Non-Cooperative Games on Networks

Martijn van der Merwe

Thesis presented in partial fulfilment of the requirements for the degree
MSc (Operations Research)
Department of Logistics, Stellenbosch University

Supervisor: Prof JH van Vuuren
Co-Supervisors: Dr AP Burger, Dr C Hui

March 2013

Declaration

By submitting this thesis electronically, I declare that the entirety of the work contained therein is my own, original work, that I am the sole author thereof (save to the extent explicitly otherwise stated), that reproduction and publication thereof by Stellenbosch University will not infringe any third party rights and that I have not previously in its entirety or in part submitted it for obtaining any qualification.

March 2013

Abstract

There are many examples of cooperation in action in society and in nature. In some cases cooperation leads to the increase of the overall welfare of those involved, and in other cases cooperation may be to the detriment of the larger society. The presence of cooperation seems natural if there is a direct benefit to individuals who choose to cooperate. However, in examples of cooperation this benefit is not always immediately obvious. The so called *prisoner's dilemma* is often used as an analogy to study cooperation and tease out the factors that lead to cooperation.

In classical game theory, each player is assumed to be rational and hence typically seeks to select his strategy in such a way as to maximise his own expected pay-off. In the case of the classical prisoner's dilemma, this causes both players to defect. In evolutionary game theory, on the other hand, it is assumed that players have limited knowledge of the game and only bounded rationality. Games in evolutionary game theory are repeated in rounds and players are afforded the opportunity to adapt and learn as this repetition occurs. Past studies have revealed that cooperation may be a viable strategy if the prisoner's dilemma is placed in an evolutionary context, where the evolutionary fitness of a strategy is directly related to the pay-off achieved by the player adopting the strategy. One of the mechanisms that promote the persistence of cooperation in the evolutionary prisoner's dilemma is structured interaction between players.

A mathematical framework for representing the *evolutionary prisoner's dilemma* (ESPD) is developed in this thesis. The mathematical framework is used to undertake an analytical approach (*i.e.* avoiding the use of simulation) towards investigating the dynamics of the ESPD with a path, cycle, plane grid or toroidal grid as underlying graph. The objective of this investigation is to determine the likelihood of the emergence of persistent cooperation between players. The ESPD on a path or a cycle admits two fundamentally different parameter regions; large values of the temptation-to-defect parameter are not capable of inducing persistent cooperation, while small values of this parameter allow for the possibility of persistent cooperation. It is found that the likelihood of cooperation increases towards certainty as the order of the underlying graph increases if the underlying graph is a path or cycle.

The state space of the ESPD with a plane or toroidal grid graph as underlying graph grows very quickly as a function of the graph order. The automorphism classes of game states are enumerated to determine exactly how fast the size of the state space of the game grows as a function of the order of the underlying graph. Finally, the dynamics of the ESPD is investigated for a grid graph as underlying graph (in cases where the state space is small enough) by means of constructing the corresponding state graphs of the ESPD.

Uittreksel

Daar is baie voorbeelde van samewerking in the gemeenskap en in die natuur. In sommige gevalle lei samewerking tot 'n toename in die algehele welvaart van die betrokkenes, terwyl samewerking in ander gevalle tot nadeel van die breër gemeenskap mag wees. Die voorkoms van samewerking blyk natuurlik te wees indien daar 'n direkte voordeel vir die individue is wat kies om saam te werk. In voorbeelde van samewerking is só 'n voordeel egter nie altyd voor-die-hand-liggend nie. Die sogenaamde *prisoniersdilemma* word dikwels as voorbeeld in die studie van samewerking gebruik om die faktore wat na samewerking lei, te ontbloot.

In *klassieke speleteorie* word daar aangeneem dat elke speler rasioneel is en dus poog om sy spelstrategie op só 'n manier te kies dat sy eie verwagte uitbetaling gemaksimeer word. In die geval van die klassieke prisoniersdilemma veroorsaak dit dat beide spelers mekaar verraai. In *evolusionêre speleteorie*, daarenteen, word daar slegs aangeneem dat elke speler oor beperkte kennis van die spel en begrensde rasionaliteit beskik. Spele in evolusionêre speleteorie word in rondtes herhaal en spelers word die geleentheid gebied om gedurende hierdie herhalingsproses aan te pas en te leer. Vorige studies het getoon dat samewerking 'n lewensvatbare strategie is indien die prisoniersdilemma in 'n evolusionêre konteks gespeel word, waar die evolusionêre fiksheid van 'n strategie direk afhang van die uitbetaling van 'n speler wat die strategie volg. Een van die meganismes wat volhoubare samewerking in die evolusionêre prisoniersdilemma voortbring, is gestruktureerde interaksie tussen spelers.

'n Wiskundige raamwerk word vir die voorstelling van die evolusionêre prisoniersdilemma in hierdie tesis ontwikkel. Hierdie wiskundige raamwerk word gebruik om 'n analitiese studie (met ander woorde sonder die gebruik van simulasie) van die dinamika van die prisoniersdilemma op 'n pad, siklus, rooster in die vlak, of rooster op die torus as onderliggende grafiek van stapel te stuur. Die doel van hierdie studie is om die waarskynlikheid vir die ontstaan van volhoubare samewerking tussen spelers te bepaal. Die prisoniersdilemma op 'n pad of siklus as onderliggende grafiek het twee fundamenteel verskillende parametergebiede tot gevolg; groot waardes van die versoeking-om-te-verraai parameter lei nie tot volhoubare samewerking nie, terwyl volhoubare samewerking wel vir klein waardes van hierdie parameter moontlik is. Daar word gevind dat die kans vir volhoubare samewerking toeneem tot sekerheid namate die orde van die onderliggende grafiek groei.

Die toestandsruimte van die prisoniersdilemma met 'n rooster in die vlak of 'n rooster op die torus as onderliggende grafiek groei baie vinnig as 'n funksie van die orde van die grafiek. Die outomorfismeklasse van die speltoestande word getel met die doel om te bepaal presies hoe vinnig die toestandsruimte van die spel as 'n funksie van die orde van die onderliggende grafiek groei. Die dinamika van die prisoniersdilemma met 'n rooster in die vlak of 'n rooster op die torus as onderliggende grafiek word laastens deur middel van konstruksies van die ooreenstemmende toestandsgrafieke ondersoek (in gevalle waar die toestandsruimte klein genoeg is).

Acknowledgements

Many people played a significant role in the work leading up to and during the writing of this thesis. I would like to acknowledge the following people and organisations. The Department of Logistics at Stellenbosch University who provided computing facilities and office space. I would like to thank my fellow students at the Operations Research division of Stellenbosch University for a couple of great conferences, shared joy and frustration, and numerous seemingly pointless debates over coffee. Though these debates seemed frivolous, they often inspired me to attack my investigations with new vigour.

There are a number of people without whom this thesis, or parts of this thesis, would never have seen the light of day to whom I would like to extend my deepest gratitude:

- My supervisor, Prof Jan van Vuuren, for his guidance, hard work and advice. He has played an influential role in my academic growth throughout my studies at Stellenbosch University.
- My co-supervisor, Dr Alewyn Burger, for his invaluable input, mathematical programming skills and dogged determination when it comes to enumerating sets. Without his assistance almost all of the theorems in this thesis would never have been proved.
- My co-supervisor, Dr Cang Hui, who introduced me to the field of evolutionary game theory. His input early in my research provided the necessary inspiration to pursue the topics covered in this thesis.
- If it was not for Gustav Paul and his googling skills, it would have been very likely that I would never have found the Transfer Matrix Method. Finding this method was one of the biggest "ah ha!" moments of my masters research and allowed for a very elegant solution to a counting problem.
- My parents, friends and family for their unwavering and continued support.
- The NRF for their financial support in the form of a bursary.

Table of Contents

List of Figures

List of Tables

List of Reserved Symbols

Symbols in this dissertation conform to the following font conventions:		
$\mathcal{A}$	Symbol denoting a **set** or a **group**	(Calligraphic capitals)
$\boldsymbol{A}$	Symbol denoting a **matrix**	(Boldface capitals)
α	Symbol denoting a general **mapping**	(Greek lower case letters)

Symbol	**Meaning**
$\times$	A binary operator symbol denoting the Cartesian product of two graphs.
C	The strategy of cooperation in the prisoner's dilemma.
C_n	A cycle of order n.
$c_{i,j}$	The pay-off achieved by a cooperator in the ESPD with i cooperators and j defectors in his open neighbourhood.
D	The strategy of defection in the prisoner's dilemma.
$\mathcal{D}_4$	The dihedral group of order 4.
$d_{i,j}$	The pay-off achieved by a defector in the ESPD with i cooperators and j defectors in his open neighbourhood.
δ_u^i	The operation of modular shifting players in the ESPD upwards by i positions.
δ_r^i	The operation of modular shifting players in the ESPD right by i positions.
$\delta^{i,j}$	The operation of modular shifting players in the ESPD upwards by i positions and to the right by j positions.
$\mathcal{G}_{n\times 2}$	The symmetry group of the ESPD with $C_n \times P_2$ as underlying graph for the case where $n > 2$.
$\mathcal{G}_r$	The symmetry group of the ESPD with $P_m \times P_n$ as underlying graph for the case where $m, n \geq 2$.
$\mathcal{G}_t$	The symmetry group of the ESPD with $C_m \times C_n$ as underlying graph for the case where $m, n \geq 3$.
ι	The identity mapping.
$\Lambda_c(n)$	The order of the state graph of the ESPD with C_n as underlying graph.
$\Lambda_p(n)$	The order of the state graph of the ESPD with P_n as underlying graph.
$\Lambda_r(m,n)$	The order of the state graph of the ESPD with $P_m \times P_n$ as underlying graph $(m > n)$.
$\Lambda_s(n)$	The order of the state graph of the ESPD with $P_n \times P_n$ as underlying graph.
$\Lambda_t(m,n)$	The order of the state graph of the ESPD with $C_m \times C_n$ as underlying graph.
m	The vertical dimension of the underlying graph of the ESPD.
n	The horizontal dimension of the underlying graph of the ESPD.

P	The pay-off to each of the players in the prisoner's dilemma if both players defect.
P_n	A path of order n.
ρ	The operation of rotating the underlying graph of the ESPD clockwise through 90°.
σ_h	The operation of reflecting the underlying graph of the ESPD about the horizontal axis of symmetry.
σ_m	The operation of reflecting the underlying graph of the ESPD about one of two diagonals.
σ_p	The operation of reflecting the underlying graph about one of two diagonals.
σ_v	The operation of reflecting the underlying graph of the ESPD about the vertical axis of symmetry.
T	The pay-off that a defecting player achieves if his opponent cooperates in the PD.

List of Acronyms

ESPD	Evolutionary spatial prisoner's dilemma
ESS	Evolutionary stable strategy
PD	Prisoner's dilemma

CHAPTER 1

Introduction

Contents

1.1 Background

There are numerous examples of cooperation in society and in nature. Often such cooperation leads to an improvement in the overall welfare of those involved. The emergence of cooperation seems to be natural if there is a direct benefit to individuals who choose to cooperate. However, in many examples of cooperation this benefit is not always immediately obvious. In some cases there may be a greater benefit to an individual seeking to exploit any cooperative behaviour by others. Furthermore, cooperation may even be to the detriment of the larger society. Consider the following examples of cooperation observed in society and in nature.

During the First World War spontaneous co-operative behaviour developed between the opposing troops, especially during prolonged trench warfare [2]. Soldiers refrained from shooting enemies even when their enemies were well within range. Artillery units deliberately aimed their rounds to miss the opposing forces, overshooting their supposed targets or having their rounds land harmlessly in no man's land.

The many examples of cleaning symbiosis found in nature, and particularly in the ocean, is another example of cooperation. In such a cleaning symbiosis within the ocean, one organism cleans another organism, usually a larger fish, of ectoparasites. The cleaner sometimes even enters the gills and mouth of the host being cleaned. These cleaner/host relationships are by no means a rare occurrence; there are more than 45 species of fish and six species of shrimp known to be cleaners, cleaning a wide variety of fish species. It would seem the most beneficial to a host to be cleaned, and then to make a meal of the cleaner once it has completed its cleaning job. However, host fish avoid eating cleaners; they typically go to great lengths not to do so, even at a cost to themselves [52].

Cooperation, however, does not always result in positive outcomes. In mid-November 2007, Tiger Brands was fined R98,8 million by the South African Competition Commission for colluding

with other bread producers to inflate the price of bread by between 30c and 35c per loaf. Pioneer Foods, another partner involved in the price fixing scandal, was the subject of the largest settlement in the history of the Competition Commission when they were fined R1-billion in penalties [16, 47]. One of the interpretations of this scenario as that the bread producers cooperated for their mutual benefit with a negative consequence to the larger society.

Cooperative behaviour typically evolves over many generations in nature, while in human societies people adapt and learn new strategies according to the perceived success of their previous strategies. This adaptation or learning process may be considered a form of evolution. The following five theories have been proposed to explain the evolution of cooperation: kin selection, direct reciprocity, indirect reciprocity, graph selection and group selection [35, 36].

Kin selection, first proposed by Hamilton [19], occurs when evolution is driven by the interaction between related individuals. The cooperation is observed when a donor pays a cost c to a recipient in order to gain a benefit b. The cost and benefit is measured in terms of the impact that the act of cooperation has on reproductive success of the individuals involved. It has been suggested that it is possible for natural selection to favour kin selection if the coefficient of genetic relatedness r is greater than the cost/benefit ratio, that is if $r > c/b$. Related individuals are more likely to have many genes in common, therefore an act of cooperation, while incurring a cost to one individual, may still benefit the set of genes.

The theory of *direct reciprocity*, put forward by Trivers [52] as an alternative to kin selection, can explain cooperative situations where organisms are not related. The *prisoner's dilemma* (PD), attributed by Durlauf & Blume [11] to A.W. Tucker, is often used as a tool for studying this kind of cooperation.

Indirect reciprocity is explained by Nowak & Sigmund [35] as follows: "Whereas direct reciprocity embodies the idea of you scratch my back I scratch yours, indirect reciprocity suggests that you scratch my back I scratch someone else's." Reputation plays a part in enforcing this kind of cooperation. Individuals are not directly punished in their act of defection, but may be punished later by a third party for a previous defection.

Selection not only acts on individuals, but may also do so in a group context. This form of cooperation is called *group selection*. A group of cooperators may be more successful than a group of defectors. It is acknowledged that group selection is a controversial theory [28].

Structured interactions in populations have been shown to facilitate cooperation in certain cases. This form of cooperation is called *network reciprocity* (or *graph selection*). Many populations (or societies) demonstrate a network-like structure in which certain individuals interact more with some individuals than with others. Graph theory may be used to study the effect of the spatial structure on the emergence of cooperation. This is the mechanism promoting cooperation which will form the focus of investigation in this thesis.

There has been a flurry of interest from the research community over the last decade in the study of games on graphs. This interest is evident by the number of citations that the review article [51] has received. The article has been cited 489 times in the literature according to *Scopus* [12] and 742 times according to *Google Scholar* [18] at the time of writing.

Understanding the factors that facilitate cooperation may allow one to install a mechanism that is capable of promoting cooperation where it is the preferred outcome, or to discourage cooperation, as in the case of price fixing, when cooperation is not desirable. Predicting where cooperation is likely to occur may also prove useful to businesses looking for effective strategies to increase their income, or governments looking to create policies that promote cooperation.

Simulation is a popular technique for studying games on graphs. The following quote by Nowak eludes to a reason why simulation is the preferred tool of investigation in this context: "Games on graphs are easy to study by computer simulation, but they are difficult to analyse mathematically because of the enormous number of possible configurations that can arise" [36].

1.2 Problem description

The examples of cooperation mentioned in §1.1 may be translated into games with player strategies and pay-offs. Possibly the simplest analogy used to investigate the emergence of cooperation is the well-known PD [2], as mentioned above. The PD is considered within an evolutionary context with structured interaction in this thesis, referred to as the *evolutionary spatial prisoner's dilemma* (ESPD). The aim of the research in this thesis may be captured by the two key questions:

1. What conditions facilitate the persistence of cooperation in the ESPD?
2. Given an underlying spatial structure to the ESPD, what is the likelihood that cooperation will persist?

As noted by Nowak [36], the mathematical analysis of games on graphs is a complicated task due to the large number of different configurations that a game can exhibit if the underlying graph is large. It is, however, possible to investigate the complete game dynamics of the ESPD on small, simple graph structures, such as paths or cycles. Three steps are required to compute the probability that cooperation will persist. The first step involves enumerating all the possible configuration that a game can exhibit. The second step is to characterise those starting configurations of the game that lead to persistent cooperation. The final step is to enumerate these 'special' cases that allow for the persistence of cooperation.

1.3 Scope and objectives

The following five objectives are pursued in this thesis:

I To perform a literature survey of previous research related to the ESPD on various underlying graph structures.

II To establish a mathematical framework in aid of the study of games on graphs.

III To determine the size of the state space of the ESPD on a grid graph.

IV To determine analytically the likelihood that cooperation will persist in the ESPD on a cycle or path.

V To determine the likelihood that cooperation will persist in the ESPD on small instances of grid-like graph structures.

The underlying graphs which are considered in this thesis are paths, cycles, grid graphs in the plane (referred to as *without wrapping*) and toroidal grid graphs (referred to as *with wrapping*). The ESPD with deterministic update rules and isomorphic graphs for the update and interaction structures of the game, is considered. The focus of this thesis is on the use of analytical techniques (*i.e.* without the aid of simulation) to study the game dynamics of the ESPD.

1.4 Thesis organisation

A number of basic mathematical concepts are introduced in the second chapter of this thesis. These concepts form the mathematical foundation upon which arguments later in the thesis are built. The first section of the chapter is a short introduction to basic notions in graph theory, while the second section is a brief introduction to basic notions in group theory. The third section contains a description of the notion of a generating function and how such a function may be applied to counting the number of paths in a directed graph.

The literature related to classical game theory, evolutionary game theory and games on graphs is briefly reviewed in the third chapter. The first section is devoted to classical game theory. A brief historical account of the development of game theory is given and important concepts and terminology are established. In the second section the focus of the literature review turns to important concepts in evolutionary game theory. In this section, the development of the field of evolutionary game theory and important results in this field are discussed. The final section is devoted to detailed descriptions of the prisoner's dilemma and its variations.

A mathematical framework for representing evolutionary games on graphs is developed in the fourth chapter. This includes defining the concept of the state of a game and defining the rules which govern how players update their strategies from round to round in such games. Finally, the notion of a state graph is introduced as a means of visually representing the game dynamics of the ESPD.

In the fifth chapter, an analytical approach (*i.e.* avoiding the use of simulation) is adopted to investigate the dynamics of the ESPD on a path or cycle as underlying graph. The likelihood of the emergence of persistent cooperation is determined. Since the game state graph captures the complete dynamics of a game, it is of interest to determine properties of the state graph without having to simulate the entire game. A number of theorems are established in this regard, describing the properties of the state graph of the ESPD with a path or cycle as underlying graph.

In the penultimate chapter, the dynamics of the ESPD with a small grid-like structure as underlying graph is investigated. The symmetries on square and rectangular grids are reviewed and the corresponding automorphism classes are enumerated. A phase plane is constructed for the ESPD with both grids with and without wrapping. It is possible to visualise the complete game dynamics for the EPSD on small grids by drawing the state graphs of the game. State graphs are constructed for the ESPD on grid graphs of dimensions 2×2, 2×3, 2×4 and 3×3 for each region in the phase plane. However, as the dimensions of the underlying graph increases the number of state automorphism classes increases exponentially and a complete analysis of the game is no longer possible if the underlying graph is sufficiently large.

The thesis closes in Chapter 7 with a summary of the work contained therein, an appraisal of the contributions of the thesis, as well as a discussion on various possibilities for future work in the area of evolutionary games on graphs.

CHAPTER 2

Preliminary concepts

Contents

A number of basic mathematical concepts which will be used in later chapters are defined and illustrated by means of examples in this chapter. The first section of the chapter is a short introduction to basic notions in graph theory, while the second section is a brief introduction to basic notions in group theory. The third section contains a description of the notion of a generating function and how such a function may be applied to counting the number of paths in a directed graph. This chapter therefore serves as a mathematical foundation on which the rest of this thesis is built.

2.1 A primer in graph theory

This section contains a number of basic definitions from graph theory in order to facilitate a description of the work presented later in this thesis. The primary source of definitions and terminology in this section is [54].

2.1.1 What is a graph?

A *graph* G is a finite, non-empty set of objects, called *vertices*, together with a (possibly empty) set of unordered pairs of distinct vertices, called *edges*. The set of vertices of a graph G is called the *vertex set* and is denoted by $V(G)$. The set of edges is called the *edge set* and is denoted by $E(G)$. An edge $e = \{u, v\}$ is said to join the vertices u and v. If $e = \{u, v\}$ (or simply $e = uv$) is an edge of G, then u and v are *adjacent vertices*, while u and e are incident, as are v and e. Two distinct edges e_1 and e_2 of G are *adjacent edges* if they are incident with a common vertex. The cardinality of the vertex set of a graph G is called the *order* of G and is denoted by $n(G)$, or more simply n when the graph under consideration is obvious, while the cardinality of its edge set is the *size* of G, denoted $m(G)$ or m. An (n, m)-*graph* has order n and size m. A graph is often represented by a diagram in which each vertex is represented by a point and each edge $e = uv$ is represented by a line or curve joining the points corresponding to u and v. To illustrate the concepts introduced above, consider the graph G_1 defined by the vertex set $V(G_1) = \{v_1, v_2, v_3, v_4, v_5\}$ and edge set $E(G_1) = \{v_1v_2, v_1v_3, v_2v_3, v_3v_4\}$ shown in Figure 2.1. The graph G_1 has order $n = 5$ and size $m = 4$. The vertices v_1 and v_3 are the only vertices adjacent to vertex v_2. The edges v_1v_2 and v_2v_3 are adjacent edges.

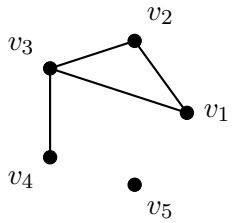

Figure 2.1: *The graph G_1.*

A *subgraph* of a graph G is a graph all of whose vertices belong to $V(G)$ and all of whose edges belong to $E(G)$. If H is a subgraph of G then we write $H \subseteq G$. If a subgraph H of G contains all the vertices of G, then H is called a *spanning subgraph* of G. For example, the graphs shown in Figure 2.2 are all subgraphs of G_1, but only $G_{1.3}$ is a spanning subgraph of G_1.

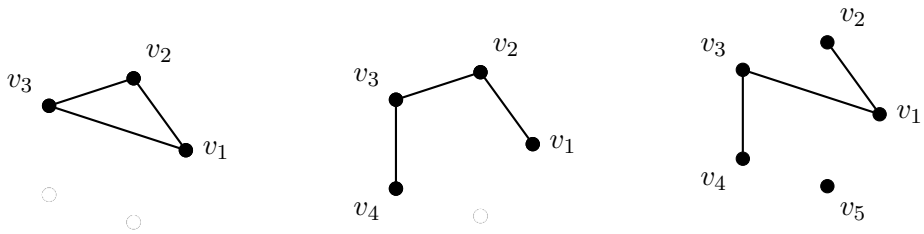

(a) $G_{1.1}$ (b) $G_{1.2}$ (c) $G_{1.3}$

Figure 2.2: *Subgraphs of the graph G_1.*

Let v be a vertex of a graph G. The *degree* of v is the number of edges of G incident with v and is denoted by $d_G(v)$, or simply $d(v)$ if G is clear from the context. The *minimum degree* of G, denoted by $\delta(G)$, is the minimum degree among all the vertices of G, while the *maximum degree* of G, denoted by $\Delta(G)$, is the maximum degree among all the vertices of G. A vertex is called *odd* or *even* depending on whether its degree is odd or even. A vertex of G with degree 0 is called an *isolated vertex* (while also being considered even) and a vertex of degree 1 is an *end-vertex* of G. To illustrate these concepts, again consider the graph G_1 in Figure 2.1. The minimum degree and maximum degree of G_1 are $\delta(G_1) = 0$ and $\Delta(G_1) = 3$, respectively.

The vertex v_4 is an end-vertex of G_1 while v_5 is an isolated vertex of G_1. The vertex v_1 of G_1 has degree $d(v_1) = 2$.

In a graph G, the *open neighbourhood* of a vertex $v \in V(G)$ is the set of all vertices adjacent to v, denoted by $N(v) = \{u | u \in V(E) \text{ and } uv \in E(G)\}$. The *closed neighbourhood* of a vertex $v \in V(G)$ is its open neighbourhood together with the vertex v itself, denoted $N[v] = N(v) \cup \{v\}$. The sets of vertices $\{v_1, v_3\}$ and $\{v_1, v_2, v_3\}$ are the open and the closed neighbourhoods, respectively, of the vertex v_2 of the graph G_1.

The *degree distribution* P of a graph is the function where $P(k)$ the fraction of nodes in the graph with degree k. The graph G_1 in Figure 2.1 has degree distribution

$$P(k) = \begin{cases} 1/5 & \text{if } k = 0, \\ 1/5 & \text{if } k = 1, \\ 2/5 & \text{if } k = 2, \\ 1/5 & \text{if } k = 3, \\ 0 & \text{otherwise.} \end{cases}$$

2.1.2 Special graphs

Certain graphs occur often in various applications, including modelling games on graphs. In this section a number of these graphs and their respective notations are described.

A graph G is called *r-regular* or *regular* of degree r if the degree of every vertex of G is r. A graph is *regular* if it is r-regular for some $r \in \mathbb{N}_0$. A 3-regular graph is also sometimes called a *cubic graph*. An example of a cubic graph is the graph G_2 shown in Figure 2.3(a).

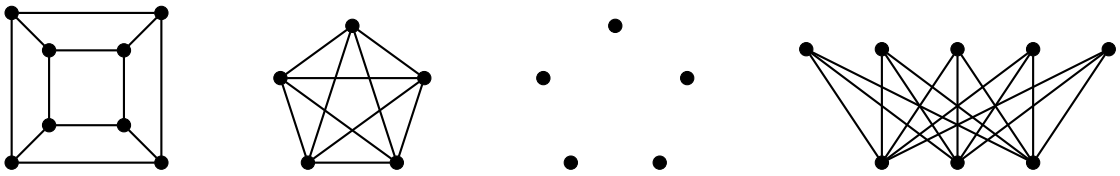

(a) G_2 (b) K_5 (c) $\overline{K_5}$ (d) $K_{5,3}$

Figure 2.3: *Examples of special graphs. (a) A 3-regular graph, (b) the complete graph K_5, (c) the empty graph $\overline{K_5}$ and (d) the complete bipartite graph $K_{5,3}$.*

A *complete graph* or *clique* is a graph in which every two distinct vertices are adjacent. A complete graph of order n is denoted by K_n and is also sometimes called an *n-clique*. A complete graph of order n has size

$$m = \binom{n}{2} = \frac{n(n-1)}{2}.$$

The *empty graph* is a graph containing no edges. An empty graph of order n is denoted by $\overline{K_n}$. Consider, as examples, the complete graph K_5 shown in Figure 2.3(b) and the empty graph $\overline{K_5}$ shown in Figure 2.3(c).

A *bipartite graph* is a graph whose vertex set can be partitioned into two disjoint sets, V_1 and V_2 (called *partite sets*), in such a way that each edge of the graph joins a vertex of V_1 to a vertex of V_2. Hence there is no adjacency amongst vertices of the same partite set. A *complete bipartite* is a bipartite graph with partite sets V_1 and V_2 having the added property that every vertex of V_1 is adjacent to every vertex of V_2. If $|V_1| = r$ and $|V_2| = s$, such a graph is denoted by $K_{r,s}$.

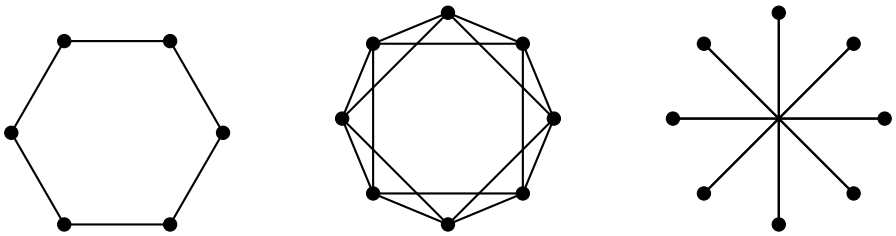

(a) $C_6\langle 1\rangle$ (b) $C_8\langle 1,2\rangle$ (c) $C_8\langle 4\rangle$

Figure 2.4: *Examples of circulants.*

A complete bipartite graph of the form $K_{1,s}$ is called a *star*, while a complete bipartite graph $K_{n,n}$ is called an *n-biclique*. An example of the complete bipartite graph, namely the graph $K_{5,3}$, is shown in Figure 2.3(d).

The *circulant* $C_n\langle i_1,\ldots,i_z\rangle$ is defined as a graph of order n with vertex set

$$V(C_n\langle i_1,\ldots,i_z\rangle) = \{v_0,\ldots,v_{n-1}\}$$

and edge set

$$E(C_n\langle i_1,\ldots,i_z\rangle) = \left\{v_\alpha v_{(\alpha+\beta)\pmod n} | \alpha \in \{0,...,n-1\} \text{ and } \beta \in \{i_1,\ldots,i_z\}\right\}$$

where $1 \leq z < n$ and $1 \leq i_1,\ldots,i_z \leq n-1$ are z distinct integers. The graph may be drawn by arranging the vertex set $\{v_0,\ldots,v_{n-1}\}$ on the edge of an imaginary circle and then joining, by means of an edge, every j-th vertex to the $(j+i)$-th vertex for each $i \in \{i_1,\ldots,i_z\}$ [54, 58]. Examples of circulants are shown in Figure 2.4.

2.1.3 Operations on graphs

In the following definitions it is assumed that F and H are two graphs with disjoint vertex sets. The *union* $G = F \cup H$ of two graphs F and H has vertex set $V(G) = V(F) \cup V(H)$ and edge set $E(G) = E(F) \cup E(H)$. A graph G consisting of k (≥ 2) disjoint copies of a graph H is written as $G = kH$.

The *cartesian product* $G = F \times H$ of F and H has vertex set $V(H) = V(F) \times V(H)$ and two vertices (u_1,u_2) and (v_1,v_2) are adjacent if and only if either $u_1 = v_1$ and $u_2v_2 \in E(H)$, or $u_2 = v_2$ and $u_1v_1 \in E(F)$. An example of the cartesian product of two graphs is shown in Figure 2.5.

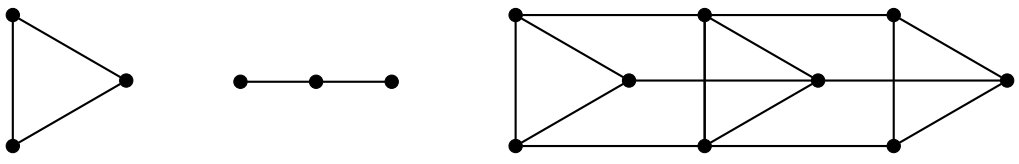

(a) G_3 (b) G_4 (c) $G_3 \times G_4$

Figure 2.5: *The Cartesian product of two graphs.*

The *complement* $\overline{G}$ of a graph has vertex set $V(\overline{G}) = V(G)$ and edge set $E(\overline{G})$ such that an edge in $\overline{G}$ joins two vertices if and only if the vertices are not adjacent in G. The graph G_1 and its complement $\overline{G_1}$ are shown in Figure 2.6.

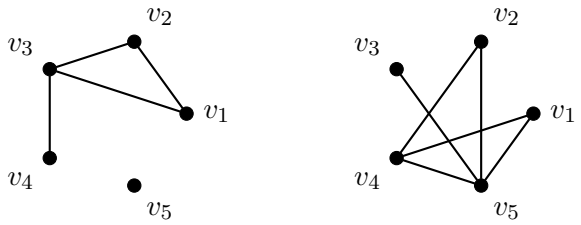

(a) G_1 (b) $\overline{G}_1$

Figure 2.6: *The graph G_1 and its compliment $\overline{G_1}$.*

2.1.4 Connectivity

A *u-v walk* in a graph G is a finite, alternating sequence of vertices and edges of G that begins with the vertex u and ends with the vertex v, and in which each edge in the sequence joins the vertex that precedes it in the sequence with the vertex which follows it in the sequence. The number of edges in the walk is called the *length* of the walk. Edges and vertices may be repeated in a walk. A *path* is a *walk* with the restriction that if an edge or a vertex occurs in the sequence, it occurs only once. Two vertices u and v are connected if $u = v$, or if $u \neq v$ and a u-v path exists in G. The edges are often omitted when indicating a path, since the edges are implied. Consider, as an example, the v_1-v_3 path v_1, v_6, v_5, v_3 of length 3 contained in the graph G_5 shown in Figure 2.7.

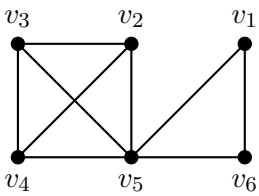

Figure 2.7: *The graph G_5.*

A u-v walk is *closed* if $u = v$ and *open* otherwise. A closed walk in which all the edges are unique is a *closed trail*. A closed trail which contains at least three vertices is called a *circuit*. A circuit in which no vertices are repeated (except the first and the last) is called a *cycle*. The length of a cycle is the number of edges in the cycle. A cycle of length n is also sometimes called an *n-cycle*, while a 3-cycle is sometimes called a *triangle*. A cycle is *even* if its length is even, or *odd* otherwise. A graph is called *acyclic* if it contains no cycles. For example, the graph G_5 in Figure 2.7 is not acyclic and contains the even cycle v_2, v_3, v_4, v_5, v_2 of length 4.

A graph G is *connected* if there exists a path in G between any two of its vertices, and is *disconnected* otherwise. Every disconnected graph can be partitioned into a number of connected subgraphs, called *components*. A component of a graph G is therefore a maximal connected subgraph of G. The number of components of G is denoted by $k(G)$. Note that $k(G) = 1$ if and only if G is connected. The *distance* $d_G(u, v)$ between two vertices u and v in a connected graph G is the minimum of the lengths of the u-v paths of G. As an example of these concepts consider the graph G_5 in Figure 2.7. There is a v_1-v_3 path in G_5, the vertices v_1 and v_3 are thus connected with the distance between them $d_{G_5}(v_1, v_3) = 2$. The graph G_5 is a connected graph, while the graph G_1 in Figure 2.6(a) is disconnected, containing $k(G_1) = 2$ components.

2.1.5 Isomorphisms

If H can be obtained from G by relabelling the vertices, then H and G are said to be *isomorphic*, written $G \cong H$. Stated alternatively, G and H are isomorphic if there is a one-to-one correspondence between the vertices of G and those of H such that an edge joins any pair of vertices in G if and only if an edge joins the corresponding pair of vertices in H. An *isomorphism* is a one-to-one mapping ϕ from $V(G)$ onto $V(H)$ such that ϕ preserves adjacency, that is $uv \in E(G)$ if and only if $\phi(u)\phi(v) \in E(H)$. If two graphs are not isomorphic, then they are *non-isomorphic*, written $G \ncong H$. The graphs G_6 and G_7, shown in Figure 2.8, are isomorphic and the mapping $\phi : V(G_6) \mapsto V(G_7)$ defined by

$$\phi(v_1) = u_1,\ \phi(v_2) = u_2,\ \phi(v_3) = u_3,\ \phi(v_4) = u_4,\ \phi(v_5) = u_5$$

is an isomorphism from $V(G_6)$ to $V(G_7)$. An isomorphism between a graph G and itself is called an *automorphism* of G.

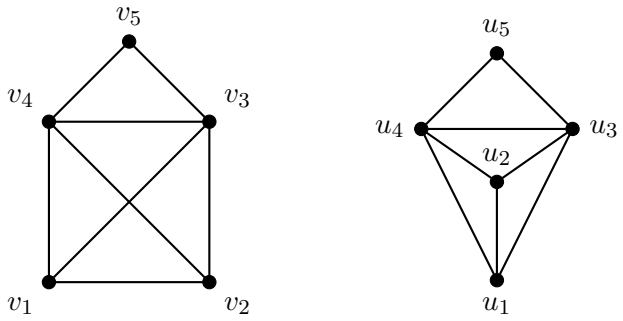

(a) G_6 (b) G_7

Figure 2.8: *Two isomorphic graphs.*

2.1.6 Directed graphs

A directed graph, or *digraph*, is a finite non-empty set of objects, called *vertices*, together with a (possibly empty) set of *ordered* pairs of distinct vertices of D, called *arcs* (or directed edges). The definitions made for graphs extend naturally to digraphs. The order m and size n of a digraph D is the cardinality of its vertex set $V(G)$ and arc set $E(G)$, respectively. The digraph D_1 shown in Figure 2.9 has order $m = 5$ and size $n = 5$.

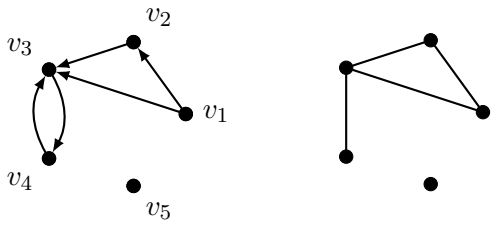

(a) D_1 (b) G_1

Figure 2.9: *The digraph D_1 and its underlying graph G_1.*

An arc (u, v) of a digraph D is said to be *incident from* u and *incident to* v. Furthermore, u is *adjacent to* v and v is *adjacent from* u. The *outdegree* of a vertex v in D is the number of vertices adjacent from v, and the *indegree* of v is the number of vertices adjacent to v. For

example, in Figure 2.9 the vertex v_3 of the digraph D_1 is adjacent to v_4, adjacent from v_2, has an outdegree of 1 and an indegree of 3.

For each digraph D, there is an associated graph G called the *underlying graph* of D. The *underlying graph* G of D has the same vertex set as that of D and is obtained by removing the directions from all the arcs, or equivalently replacing each arc (u, v) by an edge uv. The digraph D_1 and its underlying graph G_1 are shown in Figure 2.9.

A directed u-v walk in a digraph D is a finite, alternating sequence $u_0, a_1, u_1, a_2, \ldots, u_{k-1}, a_{k-1}, u_k$ of vertices and arcs that begin with the vertex u and ends with the vertex v, such that $a_i = (u_{i-1}, u_i)$ for all $i = 1, \ldots, k$. Again it is possible to omit the arcs from the specification of a u-v walk since the arcs are implied. A directed path in a graph is a directed walk with the restriction that if an arc or a vertex occurs in the sequence, it occurs only once. The digraph D_1 in Figure 2.9 contains the path v_1, v_2, v_3, v_4.

A digraph D is called *symmetric*, if whenever (u, v) is an arc of D, then (v, u) is also an arc of D, while D is called *asymmetric* if whenever (u, v) is an arc of D, then (u, v) is not an arc of D. Note that a digraph can therefore be neither symmetric nor asymmetric.

2.1.7 Pseudographs and multigraphs

When there is more than one edge between some pair of vertices, the structure is called a *multigraph*. Two or more edges in a multigraph that join the same pair of vertices are called *parallel edges*. A *loop* is an edge that joins a vertex to itself. A graph containing loops (and/or parallel edges) is called a *pseudograph*. A *pseudodigraph* is defined in a similar fashion, but with directed edges. An example of each a multigraph, a pseudograph and a pseudodigraph is shown in Figure 2.10.

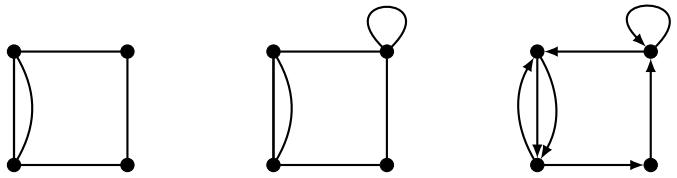

(a) A multigraph (b) A pseudograph (c) A pseudodigraph

Figure 2.10: *Different generalisations of graphs.*

2.1.8 Trees

A connected graph that contains no cycles is called a *tree*. A *forest* is a graph that has no cycles. Each component of a forest is therefore a tree. An end-vertex of a tree is called a *leaf*. In Figure 2.11, the graphs T_1 and T_2 are trees, while F_1 is a forest consisting of two components.

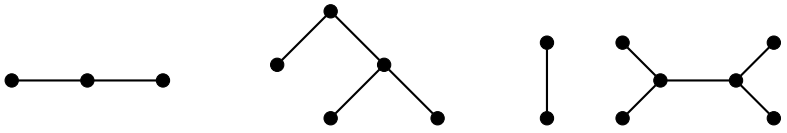

(a) T_1 (b) T_2 (c) F_1

Figure 2.11: *Examples of trees and forests.*

A *directed tree* is an asymmetric digraph for which the underlying graph is a tree. A directed tree T with a vertex r such that, for every vertex $v \neq r$, there exists a directed r-v path T, is called a *rooted tree*. The vertex r is called the *root* of the tree. When representing rooted trees graphically the root is usually placed at the top, labelled as the only vertex at level 0, the vertices adjacent from the root are then placed below the root at level 1, and so forth. The *height* of the tree is the largest integer h for which there are vertices at level h. Since all arcs are directed downwards, the arrows indicating the direction of the arcs may be omitted. The tree T_3 shown in Figure 2.12 is a rooted tree in which the vertex v_1 is the root. This rooted tree has height $h = 4$.

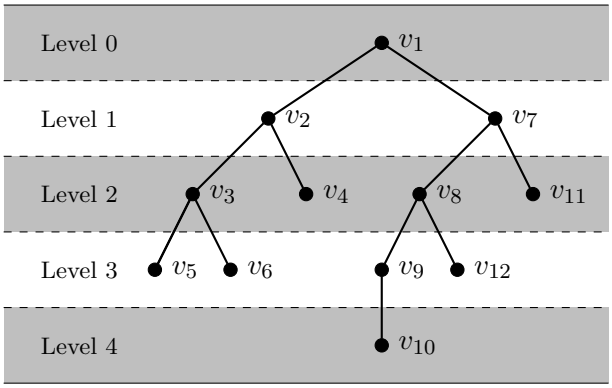

Figure 2.12: *The rooted tree T_3.*

In a rooted tree T, a vertex u adjacent to a vertex v is called the *parent* of v and the vertex v is a *child* of u. A vertex $w \in V(T)$ is a descendant of u if there exists a directed u-w path in T. In such a case u is called an *ancestor* of w. To demonstrate these concepts, consider once again the tree T_3 in Figure 2.12. The vertex v_7 is an ancestor of v_9, but not of v_3. The vertices v_9, v_{12}, v_{10} are all descendants of v_8. The vertex v_2 is the parent of its two child vertices v_3 and v_4.

2.1.9 Edge and vertex weighted graphs

An *edge-weighted graph* is a graph in which each edge e is assigned a positive real number, called the weight of e. The weight of an edge e is denoted by $w_G(e)$ or simply by $w(e)$ if the graph G is clear from the context. Similarly, a *vertex-weighted graph* is a graph in which each vertex has

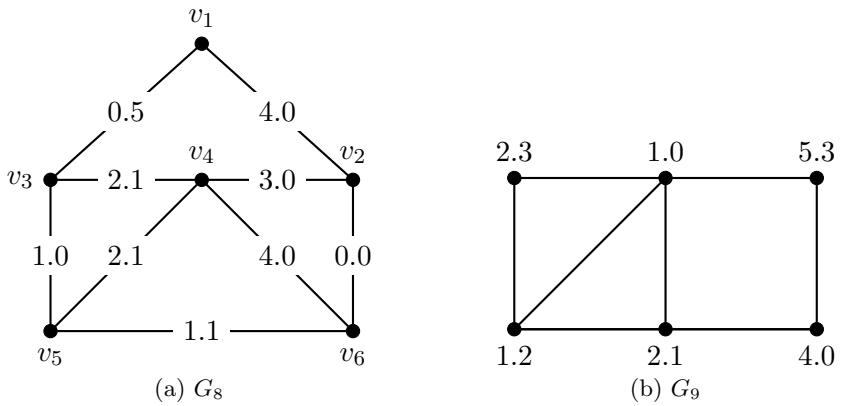

(a) G_8 (b) G_9

Figure 2.13: *(a) The edge-weighted graph G_8. (b) The vertex weighted graph G_9.*

been assigned a weight. Examples of an edge-weighted graph and a vertex-weighted graph are shown in Figure 2.13.

2.2 A primer in group theory

This section contains an introduction to some basic concepts from group theory in order to facilitate a description of the work presented later in this thesis.

2.2.1 What is a group?

A group is a set $\mathcal{G}$ together with a binary operation $\circ : \mathcal{G} \times \mathcal{G} \to \mathcal{G}$ that satisfies the following four properties:

1. For any two elements $g, h \in \mathcal{G}$, $g \circ h \in \mathcal{G}$ (closure).
2. For any three elements $g, h, k \in \mathcal{G}$, $(g \circ h) \circ k = g \circ (h \circ k)$ (associativity).
3. There exists a unique identity element $\iota \in \mathcal{G}$ such that, for all $g \in \mathcal{G}$, $g \circ \iota = \iota \circ g = g$ (identity).
4. For every element $g \in \mathcal{G}$ there exists a unique element $h \in G$, called the inverse of g, such that $h \circ g = g \circ h = \iota$ (inverses).

For the sake of brevity the expression $h \circ g$ is abbreviated as hg. An *abelian group* $(\mathcal{G}, \circ)$ is a group satisfying $ab = ba$ for any two elements a and b of $\mathcal{G}$. The *order* of $\mathcal{G}$, denoted $|\mathcal{G}|$, is the number of elements contained in $\mathcal{G}$. The order, n, of an element g in $\mathcal{G}$ is the smallest natural number n for which $g^n = \iota$, if such a number n exists, where $g^n = g \circ g \circ \cdots \circ g$ (n factors). If such a number n does not exist, then g has infinite order, written $n = \infty$. It is well known that for a finite group $\mathcal{G}$, the order $|g|$ of each $g \in \mathcal{G}$ divides $|\mathcal{G}|$ [27, Corollary on p. 78].

The set of integers $\mathbb{Z}_4 = \{0, 1, 2, 3\}$, together with the binary operation of addition modulo 4, is an example of an abelian group of order 4. The result of taking any two elements of $\mathbb{Z}_4$ and adding them together modulo 4 is again an element of $\mathbb{Z}_4$; as an example $3 + 2 = 1 \pmod 4$. The associative law holds for addition and therefore also for addition modulo 4. The identity element is 0 and there exists a unique element b for each member a of $\mathbb{Z}_4$ such that $ab = 0$ given by $b = 4 - a$.

The *Cayley table* of a group $(\mathcal{G},\circ)$ of order n is an $n \times n$ table for which the rows and columns are indexed by the elements of $\mathcal{G}$ and for which the entry at the intersection of the row indexed by a and the column indexed by b is the group product ab. The Cayley table of the group $(\mathbb{Z}_4,+)$ is given in Table 2.1 as an example.

$+$	0	1	2	3
0	0	1	2	3
1	1	2	3	0
2	2	3	0	1
3	3	0	1	2

Table 2.1: *The Cayley table of the group* $(\mathbb{Z}_4, +)$.

A group $\mathcal{G}$ with identity element ι is said to *act* on set a $\mathcal{X}$ if, for each element g in $\mathcal{G}$, there is an associated map π_g from $\mathcal{X}$ into $\mathcal{X}$ such that $\pi_\iota(x) = x$ for every x in $\mathcal{X}$ and $\pi_{hg} = \pi_h(\pi_g(x))$ for every g, h in $\mathcal{G}$ and for every x in $\mathcal{X}$ [27]. The *natural action* of $\mathcal{G}$ on $\mathcal{X}$ is defined by $\pi_g(x) = g(x)$ for each x in $\mathcal{X}$, where $\mathcal{G}$ is a group symmetries of a euclidean space E and $\mathcal{X}$ is a set of points of E [27]. Let $\mathcal{G}$ be a group acting on a set $\mathcal{X}$. If $g(x) = x$ for some $x \in \mathcal{X}$ and $g \in \mathcal{G}$, it is said that x is *fixed* by g.

2.2.2 Symmetry groups

Symmetry groups are considered in this section within the context of two-dimensional euclidean geometry. An *isometry* is a mapping between metric spaces that preserves distances. An isometry that maps a set of points to itself is called a *symmetry* for that set of points. As an example, consider a square with its centre at the origin and corner points at $(1, 1)$, $(1, -1)$, $(-1, 1)$ and $(-1, -1)$. The square has eight symmetries: clockwise rotations by 90°, 180°and 270°, reflections in the horizontal, vertical and two diagonal axes and the identity that maps every point in the plane to itself. Let ρ denote a counter clockwise rotation of 90°about the origin, let σ be the reflection in the x-axis and let ι be the identity mapping. Then the set of symmetries, $\{\iota,\ \rho,\ \rho^2,\ \rho^3,\ \sigma,\ \sigma\rho,\ \sigma\rho^2,\ \sigma\rho^3\}$, of the square forms a symmetry group, often denoted by $\mathcal{D}_4$. It holds in general that the set symmetries of a regular n-polygon forms a symmetry group called a *dihedral group*, which is denoted by $\mathcal{D}_n$.

A proof of the following well-known theorem may be found in [27, Theorem on p. 92].

Theorem 2.1 (Frobenius-Cauchy lemma, also known as Burnside's lemma) *If a group $\mathcal{G}$ acts on a set $\mathcal{X}$, then the number of equivalence classes into which $\mathcal{X}$ is partitioned by the action of $\mathcal{G}$ is the given by*

$$\frac{1}{|\mathcal{G}|}\sum_{g\in\mathcal{G}}|F_g|,$$

where $F_g = \{x \in \mathcal{X} | \pi_g(x) = x\}$ is the set of elements of $\mathcal{X}$ fixed by g.

As an example of how to apply the Frobenius-Cauchy lemma, consider counting the number of ways of colouring the four cells of a 2×2 checkerboard using two colours. The group $\mathcal{D}_4$ acts on the colourings. The identity is a symmetry of all the possible colourings, therefore $|F_\iota| = 2^4$. The operation ρ maps the first cell to the position of the second, the second to the position of the third and the third to the position of the fourth. For ρ to be a symmetry, all cells must be the same colour, so that $|F_\rho| = 2^1$. Consider next those colourings that have ρ^2 as a symmetry. The positions of the first and third cells are interchanged by ρ^2 and hence have to be the same colour. The positions of second and the fourth cells are also interchanged by ρ^2 and hence they too must have to be the same colours. There are thus 2^2 colourings that have ρ^2 as a symmetry, and so $|F_{\rho^2}| = 2^2$. The symmetries of the remaining actions may be calculated in a similar fashion with the result $|F_\iota| = 2^4$, $|F_\rho| = 2^1$, $|F_{\rho^2}| = 2^2$, $|F_{\rho^3}| = 2^1$, $|F_\sigma| = 2^2$, $|F_{\sigma\rho}| = 2^2$, $|F_{\sigma\rho^2}| = 2^3$ and $|F_{\sigma\rho^3}| = 2^3$. It follows by the Frobenius-Cauchy lemma that there are $\frac{1}{8}(16+2+4+2+4+4+8+8) = 6$ ways of colouring a 2×2 checkerboard with two colours. The six colourings are shown in Figure 2.14.

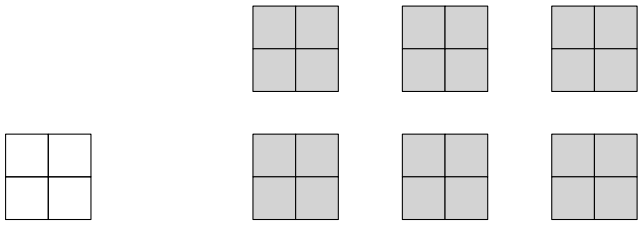

(a) (b)

Figure 2.14: *(a) A 2×2 checkerboard. (b) The six colourings of a 2×2 checkerboard, which has $\mathcal{D}_4$ as a symmetry group.*

2.3 Generating functions and the transform matrix method

This section contains a basic introduction to and definitions related to generating functions in order to facilitate a description of the work presented later in this thesis.

2.3.1 What is a generating function?

The *generating function* for a sequence $\langle a_i \rangle = a_1, a_2, a_3, \ldots$ is the power series $F(x)$ in an indeterminate x with the sequence as its coefficients [27], that is

$$F(x) = \sum_{n=0}^{\infty} a_n x^n.$$

If a generating function $F(x)$ can be written as the ratio of two polynomials, that is $F(x) = P(x)Q^{-1}(x)$, then $F(x)$ is called a *rational generating function*. As an example, $(1+x)^n$ is a rational generating function for the sequence $\binom{n}{0}, \binom{n}{1}, \binom{n}{3}, \ldots, \binom{n}{n}, 0, 0, \ldots$

2.3.2 The transfer matrix method

A method for determining the number of directed walks of a length n in a directed graph is described in this section. The method is called the *transfer matrix method* [50].

A recurrence relation for a sequence $\langle a_i \rangle$ is a formula that defines a_n in terms of $a_0, a_1, \ldots, a_{n-1}$ for all n greater than some k [27]. The terms $a_0, a_1, \ldots, a_k$ are called the initial conditions. A *linear recurrence relation* is an equation of the form $a_n = c_1 a_{n-1} + c_2 a_{n-2} + \cdots + c_d a_{n-d}$, where $c_1, c_2, \ldots, c_d \in \mathbb{R}$ for some $d \in \mathbb{N}$ not exceeding n. It is well known that the generating function of a sequence is rational if and only if the sequence is a linear recursive sequence, as stated in the following lemma.

Lemma 2.1 ([50], Theorem 4.1.1) *Let $\alpha_1, \alpha_2, \ldots, \alpha_d \in \mathbb{R}$ with $\alpha_d \neq 0$ and $d \geq 1$. The following statements are equivalent:*

1. *$\sum_{n=0}^{\infty} a_n x^n = \frac{P(x)}{Q(x)}$ where $Q(x) = 1 + \alpha_1 x + \alpha_2 x^2 + \cdots + \alpha_d x^d$ and $P(x)$ is a polynomial in x of degree less than d.*
2. *For all $n \geq 0$, $a_{n+d} + \alpha_1 a_{n+d-1} + \alpha_2 a_{n+d-2} + \cdots + \alpha_d a_n = 0$.*
3. *For all $n \geq 0$, $a_n = \sum_{i=1}^{k} P_i(n) \lambda_i^n$, where $1 + \alpha_1 x + \alpha_2 x^2 + \cdots + \alpha_d x^d = \Pi_{i=1}^{k} (1 - \lambda_i x)^{d_i}$, the λ's are distinct, and $P_i(n)$ is a polynomial in n of degree less than d_i for all $i \in \{1, \ldots, k\}$.*

The result of the following lemma allows for the enumeration of the number of paths of length n between two vertices of a digraph.

Lemma 2.2 ([50], Theorem 4.7.1) *Let $\boldsymbol{A}$ be the adjacency matrix of digraph D.[1] The entry $(\boldsymbol{A}^n)_{ij}$ is the number of walks of length n starting at vertex v_i and ending at vertex v_j.*

Proof: It follows from the definition of matrix multiplication that

$$(\boldsymbol{A}^n)_{ij} = \sum \boldsymbol{A}_{ii_1}\boldsymbol{A}_{i_1i_2}\cdots\boldsymbol{A}_{i_{n-1}j},$$

where the sum is over all sequences $(i_1,\ldots,i_{n-1})$. The summand is 1 if $v_iv_{i_1}v_{i_2}\cdots v_{i_{n-1}}v_j$ is a directed walk from v_i to v_j and 0 otherwise. □

The next lemma provides an explicit formula for determining the generating function that counts the number of closed walks in a digraph. The proof of the lemma makes use of the identity

$$\sum_{n=1}^{\infty}(ax)^n = \frac{ax}{1-ax},$$

where $|ax| < 1$.

Lemma 2.3 ([50], Theorem 4.7.3) *Let $C_D(n)$ be the number of closed walks in the digraph D of length n. Then*

$$\sum_{n\geq 1} C_D(n)x^n = \frac{-xQ'(x)}{Q(x)},$$

where $Q(x) = \det(\boldsymbol{I} - x\boldsymbol{A})$.

Proof: By Lemma 2.2, $C_D(n) = \sum_{i=1}^{p}(\boldsymbol{A}^n)_{ii} = \operatorname{tr}\boldsymbol{A}^n$. Let $\omega_1,\omega_2,\ldots,\omega_q$ be the non-zero eigenvalues of $\boldsymbol{A}$. Then $\operatorname{tr}\boldsymbol{A}^n = \omega_1^n + \omega_2^n + \cdots + \omega_q^n$ and it follows that

$$\begin{aligned}
\sum_{n=1}^{\infty} C_D(n)x^n &= \sum_{n=1}^{\infty}\omega_1^n x^n + \sum_{n=1}^{\infty}\omega_2^n x^n + \cdots + \sum_{n=1}^{\infty}\omega_q^n\lambda^n \\
&= \frac{\omega_1 x}{1-\omega_1 x} + \frac{\omega_2 x}{1-\omega_2 x} + \cdots + \frac{\omega_q x}{1-\omega_q x} \\
&= \frac{\omega_1 x(1-\omega_2 x)\cdots(1-\omega_q x) + \cdots + \omega_q x(1-\omega_1 x)\cdots(1-\omega_{q-1}x)}{(1-\omega_1 x)(1-\omega_2 x)\cdots(1-\omega_q x)} \\
&= \frac{-xQ'(x)}{Q(x)}. \quad \square
\end{aligned}$$

It follows by Lemmas 2.1 and 2.3 that there exists a recurrence relation for the number of directed walks in a digraph. Consider, as an example, the digraph D_2, shown in Figure 2.15, with associated adjacency matrix

$$\boldsymbol{A} = \begin{bmatrix} 0 & 1 & 0 & 0 & 0 \\ 0 & 0 & 1 & 0 & 0 \\ 1 & 0 & 0 & 1 & 0 \\ 0 & 0 & 1 & 0 & 0 \\ 0 & 0 & 0 & 0 & 0 \end{bmatrix}.$$

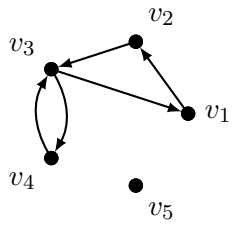

Figure 2.15: *The digraph D_2.*

The number of closed walks of length n may be enumerated by finding the associated generating function. Taking $Q(x) = \det(\boldsymbol{I} - x\boldsymbol{A}) = 1 - x^2 - x^3$, it follows by Lemma 2.3 that the generating function is given by $F(x) = \frac{-x(-2x-3x^2)}{1-x^2-x^3} = \frac{2x^2+3x^3}{1-x^2-x^3}$. The Taylor expansion of this generating function is $F(x) = 2x^2 + 3x^3 + 2x^4 + 5x^5 + 5x^6 + \ldots$ The coefficient of the term x^n is the number of closed walks of length n. There are thus two closed walks of length 4; they are v_3, v_4, v_3, v_4, v_3 and v_4, v_3, v_4, v_3, v_4. By Lemma 2.1 the recurrence relation is given by $a_n = a_{n-2} + a_{n-3}$ with the initial conditions $a_1 = 0, a_2 = 2, a_3 = 3$.

2.4 Chapter summary

In this chapter, various basic mathematical concepts were reviewed. In §2.1, some fundamentals from graph theory were considered, including basic terminology in graph theory, various types of graphs and a number of operations on graphs. §2.2 contained a brief introduction to some basic concepts from group theory. The Frobenius-Cauchy lemma, in particular, is a very useful tool in enumerative combinatorics as will become evident in later chapters. The concept of a generating function was introduced in §2.3. Generating functions may be used to enumerate the number of directed walks of a certain length in a digraph. The concepts introduced in this chapter form the mathematical building blocks for the work that is to follow later in this thesis.

[1] $\boldsymbol{A}_{ij} = 1$ if (v_i, v_j) is an element of $E(D)$, or $\boldsymbol{A}_{ij} = 0$ otherwise.

CHAPTER 3

Literature review

Contents

The literature related to game theory, evolutionary game theory and games on graphs is reviewed in this chapter. The first section concerns classical game theory. A brief historical account of the development of game theory is given and important concepts and terminology are defined. In the second section the focus is on the literature related to important concepts in evolutionary game theory. In this section the development of the field of evolutionary game theory and important results in this field are discussed. The third section concerns the prisoner's dilemma and its variations.

3.1 Classical game theory

Game theory is a subdiscipline of operations research concerned with modelling and predicting the behaviour of decision makers, also called players, when facing the problem of selecting

strategies from a set of alternatives [11]. These strategy decisions affect other players' choices and the resulting interactions are analysed from a rational point of view. A player's *strategy* determines the choices a player will make for any given scenario in a game. Each player in a game receives a *pay-off*, determined by the strategy employed in the game by the player himself and all other players involved in the game. Each player typically seeks to select his strategy in such a way as to maximise his own expected pay-off. Fields in which game theory is often applied include economics, political science, tactical and strategic military science, computer science and evolutionary biology.

3.1.1 A brief history of classical game theory

Originally, game theoretical analyses focused on a class of simple, strictly competitive games, more commonly known as two-person zero-sum games [11]. Chess and two-sided poker are examples of strictly competitive games in this class. In these games there is no point in cooperation; if one outcome is preferred to another by one player, then the preference is reversed for the other player. Although strictly competitive games seem inappropriate for applications to economic and political scenarios, concepts and results in the literature related to this simple class of games have become the cornerstone of general game theory [11].

The extensive form of the game was introduced in 1928 by von Neumann [53] and later generalised by Kuhn [26]. Other concepts developed during these early stages of game theory are the fundamental concepts of strategy, the strategic form of a game, mixed strategies and individual rationality [11]. The strategic form, often represented as a pair of matrices for two-person games, is considered one of the most significant contributions to game theory [11].

Zermelo's Theorem, published in 1913 [60], is considered the first theorem of Game Theory [11]. The original article was published in German, which led to contradictory statements in the English literature as to what Zermelo claimed in his proof. In his paper, Zermelo considered two-person zero-sum games based on perfect information and without stochastic strategic elements, called *moves* [45]. The games considered allow only a finite number of positions, but potentially infinite sequences of moves. Zermelo formalised what is meant by a *winning position* as the non-emptiness of a certain set containing all possible sequences of moves such that a player wins independently of how the other player plays. Zermelo went on to prove, given that a player is in a winning position, that it will never take more moves than there are positions available for that player to win the game. The statement was proved by means of contradiction. Zermelo used chess to illustrate his proofs. Although he proved that chess is a strictly determined game[1], the proof does not construct the winning strategy.

The Minimax Theorem is another corner stone theorem in game theory. The theorem was first proved by von Neumann [11, 53]. According to the Minimax Theorem, every two-person zero-sum game with finitely many pure strategies for each player is determined. When mixed strategies are allowed, the game has precisely one individually rational pay-off vector [11]. The Minimax Theorem paved the way for the well-known notion of a *Nash-equilibrium* [33]. In zero-sum games the so-called *minimax solution* is the same as the Nash-equilibrium. The prediction of the minimax theory was confirmed experimentally in [40] where the authors showed that, on average, human players played as predicted by the Minimax Theorem, but with high variability among players.

[1] A strictly determined game is a two-player zero-sum game that has at least one Nash-equilibrium, also sometimes called a strategic equilibrium.

A *solution concept* is a function that associates sets of outcomes with games. Solution concepts are often indicators of how a player may play in a game, but not necessarily predictions of the outcome of a game [11]. In the case of zero-sum games there is an easy answer to the question of what the solution is, namely the unique individually rational solution, but in most other cases there is not a unique solution to a game. Different solutions may be proposed for a game, depending on the assumptions made.

The 1950s was an exciting period for game theory [11]. John Nash laid the groundwork for the general non-cooperative theory and for cooperative bargaining, while Al Tucker formulated the prisoner's dilemma. Towards the end of the decade the first studies of repeated games appeared.

The 1980s saw the rise of game theory applied to biology. John Maynard Smith had a significant impact on the field when it was in its infancy [28, 29, 30]. Ordinary utility maximising rationality is easier to observe in animals and even plants than in human beings [11]. As an example, rats are found to perform better than humans in a probability matching experiment. In the experiment the subject must predict the outcome of a binary event, where each event occurs with a certain probability. The rational solution would be to always pick the variable that is most likely to occur. While rats are not especially advanced, they were found to predict the correct event significantly more often than humans [11].

3.1.2 Representing games

In classical game theory, two key assumptions are (1) that players are perfectly rational and (2) that this is common knowledge. *Perfectly rational* players have full knowledge of their own and their opponents' potential strategies and pay-off values, they always act in a way to maximize their own pay-off, and are able to deduce the best way to play the game no matter how complex the computations required to do so may be. *Common knowledge* implies that all players know that all players are rational, and all players know that all players know that all players are rational, and so on.

A game in classical game theory consists of a finite number of players, a (possibly unique) strategy space for each player, and a set of rules that determines the pay-off that each player receives at the end of the game.

Let $\Sigma_i = \{s_1^{(i)}, \ldots, s_{m_i}^{(i)}\}$ be the set of strategies available to player $i \in \{1, \ldots, N\}$. In the *strategic form* of a game, a pay-off $\pi_i(s_{j_1}^{(1)}, \ldots, s_{j_N}^{(N)})$ is associated with each possible profile $S = (s_{j_1}^{(1)}, \ldots, s_{j_N}^{(N)})$ of strategies, where $s_{j_i}^{(i)} \in \Sigma_i$ for all $i \in \{1, \ldots, N\}$, to form a pay-off profile $\Pi(S) = (\pi_1(S), \ldots, \pi_N(S))$.

The *strategic form* of a two-person game is often represented as a pair of matrices. Consider a game with two players, p_1 and p_2, and with strategy sets Σ_1 and Σ_2. If m_1 is the number of strategies in Σ_1 and m_2 is the number of strategies in Σ_2, then the $m_1 \times m_2$ pay-off matrix $\boldsymbol{M}_1$ for player p_1 is formed by labelling the rows by means of the elements of Σ_1 and the columns by means of the elements of Σ_2. The entry in the row labelled $s_i^{(1)} \in \Sigma_1$ and the column labelled $s_j^{(2)} \in \Sigma_2$ is defined to be $\pi_1(s_i^{(1)}, s_j^{(2)})$. The pay-off matrix $\boldsymbol{M}_2$ for player p_2 is formed in a similar fashion. Table 3.1 shows the matrix representation, called the strategic form, for an example of a two-person game. In this example, the strategies available to p_1 are $\Sigma_1 = \{s_1^{(1)}, s_2^{(1)}, s_3^{(1)}\}$ and those available to player p_2 are $\Sigma_2 = \{s_1^{(2)}, s_2^{(2)}, s_3^{(2)}, s_4^{(2)}\}$. If p_1 plays strategy $s_2^{(1)}$ and p_2 plays $s_4^{(2)}$ then the pay-off to player p_1 is $\boldsymbol{M}_1(2, 4) = 1$ and the pay-off to player p_2 is $\boldsymbol{M}_2(4, 2) = 3$.

A two-player game may be succinctly represented by merging the two matrices above into a

$\boldsymbol{M}_1$	$s_1^{(2)}$	$s_2^{(2)}$	$s_3^{(2)}$	$s_4^{(2)}$
$s_1^{(1)}$	1	1	5	1
$s_2^{(1)}$	2	4	2	1
$s_3^{(1)}$	4	3	1	1

(a) The pay-off matrix for player p_1.

$\boldsymbol{M}_2$	$s_1^{(1)}$	$s_2^{(1)}$	$s_3^{(1)}$
$s_1^{(2)}$	3	1	1
$s_2^{(2)}$	2	5	3
$s_3^{(2)}$	4	3	1
$s_4^{(2)}$	1	3	1

(b) The pay-off matrix for player p_2.

Table 3.1: *An example of a game in strategic form.*

single *bimatrix*. Let $\boldsymbol{B}$ be the $m_1 \times m_2$ bimatrix representation of a game. Then each entry b_{ij} of $\boldsymbol{B}$ is an ordered pair of numbers. The entries of this ordered pair represent the pay-offs to the two players, p_1 and p_2, playing the strategy profile represented by row i and column j of the bimatrix. The game shown in Table 3.1 is presented in bimatrix form in Table 3.2.

$\boldsymbol{B}$	$s_1^{(2)}$	$s_2^{(2)}$	$s_3^{(2)}$	$s_4^{(2)}$
$s_1^{(1)}$	(1,3)	(1,2)	(5,4)	(1,1)
$s_2^{(1)}$	(2,1)	(4,5)	(2,3)	(1,3)
$s_3^{(1)}$	(4,1)	(3,3)	(1,1)	(1,1)

Table 3.2: *The game of Table 3.1 in bimatrix strategic form.*

The *extensive form* representation of a game consists of a rooted tree. Each vertex of the tree represents a possible *state* of the game and each edge represents an event. An event may either be a move by a player or a stochastic event. The extensive form provides a complete formal description of how the game is played, specifying the sequence in which the players move, what they know at the times when they must move, how stochastic events are managed, and the pay-off to each player at the end of the game. Although the extensive form is especially convenient for representing a game consisting of sequential moves, it may also be used to describe games allowing simultaneous moves. The *information set* S of a player P is a set of vertices with the property that at a certain point in the game P knows that his position is described by one of the vertices in S, but does not know which one. When drawing the game tree, vertices in the same information set are connected by edges drawn as dashed lines.

Example 3.1 *The well-known prisoner's dilemma (PD) is often presented in the form of the following parable [56]. Two suspects are arrested by the police. The police, having insufficient evidence to secure a conviction, decide to offer each prisoner the same deal. Each prisoner is told that if he testifies, while the other remains silent, he will be free to go, while the silent accomplice will receive the full sentence. If both remain silent, both prisoners will be sentenced to a short term in jail for a minor charge. However, if each betrays the other, the sentence will be shared between the prisoners, in which case each will receive a medium sentence. Each prisoner must choose to betray the other or to remain silent. If each prisoner is assured that the other would not know about the betrayal, if such a betrayal were to occur, before the end of the investigation, the dilemma is that each prisoner should decide on a strategy to proceed.*

The prisoner's dilemma, attributed by [11] to A.W. Tucker, is therefore a two-person non-zero sum game. A player has the option to play one of two strategies, either to cooperate with the other (i.e. to remain silent), denoted by C, or to defect (i.e. to betray the other prisoner), denoted

by D. Traditionally the pay-off parameters are named as follows: P, the punishment for mutual defection; T, the temptation to defect; S, the sucker's pay-off; and R, the reward for mutual cooperation. The normal form of the game is given in Table 3.3 with the constraints on the pay-off values $T > R > P > S$. The 'dilemma' arises from the expected result of the game. If a player expects his opponent to cooperate, then he can gain the maximum possible pay-off by defecting. On the other hand, if the player expects his opponent to defect, it is better to settle for the punishment, P, by defecting rather than cooperating, which would result in the smallest pay-off, S. By each following this reasoning, both players eventually defect, while they could have done much better had they both cooperated.[2]

	C	D
C	(R, R)	(S, T)
D	(T, S)	(P, P)

Table 3.3: *The PD in bimatrix strategic form.*

The extensive form representation of the game is given in Figure 3.1. The vertices corresponding to the second player form an information set, reflecting the fact that the players make their choices simultaneously. □

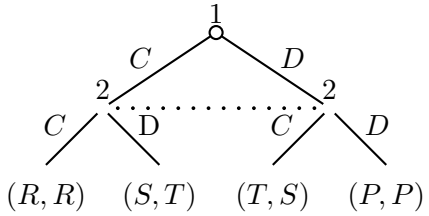

Figure 3.1: *The PD in extensive form.*

3.1.3 Classifying games

Games are often classified according to their pay-off structures and the types of rules employed. A *cooperative game* is a game in which all agreements, promises and threats are fully binding and enforceable [11]. Communication between players is allowed in cooperative games, but not in *noncooperative games*.

[2]Models incorporating the PD often use a subset of the complete parameter space in order to simplify the analysis. Nowak and May [37], for example, employed a parametrisation which gives rise to the so-called *weak prisoner's dilemma*, with parameter values $T = b, R = 1, S = 0$ and $P = 0$.

The so-called *cost benefit* parameterisation has the pay-off received in the PD interpreted in terms of the cost associated with cooperating and the benefit that an opponent will receive. Let c be the cost of cooperating in the PD and b the benefit one would receive if one's opponent cooperated. The pay-offs are then given by $T = b$, $R = b - c$, $P = 0$ and $S = -c$, or in matrix form, as

$$\begin{array}{c} \\ \text{C} \\ \text{D} \end{array} \begin{array}{c} \begin{array}{cc} \text{C} & \text{D} \end{array} \\ \begin{bmatrix} b-c & -c \\ b & 0 \end{bmatrix} \end{array}.$$

In the *scaled prisoner's dilemma* parameterisation, on the other hand, the temptation prize is fixed at 0 and the reward for cooperation at 1. The other two parameters, T and P, are allowed to vary within the bounds $T > 1$ and $0 < P < 1$. This parameterisation proves useful in games played on regular lattices and games on lattices where each player's score is scaled by the number of games played. The scaled prisoner's dilemma is discussed in more detail in the next chapter.

In a *symmetric game* the pay-off to a player playing a particular strategy depends only on the strategies adopted by the other players in the game, not on who is playing any particular strategy. A game is called *asymmetric* if it is not symmetric. If $\boldsymbol{M}$ is the pay-off matrix to player p_1 in a symmetric game with two players, then the transpose $\boldsymbol{M'}$ is the pay-off matrix to player p_2. The game given in extensive form in Figure 3.1 is a symmetric game; the entire game may be represented in strategic form by a single matrix, as shown in Table 3.4.

	C	D
C	R	S
D	T	P

Table 3.4: *The PD in matrix strategic form.*

If the pay-offs to all the players in a game sum to zero for all strategies, the game is called a *zero-sum game*. Zero-sum games model situations where there is a constant resource, and decisions made by players do not increase or decrease the total available resource. In other words, if π_i is the pay-off to player P_i in an N-person zero-sum game, then

$$\sum_{i=1}^{N} \pi_i \left(s_{j_1}^{(1)}, \ldots, s_{j_N}^{(N)} \right) = 0$$

for all possible strategy profiles $S = (s_{j_1}^{(1)}, \ldots, s_{j_N}^{(N)})$. If there are only two players in a zero-sum game, then the one player's pay-off is the negative of the other player's pay-off.

As mentioned previously, players can perform their moves simultaneously or sequentially. In a game with sequential moves, players have some knowledge of the decisions made by other players during earlier moves of the game. The extensive form is often used to represent sequential games. A game may also incorporate a combination of sequential and simultaneous events.

A game in which all players know exactly the state of the game and which decisions are made at all times is called a *game of perfect information*. An example of a game of perfect information is chess — both players know all the rules of the game and a player can observe all the moves made by the other player. If a game is not of perfect information, then it is of *imperfect information*. An example of a game of imperfect information is bridge — each player has limited knowledge of the cards held by other players. In a *game of complete information*, on the other hand, every player knows the strategies and pay-offs available to other players, but not necessarily their actions [17].

It is often useful to allow a player to choose to play each of his strategies with a certain probability; this is called a *mixed strategy*. When mixed strategies are allowed, a player's goal is to find the probabilities with which each strategy will be chosen in order to maximise his *expected* pay-off. A mixed strategy for a player i is an m_i-tuple $\mathbf{p}^{(i)} = (p_1^{(i)}, \ldots, p_{m_i}^{(i)})$ of probabilities, that is $p_j^{(i)} > 0$ for all $j \in \{1, \ldots, m_i\}$ and all $i \in \{1, \ldots, N\}$, and $\sum_{j=1}^{m_i} p_j^{(i)} = 1$ for all $i \in \{1, \ldots, N\}$. A player playing mixed strategy $\mathbf{p}^{(i)}$ will play strategy j with probability $p_j^{(i)}$ at each play of the game.

3.1.4 Solution concepts

A *solution concept* is a formal rule for predicting how a game will be played. A strategy $s_j^{(i)}$ in the strategy set Σ_i of player P_i is said to be *dominated* by a strategy $s_k^{(i)} \in \Sigma_i$ if $\pi_i\left(s_j^{(i)}, S'\right) > \pi_i\left(s_k^{(i)}, S'\right)$ for all strategy profiles $S' = \left(s_{j_1}^{(1)}, \ldots, s_{j_{i-1}}^{(i-1)}, s_{j_{i+1}}^{(i+1)}, \ldots, s_{j_N}^{(N)}\right)$. To find a dominated strategy in a two-person game in strategic form, one has to look for a dominated row in the matrix representation of the game. In the game in Table 3.1, strategy $s_4^{(2)}$ is, for example, dominated by the strategy $s_2^{(2)}$.

Rational players seeking to optimise their scores would not play dominated strategies, since playing any other strategy will lead to a higher pay-off. In some cases it is possible to find a solution to a game by simply eliminating all strictly dominated strategies. As an example, the strategy C is dominated by the strategy D in the game shown in Table 3.4. One may thus eliminate C as a possible solution, leaving D as the only remaining rational strategy. Note that a rational strategy does not necessarily optimise the total score in a game; it merely ensures the best-case scenario from a selfish perspective.

Eliminating dominated strategies may not always be sufficient to reach a single, unique solution; further refinements may be required. A very famous game theoretic notion is that of the Nash-equilibrium. In a game played by two or more players, a set of strategies is a *Nash equilibrium* if no player can do any better by changing his strategy while the other players keep to the same strategy. If the strategy profile $(s_i^{(1)}, s_j^{(2)})$ is a Nash-equilibrium in a two-person game, then $s_j^{(1)}$ is said to be the *best response* to strategy $s_j^{(2)}$. It is possible for a game to have more than one Nash equilibrium. As an example, consider the game in Table 3.2 which has two Nash equilibria, namely $(s_1^{(1)}, s_3^{(2)})$ and $(s_2^{(1)}, s_2^{(2)})$.

Backward induction is a technique used to solve a game by reasoning backward from the end of the game, eliminating all sub-optimal choices. Backward induction is based on the principle that at every decision point the player makes an optimal choice.

Example 3.2 *Suppose three politicians are voting on whether or not to give themselves a pay raise. Each stands a chance to benefit from the pay raise by an amount b, but will face a small resentment c from the voters if they vote for the pay raise. The three politicians vote sequentially and it is assumed that the benefit of the pay raise exceeds to cost of voting for it. The extensive form of the game is shown in Figure 3.2 [32].*

To solve the game using backward induction, politician 3's strategy is considered first. In the case where the first two politicians split their vote, one politician votes yes and the other no, in which case politician 3 votes yes, since this gives him a pay-off of $b - c$ which is greater than 0, the pay-off he would have received had he voted no. If both previous politicians voted yes, then politician 3 achieves the best pay-off by voting no, receiving b as opposed to $b - c$ had he voted yes. If the first two politicians both voted no, then politician 3 will vote no, receiving a pay-off of 0.

Next the best choice for politician two is considered. Politician 2 knows that politician 3 will play as described above. He can thus reduce the original game to the one shown in Figure 3.3. Now, if politician 1 votes yes, then the best option is for politician 2 to vote no, receiving a pay-off of b. If, however, politician 1 votes no, politician 2 gains the best pay-off $b - c$ by voting yes.

Finally, politician 3 anticipates how politicians 2 and 3 will vote. If politician 1 votes yes,

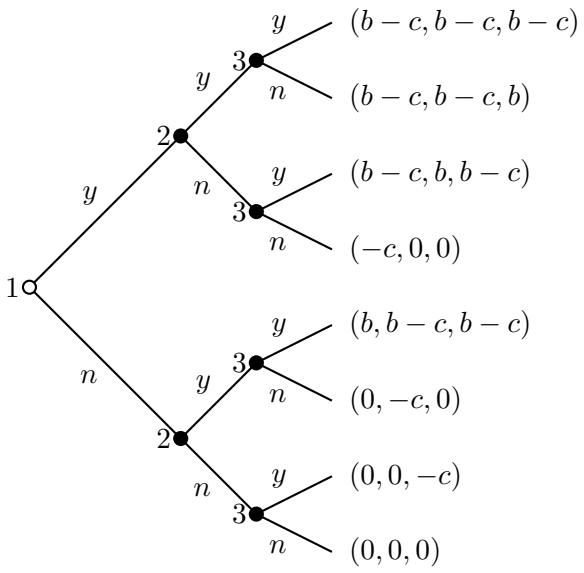

Figure 3.2: *A three-person game in extensive form.*

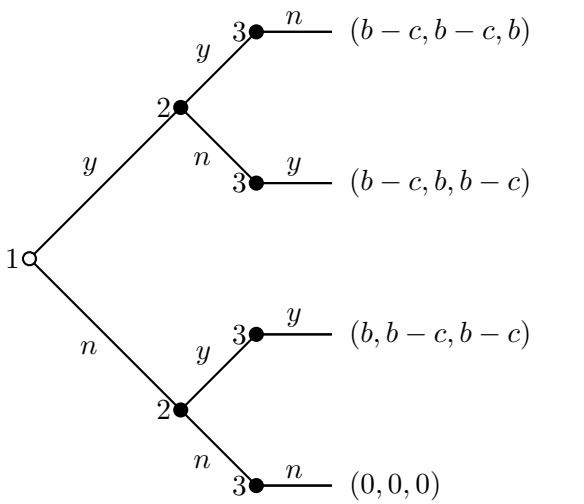

Figure 3.3: *The reduced form of the three-person game in Figure 3.2, illustrating the use of backward induction.*

then politician two will vote no and politician 3 will vote yes, resulting in a pay-off of $b - c$ to politician 1. However, if politician 1 votes no, politician 2 will vote yes and politician 3 will vote yes, giving politician 1 a pay-off of b. Thus, in the expected outcome of the game, politician 1 votes no and politicians 2 and 3 both vote yes. It is interesting to note that it is best to vote first. □

A *subgame* is a part of a game which starts at a point in the game at which the entire history of the game up to that point is common knowledge and contains all the successors of some initial node [32]. For a part of a game to be a proper subgame, all information sets must be preserved. That is, if any node in the subgame is part of an information set, then all other nodes contained in the information set must also be part of the subgame. A set of strategies is a subgame perfect Nash-equilibrium if, for every subgame, the restriction of those strategies to the subgame forms a Nash-equilibrium of the subgame.

Consider, as an example, the game in Figure 3.4, which has the two Nash-equilibria (R, R') and (L, L') [17]. The Nash-equilibrium (L, L') exists because the best response of player 1 to player 2 playing L' is to end the game by playing L. The equilibrium relies on the threat by player 2 to play strategy L' rather than strategy R' if given the opportunity. But player 2 playing rationally would not carry out this threat if given the opportunity to do so. Such a move is called a *non-credible threat*. Assuming that a rational player will never carry out a non-credible threat, it is possible to eliminate Nash-equilibria which rely on non-credible threats from the possible solutions of the game. The subgame starting at the node belonging to player 2 has strategy R' leading to the only Nash-equilibrium; for an equilibrium to be a subgame perfect it has to contain the strategy R'. Therefore (L, L') is a Nash-equilibrium which is not subgame perfect.

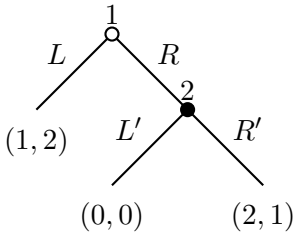

	L'	R'
L	(1,2)	(1,2)
R	(0,0)	(2,1)

Figure 3.4: *Two representations of a two-person game. The game exhibits a non-credible threat.*

3.1.5 Applications of classical game theory

Game theoretical analyses sometimes lead to surprising or counter-intuitive results. One such example is Braess' paradox [5, 6]. The paradox states that the addition of extra capacity to a network in which the entities selfishly choose their routes can in certain cases reduce the overall performance of the network. Consider, as an example, the road network represented by the digraph shown in Figure 3.5 and suppose a total of 4 000 cars wish to traverse the digraph from vertex 1 to vertex 4. Cars enter the network at vertex 1 and may then choose to head to vertex 4 via either vertices 2 or 3. The time it takes to travel from vertex 1 to vertex 2 depends on the number of drivers, x_1, choosing this route and is given by $\frac{x_1}{100}$. It takes a fixed time of 45 minutes to travel from vertex 2 to vertex 4 and similarly from vertex 1 to vertex 3. The total time needed to travel to vertex 4 along the top route is therefore $\frac{x_1}{100} + 45$ minutes. Similarly, the

bottom route takes $45 + \frac{x_2}{100}$ minutes, where x_2 is the number of drivers who choose to take the bottom route. A rational driver will choose the quickest route. At equilibrium each route has the same number of cars, namely 2 000, and the average travelling time is therefore 65 minutes. Suppose a road is built between vertices 2 and 3 with negligible travelling time. All drivers at vertex 1 will choose the top route as this has a worst-case travelling time of 40 minutes, which is better than 45 minutes for the alternate route. Upon reaching vertex 2, all drivers will choose the road from vertex 2 to vertex 3 and continue along the path from vertex 3 to vertex 4, which again has a worst-case travelling time of 40 minutes. It therefore takes drivers an average of 80 minutes to complete the route after the addition of the extra travel route. This is an example where the individual rational strategies do not result in a globally optimal outcome.

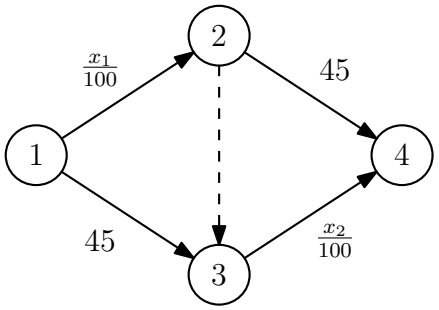

Figure 3.5: *A graph representing a simplified road network, illustrating Braess' paradox.*

Braess' paradox is not just a theoretical notion, but has been witnessed in action in real-world road networks. The closure of the congested 42nd street in New York City was expected to wreak havoc on the already congested roads of Manhattan. But, contrary to the expected results, the traffic flow actually improved when the road was closed [25].

Tactical military problems presented one of the major application areas for game theory at the beginning of the 1950s [11]. Haywood [22] demonstrated that, under certain conditions, the decision doctrine used by the United States military is equivalent to finding minimax strategies. The author used varies battles which occurred during the Second World War as case studies, drawing parallels between the decision processes followed by the generals and the methods used by game theorists. The battles were modelled as two-person zero-sum games. The emphasis of applications of game theory later shifted to deterrence and cold war strategies [11]. The largest area of application and the field of study with which game theory is most often associated is economics [11]. It was with applications in economics in mind that von Neumann and Morgenstern [34] published their book which is often credited as the single work that marks the origin of game theory as a field of study in its own right [11].

Game theory has been applied very successfully in biology. It was through inspiration from applications in biology that evolutionary game theory emerged. Evolutionary game theory is, however, no longer limited to biological applications only, but has found relevance in other fields such as economics [2]. In biology, evolutionary game theory is used, for example, to investigate the evolution of altruism and cooperation [14, 19, 28, 36, 52].

Some of the earliest appearances of notions from game theory in the field of biology, occurs in [30] and [52]. Maynard Smith and Price [30] defined the important and well-known concept of an *evolutionary stable strategy* (ESS) as "a strategy such that, if most of the members of a population adopt it, there is no 'mutant' strategy that would give a higher reproductive fitness." Maynard Smith and Price [30] used game theory to investigate conflict in animals, employing the

Hawk-Dove game[3] as analogy. It is witnessed in nature that animals often fight without harming each other, *e.g.* snakes fighting without using their fangs, buck pushing antlers against antlers, but refraining from attacking when their opponents turn away. Using game theory it is possible explain the occurrence of adaptation which may have negative impact on the individual's fitness at face value.

3.2 Evolutionary game theory

In evolutionary game theory it is assumed that players have limited knowledge of the game and only bounded rationality. Games in evolutionary game theory are repeated and players are afforded the opportunity to adapt and learn as this repetition occurs. Evolutionary game theory started out as a refinement of classical static games, but has progressed and now deals more with dynamic games of adaptation.

3.2.1 Evolution and natural selection

Evolutionary game theory has its origins in biology and is inspired by evolution, as observed in nature [19, 28]. In biology, evolution is described as the physical, genetic or behavioural change in populations of organisms from generation to generation. Natural selection is the force driving this change. A wide range of variation exists in organisms, both within and between species. This variation has the effect that some organisms are better adapted at surviving and producing offspring than others. If an individual exhibits a heritable characteristic which gives it a reproductive advantage over its peers, then it is likely that this trait will become more common in the population in future. The characteristics of an individual are encoded in its genetic makeup. *Genes* are the most basic heritable units. It is the combination of genes that gives each individual its unique phenotypical characteristics. Generally, an evolutionary process combines two basic elements: a mutation mechanism that provides variety and a selection mechanism that favours some varieties over others [57].

The *fitness* of an individual is its ability to survive and reproduce. Wright [59] was the first to introduce the concept of a fitness landscape. A measure of fitness is plotted against gene frequency. Fitness landscapes were originally considered to be fixed. However, with the aid of game theory it is possible to consider a changing fitness landscape, where the fitness of a gene depends on a variety of changing factors, such as the frequency of other genes. The book by Vincent and Brown [56] contains a detailed discussion on evolutionary game theory and its application to studying natural selection.

3.2.2 Evolving games

Vincent and Brown [55, 56] described a game in evolutionary game theory as having two parts, an inner and outer game. The *inner game* is a game similar to games in classical game theory and defines the available strategies and pay-offs players receive. The *outer game* describes the game dynamics; this is where the pay-offs are translated into changes in strategy frequencies.

As described in [56], there are a number of key features distinguishing evolutionary game theory from classical game theory. In classical game theory the focus is on the players who strive to

[3] This game will be elucidated later in the chapter.

choose strategies that optimise their pay-offs, whereas in the evolutionary game the focus is on strategies and how these strategies persist through time. Through birth and death processes the players can come and go, but their strategies pass on from generation to generation. In classical game theory, players choose their strategies from a well-defined strategy set given as part of the game definition. In evolutionary game theory, on the other hand, players generally inherit their strategies and occasionally acquire a novel strategy as a mutation. In classical game theory, each player's rationality or self-interest serves as the agent of optimisation, whereas in evolutionary game theory, the selection process serves as the agent of optimisation.

In an evolutionary game, a *population* consists of a number of players, each with a strategy chosen from a set of available strategies. During one *generation* each player in the population plays his strategy against one or more other players, receives a pay-off and updates his strategy for play during the next generation. A player's opponents are chosen according to the so-called interaction rules and the structure underlying the population. Since the focus of investigation is on the frequencies with which strategies occur, it is often convenient rather to refer to a population of strategies, implying the players. It is then also natural to refer to a strategy playing against another strategy.

3.2.3 The social structure of a game

Graphs are used to describe the social structure, or *underlying topology* of a game. Ohstuki *et al.* [39] proposed using two graphs to describe the connectivity of players. One graph determines how players interact to gain a pay-off, while the second graph describes the learning mechanism. The vertices of the graphs represent the players, and edges joining vertices represent the connections between players.

Underlying topologies commonly investigated in evolutionary game theory models include complete graphs, lattices, small-world networks and scale-free networks. *Mean-field games* have the complete graph as underlying topology, and in addition any player is equally likely to interact with every other player.

A lattice is a regular grid-like structure or "an arrangement of points or particles or objects in a regular periodic pattern in 2 or 3 dimensions" [31]. Lattice structures are often used in spatial models. The lattice structure results from using a regular tiling pattern, and considering the centre point of each tile as the representative of the tile area. Two tiling patterns often encountered in spatial modelling are square and hexagonal tilings, as shown in Figure 3.6. In game theoretical models each tile represents the position of a player (or possibly a group of players) and each player usually interacts only with players located at the neighbouring tiles.

The graph describing the topology of the game for a given tiling is constructed by placing a vertex at the centre of each tile and joining two vertices if the corresponding tiles share a common border. Constructing a graph in this fashion on a hexagonal tiling pattern results in triangular grid graph shown in Figure 3.7(a). Two different neighbourhoods are often investigated when considering players on a square lattice. In the *von Neumann neighbourhood*, each square tile neighbours each of the four nearest tiles directly north, south, east and west. A game on a square lattice with a von Neumann neighbourhood has the underlying graph shown in Figure 3.7(b) — this graph is the Cartesian product of paths. A square lattice with the *Moore neighbourhood* has each tile connected to its eight nearest neighbours, the four tiles north, east, west and south, as well as the four nearest diagonal tiles. A game played on a square lattice with a Moore neighbourhood has the underlying graph shown in Figure 3.7(c).

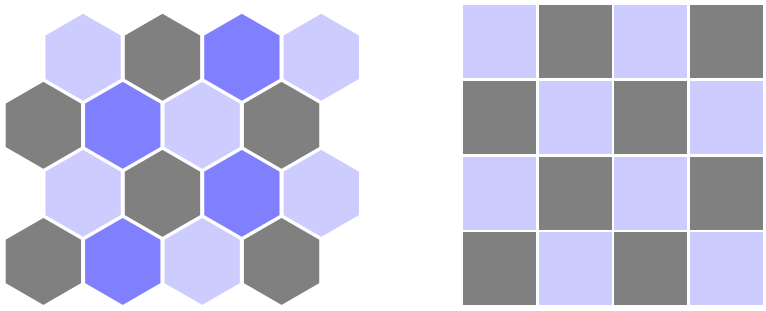

(a) (b)

Figure 3.6: *(a) Hexagonal and (b) square tiling patterns.*

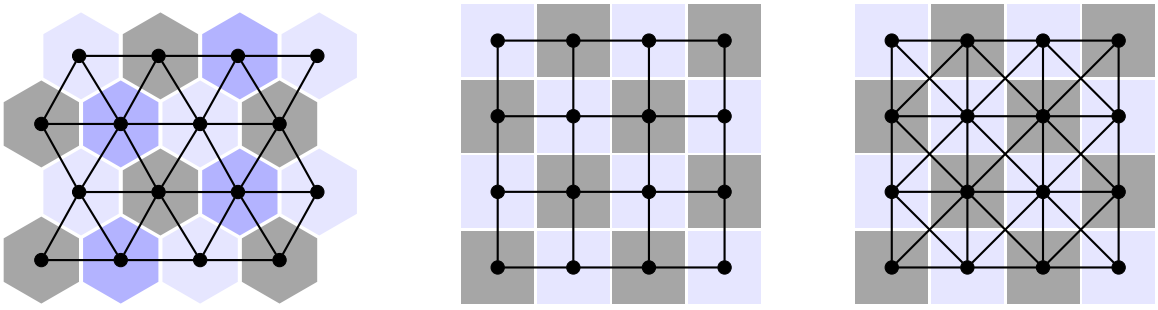

(a) (b) (c)

Figure 3.7: *Different lattice graphs, also called grid graphs. (a) A triangular grid graph may be used to model a landscape divided into hexagonal tiles. (b) A square grid graph over a square lattice with the von Neumann neighbourhood. (c) A lattice graph with the a square lattice as underlying topology, but including diagonal neighbours. This is the graph representation of a square lattice with a Moore neighbourhood.*

A *scale-free network* is a graph whose degree distribution exhibits a power law distribution $P(k) \sim k^{-\lambda}$, where $P(k)$ is the fraction of vertices in the graph which have degree k. Many real-world networks are scale-free, including the internet, citation networks and certain social networks.

The *clustering coefficient* is a measure of the degree to which vertices in a graph tend to cluster together. The *local clustering coefficient* C_v^* of a vertex v, is the number of edges incident to two vertices in the neighbourhood of v divided by the maximum number of edges that can exist between vertices in the neighbourhood of v, that is

$$C_v^* = \frac{2|\{e_{uw}\}|}{k_v(k_v - 1)},$$

where e_{uw} is an edge joining two vertices in the neighbourhood of v and k_v is the degree of vertex v. The local clustering coefficient of a vertex measures how close its neighbours are to forming a clique. Averaging over the local clustering coefficients gives rise to the *average clustering coefficient*

$$\bar{C^*} = \frac{1}{|V(G)|} \sum_{v \in V(G)} C_v^*$$

of a graph G with vertex set $V(G)$.

The characteristic path length L of graph is the average distance between vertices, averaged over all the vertex pairs in the graph. A *small-world network* is a graph which is highly clustered, yet has a small characteristic path length [10]. They are named in analogy with the so-called small-world phenomenon, popularly referred to as *six degrees of separation*. A graph is considered small-world if its average clustering coefficient is significantly larger than that of a random graph constructed on the same vertex set.

The first investigation involving an evolutionary game in a spatial context was done by Nowak and May [37], who were able to show that it is possible for cooperation to persist if players taking part in a PD occupy a two-dimensional array, interacting only with their nearest neighbours. The weak prisoner's dilemma was used and the model evolved complex Persian carpet-like patterns and also chaotic-like behaviour. The authors demonstrated their results on a lattice in which a player interacts with his eight nearest neighbours and himself, and stated that the results also hold for square lattices with four nearest neighbours or hexagonal lattices and six nearest neighbours, as well as whether or not self-interactions are included. The analysis focused on the parameter values $1.8 < b < 2$; in this region borders between clusters of cooperators are unstable, and the results exhibit chaotic spatial arrays. The asymptotic fraction of sites occupied by cooperators fluctuates around 0.318. The authors wrote a follow-up paper [38] exploring the model in more detail. These two papers initiated the exploration by various authors of numerous games in two-dimensions and many other structures connecting the players.

Games structured in this way are often referred to as *spatial games*, since it is convenient to visualise the games as being played in a spatial arena with connections between nearby players. The structure of a game may also be caused by, for example, a preference for players to interact with certain opponents via social structures or physical networks such as road networks and computer networks.

A systematic study of 2×2 games[4] on lattices was performed by Hauert [21]. Later Roca *et al.* [43] further generalised the results of Hauert [21] by including random graphs and small-world networks in their investigation. Two-dimensional regular lattices and random networks, each

[4] A game played by two players, where each player has two available strategies to choose from.

of degrees 4, 6 and 8, were considered. Roca *et al.* [43] and Hauert [21] utilised a simulation approach to investigate the two-person game with pay-off matrix

$$\begin{array}{c} \\ C \\ D \end{array} \begin{array}{c} \begin{array}{cc} C & D \end{array} \\ \begin{bmatrix} 1 & S \\ T & 0 \end{bmatrix} \end{array}$$

for values of the parameters in the ranges $-1 < S < 1$ and $0 < T < 2$. Each quadrant in the (S, T)-parameter plane represents a different known game in game theory. Roca *et al.* [43] investigated each game adopting the *replicator rule*, the *multiple replicator rule*, the *Moran rule* and the *unconditional imitation rule* as update rules.

Roca *et al.* [43] discussed their results for the PD, the stag hunt, snowdrift[5] and the harmony game. Their results related to the PD are briefly repeated here. On a complete network the cooperation is not a viable strategy. It was found that all the other networks investigated enhance the level of cooperation to a greater or lesser extent. It was also found that random graphs promoted the evolution of cooperation. Random graphs and lattices of the same degree produced very similar results. Increasing the graph order from 4 to 6 and 8 showed an increase in likelihood that cooperation will persist with lattices exhibiting higher levels of cooperation along a wide range of parameter values. These results confirmed the existence of phase transitions in the (S, T)-plane, with clear boundaries between different regions in the plane. It was further shown that the effect of spatial structure depends strongly on the update rule used. In certain contexts, structure can be inhibiting to the evolution of cooperation.

The effect of the spatial structure in promoting cooperation is directly linked to the presence of clustering in the underlying graph [43]. Small world networks have a high clustering coefficient, and therefore promote cooperation. The existence of "shortcuts" in the network allow cooperation to spread much quicker with the result that the game tends to reach equilibrium quicker than when the game is played on a regular lattice [43].

Fowler and Christakis [15] studied cooperation in human social networks, while Du *et al.* [9] considered the evolutionary PD on weighted scale-free networks. Analyses of spatial games and evolutionary games are reviewed in [42, 44, 51].

3.2.4 Solution concepts

As mentioned, the focus in evolutionary game theoretical analyses shifts from players and how they play the game, to strategies and how they persist through time. Axelrod [3] proposed a set of three criteria for a strategy to be evolutionary viable:

- **Robustness.** A strategy must be able to survive in an environment with a variety of strategies.
- **Stability.** A strategy must be able to resist invasion by another, mutant strategy.
- **Invasiveness.** A strategy must be able to invade an environment dominated by rival strategies.

An important concept in evolutionary game theory, originally developed by Maynard Smith and Price [30], is that of an ESS. An ESS is a strategy which, if adopted by a population of

[5] These games are all described in more detail later in this chapter.

players, renders them immune to invasion by a rare mutant strategy. Such an ESS is relevant when the mutation or experimentation rate is low. An ESS does not contain any reference to the game dynamics and is a static concept. It is only necessary to assume that a strategy with a higher pay-off has a higher growth rate. More specifically let, S and T be two strategies and let $E(S,T)$ be the pay-off a player playing strategy S receives after playing against a player playing strategy T. Then S is an ESS if either

$$\begin{aligned} E(S,S) &> E(T,S) \text{ or} \\ E(S,S) &= E(T,S) \text{ and } E(S,T) > E(T,T) \end{aligned}$$

is satisfied. An ESS is therefore a refinement of the notion of a Nash-equilibrium. All ESSs are Nash-equilibria, but a Nash-equilibrium is not necessarily an ESS.

3.3 The prisoner's dilemma and its variations

The PD, as described in Example 3.1, is attributed to Tucker, Dresher and Flood [11]. There exist many variations on the prisoner's dilemma, four variations are discussed in this section.

3.3.1 The hawk-dove game

Altering the constraints on the pay-off values in the PD results in variations on the PD, each with its own interpretation and applications. Changing the constraints such that the pay-off P for mutual defection is less than the sucker's pay-off S results in the *Hawk-Dove game*. This game is also sometimes referred to as the *game of chicken* [56] or the *snowdrift game* [51]. The bimatrix strategic form of the game is similar to that of the PD, given in Table 3.3, but with the distinction that the parameters are constrained by the inequality chain $T > R > S > P$.

The name *hawk-dove game* derives from the situation where there is competition for a shared resource. Players have either the option to contest or to share the resource. If both players fight for the resource, both players incur a large cost. If only one player contests the resource, referred to as *playing hawk*, and the other retreats, referred to as *playing dove*, then the hawk gets the entire resource and the dove nothing. If both players play dove, they share the resource. A hawk will always fight for sole ownership of a resource, whereas a player playing *dove* is willing to share the resource.

3.3.2 The stag hunt

The *stag hunt* is a symmetric two-person game. The game is often explained by means of the following parable [48]. Two hunters go out on a hunt and each can choose to hunt a deer (stag) or a hare. If one of the hunters decides to hunt a deer, he must have the cooperation of his partner in order to succeed. A hunter can get a hare on his own, but a hare is worth less than a deer. The game may be presented by the pay-off matrix in Table 3.3 with parameters restricted by the inequality chain $R > T > P > S$. The stag hunt has two Nash-equilibria, one is where both players cooperate and the other is where both players defect. The one equilibrium is considered payoff-dominant while the other is risk-dominant. Like the PD, the stag hunt presents a context in which to study cooperation and its problems.

3.3.3 The iterated prisoner's dilemma

Allowing for repeated rounds of the PD results in the so called *iterated prisoner's dilemma* (IPD). In the IPD a player's strategy defines what his action will be during a particular round: to defect or to cooperate. It is usually assumed that the number of rounds is unknown. In the case where the number of rounds is known, it is best to defect during the last round. But then, expecting one's opponent to defect during the last round, it is best to defect during the penultimate round. By backward induction it follows that it is best to defect during every round. Therefore, the IPD in which the number of rounds is known has both players defecting during every round as a solution. The case where the number of rounds is unknown represents a more complex situation, in which the optimal strategy is unknown.

In order to investigate which strategies are successful in the IPD, Axelrod and Hamilton [3] organised a tournament in which strategies competed in a mixed population of different strategies. Professional game theorists were invited to submit their strategies to the competition. In the tournament each strategy played against every other strategy in a round-robin fashion. The strategy scoring the highest average over all the rounds was declared the winner. It was found that a strategy called *Tit-for-Tat* does very well.

A player playing the strategy Tit-for-Tat cooperates during the very first round, while during subsequent rounds merely mirrors the opponent's move during the previous round. If the opponent therefore cooperated during the preceding round, then the Tit-for-Tat strategy cooperates during the current round, while a defection during the preceding round will be met with a defection during the current round. Consider, as an example, two players in an IPD lasting five rounds. Suppose one player adopts the Tit-for-Tat strategy and the other adopts a predetermined strategy $s = (D, C, C, D, C)$ of which the Tit-for-Tat player is not aware before the start of the game. Table 3.5 shows the resulting game. The Tit-for-Tat player plays C during the first. During the second round the Tit-for-Tat player plays the strategy played by s during the first round. Similarly, Tit-for-Tat plays the move made by s during the second, third and fourth round in the third, fourth and fifth rounds, respectively.

	Round				
Strategy	1	2	3	4	5
s	D	C	C	D	C
TFT	C	D	C	C	D

Table 3.5: *A sequence of moves in the IPD demonstrating how a player adopting the Tit-for-Tat strategy would react to another strategy, in this case called s.*

Axelrod [2] calls a strategy *collectively stable* if the condition $E(S, S) \geq E(T, S)$ is satisfied. This is a relaxation of Maynard Smith's [28] requirements for a strategy to be an ESS. The following theorem implies that in a large population of players playing only Tit-for-Tat, another strategy will not be able to invade the population.

Theorem 3.1 *Tit-for-Tat is a collectively stable strategy in the IPD provided that the probability, w, that the interaction between two players will continue to another round of the IPD satisfies*

$$w \geq \max\left(\frac{T-R}{R-S}, \frac{T-R}{T-P}\right).$$

3.3.4 The public goods game

The public goods game is played by a set of N players. Each player has the option to either cooperate, denoted by C, or defect, denoted by D. Each cooperating player contributes a benefit b to the public good, while incurring a cost c to himself. A defecting player contributes nothing with no cost to himself. The total public wealth is the distributed equally among all the players regardless of their strategy at the end of the game.

3.4 Chapter summary

Definitions and concepts in classical game theory and evolutionary game theory were reviewed in this chapter.

Notions in classical game theory were reviewed in §3.1 together with a brief historical account of important developments in the field. Two methods for representing games were considered, namely, the matrix form representation and extensive form representation. The PD was considered as an example of a very well known game in game theory. Other topics in this section included the classification of games according to their properties, solution concepts and solution methods. The section concluded with a brief description of a number of successful applications of game theory, while a description of Braess' paradox illustrated how counter-intuitive results may arise from game theory.

In §3.2 the extension of classical game theory to evolutionary game theory was described. Evolutionary game theory has its origins in classical game theory and is inspired by evolution as seen in nature. The connection between biology and evolutionary game theory was discussed. The definition and components of an evolutionary game were reviewed. Structured evolutionary games were also discussed in this section. The section concluded with a brief discussion on solution concepts in evolutionary game theory.

In the final section of the chapter, §3.3, a number of variations on the PD often encountered in the literature on evolutionary game theory were presented.

CHAPTER 4

Modelling game dynamics

Contents

Nowak and May [37, 38] were the first to introduce a spatial element to the PD by placing each player in a cell on a lattice. Each player plays a PD against the players in his neighbourhood. Nowak and May [37] considered both the von Neumann and Moore neighbourhoods. Here a similar game and game dynamics are considered with the extension that the underlying game topology may be any graph structure (*i.e.* not necessarily a grid graph). A framework for representing games on graphs is developed in this chapter.

4.1 The mathematical representation of a game

An evolutionary game may be denoted by a pair, $\Upsilon = (\Pi, G)$. In this notation $\Pi = \{T, R, S, P\}$ is the set of pay-off parameters taken from the two-player PD pay-off matrix,

$$\begin{array}{c} \\ C \\ D \end{array} \begin{array}{c} \begin{array}{cc} C & D \end{array} \\ \begin{bmatrix} R & S \\ T & P \end{bmatrix} \end{array}, \tag{4.1}$$

which is used to calculate the score of a player. The variable G is a graph representing the structure of the game and is called the *underlying graph* of the game[1]. Although the underlying graph may also be a pseudograph, it is nevertheless referred to as a "graph" for the sake of brevity and simplicity.

[1] In a more general setting two graphs, G_i and G_r, may be used to describe the structure of a game. In particular, the graph G_i may be used to calculate the score of a player and is called the *interaction graph* [39]. The graph G_r may be used to determine the update neighbourhood of a player and is called the *replacement graph* [39]. The investigation in this thesis is restricted to the case where these two graphs are equal and only one graph is therefore sufficient to describe the structure of a game.

In the remainder of this chapter the adjective *evolutionary* will be omitted when referring to evolutionary games, since all games are considered within the evolutionary paradigm.

4.2 The state of a game

The *state* of a game is a distribution of the strategies of the various players, modelled by the vertices of the underlying graph, during any particular round of the game. The state of a game may be modelled by a (vertex) 2-colouring of the underlying graph. In a 2-colouring f of a graph G one of two colours is associated with each vertex, that is a function of the form $f : V(G) \mapsto \{C, D\}$. Formally, the state $\boldsymbol{s}$ of a game is given by $\boldsymbol{s} = (G, \chi)$, where $G = (V(G), E(G))$ is the underlying graph of the game and where χ is a function according to which a colour is assigned to each vertex of G (*i.e.* χ determines f). The two strategies considered are the strategies of the single round PD, namely to cooperate (denoted by C) or to defect (denoted by D). When representing the state of a game on the underlying graph, a player playing strategy C is denoted by a solid vertex, while a player playing strategy D is denoted by an open vertex. The *weight* w of a game state is the total number of vertices associated with strategy C or equivalently the number of solid vertices in the corresponding 2-colouring of the underlying graph.

Given a number of distinct game states and an integer labelling of the underlying graph, it is possible to determine the *lexicographical order* of these states, as follows. The vertices are considered in the order in which they are labelled. A solid vertex is assumed to be lexicographically smaller than an open vertex, that is the relationship $C < D$ is assumed between the strategies C and D. The smaller of the two states is the one with the smallest strategy (*i.e.* C) corresponding to the first vertex of the underlying graph at which the states differ in strategy, in the order in which the vertices of the underlying graph are labelled. That is, if the game states are written as strings consisting of the characters C and D in the order in which the vertices of the underlying graph are labelled, then the smallest state is the one corresponding to the lexicographically smallest string. Examples of the lexicographical order of game states are shown in Figure 4.1. Note that when comparing two states, a state with a smaller weight may have a larger lexicographical ordering than a state with a large weight.

The shorthand notation $\langle C \rangle^i$ or $\langle D \rangle^i$ will be used to indicate i consecutive cooperators or defectors in a state when considering players in the order that they are labelled. Therefore $\langle C \rangle^n$ and $\langle D \rangle^n$ denote the all-cooperator and all-defector states, respectively, for a game played on a graph of order n.

The underlying graph of a game is henceforth considered to be a labelled graph (or a labelled pseudo-graph). Due to symmetry in the update rules of the game and symmetries which may exist in the underlying graph, certain states may be considered equivalent. An *automorphism* ϕ between two states $\boldsymbol{s}_1 = (G, \chi_1)$ and $\boldsymbol{s}_2 = (G, \chi_2)$ is a one-to-one mapping of the set of vertex labels in $V(G)$ onto itself such that adjacencies in and the colouring of the underlying graph are preserved, that is $uv \in E(G)$ if and only if $\phi(u)\phi(v) \in E(G)$ and $\chi_1(v) = \chi_2(\phi(v))$ for all $v \in V(G)$. Two states $\boldsymbol{s}_1$ and $\boldsymbol{s}_2$ are said to be *automorphic* if there exists an automorphism between them. Examples of automorphic states are shown in Figure 4.2. The pair of game states $\boldsymbol{s}_1$ and $\boldsymbol{s}_2$ in Figure 4.2(a) are automorphic. An automorphism between these states is the permutation $\phi_1 : \{1, 2, 3, 4, 5\} \mapsto \{1, 2, 3, 4, 5\}$ such that $\phi_1(1) = 3$, $\phi_1(2) = 4$, $\phi_1(3) = 1$, $\phi_1(4) = 2$ and $\phi_1(5) = 5$.

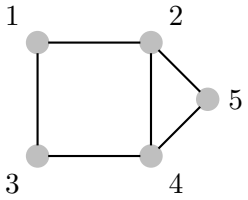

(a) $G_{4.1}$

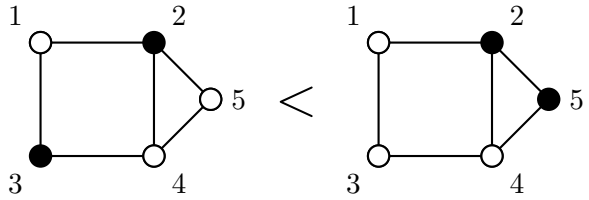

(b) Game states of the same weight.

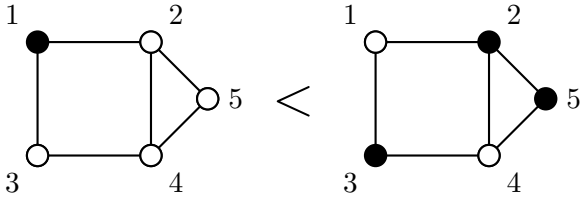

(c) Game states with different weights.

Figure 4.1: *(a) A vertex labelling of the underlying graph of the game $\Upsilon = (\Pi, G_{4.1})$ in which players may play any one of two strategies, denoted by • or ∘. Examples of the lexicographical order of two distinct game states with (b) the same weight and (c) different weights.*

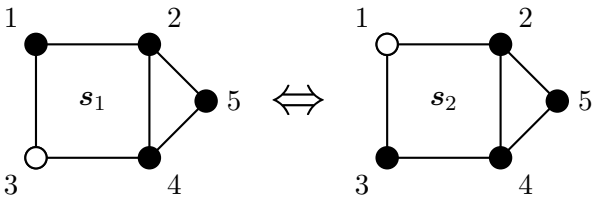

(a) Two automorphic states, $\boldsymbol{s}_1$ and $\boldsymbol{s}_2$, of weight 4.

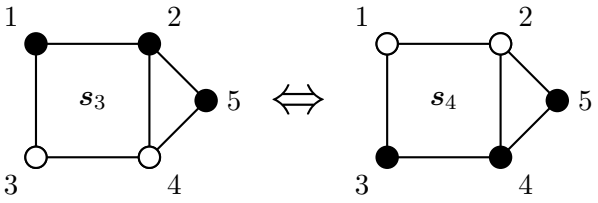

(b) Two automorphic game states, $\boldsymbol{s}_3$ and $\boldsymbol{s}_4$, of weight 3.

Figure 4.2: *Examples of automorphic game states for the underlying graph in Figure 4.1(a) and for a game in which players may play any one of two strategies, denoted by • or ∘.*

An *automorphism class* of game states is a maximal set of automorphic game states. The *class representative* of an automorphism class of game states is the state which has the smallest lexicographical order in the class. The two states shown in Figure 4.2(a) form an automorphism class and in this class the state on the left is the class representative. Table 4.1 contains all the possible states for a game which has the underlying graph $G_{4.1}$ in Figure 4.1(a), and in which players may play one of the two strategies, • or ∘. The game may be in any one of 32 distinct states. Of these states only twenty are considered non-equivalent, that is the game has twenty state automorphism classes.

An automorphism between states has been defined in such a way that if two states are automorphic, then the states obtained after one round of two instances of the game, starting from these states respectively, are again automorphic. Therefore, a description of the remaining states of a game from one state in an automorphism class, would also describe the remaining states of the game from all other states in the class.

4.3 Dynamic rules of a game

A game instance is initialised by assigning each player a strategy. Each *round* of the game consists of two phases. During the first phase each player's score is determined and during the second phase each player updates his strategy. The rounds are repeated until the system reaches a steady state, limit cycle or a pre-determined number of rounds have been played.

To determine the score of a player during a particular round, the player plays a PD against each of his neighbours. A player's score is taken to be the average pay-off value from all of these PDs. Using the average pay-off value makes it possible to compare the successes of the strategies of players with different numbers of neighbours in the underlying graph. Consider, for example, a player p who has x neighbours playing strategy C and y neighbours playing strategy D. In this case the score of player p is

$$\pi_p = \begin{cases} \frac{1}{x+y}(xT + yP) & \text{if } p \text{ is playing } D, \\ \frac{1}{x+y}(xR + yS) & \text{if } p \text{ is playing } C. \end{cases}$$

As an example of how to calculate a player's score, consider the game states shown in Figures 4.3(a) and 4.3(b), assuming the pay-off matrix

$$\begin{array}{c} \\ C \\ D \end{array} \begin{array}{c} \begin{array}{cc} C & D \end{array} \\ \begin{bmatrix} 3 & 0 \\ 5 & 1 \end{bmatrix} \end{array}.$$

The central player in Figure 4.3(a) plays strategy C, and has two neighbours playing strategy C and four neighbours playing strategy D. He therefore achieves a score of $(2 \times 3 + 4 \times 0)/6 = 1$. The central player in Figure 4.3(b) similarly achieves a score of $\frac{15}{3}$.

A player updates his strategy by adopting the strategy of the player with the largest score in his closed neighbourhood. If the player's own score is the largest in his neighbourhood, then he will continue with his current strategy during the next round. In the event of a tie between the highest scores achieved by a cooperator and a defector in the player's neighbourhood, it is assumed that he continues with his current strategy during the next round. This assumption may be interpreted as the imposition of a small cost associated with the act of a player changing his strategy. As an example of how the update rule is applied, consider the game state extract

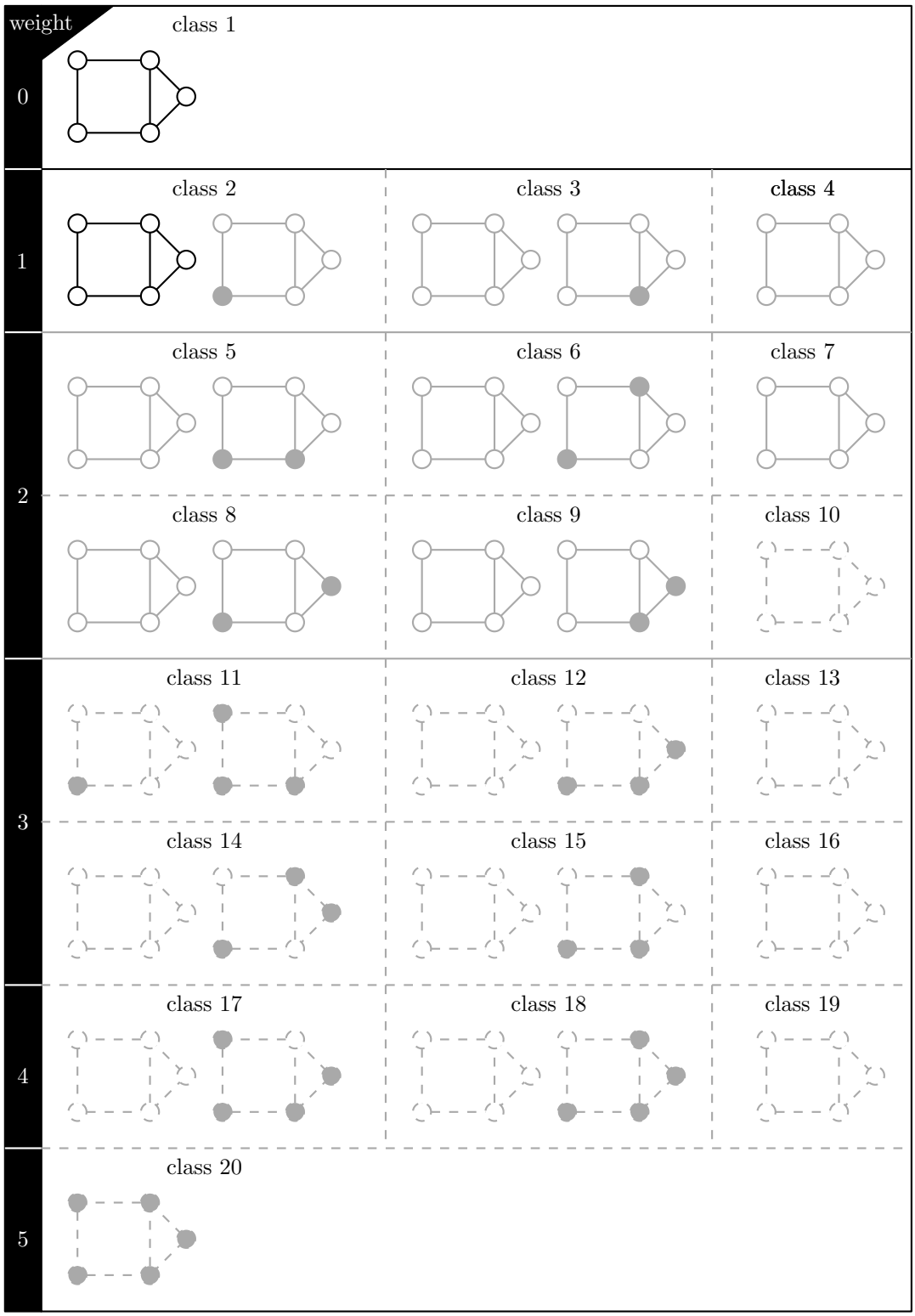

Table 4.1: *The twenty state automorphism classes of game states for the underlying graph $G_{4.1}$ in Figure 4.1(a) allowing for two strategies, denoted by • and ∘. In this example the automorphism classes have either size 1 or size 2. In the case where an automorphism class contains two states, the class leader is shown in black and the state automorphic to it is shown in grey.*

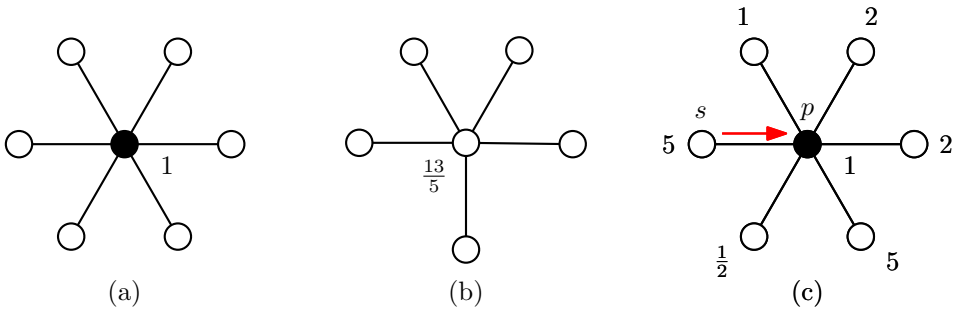

Figure 4.3: *Extracts from three game states used as examples to demonstrate how a player's score is calculated and how a player chooses a new strategy to play during the next round of the game.*

shown in Figure 4.3(c) with the scores of each player as indicated. Player p receives a score of 1. The player with the highest score in his neighbourhood is player s who is playing strategy D and receives a score of 5. Player p therefore adopts strategy D for play during the next round.

During the update process the score attained by a player depends only on the number of cooperators and defectors in his neighbourhood and on his own strategy. The positions of these neighbours playing the various strategies are not important.

As an example of the update process, consider the game $\Upsilon_1 = (\{5, 3, 1, 0\}, G_{4.1})$. The development of a game instance from a given initial state is shown in Figure 4.4. In the initial state only one player plays strategy D. This player also receives the highest score during that round; all his neighbours therefore adopt strategy D during the second round. During the second round only one player plays strategy C, which earns the lowest score during that round. The player in question therefore adopts strategy D for play during the next round. During the third round all players therefore play strategy D; there is no other strategy to consider and all players keep on playing D indefinitely after the second round.

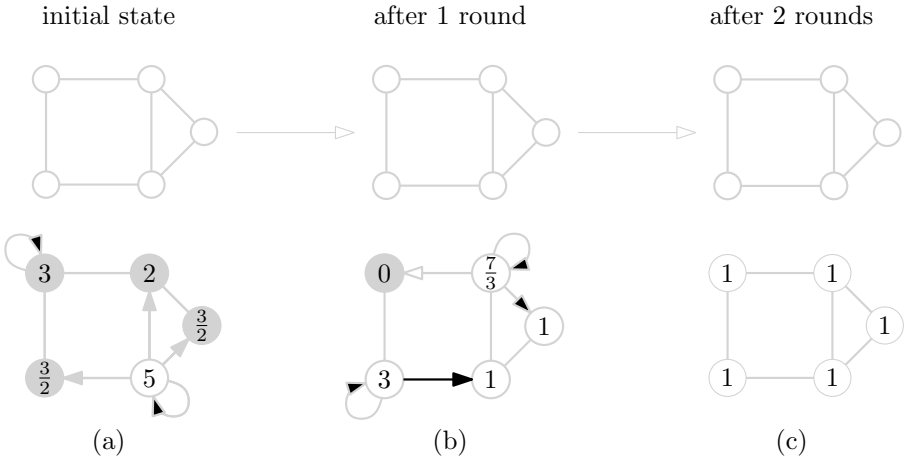

Figure 4.4: *The state transitions of an instance of the game $\Upsilon_1 = (\{5, 3, 1, 0\}, G_{4.1})$. The first row shows the transitions of the states. The second row shows the score of each player, with arrows indicating which strategy a player adopts. Here (a), (b) and (c) each represent a round of the game.*

4.4 The state graph of a game

The *state graph* G of a game is a vertex weighted pseudodigraph in which each vertex corresponds to a game state automorphism class. The state graph is a representation of the dynamics of

the game and shows the transition between states as defined by the game dynamics. Given a game Υ with associated state graph $\mathcal{G}$, a vertex u of $\mathcal{G}$ is adjacent to vertex v if and only if the state corresponding to vertex u in Υ transitions in one round to the state associated with v. The weight of a vertex in a state graph is equal to the weight of the state associated with that vertex. An example of a state graph for the game $\Upsilon_1 = (\{5, 3, 1, 0\}, G_{4.1})$ is shown in Figure 4.5. The part of the graph in Figure 4.5 enclosed by the dashed curve contains the transitions shown in Figure 4.4.

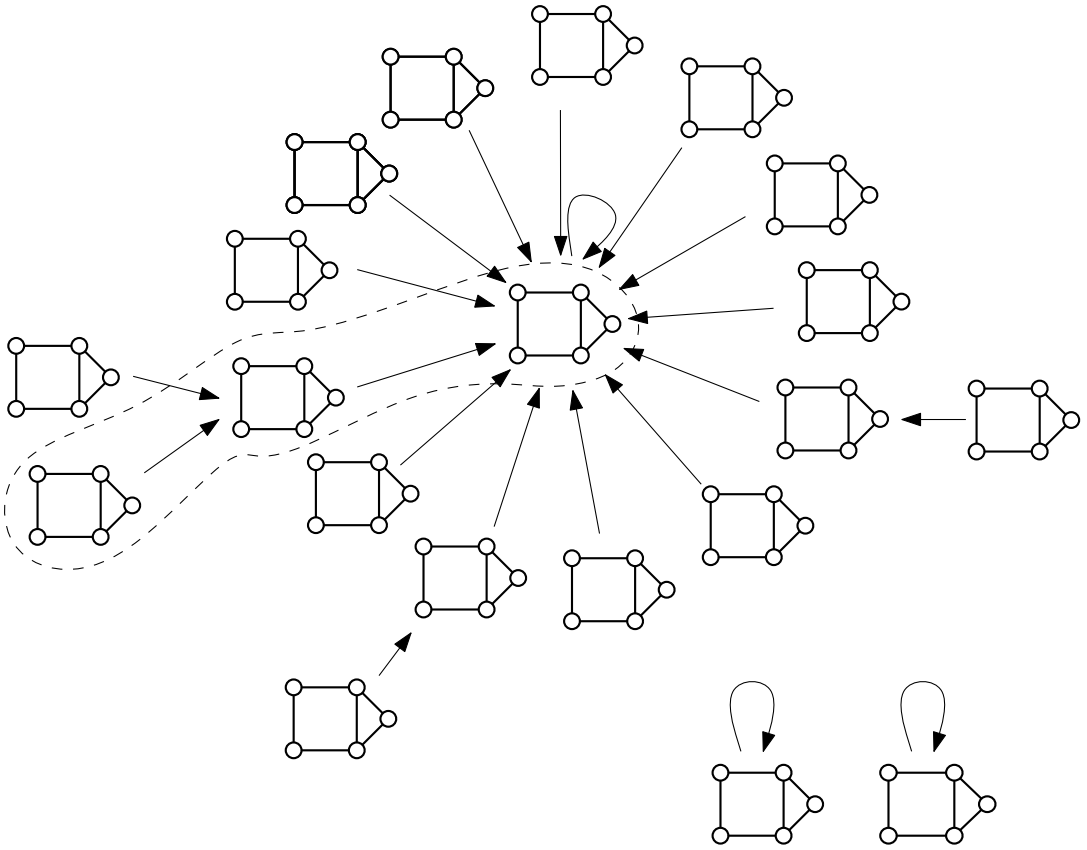

Figure 4.5: *The state graph for a game with the graph in Figure 4.1(a) as underlying graph, in which players may play any of the two strategies, • or ∘. The part of the graph highlighted by means of a closed dashed curve denotes the transition considered in Figure 4.4. The state graph comprises three components.*

A *steady state* is a state which is adjacent to itself in the state graph. It holds in general games that those game states in which all players either play strategy C or all players play strategy D are steady states. If a game has a pay-off parameter T which is sufficiently large, then the two previously mentioned states are the only steady states of the game, as is shown next.

Theorem 4.1 *Let G be any connected graph of order n with maximum degree Δ and suppose $R \leq 1$. If $T > \Delta(1-P)+P$, then the state graph of a game with underlying graph G has exactly two components. Moreover, one of these components comprises the all-cooperator steady state $\langle C\rangle^n$ only, while the other component contains all other game states, including the all-defector steady state $\langle D\rangle^n$ which attracts all states except $\langle C\rangle^n$.*

Proof: Let d_t denote the number of defectors during round $t \in \mathbb{N}_0$ of the game. It is shown that if $T > \Delta(1-P) + P$ and $d_0 > 0$, then there exists a non-negative integer t^* such that $d_{t+1} > d_t$ for all $t = 1, \ldots, t^* - 1$ and $d_t = n$ for all $t \geq t^*$.

To achieve this, it is first shown that no defector will change his strategy during subsequent rounds of the game. Let u be a defector during round t. If all players in the open neighbourhood of u also defect during round t, then u will certainly defect during round $t+1$. Therefore suppose there are $c > 0$ cooperators in the open neighbourhood of u during round t. In order to determine his strategy during round $t+1$, player u compares his pay-off value

$$\begin{aligned}\pi_u &= \frac{(\deg(u) - c)P + cT}{\deg(u)} \\ &\geq \frac{(\deg(u) - 1)P + T}{\deg(u)} \\ &> \frac{(\deg(u) - 1)P + \Delta(1 - P) + P}{\deg(u)} \\ &\geq \frac{(\deg(u) - 1)P + \deg(u)(1 - P) + P}{\deg(u)} \\ &= 1 \end{aligned} \tag{4.2}$$

to those of his cooperating neighbours during round t. But since a cooperator's pay-off value cannot exceed 1, player u will again defect during round $t+1$. This shows that

$$d_{t+1} \geq d_t \quad \text{for all} \quad t \in \mathbb{N}_0. \tag{4.3}$$

Furthermore, it follows by (4.2) that a cooperator will necessary change his strategy during the next round if there is at least one defector in his open neighbourhood. Because G is connected, it therefore follows that, in fact, $d_{t+1} > d_t$ for all t not exceeding some finite value $t^* - 1$, and that $d_{t^*} = n$, completing the proof in view of (4.3). □

4.5 Normalising the pay-off values of a game

By normalising the parameter values of a game it is possible to model the game dynamics described in the previous sections of this chapter using only two parameters instead of four, as in (4.1). This claim is demonstrated here for two games played on the same underlying graph G, but with different sets of pay-off parameters. Denote the two games in question by $\hat{\Upsilon} = (\hat{\Pi} = \{\hat{T}, \hat{R}, \hat{P}, \hat{S}\}, G)$ and $\Upsilon = (\Pi = \{T, 1, P, 0\}, G)$, respectively. Recall that the process of updating a player's strategy occurs by selecting the highest scoring strategy from his closed neighbourhood, essentially comparing the scores of the highest scoring cooperator with that of the highest scoring defector in his neighbourhood.

Consider a player p participating in the game $\hat{\Upsilon}$. Suppose p has player c and player d in his neighbourhood and assume that player c is the highest scoring cooperator in the neighbourhood of player p, with a pay-off value of $\hat{\pi}_c$, and similarly that player d is the highest scoring defector in the neighbourhood of player p, with a pay-off value of $\hat{\pi}_d$. The outcome of the strategy updating process for player p is determined by the function

$$f(\hat{\Pi}, \chi) = \begin{cases} C & \text{if } \hat{\pi}_c > \hat{\pi}_d \\ D & \text{if } \hat{\pi}_d > \hat{\pi}_c \\ \chi(p) & \text{if } \hat{\pi}_d = \hat{\pi}_c, \end{cases}$$

where χ is the current state of the game. Given an initial state χ_0, the game dynamics is a function of $\hat{T}$, $\hat{R}$, $\hat{S}$ and $\hat{P}$. Let x be the proportion of players in the open neighbourhood

of player c who are playing strategy C and let y be the proportion of players in the open neighbourhood of player d who are playing strategy C. Assuming that $\hat{\pi}_c > \hat{\pi}_d$, it follows that

$$x\hat{R} + (1-x)\hat{S} \ > \ y\hat{T} + (1-y)\hat{P}.$$

Subtracting $\hat{S}$ from both sides of the above inequality results in the inequality

$$x\hat{R} + \hat{S} - x\hat{S} - \hat{S} \ > \ y\hat{T} + \hat{P} - y\hat{P} - \hat{S}.$$

Rewriting this inequality yields

$$x(\hat{R} - \hat{S}) + 0 \ > \ y(\hat{T} - \hat{S}) + (1-y)(\hat{P} - \hat{S}). \tag{4.4}$$

After dividing both sides of (4.4) by the positive quantity $\hat{R} - S$, it holds that

$$x + 0 \ > \ y\frac{\hat{T} - \hat{S}}{\hat{R} - \hat{S}} + (1-y)\frac{\hat{P} - \hat{S}}{\hat{R} - \hat{S}}.$$

Finally, letting

$$T = \frac{\hat{T} - \hat{S}}{\hat{R} - \hat{S}} \text{ and } P = \frac{\hat{P} - \hat{S}}{\hat{R} - \hat{S}}, \tag{4.5}$$

it follows that

$$x + 0 > yT + (1-y)P.$$

Therefore the requirement $\hat{\pi}_c > \hat{\pi}_d$ implies the relationship $\pi_c > \pi_d$, where π_c and π_d are the pay-off values of player c and player d, respectively, if the pay-off parameters Π are used to calculate the scores of the players. It similarly follows that the requirement $\hat{\pi}_c < \hat{\pi}_d$ implies the relationship $\pi_c < \pi_d$ and that the requirement $\hat{\pi}_c = \hat{\pi}_d$ implies the relationship $\pi_c = \pi_d$. Therefore the outcome of the games Υ and $\hat{\Upsilon}$ are identical if (4.5) holds.

Thus, given a parameter set $\hat{\Pi} = \{\hat{T}, \hat{R}, \hat{P}, \hat{S}\}$, it is possible to rescale the parameters as in (4.5) to form a new set of parameters $\Pi = \{T, 1, P, 0\}$ without influencing the game dynamics. The analysis in this thesis is therefore restricted, without loss of generality, to the case with only two free parameters, that is, to the case where the parameter set is $\Pi = \{T, 1, P, 0\}$ and where it is assumed throughout that $T > 1$ and $0 < P < 1$.

Note, therefore, that the restriction that $R \leq 1$ in Theorem 4.1 is superfluous.

4.6 Chapter summary

This chapter contains a mathematical framework for describing spatially structured evolutionary games. A game may be presented as an ordered pair consisting of the set of pay-off parameters and an underlying graph which describes the spatial structure of the game.

Two important concepts were introduced, namely an automorphism class of game states and the state graph of a game. If the number of state automorphism classes is small, then the state graph is a useful tool for visually representing the game dynamics. It was also demonstrated in this chapter that the use of the reduced set of pay-off parameters $\Pi = \{T, 1, S, 0\}$ is sufficient to describe game dynamics in general.

CHAPTER 5

Analysing game dynamics by analytical means

Contents

In this chapter an analytical approach (*i.e.* avoiding the use of simulation) is adopted to investigate the dynamics of the *evolutionary spatial prisoner's dilemma* (ESPD) played on a path or cycle as underlying graph. The objective is to determine the likelihood of the emergence of persistent cooperation. A key question is: How does the order of the underlying graph influence the likelihood of persistent cooperation? Since the game state graph captures the complete dynamics of a game, it is of interest to determine properties of the state graph without having to simulate the entire game. A number of theorems are established in this regard, describing the properties of the state graph of the ESPD with a path or cycle as underlying graph. The ESPD on a path or a cycle admits two fundamentally different parameter regions which will be referred to as *small values of* T and *large values of* T, respectively. Large values of T are not capable of inducing persistent cooperation, while small values of T allow for the possibility of persistence of cooperation.

5.1 States of the ESPD on a path or cycle

In this section it is assumed that the underlying graph G is a path of order n whose vertices are labelled $0, 1, 2, \ldots, n-1$, or an n-cycle whose vertices are labelled $0, 1, 2, \ldots, n-1, 0$.

There are 2^n different ways of assigning one of the two strategies, C or D, to each of the n vertices in such a labelled underlying graph. There is only one possible automorphism when

the underlying graph is a path, namely the function that reverses the order of the vertices. Therefore all states which are not symmetric with respect to a mid section of the path belongs to an automorphism class of size two; the two members of each of these automorphism classes are the two states that are mirror images of one another. The game states for the case where the underlying graph is a path of order 5 are shown in Table 5.1; there are 32 states of which 20 are considered non-equivalent.

Class leader	Automorphic to	Class size
		1
		2
		2
		2
		1
		2
		2
		2
		2
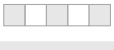		1
		2
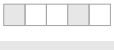		2
		1
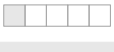	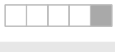	2
		1
		2
		1
		1
Total: 20		Total: $32 = 2^5$

Table 5.1: *The thirteen automorphism class leaders of game states (as well as their corresponding full automorphism classes) for the case where the underlying graph is a path of order* 5*. The two strategies C and D are represented by colouring the squares in a linear array black and white, respectively.*

Counting the number of states for the EPSD with a path as underlying graph is similar to other counting problems in the literature for which solutions are known. Related problems are described as the number of ways of creating an n-bead black-and-white reversible string [23] and the number of caterpillar graphs which can be constructed on n vertices [20]. It is known that if the underlying graph of the ESPD is a path of order n, then there are

$$\Lambda_p(n) = 2^{n-1} + 2^{\lceil n/2 \rceil - 1} \tag{5.1}$$

automorphism classes of game states [4]. The sequence $\{\Lambda_p(n)\}_{n=1}^{\infty}$ is listed as Sloane's sequence A005418 [49] and is tabulated for $1 \leq n \leq 15$ in Table 5.2.

$n \rightarrow$	1	2	3	4	5	6	7	8	9	10	11	12	13	14	15
$\Lambda_p(n)$	2	3	6	10	20	36	72	136	272	528	1056	2 080	4 160	8 256	16 512
$\Lambda_c(n)$	2	3	4	6	8	13	18	30	46	78	126	224	380	687	1 224

Table 5.2: *The order of the state graph if the underlying graph is a path or a cycle of order n, for small values of n. (Sloane's sequences A005418 and A000029, respectively [49].)*

However, there are a number of additional symmetries in the case where the underlying graph of the ESPD is a cycle: The order of the vertices may be reversed or the positions of vertices may be shifted clockwise up to $n-1$ positions. The result is an increase in the average size of an automorphism class of the ESPD on a cycle when compared to that on a path of a specific order. The thirteen class leaders of the automorphism classes of game states (as well as the full automorphism classes themselves) for the case where the underlying graph is a 6-cycle are shown in Table 5.3.

Class leader	Automorphic to	Class size
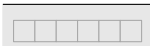		1
		6
	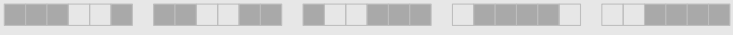	6
		6
		6
		3
		12
		6
	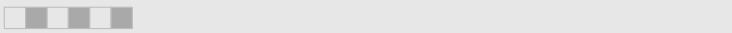	2
		6
	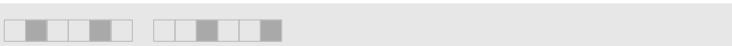	3
		6
		1
Total: 13		Total: $64 = 2^6$

Table 5.3: *The thirteen automorphism class leaders of game states (as well as their corresponding full automorphism classes) for the case where the underlying graph is a 6-cycle. The two strategies C and D are represented by colouring the squares black and white, respectively, where each game state is represented by a wrapping array of squares denoting the players.*

If the underlying graph is a cycle of order n, then there are

$$\Lambda_c(n) = \begin{cases} \sum_{d|n} \frac{\phi(d)2^{n/d}}{2n} + 2^{\frac{n-1}{2}} & \text{if } n \text{ is odd} \\ \sum_{d|n} \frac{\phi(d)2^{n/d}}{2n} + 2^{\frac{n}{2}-1} + 2^{\frac{n}{2}-2} & \text{if } n \text{ is even} \end{cases} \tag{5.2}$$

automorphism classes of game states [13], where $\phi(\cdot)$ is the well-known Euler totient. The sequence is listed as Sloane's sequence A000029 [49] and the n-th entry of this sequence is

described as the number of necklaces which can be created from a total of n black or white beads allowing for turning over the necklaces. The numbers of automorphism classes for the ESPD on an n-cycle are also shown in Table 5.2 for $1 \leq n \leq 15$.

5.2 ESPD game dynamics for large values of T

The ESPD on a path or cycle admits two fundamentally different parameter regions, namely $T > 2 - P$ or $1 < T \leq 2 - P$[1]. These two parameter regions induce different game dynamics. It was established in Theorem 4.1 that in the case of large values of the temptation-to-defect parameter, T, the strategy of defection is inherently more stable than that of cooperation on a general underlying graph. Applying Theorem 4.1 to cycles and paths, it holds that if $T > 2-P$, then the state graph has only two components. The all-cooperator state is isolated, while the other component contains the all-defector state and all other game states. Moreover, in the latter component the all-defector state attracts all other game states. As examples, the state graphs for the ESPD on a path of order 5 and for the ESPD on a 6-cycle are shown in Figure 5.1, both for the case where $T > 2 - P$. Therefore persistent cooperation is not possible for the ESPD on a path or cycle if $T > 2 - P$, unless the strategy of cooperation is universally adopted by all players initially.

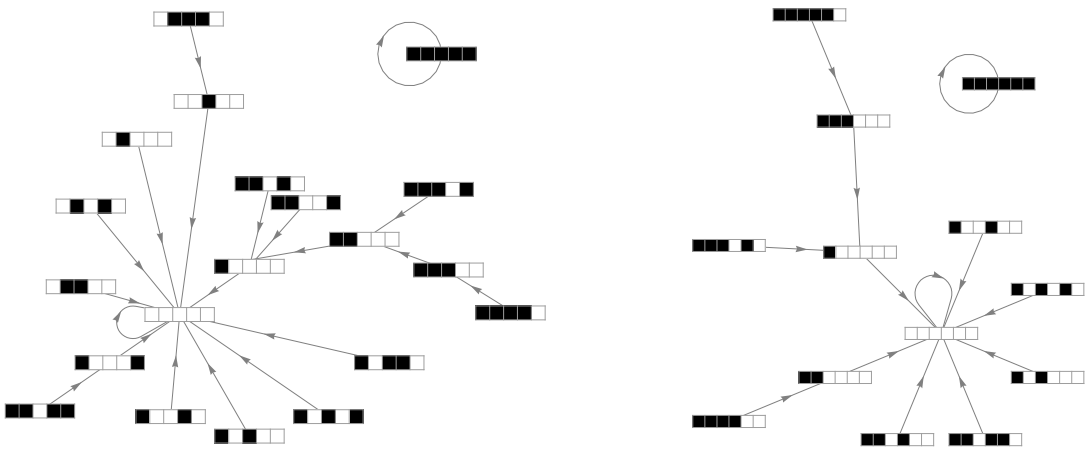

(a) (b)

Figure 5.1: *The state graph for the case where $T > 2 - P$ and the underlying graph is (a) a path of order 5 or (b) a 6-cycle. The strategy of cooperation (C) is denoted by a black square, while that of defection (D) is denoted by a white square in each state which is represented in (a) by a linear array of squares, and in (b) by a wrapping array of squares.*

The following lemma states that defection is, in fact, inherently more stable than cooperation for all values of T in the case where the underlying graph is a path or a cycle.

Lemma 5.1 *If the underlying graph of the ESPD is a path or a cycle and a player's strategy is that of defection during a specific round of the game, then his strategy remains the same for all subsequent rounds.*

[1] A player playing D can achieve one of five different scores, namely $2T$, $T + P$, $2P$, T and P, while a player playing C can achieve one of three different scores, namely 2, 1 or 0. Changing the values of T and P may have an influence on the dynamics of the game at the thresholds $T + P = 2$ and $2P = 1$. The second threshold, $2P = 1$, does not influence the game dynamics; a player with a cooperator that has a score of 1 and a defector that has a score of $2P$ in his neighbourhood is necessarily playing the underlined strategy in the configuration $DD\underline{D}CC$. The underlined player obtains a score of $T + P > 1$ and hence picks his own strategy during the next round.

Proof: If a defector is flanked by two defectors during any round of the game, he will certainly defect again during the next round, because there are only defectors in his neighbourhood. Assume, therefore, that a defector is flanked by at least one cooperator during some round of the game. Since the pay-off value received by that cooperator is at most $\frac{1}{2}$ and the pay-off value received by the defector is at least $\frac{T+P}{2} > \frac{1}{2}$, it follows that the defector will in this case also defect during the next round of the game. □

Note that there is no result similar to that of Lemma 5.1 for the strategy of cooperation. The lemma may be used to establish the structure of the state graph of the ESPD for the case where the underlying graph is a path or a cycle.

Theorem 5.1 *If the underlying graph of the ESPD is a path or cycle of order n, then each component of the state graph is a rooted pseudo-tree in which the root is a steady state of the game. Moreover, the all-cooperator steady state* $\langle C \rangle^n$ *forms a component on its own in the state graph.*

Proof: It follows by the deterministic nature of the ESPD that every vertex in the state graph has out-degree 1 (given any game state during a round of the game, there is a unique game state during the following round). It also follows by the finiteness of the state space (as a result of the finiteness of the number of players) that every component of the state graph must contain at least one steady state (a vertex with a loop from itself to itself) or a limit cycle (a directed cycle of length at least 2). But since defectors persist with their strategies as the state of the game progresses in the case where the underlying graph is a path or a cycle, by Lemma 5.1, it follows that the state graph cannot have any cycles of length at least 2. Therefore each of the state graph components is a rooted pseudo-tree containing a single steady state which attracts all states in that component. The steady state $\langle C \rangle^n$ is clearly an isolated vertex in the state graph. □

For large values of the temptation-to-defect parameter, T, the asymptotic behaviour of states in the game follows as a direct consequence of Theorems 4.1 and 5.1, as made more precise in the following result.

Corollary 5.1 *If the underlying graph of the ESPD is a path or cycle of order n, and if* $T > 2-P$*, then the state graph is a rooted pseudo-tree comprising exactly two components. Moreover, one of these components consists of the steady state* $\langle C \rangle^n$ *only. In the other component* $\langle D \rangle^n$ *is the steady state attracting all the remaining states of the game.*

The result of Corollary 5.1 may be verified in Figure 5.2 for the case where the underlying graph is a path of order $3 \leq n \leq 6$ and in Figure 5.3 for the case where the underlying graph is cycle of order $5 \leq n \leq 8$, where $T > 2 - P$ in each case.

5.3 The ESPD on a path for small values of T

In this section the focus shifts to the dynamics of the ESPD on a path of order n for small values of T. In particular, the steady states of the ESPD on paths are characterised. This is followed by a full description of the game dynamics for the case where $T \leq 2-P$. Finally the probability of randomly generating an initial state which leads to persistent cooperation is determined.

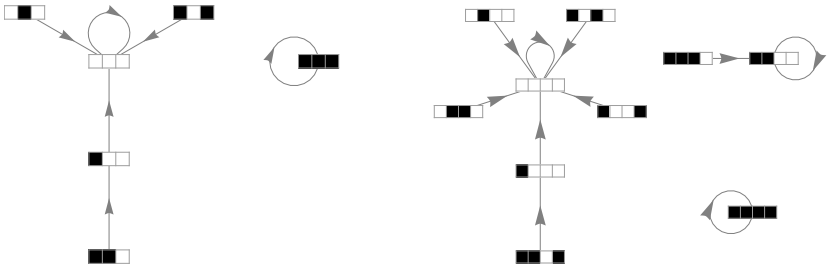

(a) $n = 3$ (b) $n = 4$

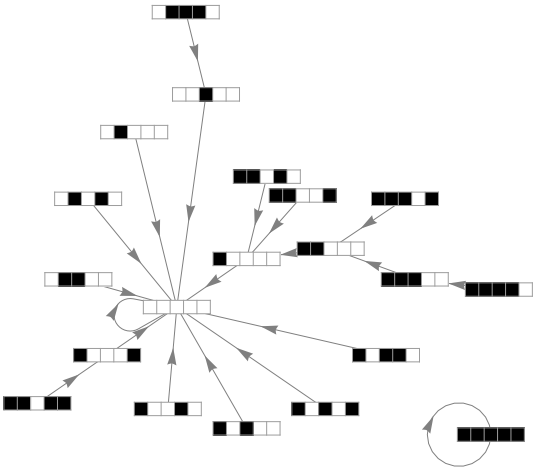

(c) $n = 5$

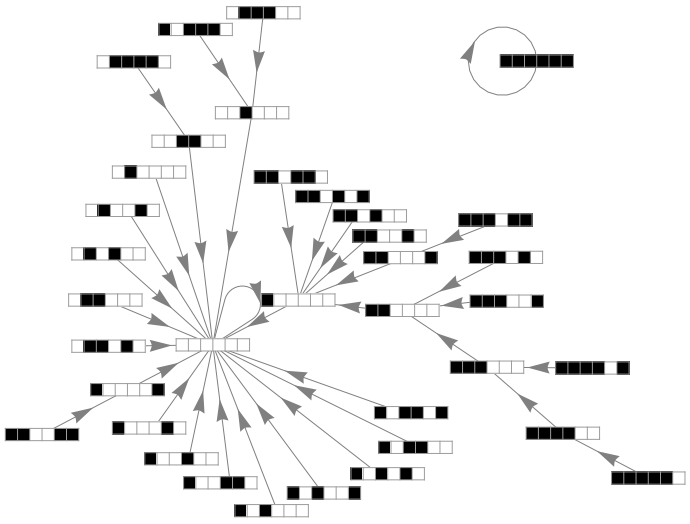

(d) $n = 6$

Figure 5.2: *The state graph of the ESPD for the case where $T > 2 - P$ and the underlying graph is a path of order n. The strategy of cooperation (C) is denoted by a black square, while that of defection (D) is denoted by a white square in each state, which is represented by a linear array of squares.*

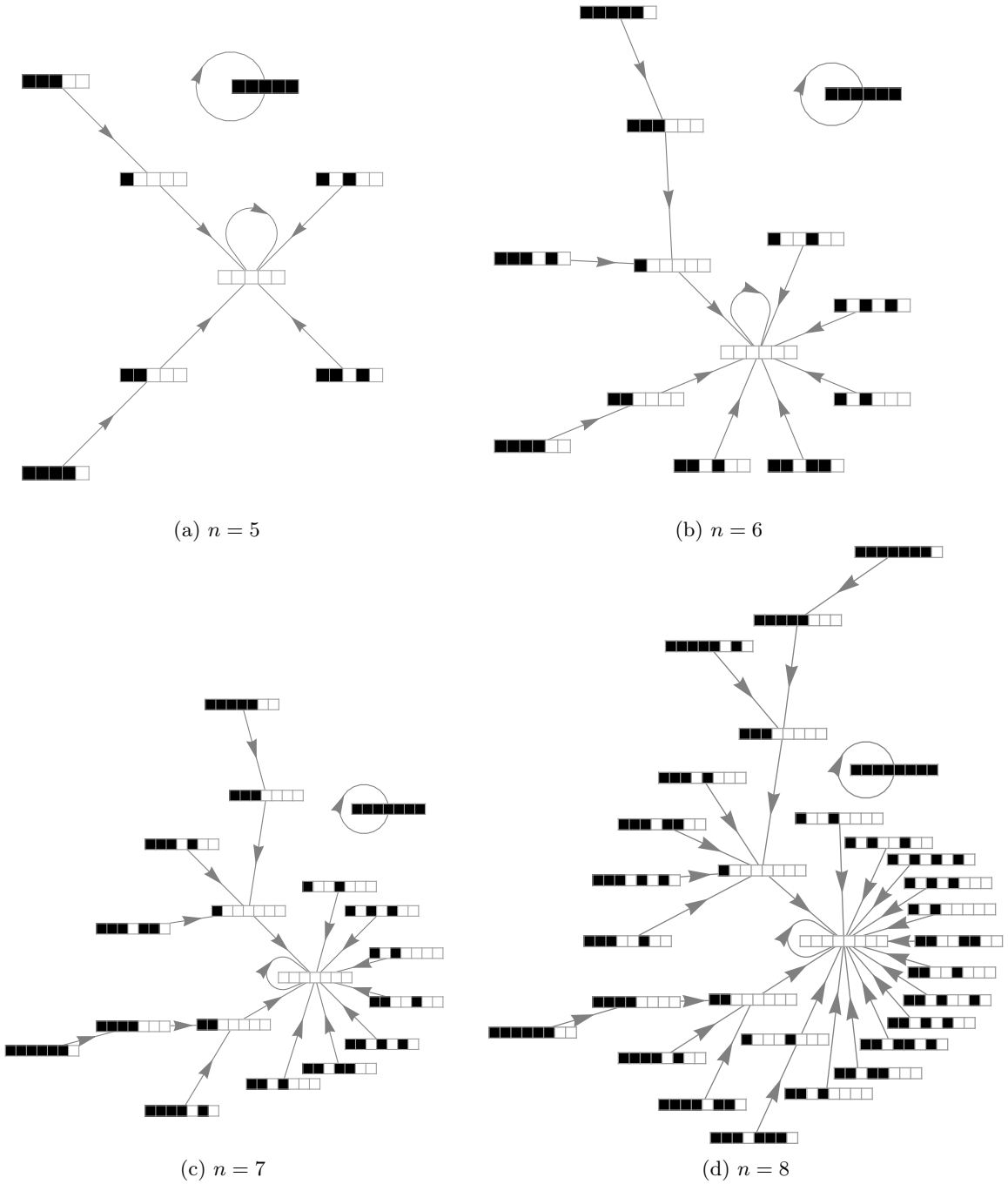

(a) $n = 5$ (b) $n = 6$

(c) $n = 7$ (d) $n = 8$

Figure 5.3: *The state graph of the ESPD for the case where $T > 2 - P$ and the underlying graph is an n-cycle. The strategy of cooperation (C) is denoted by a black square, while that of defection (D) is denoted by a white square in each state, which is represented by a wrapping array of squares.*

5.3.1 Characterisation of steady states for small values of T

The two trivial steady states of the ESPD, $\langle C\rangle^n$ and $\langle D\rangle^n$, are always present in the state graph regardless of the parameter value and/or the underlying graph. According to Corollary 5.1 no form of cooperation can persist in the long run for large values of T, except in the singular case where all players initially already cooperate. For large values of T the two trivial steady states are the only steady states. In this section the focus shifts to a characterisation of the steady states of the ESPD on a path in the more interesting case where

$$1 < T \leq 2 - P. \tag{5.3}$$

It is first shown that cooperation runs of length 1 or 2 cannot persist, while a cooperation run of length at least three can indeed persist, but only if flanked by two non-isolated defectors.

Lemma 5.2 *If the underlying graph of the ESPD is a path and (5.3) holds, then*

(a) no cooperation run of length 1 *can persist to the next round of the game,*

(b) no cooperation run of length 2 *can persist to the next round, except if the cooperation run occurs at an endpoint of the path and is adjacent to a defection run of length at least* 2*,*

(c) a cooperation run of length at least 3 *persists to the next round if and only if it is flanked by two defection runs, each of length at least* 2*, or if the cooperation run occurs at an endpoint of the path and is adjacent to a defection run of length at least* 2*.*

Proof: (a) It follows by Lemma 5.1 that the two defectors in the substate DCD of a game state during round t retain their strategies during round $t+1$. Furthermore, the pay-off value of the cooperator during round t in such a substate is 0, whilst the pay-off value of each defector during round t is at least $\frac{T+P}{2} > \frac{1}{2}$. Hence the cooperator will change his strategy to that of defection during round $t+1$. Similarly the substate[2] $[CD$ evolves to $[DD$.

(b) Again it follows by Lemma 5.1 that the two defectors in the substate $DCCD$ of a game state during round t retain their strategies during round $t+1$. Furthermore, the pay-off value of each cooperator during round t in such a substate is $\frac{1}{2}$, whilst the pay-off value of each defector during round t is at least $\frac{T+P}{2} > \frac{1}{2}$. Hence the two cooperators will change their strategy to that of defection during round $t+1$.

Similarly, the pay-off value of the left-most cooperator and the second-to-left cooperator in the substate $[CCDC$ are 1 and $\frac{1}{2}$, respectively, whilst the pay-off value of the defector in this substate is $T > 1$. Hence the second-to-left cooperator in the substate $[CCDC$ will change his strategy to that of defection during round $t+1$, resulting in the substate $[CD$ considered above.

However, the pay-off value of the left-most cooperator and the second-to-left cooperator in the substate $[CCDD$ are 1 and $\frac{1}{2}$, respectively, whilst the pay-off value of the left-most defector in this substate is $\frac{T+P}{2} \leq 1$ by (5.3). Hence neither cooperator in the substate $[CCDD$ will change his strategy to that of defection during round $t+1$, resulting in the persistence of the substate $[CCDD$.

(c) It follows by Lemma 5.1 that the defectors in the substate $DD\langle C\rangle^i DD$ or $[\langle C\rangle^i DD$ of a game state during round t retain their strategies during round $t+1$. Furthermore, all cooperators other than the two outer cooperators trivially retain their strategies during round $t+1$, each

[2]The symbols [and] are used to denote the ends of the path.

receiving a pay-off value of 1 during round t. Finally, since the pay-off value of each outer cooperator is $\frac{1}{2}$ and the pay-off value of each inner defector is $\frac{T+P}{2} \leq 1$ during round t, each outer cooperator during round t also retains his strategy during round $t+1$. This establishes the persistence of the two substates.

For the converse, consider the pay-off values of the players in the substate $DD\langle C\rangle^i DC$ or $[\langle C\rangle^i DC$ of a game state during round t, as shown in Table 5.4. The table shows that in both cases the third player from the right will change his strategy from cooperation to defection during round $t+1$ and hence that the cooperation run $\langle C\rangle^i$ will not survive intact from round t to round $t+1$. □

The substate $DD\langle C\rangle^i DC$

Player	1	2	3	4 to $i+1$	$i+2$	$i+3$	$i+4$
Strategy	D	D	C	$\langle C\rangle^{i-2}$	C	D	C
Pay-off	$\geq \frac{T+P}{2}$	$\frac{T+P}{2} \leq 1$	$\frac{1}{2}$	1 each	$\frac{1}{2}$	$T > 1$	$\leq \frac{1}{2}$

The substate $[\langle C\rangle^i DC$

Player	1 to $i-1$	i	$i+1$	$i+2$
Strategy	$\langle C\rangle^{i-1}$	i	$i+1$	$i+2$
Pay-off	1 each	$\frac{1}{2}$	$T > 1$	≥ 0

Table 5.4: *Pay-off values of the players in the two substates considered in the proof of Lemma 5.2(c).*

In order to be able to determine the structure of the state graph, a well-known fact in combinatorial analysis is required. The number of ways of distributing m indistinguishable objects among n distinguishable containers is equivalent to the number of unique strings which can be constructed from $n-1$ indistinguishable characters, denoted by "|", and m indistinguishable characters, denoted by "•". The characters denoted by "|" may be seen as dividing the characters denoted by "•" (or objects) into the distinguishable containers: those •'s occurring before the first | are placed in the first container, the •'s between the first and the second | represent objects placed into the second container, and so forth. As an example, the string | • • | • • represents placing no objects in the first container, two objects in the second container and two objects in the third container. Note that the number of dividers (*i.e.* |'s) is one fewer than the number of containers. The number of ways of forming strings from $m+n-1$ distinct characters is $(m+n-1)!$. Dividing this total by $m!$ (*i.e.* discounting the number ways of arranging the •'s) and by $(n-1)!$ (*i.e.* discounting the number of ways of arranging the |'s), gives the number of distinct strings which can be formed by $n-1$ |'s and m •'s, that is

$$\frac{(m+n-1)!}{m!(n-1)!}.$$

This argument establishes the following standard enumeration result.

Lemma 5.3 *There are* $\binom{m+n-1}{n-1}$ *distinct ways of distributing* m *indistinguishable objects among* n *distinguishable containers.*

It is now possible to characterise the steady states of the ESPD when the underlying graph is a path of order n, under the condition (5.3).

Theorem 5.2 *If the underlying graph of the ESPD is a path of order n and (5.3) holds, then the number of components, $\Xi_p(n)$, of the state graph is given by*

$$1+\sum_{i=1}^{\lfloor\frac{n+1}{5}\rfloor}\tbinom{n-3i}{2i-1}+\tfrac{1}{2}\sum_{i=1}^{\lfloor\frac{n+4}{5}\rfloor}\left[\tbinom{n-3i+2}{2i-2}+\tbinom{\lfloor\frac{n-5i+4}{2}\rfloor+i-1}{i-1}\right]+\tfrac{1}{2}\sum_{i=1}^{\lfloor\frac{n-2}{5}\rfloor}\left[\tbinom{n-3i-2}{2i}+\tbinom{\lfloor\frac{n-5i-2}{2}\rfloor+i}{i}\right]. \quad (5.4)$$

Moreover, the steady states of the game are $\langle C\rangle^n$, $\langle D\rangle^n$ and all those states in which each cooperation run has length at least 3 (or which occur at an endpoint and has length at least 2) and in which each defection run has length at least 2.

Proof: It follows by Lemma 5.2(a) and Lemma 5.2(b) that no steady state of the game can contain a cooperation run of length 1 or 2, except in the latter case if the run occurs at an endpoint and is flanked a run of defectors of length at least two. However, by Lemma 5.2(c) all steady states other than the states $\langle C\rangle^n$ and $\langle D\rangle^n$ contain cooperation runs of length 3 or more, each flanked by defection runs of length at least 2 (except if the cooperation run occurs at an endpoint of the path, in which case it may have length 2). Therefore no steady state can contain isolated defectors.

Let Q_i denote the number of states comprising i cooperation runs, starting with a run of cooperators and ending with a run of defectors, that is steady states of the form

$$\underbrace{CC\cdots}_{\text{run 1}}\underbrace{DD\cdots}_{\text{run 2}}\underbrace{CCC\cdots}_{\text{run 3}}\underbrace{DD\cdots}_{\text{run 4}}\underbrace{CCC\cdots}_{\text{run 5}}\underbrace{DD\cdots}_{\text{run 6}}\ \cdots\ \underbrace{CCC\cdots}_{\text{run }2i-1}\underbrace{DD\cdots}_{\text{run }2i}, \quad (5.5)$$

where each run has been populated above with the smallest number of cooperators and defectors, respectively, in order to ensure persistence of the cooperators according to Lemma 5.2. This partial state contains $5i-1$ symbols, leaving a total of $n-5i+1$ remaining symbols to distribute amongst the $2i$ distinguishable runs. Note that since the ordering of the cooperation and defection runs has already been fixed, these $n-5i+1$ symbols can be considered indistinguishable (that is, the symbols merely serve as place holders).

It follows by Lemma 5.3 that the number of game states of the form (5.5) is

$$Q_i=\binom{n-3i}{2i-1}. \quad (5.6)$$

However, the number of runs that a game state of this form can contain is constrained by the inequality $5i-1\leq n$. Therefore (5.6) is only valid for $i\leq\lfloor\frac{n+1}{5}\rfloor$. Since each state of the form (5.5) forms an automorphism class on its own, the total number of steady states of this form is

$$Q=\sum_{i=1}^{\lfloor\frac{n+1}{5}\rfloor}Q_i=\sum_{i=1}^{\lfloor\frac{n+1}{5}\rfloor}\binom{n-3i}{2i-1}.$$

Let R_i denote the number of steady states comprising i cooperation runs, both starting and ending in cooperation runs, that is states of the form

$$\underbrace{CC\cdots}_{\text{run 1}}\underbrace{DD\cdots}_{\text{run 2}}\underbrace{CCC\cdots}_{\text{run 3}}\underbrace{DD\cdots}_{\text{run 4}}\ \cdots\ \underbrace{CCC\cdots}_{\text{run }2i-3}\underbrace{DD\cdots}_{\text{run }2i-2}\underbrace{CC\cdots}_{\text{run }2i-1} \quad (5.7)$$

where each run has again been populated above with the smallest number of cooperators and defectors, respectively, in order to ensure persistence of the cooperators according to Lemma 5.2. The partial state (5.7) contains $5i-4$ symbols, leaving $n-5i+4$ remaining symbols to be

distributed amongst the $2i-1$ runs. It follows by Lemma 5.3 that the steady state (5.7) may be completed in $\tilde{R}_i = \binom{n-5i+4+2i-1-1}{2i-1-1} = \binom{n-3i+2}{2i-2}$ distinct ways. However, every non-symmetric state of the form (5.7) is a member of an automorphism class of cardinality 2. Hence every non-symmetric state of the form (5.7) has essentially been counted twice, while each symmetric state of the form (5.7) is the only member of its automorphism class and has been counted once. To remedy this situation the number of symmetric states of the form (5.7) is counted and added to the expression for $\tilde{R}_i$ before dividing the sum by two to obtain an expression for R_i. The symmetric states may be formed by distributing half of the remaining $n-5i+4$ symbols amongst half of the $2i-1$ runs. If the number of symbols is odd, then one symbol must be placed in the central run; hence there are $\lfloor \frac{n-5i+4}{2} \rfloor$ remaining symbols to be distributed. It follows by Lemma 5.3 that the steady state (5.7) may be completed symmetrically in

$$\bar{R}_i = \binom{\lfloor \frac{n-5i+4}{2} \rfloor + i - 1}{i-1}$$

distinct ways. The only restriction on i in (5.7) is that $5i-4 \leq n$. Hence the total number of steady states starting with a cooperation run and ending in a defection run is

$$R = \sum_{i=1}^{\lfloor \frac{n+4}{5} \rfloor} R_i = \tfrac{1}{2} \sum_{i=1}^{\lfloor \frac{n+4}{5} \rfloor} [\tilde{R}_i + \bar{R}_i] = \tfrac{1}{2} \sum_{i=1}^{\lfloor \frac{n+4}{5} \rfloor} \left[\binom{n-3i+2}{2i-2} + \binom{\lfloor \frac{n-5i+4}{2} \rfloor + i - 1}{i-1} \right].$$

The number, S, of steady states of the form

$$\underbrace{DD\cdots}_{\text{run } 1}\underbrace{CCC\cdots}_{\text{run } 2}\underbrace{DD\cdots}_{\text{run } 3}\underbrace{CCC\cdots}_{\text{run } 4} \cdots \underbrace{DD\cdots}_{\text{run } 2i-1}\underbrace{CCC\cdots}_{\text{run } 2i}\underbrace{DD\cdots}_{\text{run } 2i+1}$$

can be counted in a similar fashion as in the case above. The result is

$$S = \sum_{n=1}^{\lfloor \frac{n-2}{5} \rfloor} S_i = \tfrac{1}{2} \sum_{i=1}^{\lfloor \frac{n-2}{5} \rfloor} [\tilde{S}_i + \bar{S}_i] = \tfrac{1}{2} \sum_{i=1}^{\lfloor \frac{n-2}{5} \rfloor} \left[\binom{n-3i-2}{2i} + \binom{\lfloor \frac{n-5i-2}{2} \rfloor + i}{i} \right],$$

where the symbols S, S_i, $\tilde{S}_i$ and $\bar{S}_i$ have meanings similar to those of R, R_i, $\tilde{R}_i$ and $\bar{R}_i$, respectively. Taking into account the all-defector state, which has not been counted above, the total number of steady states is the quantity $1+Q+R+S$ in (5.4). Since every component of the state graph contains exactly one steady state by Theorem 5.1, the quantity in (5.4) is also the number of components of the state graph. □

Table 5.5 contains the number of steady states of the ESPD on a path of order $1 \leq n \leq 15$ under the condition (5.3).

n	1	2	3	4	5	6	7	8	9	10	11	12	13	14	15
$\Xi_p(n)$	2	2	2	3	4	6	9	13	19	28	42	63	95	143	216

Table 5.5: *The number of steady states, $\Xi_p(n)$, of the ESPD on a path of order $1 \leq n \leq 15$ under the condition (5.3). These values were computed via (5.4).*

5.3.2 The game dynamics for small values of T

Those states of the ESPD on a path that are not attracted by the all-defector state, $\langle D\rangle^n$, under the condition (5.3) are characterised in the following result.

Theorem 5.3 *If the underlying graph of the ESPD is a path of order n and (5.3) holds, then the game states that are not attracted by the all-defector steady-state $\langle D\rangle^n$ are exactly those states containing at least one of the substates $\langle C\rangle^5$, $DD\langle C\rangle^3DD$, $DD\langle C\rangle^4D$, $[CCDD$ or $[\langle C\rangle^3$ (or their reverses).*

Proof: First it is shown that it is sufficient for a game state $\boldsymbol{S}_t$ during round t to contain one of the five substates mentioned above in order for cooperation to persist. To achieve this, it is shown that either $\boldsymbol{S}_t$ or $\boldsymbol{S}_{t+1}$ necessarily contains the substate $DD\langle C\rangle^iDD$ for some integer $i \geq 3$; the result then follows by Lemma 5.2(c).

If $\langle C\rangle^5 \subseteq \boldsymbol{S}_t$, then there exists an integer $i \geq 5$ such that $\boldsymbol{a} = DD\langle C\rangle^iDD$, $\boldsymbol{b} = CD\langle C\rangle^iDD$, $\boldsymbol{c} = CD\langle C\rangle^iDC$ or $\boldsymbol{d} = DD\langle C\rangle^iDC$ is a substate of $\boldsymbol{S}_t$. If $\boldsymbol{a} \subseteq \boldsymbol{S}_t$, then cooperation persists by Lemma 5.2(c). If $\boldsymbol{b} \subseteq \boldsymbol{S}_t$ or $\boldsymbol{d} \subseteq \boldsymbol{S}_t$, then $\langle D\rangle^3\langle C\rangle^{i-1}DD \subseteq \boldsymbol{S}_t$ or $DD\langle C\rangle^{i-1}\langle D\rangle^3 \subseteq \boldsymbol{S}_{t+1}$, respectively, and so cooperation persists by Lemma 5.2(c). Finally, if $\boldsymbol{c} \subseteq \boldsymbol{S}_t$, then the cooperators in the underlined substates of $\boldsymbol{c} = \underline{CDC}\langle C\rangle^{i-2}\underline{CDC}$ become defectors during round $t+1$, in which case $DD\langle C\rangle^{i-2}DD \subseteq \boldsymbol{S}_{t+1}$ and so cooperation persists by Lemma 5.2(c). In all four cases it therefore follows that the states $\boldsymbol{S}_t$ and $\boldsymbol{S}_{t+1}$ are not in the component that contains the all-defector state.

If $DD\langle C\rangle^3DD \subseteq \boldsymbol{S}_t$, then it follows directly by Lemma 5.2(c) that cooperation persists and hence the state $\boldsymbol{S}_t$ is not in in the same component as the all-defector steady state.

If $DD\langle C\rangle^4D \subseteq \boldsymbol{S}_t$, then either $DD\langle C\rangle^4DD \subseteq \boldsymbol{S}_t$, $DD\langle C\rangle^4DC \subseteq \boldsymbol{S}_t$ or $DD\langle C\rangle^4D] \subseteq \boldsymbol{S}_t$. In the first case cooperation persists by Lemma 5.2(c) and hence $\boldsymbol{S}_t$ is not in the component that contains the all-defector steady state. In the second case each cooperator in the underlined substate of $DD\langle C\rangle^3\underline{CDC}$ becomes a defector during round $t+1$, so that $DD\langle C\rangle^3DD \subseteq \boldsymbol{S}_{t+1}$. In the third case the underlined cooperator in the substate $DD\langle C\rangle^3\underline{C}D]$ becomes a defector during round $t+1$, so that $DD\langle C\rangle DD \subseteq \boldsymbol{S}_{t+1}$. Therefore cooperation also persists in this case by Lemma 5.2(c) and so the states $\boldsymbol{S}_t$ and $\boldsymbol{S}_{t+1}$ are not in the component that contains the all-defector steady state.

If $[CCDD \subseteq \boldsymbol{S}_t$, then this substate persists to round $t+1$ by Lemma 5.2(b).

If $[\langle C\rangle^i \subseteq \boldsymbol{S}_t$ for some integer $i \geq 3$, then either $\boldsymbol{S}_t = [\langle C\rangle^i]$, or $\boldsymbol{S}_t = [\langle C\rangle^iD$, which evolves to $[\langle C\rangle^{i-1}DD$ during round $t+1$, a substate which persists to round $t+2$ by Lemma 5.2(b), or else $\boldsymbol{S}_t$ contains one of the substates $\boldsymbol{e} = [\langle C\rangle^iDD$ or $\boldsymbol{f} = [\langle C\rangle^iDC$. The substate $\boldsymbol{e}$ persists to round $t+1$ by Lemma 5.2(c), while the substate $\mathbf{f}$ evolves to $[\langle C\rangle^{i-1}DDD$, which persists to round $t+2$ by Lemma 5.2(b)–(c).

For the converse it is shown that it is necessary for a game state to contain one of the five stated substates in order for cooperation to persist. There are three possible ways in which a game state can contain an endpoint cooperation run of length at most 2 during round t, namely $[CD$, $[CCDD$ or $[CCDC$. The first and last of these substates evolve during round $t+1$ to $[DD$ or $[CDDD$, respectively. Therefore $[CCDD$ is the only endpoint substate containing a cooperation run of length at most 2 which allows for the persistence of cooperation (by Lemma 5.2(b)). Any endpoint substate containing a cooperation run of length at least 3 persists to the next round, as shown above.

It follows from Lemma 5.2(b)–(c) that an interior cooperation run of length at least 3 is required for the persistence of cooperation.

The four possible substates containing a run of three cooperators are $DD\langle C\rangle^3 DD$, $CD\langle C\rangle^3 DC$, $CD\langle C\rangle^3 DD$ and $DD\langle C\rangle^3 DC$, but only the first of these substates allows for the persistence of cooperation by Lemma 5.2(c), since the other three substates lead to the progressions $CD\langle C\rangle^3 DC \to \langle D\rangle^3 C\langle D\rangle^3$, $CD\langle C\rangle^3 DD \to \langle D\rangle^3 CCDD$ and $DD\langle C\rangle^3 DC \to DDCC\langle D\rangle^3$ during the following round of the game.

Two game substates containing a cooperation run of length 3 that have not yet been considered are those in which the run is adjacent to an endpoint defector, namely $[D\langle C\rangle^3 DD$, $[D\langle C\rangle^3 DC$ and $[D\langle C\rangle^3 D]$. These three substates evolve to $[DDCCDD$, $[DDC\langle D\rangle^3$ and $[DDCDD]$, respectively. Therefore $DD\langle C\rangle^3 DD$ is the only substate in which an internal cooperation run persists.

There are only three cases in which a cooperation run of length 4 is not flanked on at least one end by a defection run of length at least 2, namely $CD\langle C\rangle^4 DC$, $[D\langle C\rangle^4 D]$ or $[D\langle C\rangle^4 DC$. Since these substates evolve to $\langle D\rangle^3 CC\langle D\rangle^3$, $[DDCCDD]$ and $[DDCC\langle D\rangle^3$ within one round, respectively, the only case in which an internal cooperation run of length 4 can persist is if it is flanked on at least one end by two defectors.

Finally, every possible substate containing a run of length at least five cooperators leads to persistent cooperation, as shown above. □

The state graphs for the ESPD on a path of order n is shown in Figure 5.4 for $3 \leq n \leq 6$. Note that the state graphs in the figure are pseudo-forests and that the number of cooperators is non-increasing from round to round. The results of Theorems 5.2 and 5.3 may be verified for $3 \leq n \leq 6$ in the figure.

5.3.3 The probability of persistent cooperation for small values of T

In this section the probability, $P_p(n)$, that some form of cooperation will persist from a randomly generated initial state of the ESPD on a path of order n is determined. Denote by $\mathcal{S}_n$ the set containing all binary strings of length n that do not contain any of the substrings $\boldsymbol{s}_1 = DDCCCDD$, $\boldsymbol{s}_2 = DCCCCDD$, $\boldsymbol{s}_3 = DDCCCCD$, $\boldsymbol{s}_4 = CCCCC$, $\boldsymbol{s}_5 = [CCDD$, $\boldsymbol{s}_6 = DDCC]$, $\boldsymbol{s}_7 = [CCC$ or $\boldsymbol{s}_8 = CCC]$ as listed in Table 5.6(a). The symbols '[' and ']' again indicate that the substring occurs on a left or right endpoint of the path. Furthermore, let a_n be the number of strings contained in the set $\mathcal{S}_n$. Then the number of initial states leading to some form of persistence of cooperation is $\psi_p(n) = 2^n - a_n$ by Theorem 5.3.

Let z_n be the number of binary strings contained in $\mathcal{S}_n$ starting with $[D$. Similarly, let u_n, w_n and v_n be the number of binary strings contained in $\mathcal{S}_n$ starting with $[C$, $[DD$ and $[DC$, respectively. A summary of the variables introduced in this section and their definitions is given in Table 5.6(b).

It follows directly from the definitions of a_n, z_n and u_n that

$$a_n = z_n + u_n \text{ and} \tag{5.8}$$

$$z_n = w_n + v_n. \tag{5.9}$$

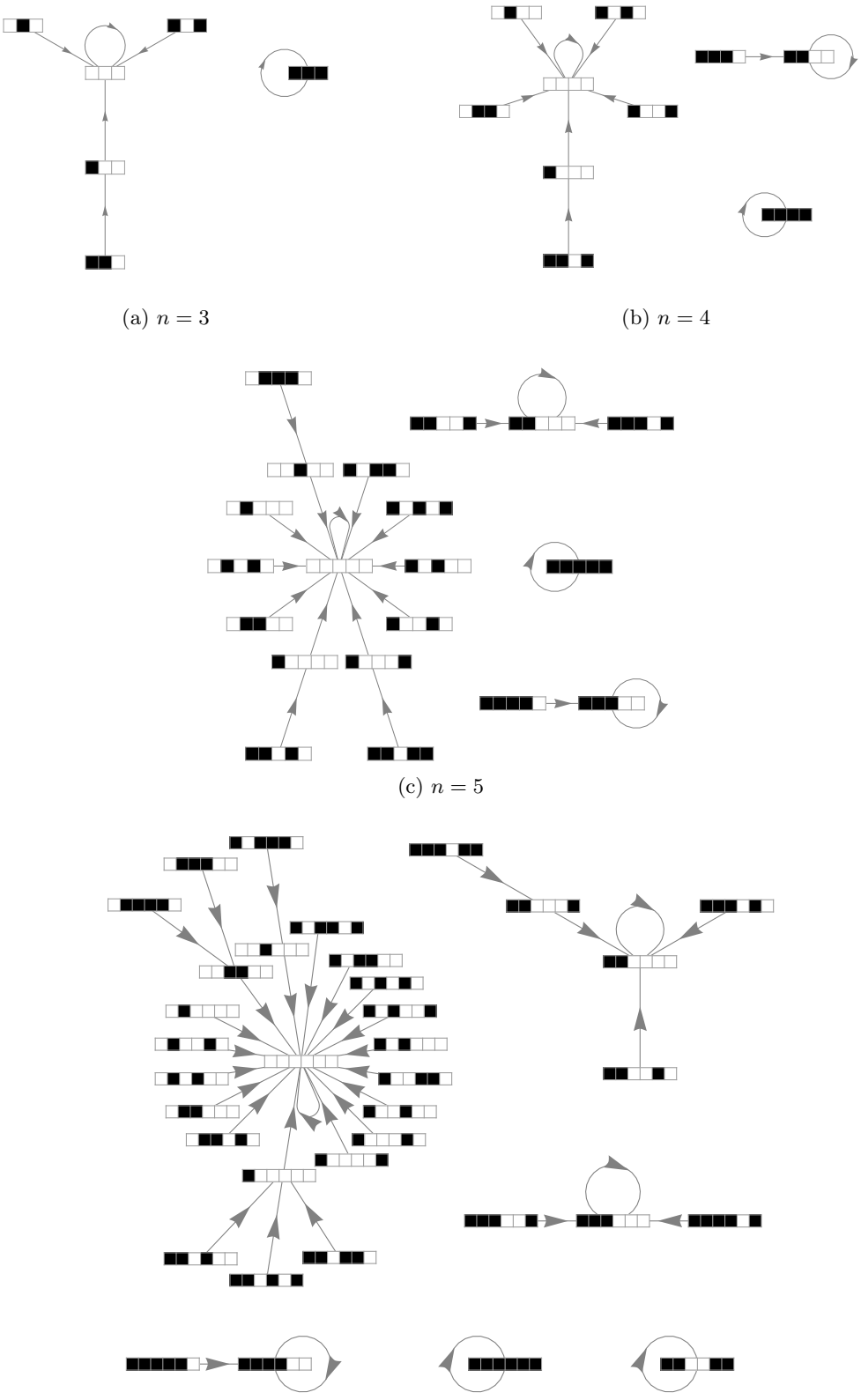

(a) $n = 3$

(b) $n = 4$

(c) $n = 5$

(d) $n = 6$

Figure 5.4: *The ESPD state graph for the case where $T \leq 2 - P$ and the underlying graph is a path of order n. The strategy of cooperation (C) is denoted by a black square, while that of defection (D) is denoted by a white square in each state which is represented by a linear array of squares.*

Substring
$\boldsymbol{s}_1 = DDCCCDD$
$\boldsymbol{s}_2 = DCCCCDD$
$\boldsymbol{s}_3 = DDCCCCD$
$\boldsymbol{s}_4 = CCCCC$
$\boldsymbol{s}_5 = [CCDD$
$\boldsymbol{s}_6 = DDCC]$
$\boldsymbol{s}_7 = [CCC$
$\boldsymbol{s}_8 = CCC]$

(a)

Variable	Value
a_n	$\lvert\mathcal{S}_n\rvert$
u_n	$\lvert\{\boldsymbol{s} \in \mathcal{S}_n \lvert \boldsymbol{s} = C...\}\rvert$
v_n	$\lvert\{\boldsymbol{s} \in \mathcal{S}_n \lvert \boldsymbol{s} = DC...\}\rvert$
w_n	$\lvert\{\boldsymbol{s} \in \mathcal{S}_n \lvert \boldsymbol{s} = DD...\}\rvert$
z_n	$\lvert\{\boldsymbol{s} \in \mathcal{S}_n \lvert \boldsymbol{s} = D...\}\rvert$

(b)

Table 5.6: *(a) Persistence of cooperation is possible on paths of order 3 or more if and only if one of these substrings are present, according to Theorem 5.3. (b) A summary of the variables used to enumerate the initial game states leading to some form of persistent cooperation and their definitions. Each variable represents the size of a subset of $\mathcal{S}_n$.*

The value u_n, representing the number of binary strings contained in $\mathcal{S}_n$ starting with $[C$, is given by

$$u_n = a_{n-1} - x + y,$$

where x is the number of strings that are in $\mathcal{S}_{n-1}$, but would not be in $\mathcal{S}_n$ if 'C' is joined to the front of the strings and y is the number of strings that are not in $\mathcal{S}_{n-1}$, but would be in $\mathcal{S}_n$ if 'C' is joined to the front of the strings. Here $y = 0$ since all the strings containing one or more of the substrings listed in Table 5.6(a) would still contain those substrings after joining C to the front of the binary string. To determine the value of x, note that only the substrings s_5 or s_7 can be created by joining a 'C' to the front of a string contained in $\mathcal{S}_{n-1}$. For these substrings to be introduced, the string of length $n-1$ must be of either the form $[CDD\ldots$ or $[CCDC\ldots$ A binary string of the form $[CDD\ldots$ contained in $\mathcal{S}_{n-1}$ becomes $[CCDD\ldots$, which is not in $\mathcal{S}_n$ and a binary string of the form $[CCDC\ldots$ in S_{n-1} becomes $[CCCDC\ldots$, which is not in $\mathcal{S}_n$. The number of strings of the form $[CDD\ldots$ not in $\mathcal{S}_{n-1}$ is w_{n-2} and the number of strings of the form $[CCDC\ldots$ not in $\mathcal{S}_{n-1}$ is v_{n-3}. Therefore,

$$u_n = a_{n-1} - v_{n-3} - w_{n-2}. \tag{5.10}$$

The number of binary strings z_n is given by

$$z_n = a_{n-1} - x' + y',$$

where x' is the number of strings that are in $\mathcal{S}_{n-1}$ but would not be in $\mathcal{S}_n$ if a 'D' is joined to the front of the strings and y' is the number of strings that are not in $\mathcal{S}_{n-1}$ but would be in $\mathcal{S}_n$ if 'D' is joined to the front of the strings.

The substrings that can be introduced by joining a 'D' to the front of a string contained in $\mathcal{S}_{n-1}$ are $\boldsymbol{s}_1$, $\boldsymbol{s}_2$ and $\boldsymbol{s}_3$. For these substrings to be introduced, the string of length $n-1$ must be of the form $[DCCCDD\ldots$, $[CCCCDD\ldots$ or $[DCCCCD\ldots$ Note that no string of length $n-1$ of the form $[CCCCDD\ldots$ or $[DCCCCDD\ldots$ is in $\mathcal{S}_{n-1}$ since it already contains substring $\boldsymbol{s}_7$ and $\boldsymbol{s}_2$ respectively. The number of strings in $\mathcal{S}_{n-1}$ of the form $[DCCCDD\ldots$ and $[DCCCCDC\ldots$ are w_{n-5} and v_{n-6}, respectively. Therefore $x' = w_{n-5} + v_{n-6}$.

The variable y' counts those strings which contain only one of the substrings at an endpoint that would 'break' if a 'D' is joined to the front of the string. The strings that have this property are

those that contain one of the endpoint substrings $\boldsymbol{s}_5$ or $\boldsymbol{s}_7$, while containing none of the other substrings $\boldsymbol{s}_1$, $\boldsymbol{s}_2$, $\boldsymbol{s}_3$, $\boldsymbol{s}_4$ or $\boldsymbol{s}_6$. That is, strings of length $n-1$ of the form $[CCDD\ldots$, $[CCCD\ldots$, $[CCCCDC\ldots$ and $[CCCCDD\ldots$, which become $[DCCDD\ldots$, $[DCCCD\ldots$, $[DCCCCDC\ldots$ and $[DCCCCDD\ldots$, respectively. All of these binary strings, except the last, is in $\mathcal{S}_n$. The number of binary strings of length $n-1$ of the form $[CCDD\ldots$ not containing any of the substrings, except $\boldsymbol{s}_5$, is w_{n-3}. The number of strings of the forms $[CCCD\ldots$ and $[CCCCDC\ldots$ are z_{n-4} and v_{n-5}, respectively. Therefore $y' = w_{n-3} + z_{n-4} + v_{n-5}$, and so

$$\begin{aligned} z_n &= a_{n-1} - (w_{n-5} + v_{n-6}) + (w_{n-3} + z_{n-4} + v_{n-5}) \\ &= a_{n-1} + v_{n-5} - v_{n-6} + w_{n-3} - w_{n-5} + z_{n-4}. \end{aligned} \tag{5.11}$$

An expression for v_n in terms of u_n, v_n, w_n and z_n can be found by using a similar approach to that used to derive (5.11), with the result that

$$v_n = u_{n-1} + v_{n-5} + w_{n-3} + z_{n-4}. \tag{5.12}$$

Substituting (5.9) and (5.10) into (5.8) and rewriting the result, yields

$$a_n - a_{n-1} = w_n - w_{n-2} + v_n - v_{n-3}. \tag{5.13}$$

Replacing z_n and z_{n-4} in (5.11) using (5.9) and rewriting the equation to make a_{n-1} the subject yields

$$a_{n-1} = v_n - v_{n-4} - v_{n-5} + v_{n-6} + w_n - w_{n-3} - w_{n-4} + w_{n-5}. \tag{5.14}$$

Substituting (5.9) into (5.12) and rewriting to make u_n the subject of the equation yields

$$u_{n-1} = v_n - v_{n-4} - v_{n-5} - w_{n-3} - w_{n-4}. \tag{5.15}$$

The equation (5.10) can be written as

$$u_{n-1} = a_{n-2} - v_{n-4} - w_{n-3},$$

and substituting this into (5.15) yields

$$w_{n-4} = -a_{n-2} + v_n - v_{n-5}.$$

Using this equation to substitute the expressions for w_n in (5.13) and (5.14) yields the system of equations

$$a_{n+2} - a_{n-1} = v_{n+4} - v_{n+2} + v_n - v_{n-1}, \tag{5.16}$$

$$a_{n+2} - a_{n-2} + a_n - 3 = v_{n+4} - v_{n+1}. \tag{5.17}$$

It follows from (5.16) and (5.17) themselves, as well as from appropriate left and right shifts of their indices, that the linear system

$$\begin{aligned} a_{n+2} - a_{n-1} &= v_{n+4} - v_{n+2} + v_n - v_{n-1}, \\ a_{n+2} - a_{n-2} + a_{n-3} &= v_{n+4} - v_{n+1}, \\ a_{n+3} - a_n &= v_{n+5} - v_{n+3} + v_{n+1} - v_n, \\ a_{n+3} - a_{n-1} + a_{n-2} &= v_{n+5} - v_{n+2}, \\ a_{n+1} - a_{n-2} &= v_{n+3} - v_{n+1} + v_{n-1} - v_{n-2}, \\ a_{n-1} - a_{n-5} + a_{n-6} &= v_{n+1} - v_{n-2} \end{aligned}$$

must be satisfied. The aim is to find a combination of these equations such that all the v-variables add to zero, leaving a single equation containing only the a-variable, in other words, to find values for Z_1, Z_2, Z_3, Z_4 and Z_5 such that

$$\begin{aligned} v_{n+4} - v_{n+2} + v_n - v_{n-1} &= Z_1(v_{n+4} - v_{n+1}) + Z_2(v_{n+5} - v_{n+3} + v_{n+1} - v_n) \\ &+ Z_3(v_{n+5} - v_{n+2}) + Z_4(v_{n+3} - v_{n+1} + v_{n-1} - v_{n-2}) + Z_5(v_{n+1} - v_{n-2}). \end{aligned} \tag{5.18}$$

Solving the over-specified system

$$\begin{bmatrix} 0 & 1 & 1 & 0 & 0 \\ 1 & 0 & 0 & 0 & 0 \\ 0 & -1 & 0 & 1 & 0 \\ 0 & 0 & -1 & 0 & 0 \\ -1 & 1 & 0 & -1 & 1 \\ 0 & -1 & 0 & 0 & 0 \\ 0 & 0 & 0 & 1 & 0 \\ 0 & 0 & 0 & -1 & -1 \end{bmatrix} \begin{bmatrix} Z_1 \\ Z_2 \\ Z_3 \\ Z_4 \\ Z_5 \end{bmatrix} = \begin{bmatrix} 0 \\ 1 \\ 0 \\ -1 \\ 0 \\ 1 \\ -1 \\ 0 \end{bmatrix},$$

which results from collecting similar terms in (5.18), yields the values $Z_1 = 1$, $Z_2 = -1$, $Z_3 = 1$, $Z_4 = -1$ and $Z_5 = 1$, which, in turn, results in the recursive expression

$$a_n = a_{n-1} + a_{n-2} + a_{n-3} + a_{n-4} - a_{n-6} + a_{n-7}. \tag{5.19}$$

The values required to seed (5.19) are listed in Table 5.7 and were determined by brute force counting. The arguments of this section lead to the following result.

Theorem 5.4 *The probability that a randomly generated initial state of the ESPD on a path of order n will lead to some form of persistent cooperation is given by*

$$P_p(n) = 1 - \frac{a_n}{2^n},$$

where a_n satisfies (5.19) with seed values as specified in Table 5.7.

a_1	a_2	a_3	a_4	a_5	a_6	a_7
1	3	7	11	21	42	81

Table 5.7: *The values required to seed the recurrence relation for a_n in (5.19).*

The values of a_n are given in Table 5.8 for small values of n and the probability that cooperation will persist for a randomly generated initial state is shown in Figure 5.5.

In order to study the asymptotic behaviour of $P_p(n)$ as $n \to \infty$ the following intermediate result is required.

Lemma 5.4 *The terms in the sequence $(a_1, a_2, a_3, \ldots)$ are positive and strictly increasing.*

Proof: By the strong form of induction. It follows directly from the observed values in Table 5.7 that the result of the lemma holds for $1 \leq n \leq 7$. This establishes the base case. Assume, as induction hypothesis, that $a_n > a_{n-1} > 0$ for all $n \leq k$. Substituting $k+1$ for n in (5.19) gives

$$a_{k+1} = a_k + a_{k-1} + a_{k-2} + a_{k-3} - a_{k-5} + a_{k-6}.$$

$n \to$	1	2	3	4	5	6	7	8	9	10	11	12	13
a_n	1	3	7	11	21	42	81	153	293	565	1 082	2 072	3 973
2^n	2	4	8	16	32	64	128	256	512	1 024	2 048	4 096	8 192

$n \to$	14	15	16	17	18	19	20	21	22
a_n	7 620	14 607	28 000	53 683	102 920	197 309	378 265	725 190	1 390 291
2^n	16 384	32 768	65 536	131 072	262 144	524 288	1 048 576	2 097 152	4 194 304

Table 5.8: *Information for computing the probability of randomly generating a state of the ESPD on a path of order n which is not attracted by the all-defector steady state $\langle D \rangle^n$. The probability is $1 - a_n/2^n$ according to Theorem 5.4.*

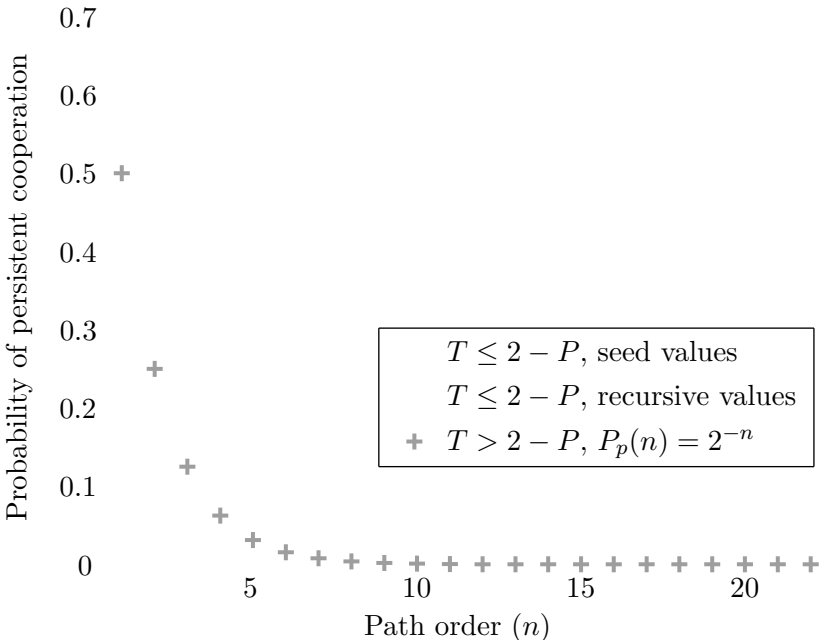

Figure 5.5: *The probability of randomly generating a game state for the ESPD on a path of order n which is not attracted by the all-defector steady state.*

Since $a_{k-3} > a_{k-5}$ by the induction hypothesis and all the other terms in the above equation are positive, it follows that $a_{k+1} > a_k > 0$. □

The result above may be used to establish the limiting behaviour of the probability $P_p(n)$ as $n \to \infty$.

Theorem 5.5 *Let $P_p(n)$ denote the probability that a randomly generated initial state of the ESPD on a path of order n is not attracted by the all-defector steady state, $\langle D \rangle^n$. Then*

$$\lim_{n\to\infty} P_p(n) = 1.$$

Proof: Let $R_n = a_{n-2} + a_{n-3} + a_{n-4} - a_{n-6} + a_{n-7}$. Then it follows by (5.19) that

$$a_n = a_{n-1} + R_n. \tag{5.20}$$

Shifting the indices in (5.19) yields

$$a_{n-1} = a_{n-2} + a_{n-3} + a_{n-4} + a_{n-5} - a_{n-7} + a_{n-8}.$$

Taking the difference between a_{n-1} and R_n gives

$$a_{n-1} - R_n = a_{n-5} + a_{n-6} - a_{n-7} + a_{n-8},$$

and since $a_n > a_{n-1}$ by Lemma 5.4, the right-hand side of the above expression is positive, which implies that $R_n < a_{n-1}$. Hence it follows by (5.20) that $0 < a_n < 2a_{n-1}$. Dividing by 2^n yields

$$0 < \frac{a_n}{2^n} < \frac{a_{n-1}}{2^{n-1}}.$$

and therefore the sequence $\frac{a_1}{2}, \frac{a_2}{2^2}, \frac{a_3}{2^3}, \ldots$ is monotonically decreasing and strictly positive. It thus follows by [1, Theorem 8.6] that the sequence $(a_n/2^n)_{n=1}^{\infty}$ converges. Assume that the value to which the sequence converges is L, that is

$$\lim_{n\to\infty} \frac{a_n}{2^n} = L. \tag{5.21}$$

From (5.19) the left-hand side of (5.21) can be written as

$$\begin{aligned}\lim_{n\to\infty} \frac{a_n}{2^n} &= \lim_{n\to\infty} \frac{a_{n-1} + a_{n-2} + a_{n-3} + a_{n-4} - a_{n-6} + a_{n-7}}{2^n} \\ &= \lim_{n\to\infty} \left(\frac{a_{n-1}}{2 \cdot 2^{n-1}} + \frac{a_{n-2}}{2^2 \cdot 2^{n-2}} + \frac{a_{n-3}}{2^3 \cdot 2^{n-3}} + \frac{a_{n-4}}{2^4 \cdot 2^{n-4}} - \frac{a_{n-6}}{2^6 \cdot 2^{n-6}} + \frac{a_{n-7}}{2^7 \cdot 2^{n-7}} \right).\end{aligned}$$

Rewriting and taking the limits therefore yields

$$\begin{aligned}\lim_{n\to\infty} \frac{a_n}{2^n} &= \frac{1}{2} \lim_{n\to\infty} \frac{a_{n-1}}{2^{n-1}} + \frac{1}{2^2} \lim_{n\to\infty} \frac{a_{n-2}}{2^{n-2}} + \frac{1}{2^3} \lim_{n\to\infty} \frac{a_{n-3}}{2^{n-3}} + \frac{1}{2^4} \lim_{n\to\infty} \frac{a_{n-4}}{2^{n-4}} \\ &\quad - \frac{1}{2^6} \lim_{n\to\infty} \frac{a_{n-6}}{2^{n-6}} + \frac{1}{2^7} \lim_{n\to\infty} \frac{a_{n-7}}{2^{n-7}} \\ &= L \cdot \left(\frac{1}{2} + \frac{1}{2^2} + \frac{1}{2^3} + \frac{1}{2^4} - \frac{1}{2^6} + \frac{1}{2^7} \right).\end{aligned}$$

It follows by (5.21) that

$$L \cdot \left(\frac{1}{2} + \frac{1}{2^2} + \frac{1}{2^3} + \frac{1}{2^4} - \frac{1}{2^6} + \frac{1}{2^7} \right) = L,$$

which implies $L = 0$. □

5.4 The ESPD on a cycle for small values of T

In this section the focus is on the dynamics of the ESPD on a cycle of order n. The same approached is followed as for the ESPD on a path and the corresponding proofs are similar to some extent. The steady states of the ESPD on a cycle are characterised, and this is followed by a description of the game dynamics in the case where $T \leq 2 - P$. Finally, the probability of randomly generating an initial state which leads to some form of persistent cooperation is determined.

5.4.1 Characterisation of steady states for small values of T

According to Corollary 5.1 no form of cooperation can persist in the long run for large values of T, except in the singular case where all players initially already cooperate. For large values of T the two trivial steady states, $\langle C \rangle^n$ and $\langle D \rangle^n$, are the only steady states. It is shown next that, as for the case of the ESPD on a path, cooperation runs of length 1 or 2 cannot persist in the ESPD on a cycle, while a cooperation run of length at least three can indeed persist, but only if flanked by two non-isolated defectors.

Lemma 5.5 *If the underlying graph of the ESPD is a cycle and (5.3) holds, then*

(a) no cooperation run of length 1 *can persist to the next round of the game,*

(b) no cooperation run of length 2 *can persist to the next round of the game,*

(c) a cooperation run of length at least 3 *persists to the next round of the game if and only if it is flanked by two defection runs, each of length at least* 2*.*

The proof of Lemma 5.5 is similar to that of Lemma 5.2. Using Lemma 5.5 it is possible to characterise the steady states of the ESPD on a cycle. Note that again the number of steady states, up to automorphism, is the same as the number of components contained in the state graph.

Theorem 5.6 *If the underlying graph of the ESPD is a cycle of order n and (5.3) holds, then the number of components, $\Xi_c(n)$, of the state graph is given by*

$$2 + \sum_{i=1}^{\lfloor \frac{n}{5} \rfloor} \frac{1}{2i} \left[\binom{n-3i-1}{2i-1} + \sum_{j \in S} \binom{(n-3i)\gcd(i,j)/i-1}{2\gcd(i,j)-1} + i \sum_{k=0}^{\lfloor \frac{n-5i}{2} \rfloor} (n-5i-2k+1) \binom{k+i-2}{i-2} \right], \tag{5.22}$$

where $S = \{x \in \mathbb{N} \mid i \text{ divides } n\gcd(i,x) \text{ and } x < i\}$. Moreover, the steady states of the game are $\langle C \rangle^n$, $\langle D \rangle^n$ and all those states in which each cooperation run has length at least 3 and each defection run has length at least 2.

Proof: Let Q_i denote the number of states, up to automorphism, comprising i defection runs starting with a run of cooperators and ending with a run of defectors, that is, steady states of the form

$$\underbrace{CCC\cdots}_{\text{run } 1}\underbrace{DD\cdots}_{\text{run } 2}\underbrace{CCC\cdots}_{\text{run } 3}\underbrace{DD\cdots}_{\text{run } 4} \quad \cdots \quad \underbrace{CCC\cdots}_{\text{run } 2i-1}\underbrace{DD\cdots}_{\text{run } 2i}, \tag{5.23}$$

where each run has been populated above with the smallest number of cooperators and defectors, respectively, in order to ensure the persistence of cooperators and defectors according to Lemma 5.5.

The partial state (5.23) contains $5i$ symbols, leaving a total of $n-5i$ indistinguishable symbols to distribute amongst the $2i$ distinguishable runs. Since the underlying graph is a cycle, the endpoints in the representation (5.23) are chosen arbitrarily. Therefore, all steady states or their mirror images can be represented by (5.23), except the all-defector and all-cooperator steady states. The total number of steady states is given by

$$2+\sum_{i=1}^{\lfloor \frac{n}{5} \rfloor} Q_i$$

which, by Theorem 5.1, is the same as the number of components in the state graph.

The value of Q_i for $i \in \{1,2,\ldots,\lfloor \frac{n}{5} \rfloor\}$ may be determined using the Cauchy-Frobenius lemma (see Theorem 2.1). Let $\mathcal{X}$ be the set of all states of the form (5.23), let ι be the identity permutation on the sequence of runs of a state $\boldsymbol{s} \in \mathcal{X}$, let ρ^j be the permutation which modular shifts each run $2j$ positions to the right, and let δ be the operation which reverses the order of the runs such that the first run remains in its original position, followed by run $2i$, $2i-1$ and so on. It can be shown that the set $\{\iota,\ \rho^1,\ \rho^2,\ \ldots\ ,\ \rho^{i-1},\ \delta,\ \delta\rho^1,\ \delta\rho^2,\ \ldots\ ,\ \delta\rho^{i-1}\}$ forms a group, $\mathcal{G}$, of order $2i$, under the binary operator of the composition of functions. According to Theorem 2.1, the number of equivalence classes into which $\mathcal{X}$ is partitioned by $\mathcal{G}$ is

$$Q_i = \frac{1}{|\mathcal{G}|}\sum_{g\in\mathcal{G}} |F_g|, \tag{5.24}$$

where $|F_g|$ is the number of states in $\mathcal{X}$ that remain invariant under g.

The identity operator ι leaves all elements of $\mathcal{X}$ unchanged. Therefore $|F_\iota| = |\mathcal{X}|$, which is the number of ways of distributing the remaining $n-5i$ indistinguishable symbols amongst the $2i$ distinguishable runs, that is

$$|F_\iota| = \binom{n-3i-1}{2i-1}. \tag{5.25}$$

Applying ρ^1 to a state $\boldsymbol{s} \in \mathcal{X}$ maps run i of $\boldsymbol{s}$ to run $i+2$; the number of symbols in runs 1 and 2 determine the number of symbols in runs 3 and 4 which, in turn, determine the number of symbols in runs 5 and 6, and so on. The result of applying the operator ρ^1 to a state is illustrated in Figure 5.6. In order for the a state to remain invariant under ρ^1 each pair of runs must contain the same number of symbols. Therefore, distributing $(n-5i)\frac{2}{2i}$ symbols among the first two runs determines the structure of the entire state. There are

$$|F_{\rho^1}| = \binom{\frac{n-5i}{i}+1}{1} = \frac{n-5i}{i}+1$$

ways of distributing $\frac{n-5i}{i}$ indistinguishable symbols among two distinguishable runs.

In general, if the shift ρ^j is applied to a state $\boldsymbol{s}$, fixing at most the first j pairs of runs would determine all the subsequent runs. The operation may be seen as modular shifting the pairs of cooperator-defector runs in blocks of length j. If j divides i, then exactly the first j pairs of runs determines the remaining $2(i-j)$ runs. Otherwise the number of runs that need to be fixed is determined by the greatest common denominator $d = \gcd(i,j)$. Fixing the first d pairs

$\boldsymbol{s}$	1	2	3	4	5	$\cdots$	$2i-1$	$2i$
$\pi_{\rho^1}(\boldsymbol{s})$	$2i-1$	$2i$	1	2	3	$\cdots$	$2i-3$	$2i-2$

Figure 5.6: *Applying the permutation ρ^1 to the labels of a state $\boldsymbol{s}$. The highlighted runs are those that determine the remaining runs in order to leave the state $\boldsymbol{s}$ invariant under ρ^1.*

of runs determines the remaining states. Therefore, $(n-5i)\frac{2d}{2i}$ symbols need to be distributed among the first $2d$ runs, which can be done in

$$|F_{\rho^j}| = \binom{(n-5i)d/i + 2d - 1}{2d-1} = \binom{(n-3i)d/i - 1}{2d-1}$$

distinct ways. However, if $n\frac{d}{i}$ is not an integer, then there are not enough symbols available to complete the pattern of runs in the state that would be invariant under ρ^j with the result that $|F_{\rho^j}| = 0$. Therefore

$$|F_{\rho^j}| = \begin{cases} \binom{(n-3i)\gcd(i,j)/i-1}{2\gcd(i,j)-1} & \text{if } i \mid n\gcd(i,j), \\ 0 & \text{otherwise.} \end{cases} \tag{5.26}$$

The result of applying the permutation δ to the runs in a state $\boldsymbol{s}$ is shown in Figure 5.7. The runs labelled 1 to $i+1$ determine the number of symbols in the runs labelled $i+2$ to $2i$. Two of the runs, 1 and $i+1$, are projected onto themselves under the permutation δ.

$\boldsymbol{s}$	1	2	3	$\cdots$	i	$i+1$	$i+2$	$\cdots$	$2i-1$	$2i$
$\pi_\delta(\boldsymbol{s})$	1	$2i$	$2i-1$	$\cdots$	$i+2$	$i+1$	i	$\cdots$	3	2

Figure 5.7: *Applying the permutation δ to the labels of a state $\boldsymbol{s}$. The highlighted runs are those that determine the remaining runs in order to leave the state $\boldsymbol{s}$ invariant under δ.*

For a state to be invariant under the permutation δ, the state must contain an equal number of players in each run and the run's equivalent under the permutation. Therefore, distributing k indistinguishable symbols among the $i-1$ distinguishable runs that do not map onto themselves under the permutation δ determines the placement of $2k$ symbols. This can be done in $\binom{k+i-2}{i-2}$ different ways. Note that $0 \leq 2k \leq n-5i$. The remaining $n-5i-2k$ symbols must then be distributed among the two runs that do map onto themselves under δ. There are $\binom{n-5i-2k+1}{1} = n-5i-2k+1$ different ways of doing this. There are thus $(n-5i-2k+1)\binom{k+i-2}{i-2}$ different ways of distributing the symbols among the runs such that the state remains invariant under the permutation δ and a total of k symbols are distributed among runs 2 to $i+1$. Summing over the possible values of k gives the total number of states that remain invariant under δ, that is

$$|F_\delta| = \sum_{k=0}^{\lfloor \frac{n-5i}{2} \rfloor} (n-5i-2k+1)\binom{k+i-2}{i-2}.$$

$\boldsymbol{s}$	1	2	3	$\cdots$	$i+1$	$i+2$	$i+3$	$\cdots$	$2i-1$	$2i$
$\pi_{\delta\rho^1}(\boldsymbol{s})$	3	2	1	$\cdots$	$i+3$	$i+2$	$i+1$	$\cdots$	5	4

Figure 5.8: *Applying the permutation $\delta\rho^1$ to the labels of a state. The highlighted runs are those that determine the remaining runs in order to leave the state $\boldsymbol{s}$ invariant under $\delta\rho^1$.*

Figure 5.8 shows the result of applying the permutation $\delta\rho^1$ to the labels of the runs of a game state $\boldsymbol{s}$. Note that the runs labelled 2 and $i+2$ are mapped to themselves, while runs 3 to $i+1$ map to runs $i+3$ to 1, considering the labels in a modular fashion. The result of applying $\delta\rho^2$ is shown in Figure 5.9. In general, it holds for the permutation which reverses the order of the runs and then shifts the runs j positions to the left, $\delta\rho^j$, that runs $j+1$ and $i+j+1$ map onto themselves, while runs $j+2$ through $i+j$ are mapped to runs $i+j+1$ through j. Therefore, distributing k symbols among the runs that do not map to themselves determines the placement of $2k$ symbols, leaving $n-5i-k$ symbols to be distributed among runs $j+1$ and $i+j+1$. Hence there are

$$|F_{\delta\rho^j}| = \sum_{k=0}^{\lfloor \frac{n-5i}{2} \rfloor} (n-5i-2k+1)\binom{k+i-2}{i-2} \tag{5.27}$$

states that remain invariant under $\delta\rho^j$.

$\boldsymbol{s}$	1	2	3	$\cdots$	$i+2$	$i+3$	$i+4$	$\cdots$	$2i-1$	$2i$
$\pi_{\delta\rho^2}(\boldsymbol{s})$	5	4	3	$\cdots$	$i+4$	$i+3$	$i+2$	$\cdots$	7	6

Figure 5.9: *Applying the permutation $\delta\rho^2$ to the labels of a state. The highlighted runs are those that determine the remaining runs in order to leave the state $\boldsymbol{s}$ invariant under $\delta\rho^2$.*

Substituting (5.25), (5.26) and (5.27) into (5.24) gives

$$Q_i = \frac{1}{2i}\left[\tbinom{n-3i-1}{2i-1} + \sum_{j\in S}\tbinom{(n-3i)\gcd(i,j)/i-1}{2\gcd(i,j)-1} + i\sum_{k=0}^{\lfloor \frac{n-5i}{2} \rfloor}(n-5i-2k+1)\tbinom{k+i-2}{i-2}\right],$$

where $S = \{x \in \mathbb{N} \mid i \text{ divides } n\gcd(i,x) \text{ and } x < i\}$, which completes the proof. □

The number of steady states, or components, in the state graph of the ESPD on a cycle of order n are tabulated in Table 5.5 for small values of n.

n	1	2	3	4	5	6	7	8	9	10	11	12	13	14	15	16	17	18	19	20
$\Xi_c(n)$	2	2	2	2	3	4	5	6	7	9	11	15	19	26	34	46	61	85	115	162

Table 5.9: *The number of steady states, $\Xi_c(n)$, of the ESPD on a cycle of order $1 \leq n \leq 20$ under the condition (5.3). These values were computed via (5.22).*

5.4.2 The game dynamics for small values of T

The following theorem characterises those initial game states of the ESPD on a cycle which lead to some form of persistent cooperation for small values of the parameter T.

Theorem 5.7 *If the underlying graph of the ESPD is a cycle and (5.3) holds, then any state containing at least one of the substates $\langle C\rangle^5$, $DD\langle C\rangle^3DD$ or $DD\langle C\rangle^4D$ (or its reverse substate $D\langle C\rangle^4DD$) is not in the component of the state graph which contains the all-defector steady state.*

The proof of Theorem 5.7 is similar to that of Theorem 5.3.

The state graphs for the ESPD on an n-cycle are shown in Figure 5.10 for $5 \leq n \leq 8$. Note that the state graph graphs are pseudo-forests and that the number of cooperators is non-increasing from round to round.

5.4.3 The probability of persistent cooperation for small values of T

In this section the probability, $P_c(n)$, that some form of cooperation will persist from a randomly generated intial state of the ESPD on an n-cycle is determined. Let b_n be the total number of words of length n containing none of the forbidden substrings $CCCCC$, $DCCCCDD$, $DDCCCCD$ or $DDCCCDD$ mentioned in Theorem 5.7, but containing at least one D. The value of b_n for $n \geq 7$ may be determined using the transfer matrix method described in §2.3. A similar approach as the one used to derive (5.19) was attempted, but yielded a large set of interdependent variables which were difficult to determine. The transfer matrix method, on the other hand, proved to be a much simpler and a more direct approach when the underlying graph is a cycle.

A string is said to be a *legal string* if it contains none of the substrings mentioned in Theorem 5.7. Let D_6 be the digraph of order 64 in which each vertex represents one of the 64 binary strings of length six. A vertex v_i, representing the string $s_1s_2s_3s_4s_5s_6$, is incident to a vertex v_j, representing string $s_2s_3s_4s_5s_6s_7$ in D_6 if and only if $s_1s_2s_3s_4s_5s_6s_7$ is a legal string. The graph D_6 is shown in Figure 5.12. Counting the number of strings, b_n, for values of $n \geq 7$ is equivalent to counting the number of closed directed walks of length n in D_6. Note that every legal string of length $n \geq 7$ has a corresponding closed directed walk in D_6. Consider, as an example, the closed walk associated with the string $DCDDDCDD$ in Figure 5.11.

Let $\boldsymbol{A}$ be the adjacency matrix of the digraph D_6, as shown in Table 5.13. Then $\det(\boldsymbol{I} - x\boldsymbol{A}) = 1 - x - x^2 - x^3 - x^4 + x^6 - x^7$, and it follows by Lemma 2.2 that

$$\sum_{n=1}^{\infty} b_n x^n = -\frac{x\left(-1 - 2x - 3x^2 - 4x^3 + 6x^5 - 7x^6\right)}{1 - x - x^2 - x^3 - x^4 + x^6 - x^7}. \tag{5.28}$$

It therefore follows by Lemma 2.1 that b_n may be calculated recursively by means of the relationship

$$b_n = b_{n-1} + b_{n-2} + b_{n-3} + b_{n-4} - b_{n-6} + b_{n-7}, \tag{5.29}$$

The seed values for (5.29) may be found by taking the McClaurin expansion of (5.28), that is

$$-\frac{x\left(-1 - 2x - 3x^2 - 4x^3 + 6x^5 - 7x^6\right)}{1 - x - x^2 - x^3 - x^4 + x^6 - x^7} = x + 3x^2 + 7x^3 + 15x^4 + 26x^5 + 45x^6 + 99x^7 + \cdots.$$

These seed values are the coefficients of the expansion above, and are listed in Table 5.10. The values $b_1^*, \ldots, b_6^*$ mereley serve to seed (5.29) and are not equivalent to $b_1, \ldots, b_6$.

b_1^*	b_2^*	b_3^*	b_4^*	b_5^*	b_6^*	b_7
1	3	7	15	26	45	99

Table 5.10: *The values required to seed the recurrence equation for b_n in (5.29).*

The arguments of this section lead to the following result.

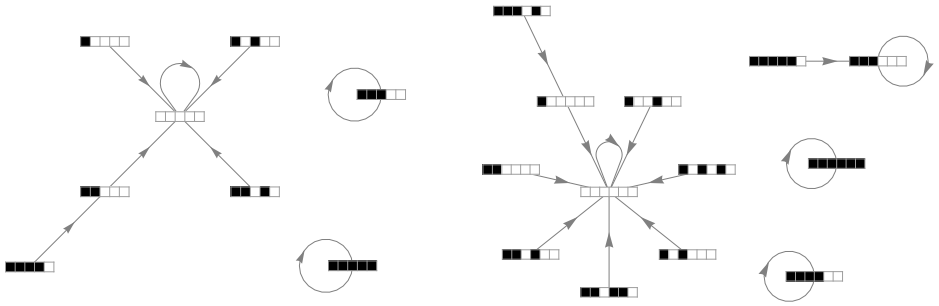

(a) $n = 5$ (b) $n = 6$

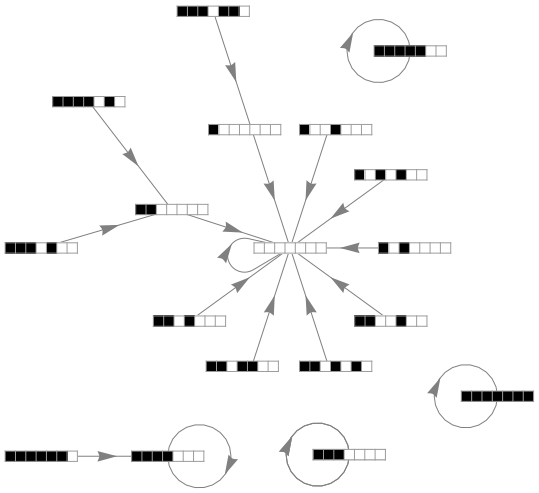

(c) $n = 7$

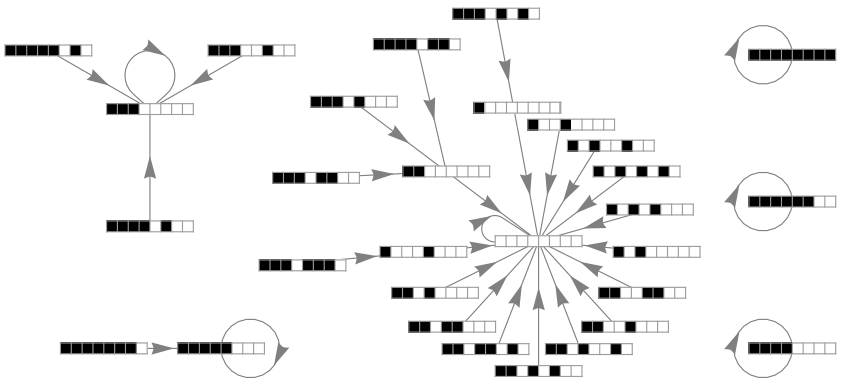

(d) $n = 8$

Figure 5.10: *The state graph of the ESPD on an n-cycle, for $5 \leq n \leq 8$, for the case where $T \leq 2 - P$. The strategy of cooperation (C) is denoted by a black square, while that of defection (D) is denoted by a white square in each state which is represented by a wrapping array of squares.*

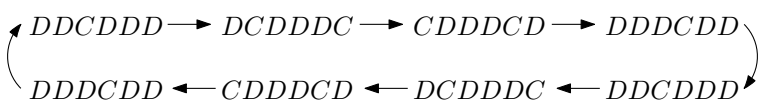

Figure 5.11: *The closed directed walk in the digraph D_6 associated with the string DCDDDCDD.*

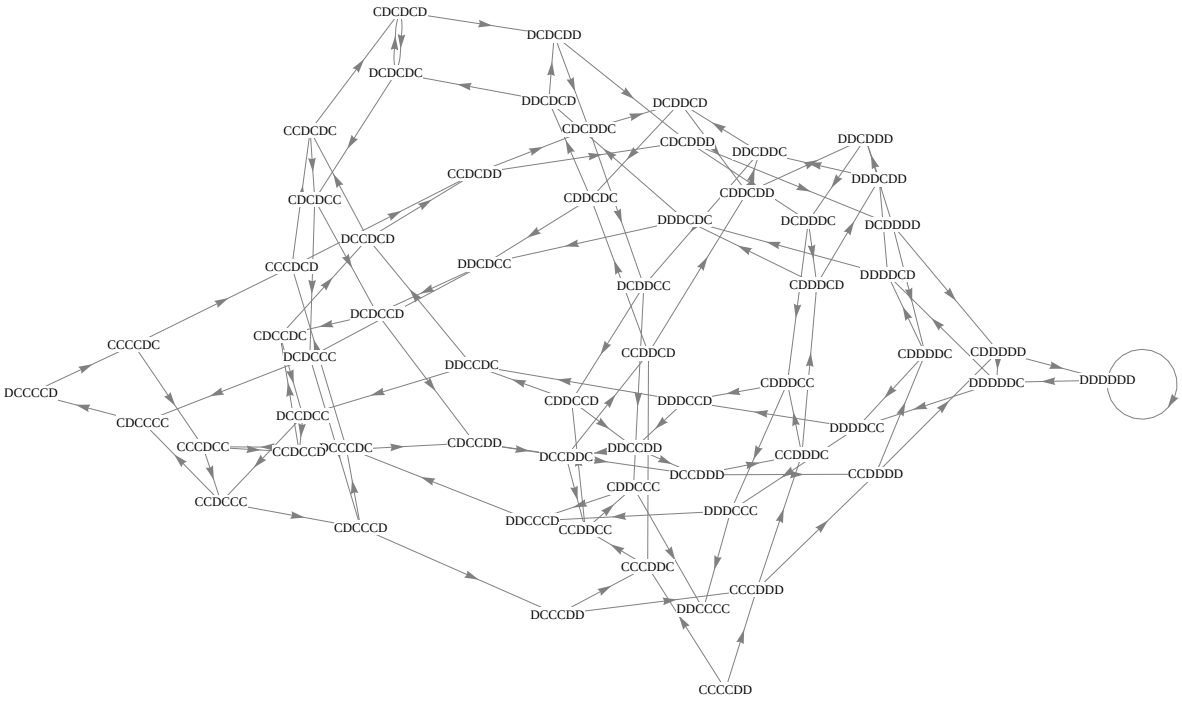

Figure 5.12: *The digraph D_6 used to calculate the number of words of length n which do not contain any of the substrings listed in Theorem 5.7.*

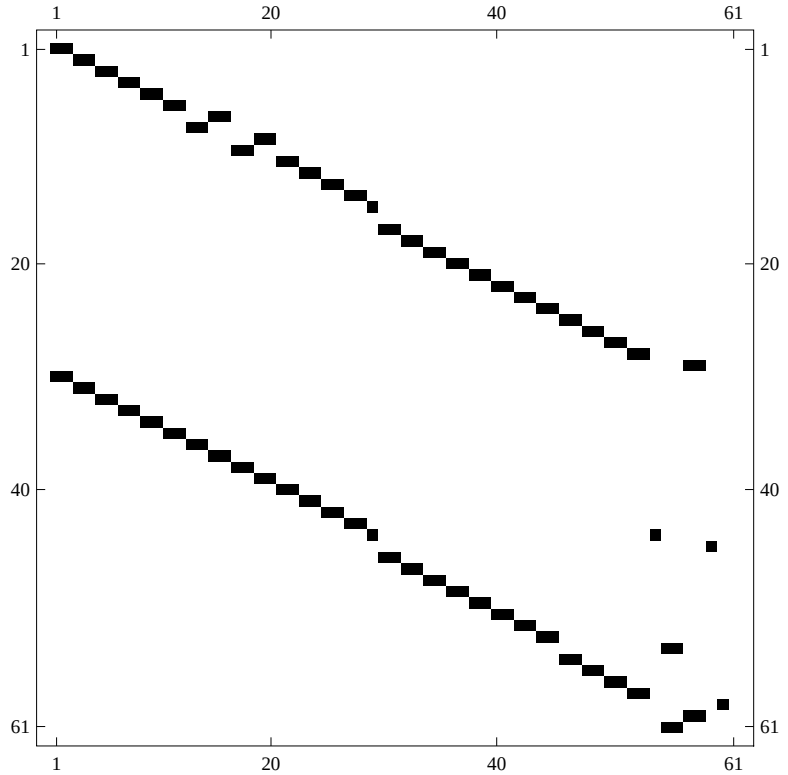

Figure 5.13: *A visual representation of the adjacency matrix $\boldsymbol{A}$ of the digraph D_6. Black squares indicate entries of the matrix equal to 1; the remaining entries are all 0.*

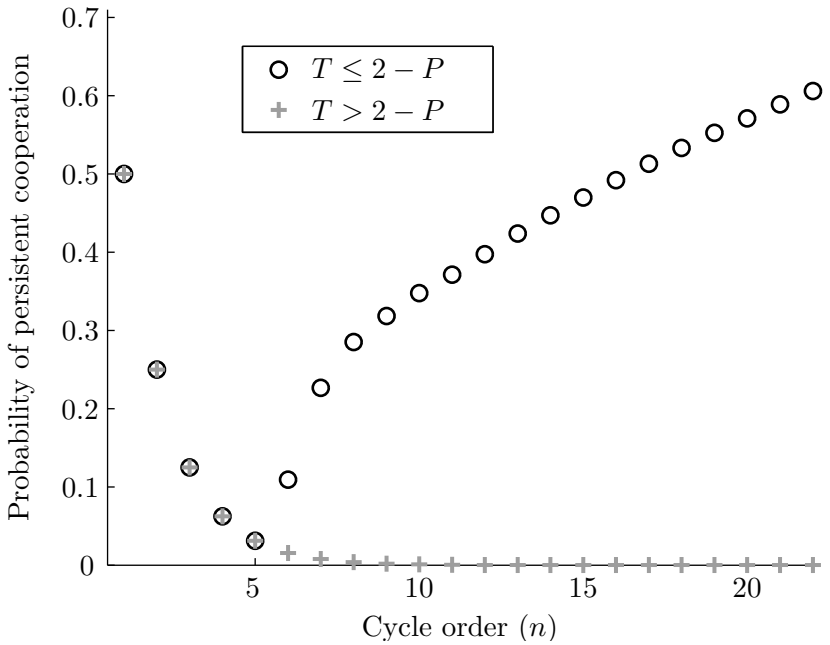

Figure 5.14: *The probability of randomly generating an initial state for the ESPD on a cycle of order n which is not attracted by the all-defector steady state.*

Theorem 5.8 *The probability that a randomly generated initial state of the ESPD on a cycle of order $n \geq 7$ will lead to persistent cooperation is given by*

$$P_c(n) = 1 - \frac{b_n}{2^n},$$

where b_n satisfies (5.29) with seed values as specified in Table 5.10.

The values of b_n for small values of n are listed in Table 5.11 and the probability that some form of cooperation will persist from a randomly generated initial game state is shown graphically in Figure 5.14. The asymptotic behaviour of $P_c(n)$ as $n \to \infty$ is described in the following theorem.

Theorem 5.9 *Let $P_c(n)$ denote the probability that a randomly generated intial state of the ESPD on a cycle of order n is not attracted by the all-defector steady state, $\langle D \rangle^n$. Then*

$$\lim_{n \to \infty} P_c(n) = 1.$$

The proof of Theorem 5.9 is similar to that of Theorem 5.5.

5.5 Chapter summary

Analytical means were employed in this chapter to analyse the game dynamics of the ESPD on a path or cycle. It was found that the number of states in the ESPD on a path or a cycle of order n increases exponentially as the order n of the underlying graph increases. This number of components is shown graphically in Figure 5.15 as a function of the underlying graph order.

$n \to$	1	2	3	4	5	6	7	8	9	10	11	12	13
b_n	1	3	7	15	31	57	99	183	349	668	1 288	2 469	4 720
2^n	2	4	8	16	32	64	128	256	512	1 024	2 048	4 096	8 192

$n \to$	14	15	16	17	18	19	20	21	22
b_n	9 061	17 372	33 303	63 836	122 391	234 651	449 840	862 407	1 653 358
2^n	16 384	32 768	65 536	131 072	262 144	524 288	1 048 576	2 097 152	4 194 304

Table 5.11: *Information for computing the probability of randomly generating an initial state of the ESPD on a cycle of order n which is not attracted by the all-defector steady state $\langle D \rangle^n$. This probability is $1 - b_n/2^n$ according to Theorem 5.8.*

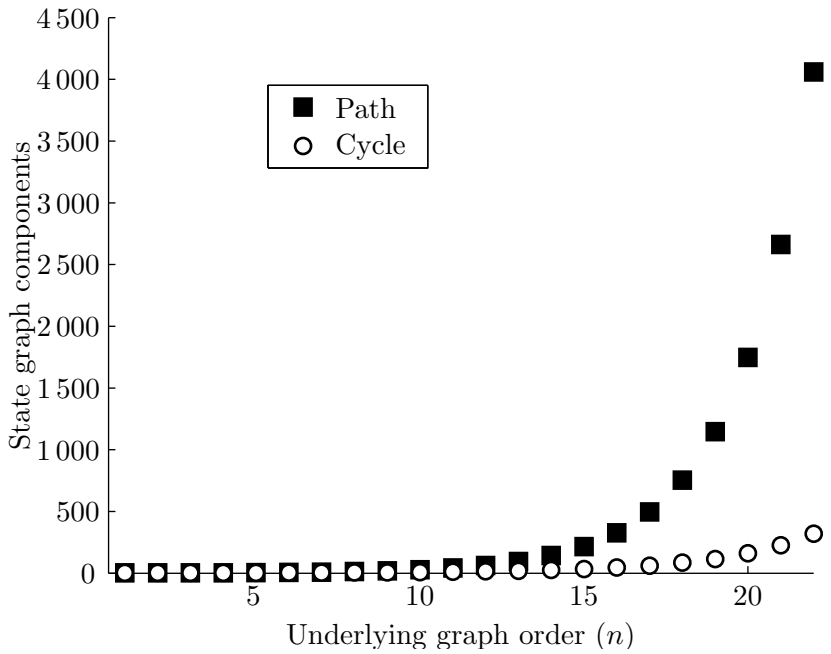

Figure 5.15: *The number of components of the state graph for the ESPD where the underlying graph is either a path of order n or an n-cycle.*

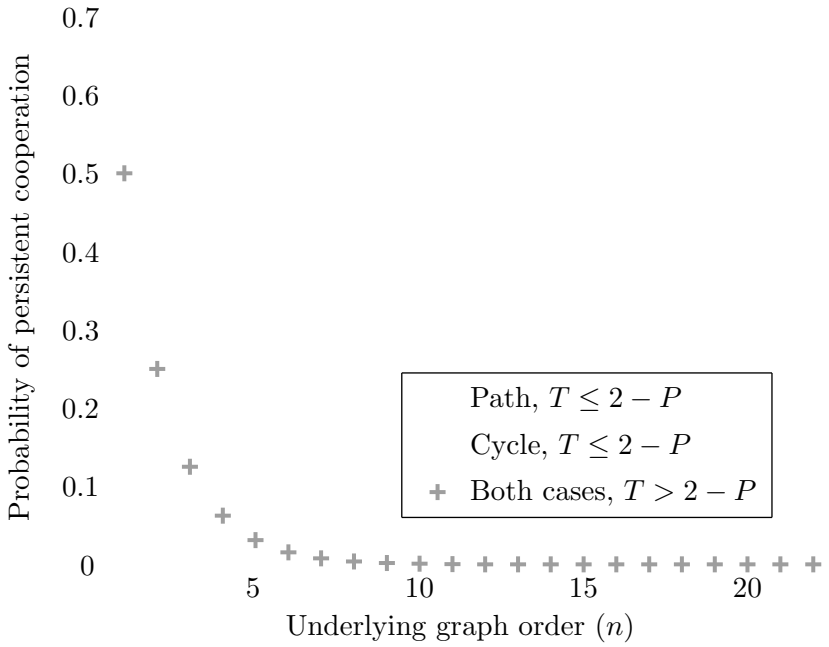

Figure 5.16: *The probability of randomly generating an initial state for the ESPD on a path of order n or an n-cycle which is not attracted by the all-defector steady state.*

It was shown that for large values of T (*i.e.* for $T > 2 - P$), cooperation is only possible if the initial game state contains cooperators only. However, it is possible for cooperation to persist in the case were $T \leq 2 - P$ even if the initial state does not contain cooperators only. The initial states which lead to persistent cooperation were characterised for the ESPD on a path or cycle. If the underlying graph is a path or a cycle of order $n > 7$, then the number of states which do not lead to persistent cooperation may be calculated by means of the recursive relationship

$$f_n = f_{n-1} + f_{n-2} + f_{n-3} + f_{n-4} - f_{n-6} + f_{n-7}.$$

The values used to seed the above relationship depends on whether the underlying graph is a path or a cycle. If the underlying graph is a path, then the values used to seed the relationship are $f_1 = 1$, $f_2 = 3$, $f_3 = 7$, $f_4 = 11$, $f_5 = 21$, $f_6 = 42$, and $f_7 = 81$. However, if the underlying graph is a cycle, then the values used to seed the relationship are $f_1 = 1$, $f_2 = 3$, $f_3 = 7$, $f_4 = 15$, $f_5 = 26$, $f_6 = 45$ and $f_7 = 99$. The probability of randomly generating an initial game state that will lead to some form of persistent cooperation may be computed using the formula $P(n) = 1 - f_n/2^n$. It was found that the likelihood of cooperation increases towards certainty as the order of the underlying graph increases; this is illustrated graphically in Figure 5.16.

CHAPTER 6

The ESPD on a grid graph

Contents

In this chapter the dynamics of the ESPD is investigated with a grid graph as underlying graph. A grid graph has a number of symmetries which give rise to more interesting game state automorphism classes than in the case with paths and cycles as underlying graphs. These symmetries on square and rectangular grids are determined and the corresponding automorphism classes are enumerated.

The P-T phase plane is constructed for both grids with and without wrapping. It is possible to visualise the complete game dynamics for the EPSD on small grids by drawing the state graphs of the game. State graphs are constructed for the ESPD on grid graphs of dimensions 2×2, 3×3, 2×3 and 2×4 for each region in the phase plane. However, as the dimensions of the underlying graph increases the number of state automorphism classes increases exponentially and a complete analysis of the game is no longer possible if the underlying graph is sufficiently large.

6.1 Automorphism classes of game states

There are 2^{nm} ways of assigning one of the strategies C or D to the players in the ESPD on a grid graph of dimensions $m \times n$. Due to the symmetries in the underlying graph, a number of these states may be considered equivalent. The game states of the ESPD with the cartesian product $C_3 \times C_3$ as the underlying graph are shown as an example in Table 6.1, where C_n

Class	Class leader	Automorphic to	Class size
1			1
2			9
3			18
4			6
5			18
6			36
7			9
8			36
9			36
10			36
11			36
12			6
13			9
14			9
15			6
16			36
17			36
18			9
19			36
20			36
21			36
22			18
23			6
24			18
25			9
26			1
		Total: 512	

Table 6.1: *All the possible states of the ESPD on a 3×3 grid with periodic boundary conditions. The second column contains the class leaders of the various state automorphism classes (the rows of the table).*

denotes a cycle of order n, as in Chapter 5. Although there are $2^9 = 512$ distinct game states, these states organise themselves into 26 automorphism classes, as indicated in the table.

6.1.1 Game state automorphism classes for grids without wrapping

Counting the number of game state automorphism classes for the ESPD on a grid graph is equivalent to counting the number of ways that a checkerboard can be coloured using two colours; this may be achieved using the Cauchy-Frobenius lemma, as discussed by Martin [27]. Martin [27] applied this enumeration method to square checkerboards, whereas the method is presented here for counting the number of state automorphism classes for square grid graphs without wrapping and is then extended to include rectangular grid graphs as well.

The dimensions of the graph influence the number of symmetries present in the graph and hence also the automorphisms that need to be considered. The underlying graph may be a square grid with odd or even dimensions, or a rectangular grid with none, one or both of its dimensions odd.

Consider first the square Cartesian product $P_n \times P_n$ as underlying graph of the ESPD, where P_n again denotes a path of order n. There are eight transformations that may be applied to the graph G which preserves the adjacencies of the graph; these are exactly the elements of the dihedral group $\mathcal{D}_4$, namely: identity (ι), rotation through 90° (ρ), rotation through 180° (ρ^2), rotation through −90° (ρ^3), the two reflections about the diagonals (σ_p and σ_m), and the two reflections about the perpendicular bisector of the sides (σ_v and σ_h). The axes of symmetry for grids of odd and even dimensions are shown in Figure 6.1(a) and (b), respectively. Note that in the case where the grid has odd dimensions, the axes of symmetry intersect at the centre point of the centre cell, whereas if the dimensions are even, the axes of symmetry intersect at the common corner of the four centre cells.

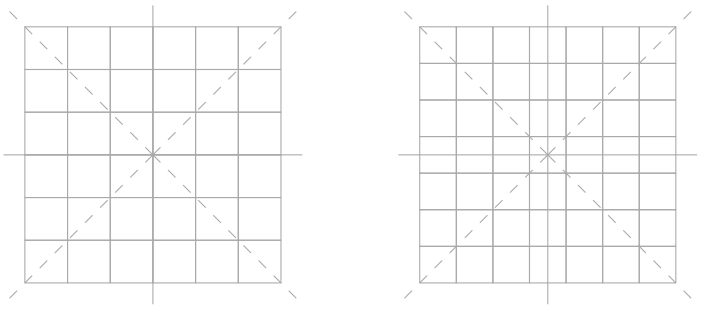

(a) (b)

Figure 6.1: *Square grids of (a) even and (b) odd dimensions, with the axes of symmetry indicated by means of black dashed and solid lines.*

Let $\mathcal{X}$ be the set of all the states of the ESPD with $G = P_n \times P_n$ as the underlying graph and let $\mathcal{G} = \{\iota, \rho, \rho^2, \rho^3, \sigma_v, \sigma_h, \sigma_p, \sigma_m\}$ be the symmetry group explained above. Then, according to Theorem 2.1, the number of equivalence classes into which $\mathcal{X}$ is partitioned by $\mathcal{G}$ is

$$\frac{1}{|\mathcal{G}|} \sum_{g \in \mathcal{G}} |F_g|, \tag{6.1}$$

where $|F_g|$ is the number of states in $\mathcal{X}$ that are invariant under g. In order to count the number of states which remain unchanged under an isometry g, the two cases where n is even or odd need to be considered separately.

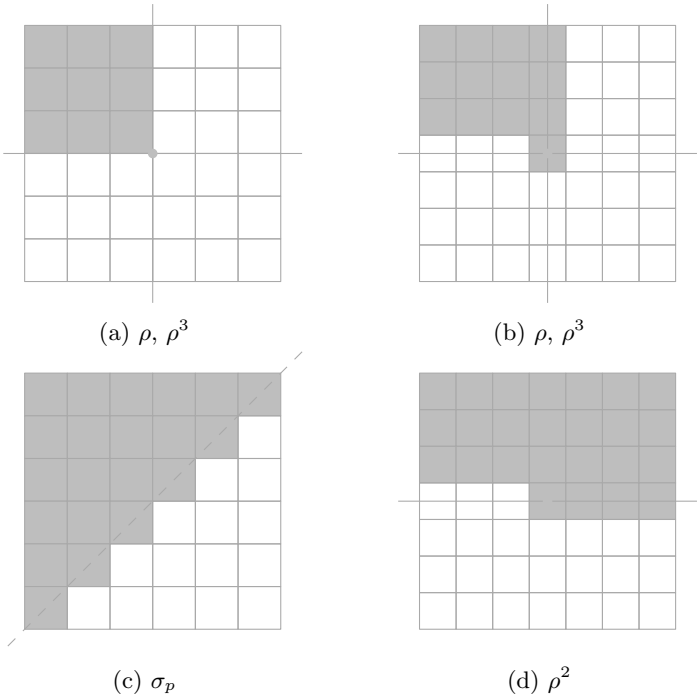

(a) ρ, ρ^3 (b) ρ, ρ^3

(c) σ_p (d) ρ^2

Figure 6.2: *Shaded cells indicate those players which, once assigned strategies, determine the strategies of the remaining players in order for a state to remain unchanged under the relevant transformations.*

When n is even, the centre of the grid, as well as the axis of rotation, is at the common corner of the four centre cells. The grid can be divided into four disjoint quadrants each containing $\frac{n^2}{4}$ players. When considering ρ, the transformation which rotates the grid through 90°, assigning strategies to the players in the first quadrant fixes the strategies of the players in the second quadrant, the second fixes the third and the third the fourth. There are $2^{n^2/4}$ ways of assigning strategies to the players in the first quadrant, indicated by the shaded cells in Figure 6.2(a), and hence the number of states that are invariant under ρ is given by $|F_\rho| = 2^{n^2/4}$. Similarly, $|F_{\rho^3}| = 2^{n^2/4}$. Next consider the transformation ρ^2, which represents a rotation through 180°. Assigning strategies to the top half of the players fixes the strategies of the bottom half, and so $|F_{\rho^2}| = 2^{n^2/2}$. In order for a state to remain unchanged upon reflection about the vertical axis, the assignment of strategies to the players has to be symmetric with respect to the vertical axis; again $2^{n^2/2}$ assignments of strategies have this property. Reflection about the diagonal calls for the assignment of strategies under the diagonal to be a mirror image of the assignment of strategies above it. Assigning strategies to the $1 + 2 + 3 + \ldots + n = (n^2 + n)/2$ players on and above the diagonal, indicated by the shaded cells in Figure 6.2(c), and repeating the pattern below the diagonal would result in a game state which is symmetric with respect to a diagonal; hence $|F_{\sigma_p}| = |F_{\sigma_m}| = 2^{(n^2+n)/2}$.

When n is odd, the centre of the grid coincides with the midpoint of the centre cell and each quadrant shares a number of cells with the neighbouring quadrant. For each transformation $g \in \mathcal{G}$ the centre player is mapped to itself and can therefore be assigned a strategy independently of those of the other players. Assigning strategies to the shaded players in Figure 6.2(b) fixes the strategies of all the players when the transformation ρ or ρ^3 is applied. Assigning strategies to the $\left(\frac{n-1}{2}\right)^2$ players in the first quadrant which are not on the axis of symmetry and to the $(n + 1)/2$ players on the boundary between two quadrants, including the centre cell, fixes the

strategies of the remaining players under the transformations ρ and ρ^3. Therefore,

$$|F_\rho| = |F_{\rho^3}| = 2^{\left(\frac{(n+1)^2}{4} + \frac{n+1}{1}\right)} = 2^{(n^2+3)/4}.$$

Assigning strategies to half of the players, including the centre player as indicated by the shaded cells in Figure 6.2(d), determines the strategies of the remaining players in order for the state to remain invariant under ρ^3. Therefore, $|F_{\rho^3}| = 2^{(n^2+1)/2}$. It may similarly be shown that $|F_{\sigma_m}| = |F_{\sigma_p}| = 2^{(n^2+n)/2}$.

A summary of the values of $|F_g|$ for $g \in \mathcal{G}$ are tabulated in Table 6.3. It follows by (6.1) that the number of game state automorphism classes for an $n \times n$ grid without wrapping is given by

$$\Lambda_s(n) = \begin{cases} \frac{1}{8}\left(2^{n^2} + 2 \cdot 2^{n^2/4} + 3 \cdot 2^{n^2/2} + 2 \cdot 2^{(n^2+n)/2}\right) & \text{if } n \text{ is even,} \\ \frac{1}{8}\left(2^{n^2} + 2 \cdot 2^{(n^2+3)/4} + 2^{(n^2+1)/2} + 4 \cdot 2^{(n^2+n)/2}\right) & \text{if } n \text{ is odd.} \end{cases}$$

The sequence $\{\Lambda_s(n)\}_{n=1}^{7}$ is listed along the diagonal of Table 6.2 and is Sloane's sequence A054247 [49].

m \ n	1	2	3	4	5	6	7
1	**2**	**3**	**6**	**10**	**20**	**36**	**72**
2		**6**	**24**	**76**	288	1 072	4 224
3			**102**	1 120	8 640	66 816	529 920
4				8 548	263 680	4 197 376	67 133 440
5					4 211 744	268 517 376	8 590 786 560
6						8 590 557 312	1 099 516 870 656
7							70 368 882 591 744

Table 6.2: *The number of game state automorphism classes for the ESPD with the grid graph $P_n \times P_m$ as underlying graph. The complete state graphs corresponding to the entries in boldface may be found in Chapter 5, later in this chapter and in Appendix B.*

Consider next the ESPD with the rectangular Cartesian product $P_n \times P_m$ as underlying graph, where $n \neq m$. In this case the automorphism classes may be counted in a similar fashion as in the case of a square grid. The symmetries which have to be considered are the identity operation (ι), rotation through 180° (ρ^2), reflection along the horizontal axis of symmetry (σ_h) and reflection along the vertical axis of symmetry (σ_v). The group acting on the set of states is $\mathcal{G}_r = \{\iota, \rho^2, \sigma_h, \sigma_v\}$. As an example, the shaded cells in Figure 6.3 indicate those players which, once assigned strategies, would determine the strategies of the remaining players in order for the state to remain invariant under the transformation ρ^2. A summary of the values of $|F_g|$ for $g \in \mathcal{G}_r$ is given in Table 6.4.

	ι	ρ	ρ^2	ρ^3	σ_v	σ_h	σ_p	σ_m
n even	2^{n^2}	$2^{n^2/4}$	$2^{n^2/2}$	$2^{n^2/4}$	$2^{n^2/2}$	$2^{n^2/2}$	$2^{\frac{n^2+n}{2}}$	$2^{\frac{n^2+n}{2}}$
n odd	2^{n^2}	$2^{(n^2+3)/4}$	$2^{(n^2+1)/2}$	$2^{(n^2+3)/4}$	$2^{(n^2+n)/2}$	$2^{(n^2+n)/2}$	$2^{(n^2+n)/2}$	$2^{(n^2+n)/2}$

Table 6.3: *The number of states invariant under the transformations belonging to the dihedral group $\mathcal{D}_4$.*

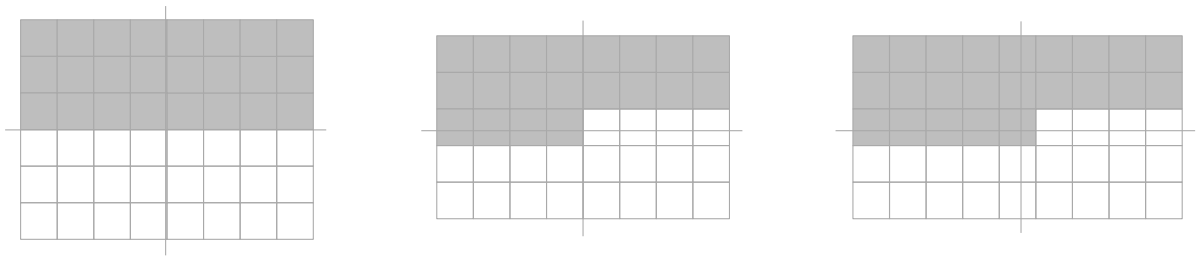

(a) (b) (c)

Figure 6.3: *The axes of symmetry (shown in black) for rectangular lattice. The grey shaded cells are those which determine the identical states under a 180 degree rotation for (a) a lattice with even dimensions, (b) one of the dimensions odd and (c) both dimensions odd.*

	$\lvert F_\iota\rvert$	$\lvert F_{\rho^2}\rvert$	$\lvert F_{\sigma_v}\rvert$	$\lvert F_{\sigma_h}\rvert$
m, n both even	2^{nm}	$2^{mn/2}$	$2^{mn/2}$	$2^{mn/2}$
m even, n odd	2^{nm}	$2^{mn/2}$	$2^{(mn+m)/2}$	$2^{mn/2}$
m odd, n even	2^{nm}	$2^{mn/2}$	$2^{mn/2}$	$2^{(mn+n)/2}$
m, n both odd	2^{nm}	$2^{(nm+1)/2}$	$2^{(mn+m)/2}$	$2^{(mn+n)/2}$

Table 6.4: *The values of $|F_g|$, the number of game states fixed by the isometry $g \in \mathcal{G}_r$.*

It follows by (6.1) that the number of game state automorphism classes for an $m \times n$ grid without wrapping is given by

$$\Lambda_r(n,m) = \begin{cases} \frac{1}{4}\left(2^{nm} + 3 \cdot 2^{mn/2}\right) & \text{if both } m \text{ and } n \text{ are even,} \\ \frac{1}{4}\left(2^{nm} + 2 \cdot 2^{mn/2} + 2^{m(n+1)/2}\right) & \text{if } m \text{ is even and } n \text{ is odd,} \\ \frac{1}{4}\left(2^{nm} + 2 \cdot 2^{mn/2} + 2^{n(m+1)/2}\right) & \text{if } m \text{ is odd and } n \text{ is even,} \\ \frac{1}{4}\left(2^{nm} + 2^{(nm+1)/2} + 2^{n(m+1)/2} + 2^{m(n+1)/2}\right) & \text{if both } m \text{ and } n \text{ are odd.} \end{cases}$$

The values of $\Lambda_r(n,m)$ are tabulated off the diagonal in Table 6.2 for $1 \leq n < m \leq 7$.

6.1.2 Game state automorphism classes for grids with wrapping

The Cauchy Frobenius Lemma (Theorem 2.1) may again be employed to enumerate the game state automorphism classes $\Lambda_t(m,n)$ of the ESPD with the toroidal grid graph $C_m \times C_n$ as underlying graph. To make use of the Cauchy Frobenius lemma, the relevant symmetry groups and the value of $|F_g|$ for the appropriate isometries g are discussed in this section. A description of the symmetry groups of the toroidal grid graphs $C_2 \times C_n$ for $n > 2$ and $C_m \times C_n$ for $3 \leq m < n$ follow below.

The symmetry group $\mathcal{G}_t$ of the game states of the ESPD with $C_m \times C_n$ as underlying graph, where $3 \leq m < n$, is equivalent to the wallpaper group **pmm**. The group $\mathcal{G}_t$ contains the following members: the identity ι; rotation through 180° (ρ^2); reflection about the vertical (σ_v) and horizontal (σ_h) axes of symmetry; the vertical translation of rows by i positions (δ_u^i); the horizontal translation of columns by j positions (δ_r^j); the combination of the vertical and horizontal translation isometries ($\delta_u^i \delta_r^j = \delta^{i,j}$); and the glide reflections $\sigma_v\delta^{i,j}$, $\sigma_h\delta^{i,j}$ and $\rho_v^2\delta^{i,j}$ for values $1 \leq i \leq m-1$ and $1 \leq j \leq n-1$. That is

$$\mathcal{G}_t = \{\iota,\ \sigma_v,\ \sigma_h,\ \rho^2,\ \delta_u^i,\ \delta_r^j,\ \delta^{i,j},\ \sigma_v\delta_u^i,\ \sigma_h\delta_u^i,\ \rho^2\delta_u^i,\ \sigma_v\delta_r^j,\ \sigma_h\delta_r^j,\ \rho^2\delta_r^j,\ \sigma_v\delta^{i,j},\ \sigma_h\delta^{i,j},\ \rho^2\delta^{i,j}\}$$

for all $1 \leq i \leq m-1$ and $1 \leq j \leq n-1$.

The symmetry group $\mathcal{G}_s$ of a square $n \times n$ torus are the members of the wallpaper group **p4m**.

The group of symmetries $\mathcal{G}_{2\times n}$ of the ESPD with the grid graph $C_2 \times C_n$ as underlying graph, is a subgroup of $\mathcal{G}_t$. The isometries σ_h and δ_u^1 are equivalent; therefore $\mathcal{G}_{2\times n}$ contains only one of these two isommetries. The symmetry group is

$$\mathcal{G}_{2\times n} = \{\iota, \sigma_v, \sigma_h, \rho^2, \delta_r^1, \ldots, \delta_r^{n-1}, \sigma_v\delta_r^1, \ldots, \sigma_v\delta_r^{n-1}, \sigma_h\delta_r^1, \ldots, \sigma_h\delta_r^{n-1}, \rho^2\delta_r^1, \ldots, \rho^2\delta_r^{n-1}\}.$$

Enumerating $|F_g|$ for the simple case where the relevant group is $\mathcal{G}_{2\times n}$ is considered here as an example. Let $|F_g|$ be the the number of states fixed by $g \in \mathcal{G}_{2\times n}$. The values of $|F_\iota|$, $|F_{\rho^2}|$, $|F_{\sigma_v}|$ and $|F_{\sigma_h}|$ have been computed previously and may be found in Table 6.4, that is $|F_\iota| = 2^{mn} = 2^{2n}$, $|F_{\rho^2}| = 2^{\frac{mn}{2}} = 2^n$ and $|F_{\sigma_h}| = 2^{mn/2} = 2^n$. Furthermore, $|F_{\sigma_v}| = 2^{mn/2} = 2^n$ in the case where n is even and $|F_{\sigma_v}| = 2^{(mn+n)/2} = 2^{n+1}$ when n is odd.

Derivation of the values of $|F_{\delta_r^j}|$, $|F_{\sigma_h\delta_r^i}|$, $|F_{\sigma_h\delta_r^i}|$ and $|F_{\rho^2\delta_r^j}|$ may be performed similarly, as described in Lemmas A.1–A.4 in Appendix A. A summary of the values of $|F_g|$ for each isometry $g \in \mathcal{G}_{2\times n}$ is provided in Table 6.5. It follows from the table and the Cauchy-Frobenius Lemma (Lemma 2.1) that

$$\begin{aligned}\Lambda_t(2,n) &= \frac{1}{|\mathcal{G}_{n\times 2}|}\sum_{g\in\mathcal{G}_{2\times n}} |F_g| \\ &= \frac{1}{4n}\left(2^{2n} + \sum_{i=1}^{n-1}[2^{2\gcd(n,i)} + 2^{\gcd(2i,n)}] + \begin{cases}(\frac{7}{2}n+1)2^n & \text{if } n \text{ is even}\\ (3n+1)2^n & \text{if } n \text{ is odd}\end{cases}\right).\end{aligned}$$

Isometry (g)	$\lvert F_g\rvert$ (even n)	$\lvert F_g\rvert$ (odd n)	isometries
ι	2^{2n}	2^{2n}	1
σ_v	2^n	2^{n+1}	1
σ_h	2^n	2^n	1
ρ^2	2^n	2^n	1
δ_r^j	$2^{2\gcd(n,j)}$	$2^{2\gcd(n,j)}$	$n-1$
$\sigma_v\delta_r^j$	$\begin{cases}2^n & \text{if } j \text{ is even}\\ 2^{n+2} & \text{otherwise}\end{cases}$	2^{n+1}	$n-1$
$\sigma_h\delta_r^i$	$2^{\gcd(2j,n)}$	$2^{\gcd(2j,n)}$	$n-1$
$\rho^2\delta_r^j$	2^n	2^n	$n-1$
		Total:	$4n$

Table 6.5: *The number of game states fixed by each $g \in \mathcal{G}_{n\times 2}$, where $\mathcal{G}_{n\times 2}$ is the group of isommetries belonging to the game states of the ESPD with the toroidal grid graph $C_2 \times C_n$ as underlying graph. The inequality chain $1 \leq j < n$ is assumed to hold in the table.*

The enumeration of $|F_g|$ for isometries in $\mathcal{G}_t$ not yet considered above is rather technical. The derivations may be found in Lemmas A.5–A.10 in Appendix A. A summary of the values of $|F_g|$ for each isometry $g \in \mathcal{G}_t$ may be found in Table 6.6.

Isometry (g)	Ref	$\lvert F_g\rvert$				
		m and n both even	m even and n odd	m odd and n even	m and n both odd	isometries
ι	T6.4	2^{mn}	2^{mn}	2^{mn}	2^{mn}	1
ρ^2	T6.4	$2^{mn/2}$	$2^{mn/2}$	$2^{mn/2}$	$2^{(nm+1)/2}$	1
σ_v	T6.4	$2^{mn/2}$	$2^{(mn+m)/2}$	$2^{mn/2}$	$2^{(mn+m)/2}$	1
σ_h	T6.4	$2^{mn/2}$	$2^{mn/2}$	$2^{(mn+n)/2}$	$2^{(mn+n)/2}$	1
δ_r^j	LA.1	$2^{m\gcd(n,j)}$	$2^{m\gcd(n,j)}$	$2^{m\gcd(n,j)}$	$2^{m\gcd(n,j)}$	$n-1$
δ_u^i	LA.1*	$2^{n\gcd(m,i)}$	$2^{n\gcd(m,i)}$	$2^{n\gcd(m,i)}$	$2^{n\gcd(m,i)}$	$m-1$
$\sigma_v\delta_r^j$	LA.2	$2^{\frac{mn}{2}+m}$ odd j, $2^{\frac{mn}{2}}$ even j	$2^{\frac{m(n+1)}{2}}$	$2^{\frac{mn}{2}+m}$ odd j, $2^{\frac{mn}{2}}$ even j	$2^{\frac{m(n+1)}{2}}$	$n-1$
$\sigma_h\delta_u^i$	LA.2*	$2^{\frac{mn}{2}+n}$ odd i, $2^{\frac{mn}{2}}$ even i	$2^{\frac{mn}{2}+n}$ odd i, $2^{\frac{mn}{2}}$ even i	$2^{\frac{(m+1)n}{2}}$	$2^{\frac{(m+1)n}{2}}$	$m-1$
$\sigma_h\delta_r^j$	LA.3	$2^{\frac{m}{2}\gcd(2j,n)}$	$2^{\frac{m}{2}\gcd(2j,n)}$	$2^{\frac{m-1}{2}\gcd(2j,n)+\gcd(j,n)}$	$2^{\frac{m-1}{2}\gcd(2j,n)+\gcd(j,n)}$	$n-1$
$\sigma_v\delta_u^i$	LA.6	$2^{\frac{n}{2}\gcd(2i,m)}$	$2^{\frac{n-1}{2}\gcd(2i,m)+\gcd(i,m)}$	$2^{\frac{n}{2}\gcd(2i,m)}$	$2^{\frac{n-1}{2}\gcd(2i,m)+\gcd(i,m)}$	$m-1$
$\rho^2\delta_r^j$	LA.4	$2^{\frac{mn}{2}}$	$2^{\frac{mn}{2}}$	$2^{\frac{mn}{2}}$ even j, $2^{\frac{mn}{2}+1}$ odd j	$2^{\frac{mn}{2}+\frac{1}{2}}$	$n-1$
$\rho^2\delta_u^i$	LA.7	$2^{\frac{mn}{2}}$	$2^{\frac{mn}{2}}$ even i, $2^{\frac{mn}{2}+1}$ odd i	$2^{\frac{mn}{2}}$	$2^{\frac{mn}{2}+\frac{1}{2}}$	$m-1$
$\delta^{i,j}$	LA.5	$2^{\gcd[n\gcd(i,m),m\gcd(j,n)]}$	$2^{\gcd[n\gcd(i,m),m\gcd(j,n)]}$	$2^{\gcd[n\gcd(i,m),m\gcd(j,n)]}$	$2^{\gcd[n\gcd(i,m),m\gcd(j,n)]}$	$(m-1)(n-1)$
$\rho^2\delta^{i,j}$	LA.8	$(\frac{7}{4}mn-m-n+1)2^{\frac{mn}{2}}$	$(\frac{3}{2}mn-\frac{3}{2}m-n+1)2^{\frac{mn}{2}}$	$(\frac{3}{2}mn-m-\frac{3}{2}n+1)2^{\frac{mn}{2}}$	$(m-1)(n-1)2^{\frac{mn+1}{2}}$	$(m-1)(n-1)$
$\sigma_v\delta^{i,j}$	LA.9	$2^{\frac{n}{2}\gcd(2i,m)}$ even j, $2^{\left(\frac{n}{2}-1\right)\gcd(2i,m)+2\gcd(m,i)}$ odd j	$2^{\frac{n-1}{2}\gcd(2i,m)+\gcd(m,i)}$	$2^{\frac{n}{2}\gcd(2i,m)}$ even j, $2^{\left(\frac{n}{2}-1\right)\gcd(2i,m)+2\gcd(m,i)}$ odd j	$2^{\frac{n-1}{2}\gcd(2i,m)+\gcd(m,i)}$	$(m-1)(n-1)$
$\sigma_h\delta^{i,j}$	LA.10	$2^{\frac{m}{2}\gcd(2j,n)}$ even i, $2^{\left(\frac{m}{2}-1\right)\gcd(2j,n)+2\gcd(n,j)}$ odd i	$2^{\frac{m}{2}\gcd(2j,n)}$ even i, $2^{\left(\frac{m}{2}-1\right)\gcd(2j,n)+2\gcd(n,j)}$ odd i	$2^{\frac{m-1}{2}\gcd(2j,n)+\gcd(n,j)}$	$2^{\frac{m-1}{2}\gcd(2j,n)+\gcd(n,j)}$	$(m-1)(n-1)$
					Total:	$4mn$

Table 6.6: *The number of game states fixed by each $g \in \mathcal{G}_r$, where $\mathcal{G}_r$ is the group of isommetries belonging to the game states of the ESPD with the toroidal grid graph $C_m \times C_n$ as underlying graph. The inequalities $1 \leq i \leq m$ and $1 \leq j \leq m$ are assumed to hold in the table. The second column contains a reference to the table (T) or lemma (L) where the value of $|F_g|$ may be found, the * symbol indicates that the same lemma applies but with m substituted for n and vice versa. The entries in the row for the isometry $\rho^2\delta^{i,j}$ have been summed over the possible values of i and j for the sake of brevity.*

It follows by Lemma 2.1 and Table 6.6 in the case when m and n are both even, that

$$\begin{aligned}\Lambda_t(m,n) =& \frac{1}{4mn}\Bigg(2^{mn} + 3\,2^{\frac{mn}{2}} + \sum_{i=1}^{m-1} 2^{n\gcd(m,i)} + \sum_{j=1}^{n-1} 2^{m\gcd(n,j)} + \left(\frac{n}{2}2^{\frac{mn}{2}+m} + \left(\frac{n}{2}-1\right)2^{\frac{mn}{2}}\right)\\ &+ \left(\frac{m}{2}2^{\frac{mn}{2}+n} + \left(\frac{m}{2}-1\right)2^{n\left(\frac{m}{2}\right)}\right) + \sum_{i=1}^{n-1} 2^{\frac{1}{2}m\gcd(2i,n)} + \sum_{i=1}^{m-1} 2^{\frac{1}{2}n\gcd(2i,m)}\\ &+ (m+n-2)2^{\frac{mn}{2}} + \sum_{j=1}^{n-1}\sum_{i=1}^{m-1} 2^{\gcd(n\gcd(i,m),m\gcd(j,n))}\\ &+ \left(\frac{7mn}{4} - m - n + 1\right)2^{\frac{mn}{2}} + \left(\frac{n}{2}-1\right)\sum_{i=1}^{m-1} 2^{\frac{1}{2}n\gcd(2i,m)}\\ &+ \frac{1}{2}n\sum_{i=1}^{m-1} 2^{\left(\frac{n}{2}-1\right)\gcd(2i,m)+2\gcd(m,i)} + \left(\frac{m}{2}-1\right)\sum_{j=1}^{n-1} 2^{\frac{1}{2}m\gcd(2j,n)}\\ &+ \frac{1}{2}m\sum_{j=1}^{n-1} 2^{\left(\frac{m}{2}-1\right)\gcd(2j,n)+2\gcd(n,j)}\Bigg).\end{aligned}$$

The values of $\Lambda_t(m,n)$ are tabulated off the diagonal in Table 6.7 for $1 \leq n < m \leq 6$. The values of $\Lambda_t(n,n)$ are tabulated along the diagonal of the Table 6.7 for $1 \leq n \leq 6$ and are listed as Sloane's sequence A093466 [49]. Finally, $\Lambda_t(6,6)$ is the sum the of the members in Sloane's sequence A093469 [49].

m \ n	1	2	3	4	5	6
1	**2**	**3**	**4**	**6**	**8**	**13**
2		**6**	**13**	**34**	**78**	237
3			**26**	158	708	4 236
4				805	14 676	184 854
5					172 112	8 999 762
6						239 114 084

Table 6.7: *The number of game state automorphism classes for the ESPD with the toroidal grid graph $C_n \times C_m$ as underlying graph. The complete state graphs of the entries in boldface may be found in Chapter 5, later in this chapter and in Appendix B. The value for $m = 6$ and $n = 6$ may be found in Sloane's database as a result of sequence A093469 [49], the remaining entries on the diagonal were confirmed via brute force enumeration using Mathematica.*

6.2 The phase plane

Varying the values of T and P may result in a change in the dynamics of the game. Such a change in game dynamics may occur if a change in the parameter values influences the outcome of the update process of one or more players in the game and is called a *phase transition*. As witnessed in the previous chapters, the ESPD on a path or a cycle has only one phase transition at $T = 2 - P$, which results in two parameter regions. A *phase plane* may be constructed by plotting the values of T and P where phase transitions occur. The lines in the phase plane

associated with phase transitions are called *isoclines*. The isoclines divide the phase plane into disjoint parameter regions. Two pairs of values of T and P in the same region of the phase plane result in equivalent game dynamics. Schweitzer *et al.* [46] applied phase plane analysis to investigate the behaviour of the ESPD on grid graphs with wrapping. In their work the authors considered the ESPD on a large (essentially infinite) underlying grid graph with periodic boundary conditions (*i.e.* wrapping boundaries) and constructed a single phase plane. Here their work is extended by constructing the phase planes for the ESPD with a grid graph without wrapping as underlying graph. Furthermore, the effect of the size of the underlying graph on the phase plane is investigated.

During the update process a player compares the values of the pay-off of the highest scoring cooperator and the highest scoring defector in his closed neighbourhood. Let the pay-off to player v with i cooperators and j defectors in his open neighbourhood be denoted by $c_{i,j}$ if player v is a cooperator, or by $d_{i,j}$ if player v is a defector. The values of $c_{i,j}$ and $d_{i,j}$ are functions of T and P. The potential transitions in the P-T phase plane are found by determining the values of T and P such that $c_{i,j} = d_{k,\ell}$ for fixed values of i, j, k and ℓ. Since the pay-off a player achieves is the average of his interaction with all of his neighbours, an important quantity in the analysis of phase plane transitions is the proportion of cooperators (or defectors) in a player's closed neighbourhood. It follows by the definitions of the variables that $c_{i,0} = c_{j,0}$, $d_{i,0} = d_{j,0}$, $c_{i,i} = c_{j,j}$ and $d_{i,i} = d_{j,j}$ for all $i, j \in \mathbb{N}_0$. There are no isoclines associated with the value of $d_{0,i}$ as proved in the following lemma.

Lemma 6.1 *The value of $d_{0,i}$ does not affect the game dynamics of the ESPD with $P_m \times P_n$ or $C_m \times C_n$ as underlying graph.*

Proof: If, during round t of the ESPD a player v has a neighbour achieving a pay-off of $d_{0,i} = P$ in his closed neighbourhood, then player v is a defector. If player v does not have a cooperator in his neighbourhood, he will adopt the strategy of defection during the following round of the game; this decision is made independent of the values of T and P. If player v has a cooperator in his neighbourhood, then, since $T > P$, player v achieves a pay-off $\pi \geq P$. □

The following Lemma may be used in the construction of a phase plane.

Lemma 6.2 *If $i + j \neq 0$, $k + \ell \neq 0$ and $\frac{i}{i+j} \geq \frac{k}{k+\ell}$, then $d_{i,j} > c_{k,\ell}$.*

Proof: Suppose $i, j, k, \ell \in \mathbb{N}_0$ with $i + j \neq 0$ and $k + \ell \neq 0$ such that $\frac{i}{i+j} \geq \frac{k}{k+\ell}$. Then it follows by the requirements $T > 1$ and $P > 0$ that

$$d_{i,j} = \frac{1}{i+j}(iT + jP) > \frac{i}{i+j}T > \frac{i}{i+j} \geq \frac{k}{k+\ell} = c_{k,\ell}. \quad \square$$

The above lemma states that a defector with a larger proportion of cooperators in his neighbourhood achieves a higher pay-off than a cooperator with an equivalent or smaller proportion of cooperators in his neighbourhood. Thus, when considering the ESPD on any graph, values of T and P may only satisfy $d_i, j = c_{k,\ell}$ if $\frac{i}{i+j} < \frac{k}{k+\ell}$.

6.2.1 Grids without wrapping

Consider the ESPD with the Cartesian product $P_n \times P_m$ as underlying graph. The size of a player's neighbourhood is determined by his position in the grid; each of the four corner players have two neighbours, players along the edges of the grid each has three neighbours and the remaining players each has four neighbours. The pay-off values that a cooperator may receive are $c_{2,0}$, $c_{1,1}$, $c_{0,2}$, $c_{3,0}$, $c_{2,1}$, $c_{1,2}$, $c_{0,3}$, $c_{4,0}$, $c_{3,1}$, $c_{2,2}$, $c_{1,3}$ and $c_{0,4}$. The pay-off values that a defector may receive are $d_{2,0}$, $d_{1,1}$, $d_{0,2}$, $d_{3,0}$, $d_{2,1}$, $d_{1,2}$, $d_{0,3}$, $d_{4,0}$, $d_{3,1}$, $d_{2,2}$, $d_{1,3}$ and $d_{0,4}$. The scoring possibilities that need to be considered when constructing the phase plane for a grid graph without wrapping are therefore as tabulated in Table 6.8.

C	D
$c_{0,i}$	—
$c_{1,3}$	$d_{1,3}$
$c_{1,2}$	$d_{1,2}$
$c_{i,i}$	$d_{i,i}$
$c_{2,1}$	$d_{2,1}$
$c_{3,1}$	$d_{3,1}$
$c_{i,0}$	$d_{i,0}$

(a)

C	D
0	—
$\frac{1}{4}$	$\frac{1}{4}T + \frac{3}{4}P$
$\frac{1}{3}$	$\frac{1}{3}T + \frac{2}{3}P$
$\frac{1}{2}$	$\frac{1}{2}T + \frac{1}{2}P$
$\frac{2}{3}$	$\frac{2}{3}T + \frac{1}{3}P$
$\frac{3}{4}$	$\frac{3}{4}T + \frac{1}{4}P$
1	T

(b)

Table 6.8: *Different pay-off values for players playing strategies C and D. (a) Adjacency possibilities for cooperators, $c_{i,j}$, and defectors, $d_{i,j}$, where i and j are the number of cooperators and defectors, respectively, in the player's neighbourhood. (b) The possible pay-off values in the ESPD on a grid without wrapping and with parameter values $\pi = (T, 1, P, 0)$.*

It follows by Lemmas 6.1 and 6.2 that the isoclines in the phase plane are given by the fifteen equations

$$
\begin{aligned}
d_{1,3} = c_{1,2} &\Rightarrow T = \tfrac{4}{3} - 3P, & d_{1,3} = c_{i,i} &\Rightarrow T = 2 - 3P,\\
d_{1,3} = c_{2,1} &\Rightarrow T = \tfrac{8}{3} - 3P, & d_{1,3} = c_{3,1} &\Rightarrow T = 3 - 3P,\\
d_{1,3} = c_{i,0} &\Rightarrow T = 4 - 3P, & d_{1,2} = c_{i,i} &\Rightarrow T = \tfrac{3}{2} - 2P,\\
d_{1,2} = c_{2,1} &\Rightarrow T = \tfrac{6}{3} - 2P, & d_{1,2} = c_{3,1} &\Rightarrow T = \tfrac{9}{4} - 2P,\\
d_{1,2} = c_{i,0} &\Rightarrow T = 3 - 2P, & d_{i,i} = c_{2,1} &\Rightarrow T = \tfrac{4}{3} - P,\\
d_{i,i} = c_{3,1} &\Rightarrow T = \tfrac{3}{2} - P, & d_{i,i} = c_{i,0} &\Rightarrow T = 2 - P,\\
d_{2,1} = c_{3,1} &\Rightarrow T = \tfrac{9}{8} - \tfrac{1}{2}P, & d_{2,1} = c_{i,0} &\Rightarrow T = \tfrac{3}{2} - \tfrac{1}{2}P \text{ and}\\
d_{3,1} = c_{i,0} &\Rightarrow T = \tfrac{4}{3} - \tfrac{1}{3}P.
\end{aligned}
$$

The phase plane of the ESPD with the graph $P_n \times P_m$ as underlying graph is shown in Figure 6.4. Not all of the phase transitions in the phase plane may be realised for small grids as certain combinations of neighbourhoods are not possible. As an example, rectangular grid graphs of dimension $2 \times n$ do not contain any players with neighbourhoods of size four.

6.2.2 Grids with wrapping

Next the ESPD with the Cartesian product $C_n \times C_m$ as the underlying graph is considered. The graph is 4-regular (*i.e.* each player has four other players in his open neighbourhood). In this case, the pay-off to a player with i cooperators in his neighbourhood is simply denoted c_i

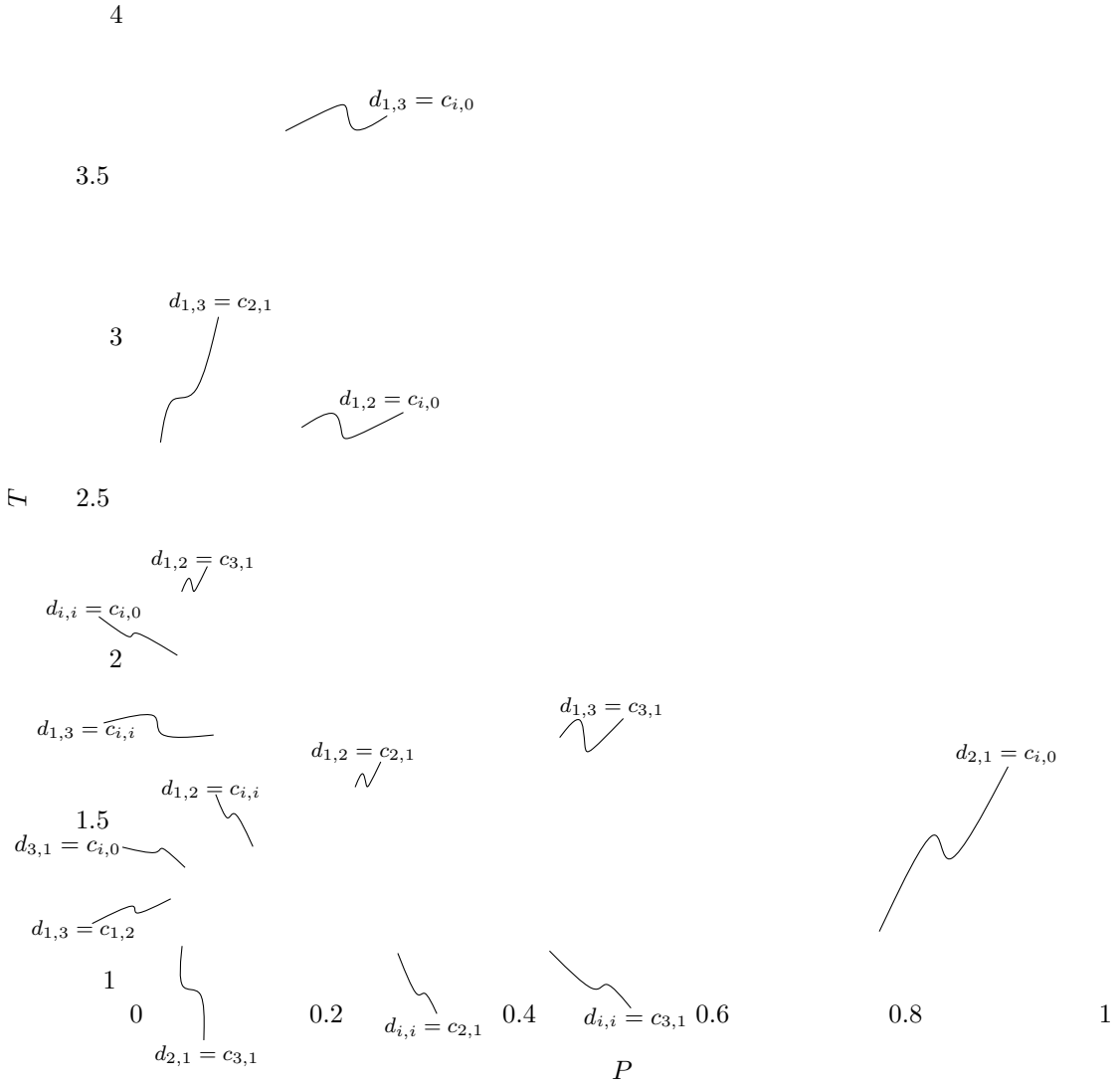

(a) $m, n > 3$

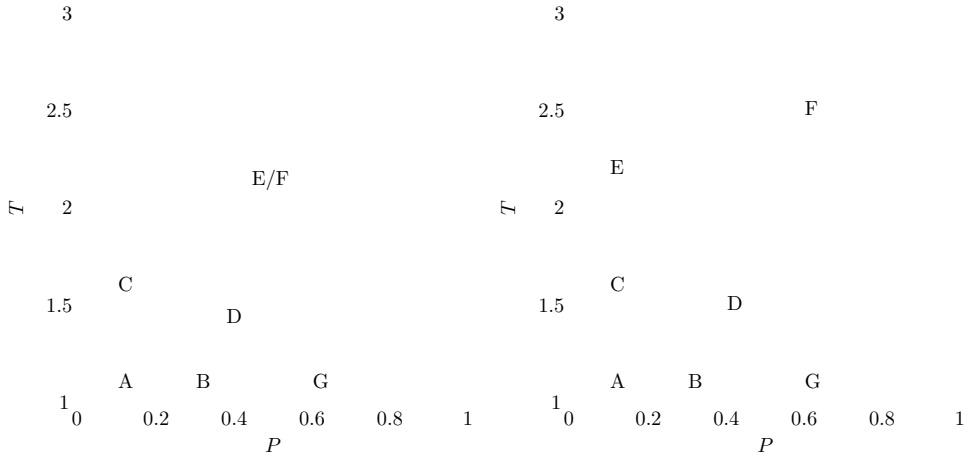

(b) $m = 2$, $n = 3$

(c) $m = 2$, $n = 4$

Figure 6.4: *The P-T phase plane for the ESPD with the grid graph $P_n \times P_m$ as underlying graph.*

or d_i. If the number of cooperators is known, the number of defectors j may be calculated as $j = i - 4$. The different pay-off values that a player may achieve are listed in Table 6.9.

C	D
c_0	d_0
c_1	d_1
c_2	d_2
c_3	d_3
c_4	d_4

(a)

C	D
0	P
$\frac{1}{4} + \frac{3}{4}S$	$T + \frac{3}{4}P$
$\frac{1}{2}$	$\frac{1}{2}T + \frac{1}{2}P$
$\frac{3}{4}$	$\frac{3}{4}T + P$
1	T

(b)

Table 6.9: *Different pay-off values for players playing strategies C and D. (a) Adjacency possibilities for cooperators, c_i, and defectors, d_i, where i is the number of cooperators in the player's neighbourhood. (b) The possible pay-off values in the ESPD on a grid with wrapping and with parameter values $\pi = (T, 1, P, 0)$.*

Again it is true that $d_i > c_j$ for values of i and j satisfying $i \geq j$ and that the pay-off value d_0 does not play a role when determining how a player will update his strategy. Furthermore, it holds that $d_i > d_j$ for all values of i and j satisfying the inequality $i \geq j$. It thus follows that the transitions in the phase plane are given by the six equations

$$\begin{aligned}
c_4 = d_3 &\Rightarrow 4 = 3T + P,\\
c_4 = d_2 &\Rightarrow 4 = 2T + 2P,\\
c_4 = d_1 &\Rightarrow 4 = T + 3P,\\
c_3 = d_2 &\Rightarrow 3 = 2T + 2P,\\
c_3 = d_1 &\Rightarrow 3 = T + 3P, \text{ and}\\
c_2 = d_1 &\Rightarrow 2 = T + 3P.
\end{aligned}$$

These critical lines in the phase plane separate eleven distinct areas which potentially result in different game dynamics. The phase plane for the ESPD on a grid with wrapping is shown in Figure 6.5.

6.3 State graphs of the ESPD on grid graphs

In this section the state graphs for grids with and without wrapping are constructed for games which have 102 or fewer state automorphism classes. The number of state automorphism classes for given dimensions of the underlying graphs is tabaluted in Tables 6.2 and 6.7.

6.3.1 Grids with wrapping

The state graphs of the ESPD on toroidal grid graphs $C_n \times C_m$ are considered in this section.

State graphs of the ESPD with $C_2 \times C_2$ as underlying graph

The EPSD with the graph $C_2 \times C_2$ as underlying graph has six automorphism classes of game states. The six class leaders of each automorphism class, together with the pay-off that each player achieves in each game state, is shown is shown in Figure 6.6. Since $d_i > c_j$ if $i \geq j$, it

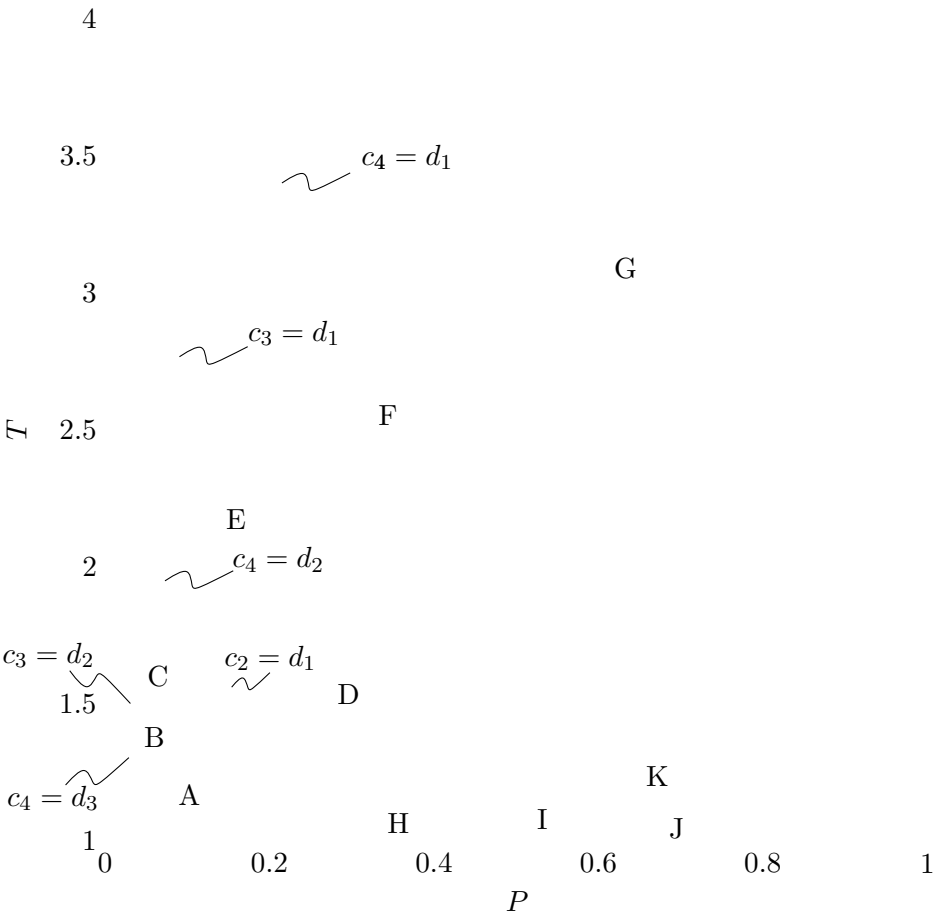

(a) $n, m > 3$

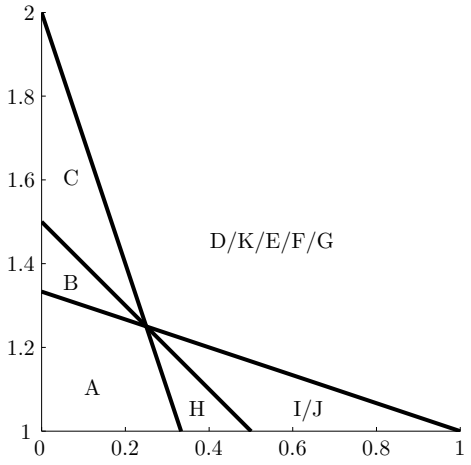

(b) $m = 2$, $n = 3$

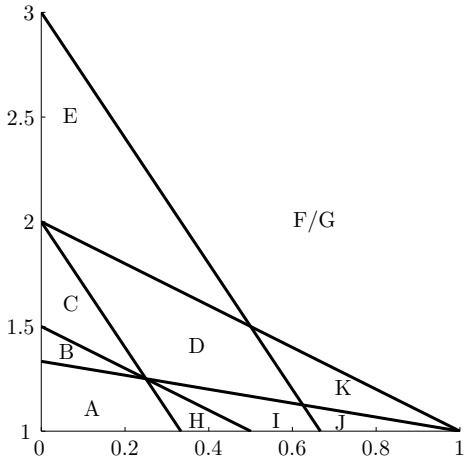

(c) $m = 2$, $n = 4$

Figure 6.5: *The P-T phase plane for the ESPD with $C_n \times C_m$ as underlying graph. The eleven parameter regions are labelled A through K. The phase plane for the ESPD with $C_3 \times C_3$ as underlying graph is shown in Figure 6.10(d).*

follows that the outcome of every player's update decision is unaffected by the the values of T and P. The single state graph of the ESPD with $C_2 \times C_2$ as underlying graph is shown in Figure 6.7.

Figure 6.6: *The class leaders of the six automorphism classes of games states for the ESPD with the graph $C_2 \times C_2$ as underlying graph, with the pay-off achieved by each player indicated.*

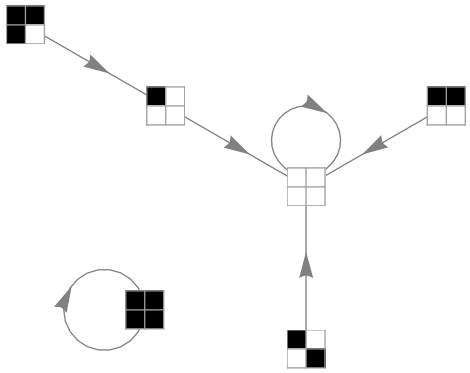

Figure 6.7: *The state graph for the ESPD with $C_2 \times C_2$ or $P_2 \times P_2$ as underlying graph. The outcome of the game is independent of the values of T and P.*

State graphs of the ESPD with $C_3 \times C_3$ as underlying graph.

The phase plane of the ESPD with the graph $C_3 \times C_3$ as underlying graph has fewer isoclines than in the general case where the underlying graph is $C_n \times C_m$ $(n, m > 3)$. If a cooperator achieving a score c_4 is present in the game, then the lowest score a defector can achieve is d_2. The minimum number of cooperators in the game is four, as illustrated in Figure 6.8(a), and each defector in the game achieves a score of d_2. Note that a player achieving a pay-off of c_4 or d_1 cannot be present in the game during the same round; therefore the isocline on the phase plane which is given by $d_1 = c_4$ is absent.

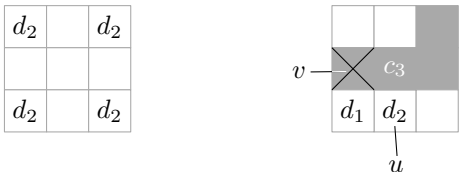

(a) (b)

Figure 6.8: *(a) A game state of the ESPD with $C_3 \times C_3$ as underlying graph containing a cooperator with a pay-off of c_4. The lowest score a defector can achieve if a cooperator scoring c_4 is present, is d_2. (b) A game state containing players achieving pay-offs c_3 and d_1, respectively.*

A player having to choose between adopting the strategies of a player with pay-off c_3 and a players achieving a pay-off of d_1, is considered next. The game states containing both a player achieving a pay-off of c_3 and a player achieving a pay-off of d_1 is shown in Figure 6.8(b).

The player indicated by the grey shaded cell may be playing either cooperate or defect. There are two players, the players labelled u and v, in the game state with a player scoring c_3 and a player scoring d_1 in their neighbourhoods. Player u achieves a pay-off of $d_2 > d_1$; therefore the value of d_1 does not affect the outcome of players u's update decisions. Player v has a player achieving d_2 in his neighbourhood, and again, the value of d_1 does not affect his update process. Hence there is no isocline in the phase plane associated with the values of T and P satisfying $c_3 = d_1$.

The phase plane of the ESPD with $C_3 \times C_3$ as the underlying graph is shown in Figure 6.10(d) and the state graphs are shown in Figures 6.9(a)–(d) and 6.10(a)–(c). A summary of the properties of the state graphs may be found in Table 6.10.

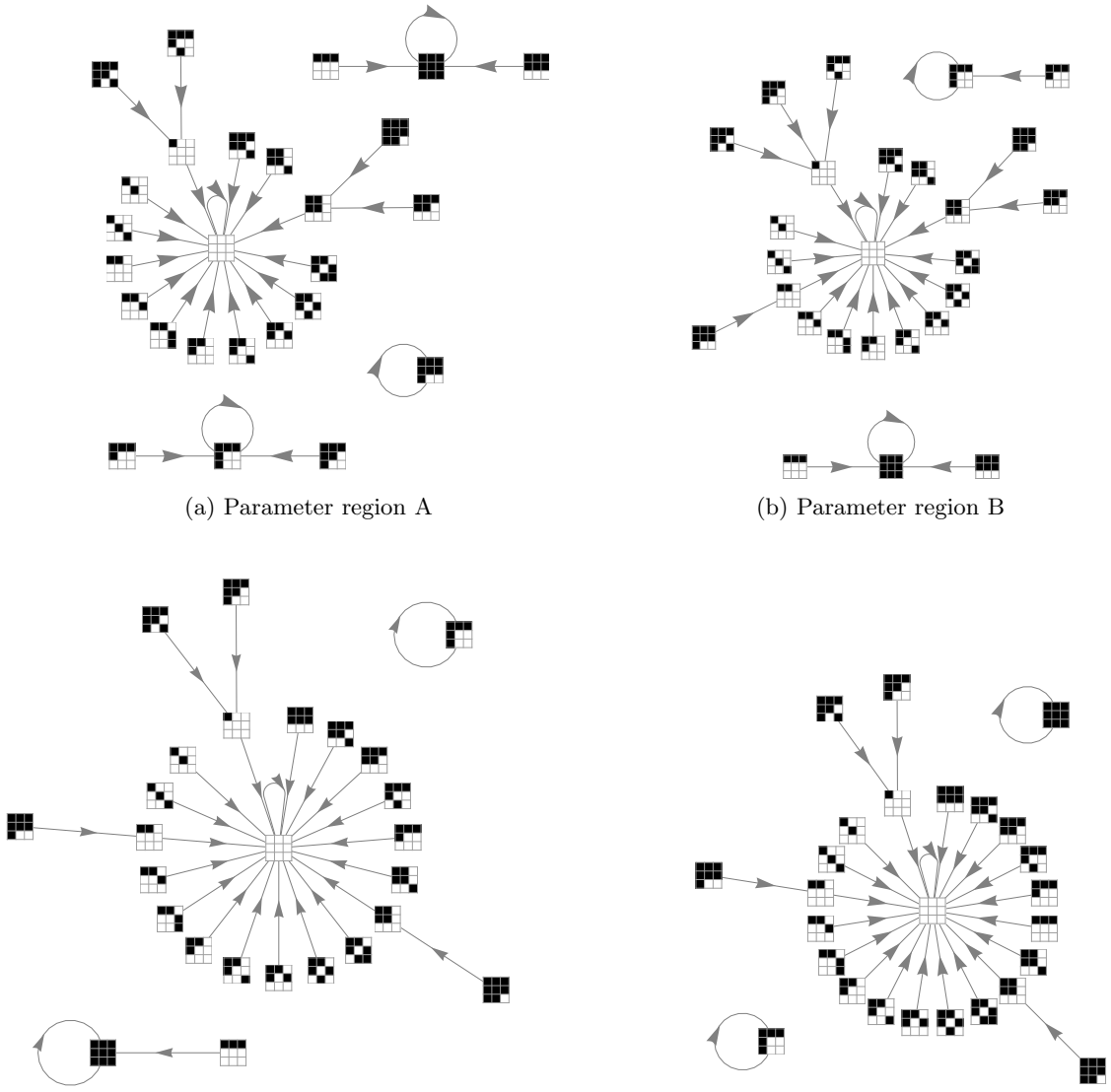

(a) Parameter region A

(b) Parameter region B

(c) Parameter region C

(d) Parameter region D

Figure 6.9: *The state graphs of the ESPD with $C_3 \times C_3$ as underlying graph for the different parameter regions in the T-P phase plane. The phase plane is shown in Figure 6.10(d).*

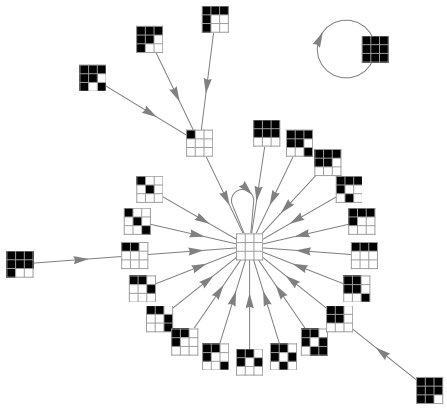

(a) Parameter region E/F/G

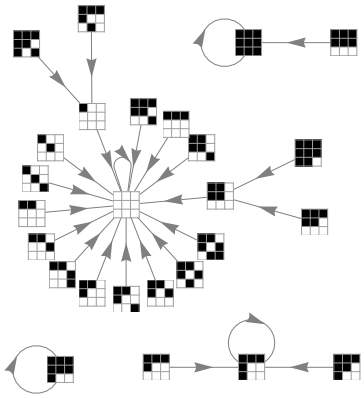

(b) Parameter region H

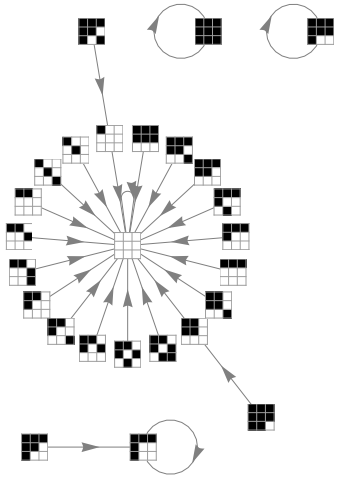

(c) Parameter region I/J

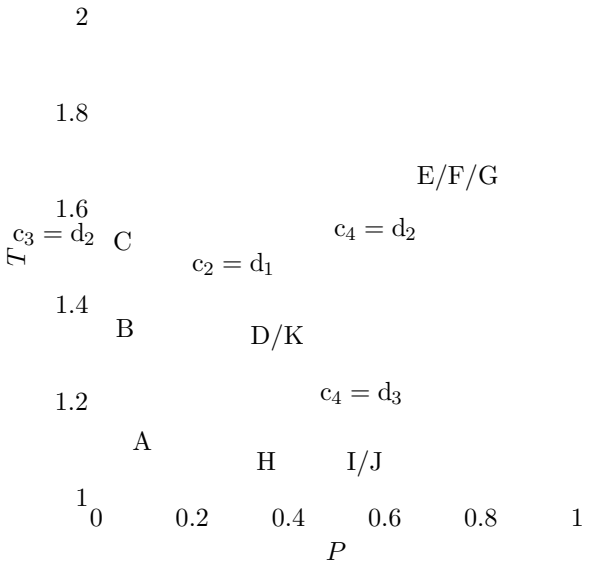

(d) The phase plane of the ESPD with $C_3 \times C_3$ as underlying graph. Regions are labelled A through J. Regions with multiple labels are those that correspond to more than one region of the phase plane in Figure 6.5(a).

Figure 6.10: *The state graphs of the ESPD with underlying graph $C_3 \times C_3$ for the different parameter regions in the T-P phase plane.*

Region	Components	Probability of persistent cooperation	Max path length	Average path length
A	4	0.219	2	1
B	3	0.113	2	1.115
C	3	0.031	2	1.038
D/K	3	0.020	2	1.038
E/F/G	2	0.002	2	1.115
H	4	0.207	2	1
I/J	4	0.125	2	0.923

Table 6.10: *Analytical results for the properties of the state graph of the ESPD with $C_3 \times C_3$ as underlying graph.*

State graphs of the ESPD with $C_2 \times C_3$ as underlying graph

As the size of the underlying graph decreases, the possible combinations of neighbourhoods decreases. The number of isoclines thus also decreases as the dimensions of the underlying graph decreases. The phase plane of the ESPD with $C_2 \times C_3$ as underlying graph contains a subset of the isoclines of the phase plane of the ESPD with $C_3 \times C_3$ as underlying graph. A game state containing a player achieving a pay-off value of c_4 is shown in Figure 6.11; it is not possible for a player to achieve a pay-off of d_2 if a player acheiving c_4 is present in the game state. Therefore the isocline $c_4 = d_2$ is absent from the P-T phase plane. The phase plane of the ESPD with the underlying graph $C_2 \times C_3$ is shown in Figure 6.5(b). The state graphs of the ESPD with $C_2 \times C_3$ as underlying graph may be found in Appendix B (section B.4).

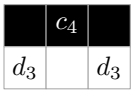

Figure 6.11: *A game state of the ESPD with $C_2 \times C_3$ as underlying graph containing a player achieving a pay-off of c_4.*

State graphs for the ESPD with $C_2 \times C_4$ as underlying graph

A game state containing a player achieving a pay-off of c_4 is shown in Figure 6.12(a), where grey shaded cells indicate those players whose strategies do not affect the pay-off of the player achieving a pay-off of c_4. All except one of the grey shaded cells are adjacent to two or more defectors. The top left-most cell is the only one which can contain a defector achieving a pay-off of d_1. The two possible game states containing both a player achieving a pay-off of d_1 and a player achieving a pay-off of c_4 are shown in Figure 6.12(b). Therefore, a player cannot have both a neighbouring player achieving a pay-off of c_4 and a neighbouring player achieving a pay-off of d_1; the isocline associated with $c_4 = d_1$ is absent from the phase plane. The P-T phase plane of the ESPD with $C_2 \times C_4$ as underlying graph is shown in Figure 6.5(c). The state graphs of the ESPD with $C_2 \times C_4$ as underlying graph may be found in Appendix B (section B.5).

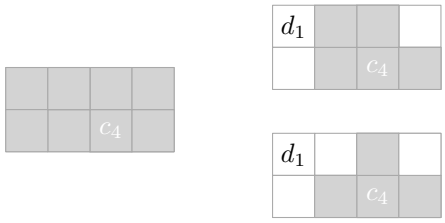

(a) (b)

Figure 6.12: *Game states of the ESPD with $C_2 \times C_4$ as underlying graph containing (a) a player achieving a pay-off of c_4 and (b) players achieving pay-offs of d_1 and c_4. The grey shaded shells in (a) indicate cells which do not affect the pay-off of the player acheiving a pay-off of c_4.*

6.3.2 Grids without wrapping

The phase planes of the ESPD with the graph $P_n \times P_m$ as underlying may be constructed in a similar fashion as in the case with wrapping. On underlying graphs of smaller dimension, once again, there may be equivalent game dynamics across regions. As the dimensions of the underlying graph decreases, more and more of the regions in the phase plane, shown in Figure 6.4, result in identical state graphs. The single state graph of the ESPD with $P_2 \times P_2$ as underlying graph is shown in Figure 6.7. The state graphs of the the ESPD with $P_2 \times P_3$, $P_2 \times P_4$ or $P_3 \times P_3$ as underlying graph may be found in Appendix B (sections B.1–B.3).

6.4 Chapter summary

The ESPD with a grid graph as the underlying graph was considered in this chapter. Both grids with and without wrapping boundary conditions were investigated. The automorphism classes of game states for the cases where $C_n \times C_m$ or $P_n \times P_m$ are the underlying graph of the ESPD where enumerated. The number of automorphism classes of game states is equivalent to the number of distinct binary matrices or two-colourings of lattices under the wallpaper groups pmm and $p4m$.

The P-T phase planes were constructed for the ESPD on the various grid graphs as underlying graphs. It was shown that the game dynamics become more complex as the dimensions of the underlying graph increases. Grids without wrapping have a larger number of regions in the P-T phase plane, each region resulting in different game dynamics, whereas the the ESPD on a grid with wrapping has at most eleven parameter regions in the P-T phase plane.

The entire state graphs were constructed for the ESPD with $C_2 \times C_2$ or $C_3 \times C_3$ as underlying graph. The state graphs of the ESPD for the cases where $P_2 \times P_3$, $P_2 \times P_4$, $P_3 \times P_3$, $C_2 \times C_3$, $C_2 \times C_4$ or $C_2 \times C_5$ is the underlying graph may be found in Appendix B.

CHAPTER 7

Conclusion

Contents

This chapter concludes the thesis with a summary of the work contained therein, an appraisal of the contributions of the thesis as well as a discussion on possibilities for future work.

7.1 Thesis summary

Various basic mathematical concepts were reviewed in Chapter 2. Some basic concepts from graph theory, including basic terminology in graph theory, various types of graphs and a number of operations on graphs. A brief introduction to some basic concepts from group theory follows. The Frobenius-Cauchy lemma, in particular, proved to be a very useful result and was used extensively throughout the thesis. The concept of a generating function was introduced in the final section of the chapter. A generating function was used to enumerate the number of walks of a certain length in a digraph.

Definitions and concepts in classical game theory and evolutionary game theory were reviewed in Chapter 3 (in fulfilment of Thesis Objective I). Notions in classical game theory were reviewed in §3.1 together with a brief historical account of important developments in the field. Two methods for representing games were considered, namely, the matrix form representation and extensive form representation. The PD was considered as an example of a very well known game in game theory. Other topics in this section included the classification of games according to their properties, solution concepts and solution methods. The section concluded with a brief description of a number of successful applications of game theory, while a description of Braess' paradox illustrated how counter-intuitive results may arise from game theory. In §3.2 the extension of classical game theory to evolutionary game theory was described. Evolutionary

game theory has its origins in classical game theory and is inspired by evolution as seen in nature. The connection between biology and evolutionary game theory was discussed. The definition and components of an evolutionary game were reviewed. Structured evolutionary games were also discussed in this section. The section concluded with a brief discussion on solution concepts in evolutionary game theory. In the final section of the chapter, §3.3, a number of variations on the PD often encountered in the literature on evolutionary game theory were presented.

Chapter 4 contains a mathematical framework for describing spatially structured evolutionary games (in fulfilment of Thesis Objective II). A game may be presented as an ordered pair consisting of the set of pay-off parameters and an underlying graph which describes the spatial structure of the game. Two important concepts were introduced, namely an automorphism class of game states and the state graph of a game. If the number of state automorphism classes is small, then the state graph is a useful tool for visually representing the game dynamics. It was also demonstrated in Chapter 4 that the use of the reduced set of pay-off parameters $\Pi = \{T, 1, S, 0\}$ is sufficient to describe game dynamics in general.

Analytical means were employed in Chapter 5 to analyse the game dynamics of the ESPD on a path or cycle. It was found that the number of states in the ESPD on a path or a cycle of order n increases exponentially as the order n of the underlying graph increases (in partial fulfilment of Thesis Objective III). It was shown that for large values of T (*i.e.* for $T > 2-P$), cooperation is only possible if the initial game state contains cooperators only. However, it is possible for cooperation to persist in the case were $T \leq 2 - P$ even if the initial state does not contain cooperators only. The initial states which lead to persistent cooperation were characterised for the ESPD on a path or cycle. If the underlying graph is a path or a cycle of order $n > 7$, then the number of states which do not lead to persistent cooperation may be calculated by means of the recursive relationship

$$f_n = f_{n-1} + f_{n-2} + f_{n-3} + f_{n-4} - f_{n-6} + f_{n-7}.$$

The values used to seed the above relationship depends on whether the underlying graph is a path or a cycle. If the underlying graph is a path, then the values used to seed the relationship are $f_1 = 1$, $f_2 = 3$, $f_3 = 7$, $f_4 = 11$, $f_5 = 21$, $f_6 = 42$ and $f_7 = 81$. However, if the underlying graph is a cycle, then the values used to seed the relationship are $f_1 = 1$, $f_2 = 3$, $f_3 = 7$, $f_4 = 15$, $f_5 = 26$, $f_6 = 45$ and $f_7 = 99$. The probability of randomly generating an initial game state that will lead to some form of persistent cooperation may be computed using the formula $P(n) = 1 - f_n/2^n$. It was found that the likelihood of cooperation increases towards certainty as the order of the underlying graph increases (in fulfilment of Thesis Objective IV).

The ESPD with a grid graph as the underlying graph was considered in Chapter 6. Both grids with and without wrapping boundary conditions were investigated. The automorphism classes of game states for the cases where $C_n \times C_m$ and $P_n \times P_m$ are the underlying graph of the ESPD where enumerated (in fulfilment of Thesis Objective III). The number of automorphism classes of game states is equivalent to the number of distinct binary matrices or two-colourings of lattices under the wallpaper groups **pmm** and **p4m**. The P-T phase planes were constructed for the ESPD on the various grid graphs as underlying graphs (in fulfilment of Thesis Objective V). It was shown that the game dynamics become more complex as the dimensions of the underlying graph increases. Grids without wrapping result in a larger number of regions in the P-T phase plane, each region inducing different game dynamics, whereas the ESPD on a grid with wrapping exhibits at most eleven parameter regions in the P-T phase plane (in fulfilment of Thesis Objective V). Entire state graphs were constructed for the ESPD with $C_2 \times C_2$, $C_3 \times C_3$, $C_2 \times C_3$, $C_2 \times C_4$, $C_2 \times C_5$, $P_2 \times P_2$, $P_3 \times P_3$, $P_2 \times P_3$ or $P_2 \times P_4$ as underlying graph.

7.2 Appraisal of the work contained in this thesis

The four main contributions of this thesis towards the fields of evolutionary games on graphs are summarised in this section.

Contribution 1 *Pay-off normalisation of the ESPD.*

A method was introduced to normalise the pay-off values without influencing the game dynamics. The *weak parameterisation* and the *cost-benefit parameterisation* are often encountered in the literature. These parameterisations explore only a subset of the full parameter space. The results in this thesis present a case for using the normalised pay-off to investigate games on graphs.

Contribution 2 *The asymptotic analysis of the ESPD on paths and cycles.*

The steady states were characterised for the cases where the underlying graph of the EPSD is a path or a cycle. The structures of those initial states that lead to the emergence of persistent cooperation were characterised. An analytical (*i.e.* without using simulation) method was used to compute the probability that the game states will evolve from a randomly generated initial state towards a steady state which accommodates some form of persistent cooperation. These contributions were published in [7] for the case where the underlying graph is a cycle, and in [8] for the case where the underlying graph is a path.

Contribution 3 *Phase plane and state graph construction of the ESPD on a grid graph.*

The phase planes were constructed for the ESPD where the underlying graph is a grid with or without wrapping. Furthermore, the influence of the size of the underlying graph on the isoclines present in the phase plane was also determined. The complete sets of state graphs were constructed for the underlying graphs $C_2 \times C_2$, $C_2 \times C_3$, $C_2 \times C_4$, $C_2 \times C_5$, $C_3 \times C_3$, $P_2 \times P_2$, $P_2 \times P_3$, $P_2 \times P_4$ and $P_3 \times P_3$.

Contribution 4 *The enumeration of the ESPD state space with $P_n \times P_m$ or $C_n \times C_m$ as underlying graph.*

The size of the automorphism classes of ESPD game states were enumerated for the ESPD with $P_n \times P_m$ or $C_n \times C_m$ (excluding the case where $m = n$) as underlying graph.

7.3 Ideas for further work

A number of ideas for further work related to the ESPD are highlighted in this section.

7.3.1 Enumeration of the automorphism classes of the ESPD on $C_n \times C_n$

A closed formula was determined in this thesis for $\Lambda_t(m, n)$ for all m, n satisfying $1 \leq n < m$. This formula, however, does not include the case of $\Lambda_t(n, n)$. Note that $\Lambda_t(n, n)$ corresponds

to the number two-colourings of a lattice or the number of a binary matrices, in both cases up to isomorphism involving modular shift of rows and columns, reflection about the horizontal and vertical axis, reflection through main diagonal and combinations of these operations (*i.e.* corresponding to the symmetry group **p4m**).

The Cauchy-Frobenius Lemma may also be applied to this enumeration problem. The members of the relevant symmetry group must first be determined. All the symmetries of the a rectangular lattice apply to a square lattice. However, the symmetry group of the square lattice has the additional symmetries σ_m and σ_p, as well as the combination of these, and the symmetries in $\mathcal{G}_r$ to ensure the closure of the group. The next step involves calculating the number of states fixed by each element in the symmetry group of the ESPD with $C_n \times C_n$ as underlying graph.

7.3.2 The global shipping network and the spread of invasive species

Invasive species bear an economic cost to the countries were they establish themselves. The spread of these invasive species is often facilitated by the movement of freight ships as they travel from port to port. Kaluza *et al.* [24] investigated the structure of the international shipping network and the number of vessels along each route. The authors also considered the implications of this network structure on bioinvasion. The global shipping network is shown in Figure 7.1.

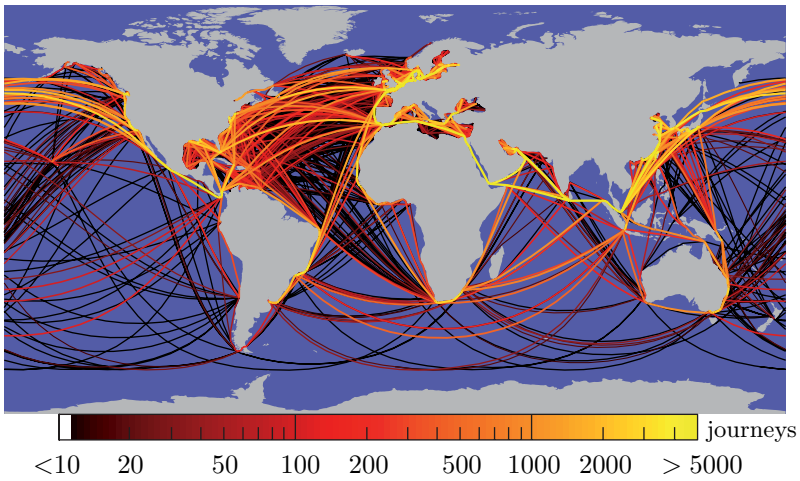

Figure 7.1: *The global shipping network. The routes travelled by large cargo ships (larger than* 10 000 *GT) during 2007. The colour scaling indicates the number of ships travelling along each route [24].*

Managing biological invasive species exhibits characteristics similar to those of the ESPD on the graph in Figure 7.1. A cost is associated with preventing the spread of invasive species, such as when a port's authorities have to inspect and clean the hulls of the ships before they leave the port, a cost would be incurred. The cost of this screening process is thus to the exporter, but the benefit gained by such screening practices is to the importers. This scenario may be translated into a cost-benefit parameterisation of the ESPD with the global shipping network as underlying graph.

The following research question naturally arises: Is it possible for a sustainable, efficient invasive biological control programme to emerge among a cluster of countries in the form of persistent cooperation?

7.3.3 Determining the fraction of cooperators present in a steady state

Another quantity of interest when it comes to the persistence of cooperation, is the fraction of cooperators present in a steady state. A natural extension of the work carried out in Chapter 5 would be to derive an expression for the average fraction of cooperators present in the steady state of the ESPD with C_n or P_n as underlying graph. In Chapter 5, the probability that cooperation will persist in the ESPD with a path or a cycle as underlying graph was determined. It was found that the probability of persistent cooperation tends to certainty as the underlying graph size increases. This, however, does not indicate what the final proportion of cooperators in the steady state will be.

7.3.4 The ESPD on trees, grid graphs and small-world networks

It would be interesting to conduct asymptotic analyses for the ESPD on trees, larger grid graphs, circulant graphs and small-world networks. However, such analyses are expected to be considerably more difficult due to an increase in symmetry involved in the underlying graphs and since the state graph will no longer be a rooted pseudo-forest. Much more complex (in fact, seemingly chaotic) structures of persistent cooperation are expected to emerge in these cases. For example, the limit cycle containing "persistent" behaviour in Figure 7.2 emerges for the ESPD with $C_{12} \times C_{12}$ as underlying graph.

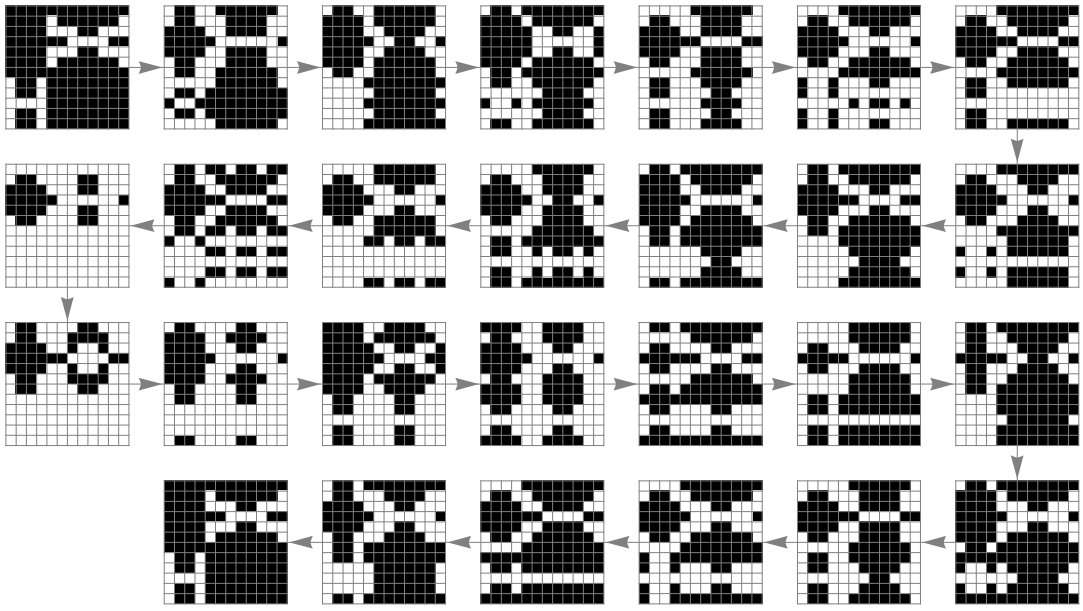

Figure 7.2: *A limit cycle of length 26 for the ESPD with $C_{12} \times C_{12}$ as underlying graph for values of T and P corresponding to parameter region D in the P-T phase plane shown in Figure 6.5.*

7.3.5 Variations on the ESPD

Many variations on the ESPD may be imagined. As an example, Ohtsuki *et al.* [39] considered two separate graphs, the so-called *interaction graph* and the *replacement graph*, to define the

structure of the ESPD. The interaction between players may also not necessarily be static from round to round; the co-evolution of strategies and networks are investigated in [41, 61]. These are just two examples of potential variations on the ESPD. Though many variations have been studied in the literature, these studies are by no means exhaustive with respect to all the potential variations under every condition. Investigating these variations may lead to a comprehensive theoretical understanding of the conditions necessary to promote (or discourage) the evolution of cooperation.

Bibliography

[1] Apostol T, 1974, *Mathematical analysis*, World student series, 2nd Edition, Addison-Wesley Publishing Company, Reading (MA).

[2] Axelrod R, 1984, *The Evolution of Cooperation*, Basic Books, New York (NY).

[3] Axelrod R & Hamilton WD, 1981, *The evolution of cooperation*, Science, **211**(4489), pp. 1390–1396.

[4] Balasubramanian K, 1978, *Combinatorial enumeration of chemical isomers*, Indian Journal of Chemistry, **16B**, pp. 1094–1096.

[5] Braess D, 1968, *Über ein Paradoxon aus der Verkehrsplanung*, Unternehmensforschung Operations Research - Recherche Opérationnelle, **12**(1), pp. 258–268.

[6] Braess D, Nagurney A & Wakolbinger T, 2005, *On a paradox of traffic planning*, Transportation Science, **39**(4), pp. 446–450.

[7] Burger AP, van der Merwe M & van Vuuren JH, 2012, *An asymptotic analysis of the evolutionary spatial prisoner's dilemma on a path*, Discrete Applied Mathematics, **160**(15), pp. 2075–2088.

[8] Burger AP, Van der Merwe M & Van Vuuren JH, 2012, *The evolutionary spatial prisoner's dilemma on a cycle*, ORiON, **Article in Press**.

[9] Du W, Zheng H & Hu M, 2008, *Evolutionary prisoner's dilemma game on weighted scale-free networks*, Physica A: Statistical Mechanics and its Applications, **387**(14), pp. 3796–3800.

[10] Duncan J & Steven H, 1998, *Collective dynamics of 'small-world' networks*, Nature, **393**, pp. 440–442.

[11] Durlauf SN & Blume LE (Eds), 2008, *New Palgrave Dictionary of Economics*, volume 3, 2nd Edition, Palgrave Macmillan, New York (NY).

[12] Elsevier, 2012, *Scopus*, [Online], [Cited December 01st, 2012], Available from `http://www.scopus.com/`.

[13] Fine N, 1958, *Classes of periodic sequences*, Illinois J. Math., **2**, pp. 385–302.

[14] Fletcher JA & Doebeli M, 2009, *A simple and general explanation for the evolution of altruism*, Proceedings of the Royal Society B, **276**(1654), p. 13.

[15] Fowler JH & Christakis NA, 2010, *Cooperative behavior cascades in human social networks*, Proceedings of the National Academy of Sciences, **107**(12), pp. 5334–5338.

[16] Gedye L, 2011, *Bread price respite is over*, [Online], [Cited December 1st, 2012], Available from `http://mg.co.za/article/2011-05-30-bread-price-respite-is-over`.

[17] Gibbons R, 1997, *An introduction to applicable game theory*, The Journal of Economic Perspectives, **11**(1), pp. 127–149.

[18] Google, 2012, *Google scholar*, [Online], [Cited December 01st, 2012], Available from `http://scholar.google.com/`.

[19] Hamilton WD, 1963, *The evolution of altruistic behavior*, American Naturalist, **97**(896), pp. 354–356.

[20] Harary F & Schwenk A, 1973, *The number of caterpillars*, Discrete Mathematics, **6**(4), pp. 359–365.

[21] Hauert CH, 2002, *Effects of space in 2 × 2 games*, International Journal of Bifurcation and Chaos, **12**(7), pp. 1531–1548.

[22] Haywood OG, 1954, *Military decision and game theory*, Journal of the Operations Research Society of America, **2**(4), pp. 365–385.

[23] Hoffman N, 1978, *Binary grids and a related counting problem*, The Two-Year College Mathematics Journal, **9**(5), pp. 267–272.

[24] Kaluza P, Kölzsch A, Gastner MT & Blasius B, 2010, *The complex network of global cargo ship movements*, Journal of The Royal Society Interface, **7**(48), pp. 1093–1103.

[25] Kolata G, 1990, *What if they closed 42d street and nobody noticed?*, [Online], [Cited May 26th, 2010], Available from `http://www.nytimes.com/1990/12/25/health/what-if-they-closed-42d-street-and-nobody-noticed.html`.

[26] Kuhn H, 1953, *Extensive games and the problem of information*, Contributions to the Theory of Games, **2**(28), pp. 193–216.

[27] Martin GE, 2001, *Counting: The art of enumerative combinatorics*, Springer-Verlag, New York (NY).

[28] Maynard Smith J, 1964, *Group selection and kin selection*, Nature, **201**(4924), pp. 1145–1146.

[29] Maynard Smith J, 1982, *Evolution and the theory of games*, Cambridge University Press, Cambridge.

[30] Maynard Smith J & Price G, 1973, *The logic of animal conflict*, Nature, **246**(5427), pp. 15–18.

[31] Miller GA, 2011, *WordNet Search - 3.0*, [Online], [Cited January 31st, 2011], Available from `http://wordnetweb.princeton.edu/`.

[32] Morrow JD, 1994, *Game theory for political scientists*, Princeton University Press, Princeton (NJ).

[33] Nash J, 1951, *Non-cooperative games*, Annals of mathematics, pp. 286–295.

[34] Neumann JV, Morgenstern O, Rubinstein A & Kuhn H, 1944, *Theory of games and economic behavior*, Princeton University Press, Princeton (NJ).

[35] Nowak M & Sigmund K, 2007, *How populations cohere: five rules for cooperation*, Theoretical Ecology: Principles and Applications, **314**, pp. 1560–1563.

[36] Nowak MA, 2006, *Five rules for the evolution of cooperation*, Science, **314**(5805), pp. 1560–1563.

[37] Nowak MA & May RM, 1992, *Evolutionary games and spatial chaos*, Nature, **359**(6398), pp. 826–829.

[38] Nowak MA & May RM, 1993, *The spatial dilemmas of evolution*, International Journal of Bifurcation and Chaos, **3**, pp. 35–35.

[39] Ohtsuki H, Pacheco JM & Nowak MA, 2007, *Evolutionary graph theory: breaking the symmetry between interaction and replacement*, Journal of Theoretical Biology, **246**(4), pp. 681–694.

[40] O'Neill B, 1987, *Nonmetric test of the minimax theory of two-person zerosum games.*, Proceedings of the National Academy of Sciences of the United States of America, **84**(7), pp. 2106–9.

[41] Pacheco JM, Traulsen A & Nowak MA, 2006, *Coevolution of strategy and structure in complex networks with dynamical linking*, Physical Review Letters, **97**, p. 258103.

[42] Perc M & Szolnoki A, 2010, *Coevolutionary games–a mini review*, BioSystems, **99**(2), pp. 109–125.

[43] Roca CP, Cuesta JA & Sánchez A, 2009, *Effect of spatial structure on the evolution of cooperation*, Physical Review E, **80**(4), p. 046106.

[44] Roca CP, Cuesta JA & Sánchez A, 2009, *Evolutionary game theory: Temporal and spatial effects beyond replicator dynamics*, Physics of Life Reviews, **6**(4), pp. 208–249.

[45] Schwalbe U, 2001, *Zermelo and the early history of game theory*, Games and Economic Behavior, **34**(1), pp. 123–137.

[46] Schweitzer F, Behera L & Mühlenbein H, 2002, *Evolution of cooperation in a spatial prisoner's dilemma*, Advances in Complex Systems, **5**(2–3), pp. 269–299.

[47] Seria N, 2007, *Tiger brands*, [Online], [Cited November 29th, 2012], Available from `http://www.moneyweb.co.za/moneyweb-corporate-governance/tiger-brands-admits-to-bread-pricefixing-pays-fine`.

[48] Skyrms B, 2001, *The stag hunt*, Proceedings and Addresses of the American Philosophical Association, **75**(2), pp. 31–41.

[49] Sloane NJA, 2011, *The on-line encyclopedia of integer sequences*, [Online], [Cited April 14th, 2011], Available from `http://oeis.org/`.

[50] Stanley R, 2012, *Enumerative combinatorics*, 2nd Edition, Cambridge University Press, Cambridge.

[51] Szabó G & Fáth G, 2007, *Evolutionary games on graphs*, Physics Reports, **446**(4-6), pp. 97–216.

[52] Trivers RL, 1971, *The evolution of reciprocal altruism*, The Quarterly Review of Biology, **46**(1), pp. 35–57.

[53] v Neumann J, 1928, *Zur theorie der gesellschaftsspiele*, Mathematische Annalen, **100**(1), pp. 295–320.

[54] Van Vuuren JH, 2011, *Graph theory*, In Press.

[55] Vincent TL & Brown JS, 1984, *Stability in an Evolutionary Game*, Theoretical Population Biology, **427**, pp. 408–427.

[56] Vincent TL & Brown JS, 2005, *Evolutionary game theory, natural selection, and Darwinian dynamics*, Cambridge University Press, Cambridge.

[57] Weibull JW, 1997, *Evolutionary game theory*, MIT Press, Cambridge (MA).

[58] Weisstein EW, 2012, *Circulant graph – from Wolfram MathWorld*, [Online], [Cited November 28th, 2012], Available from `http://mathworld.wolfram.com/CirculantGraph.html`.

[59] Wright S, 1932, *The roles of mutation, inbreeding, crossbreeding, and selection in evolution*, Proceedings of the 6$^{\text{th}}$ International Congress of Genetics, Ithaca (NY), pp. 356–366.

[60] Zermelo E, 1912, *Über eine anwendung der mengenlehre auf die theorie des schachspiels*, Proceedings of the 5$^{\text{th}}$ International Congress of Mathematicians, Cambridge, pp. 501–504.

[61] Zimmermann MG, Eguíluz VM & San Miguel M, 2004, *Coevolution of dynamical states and interactions in dynamic networks*, Physical Review E, **69**, p. 065102.

APPENDIX A

Enumeration lemmas for the toroidal grid graph

A number of lemmas and a corollary, which are required to enumerate the automorphism classes of the ESPD on toroidal grid graphs, are provided in this appendix. The isometry δ_r^i is considered first.

Lemma A.1 *Let $\mathcal{X}$ be the set of all the game states of the ESPD with the toroidal $m \times n$ grid graph as underlying graph. Then the number of game states in $\mathcal{X}$ fixed by δ_r^i is $|F_{\delta_r^i}| = 2^{m \gcd(i,n)}$.*

Proof: Applying the isometry δ_i to a game state modulo shifts each column i positions to the right. Let $d = \operatorname{lcm}(i,n) = \frac{in}{\gcd(i,n)}$. Applying δ_i to a state $\frac{d}{i}$ times maps a column to its original position, as illustrated in Figure A.1. Therefore, assigning strategies to a single column fixes the strategies of the players in $\frac{d}{i}$ other columns. It therefore follows that assigning strategies to the players in the first $n\frac{i}{d} = \gcd(i,n)$ columns fixes all the remaining strategies of the state under the isometry δ_r^i. Since each of the m players can be assigned one of two strategies, it follows that $|F_{\delta_r^i}| = 2^{m \gcd(i,n)}$. $\square$

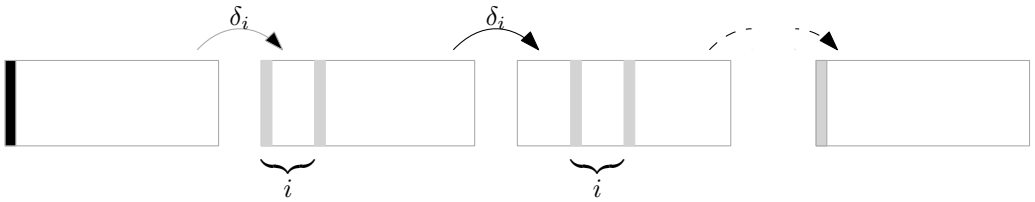

Figure A.1: *An illustration of applying the isometry δ_i to a toroidal grid graph. The translation of a single column is demonstrated; the position of the column before each application of the isometry δ_i is indicated in grey.*

The isometry $\sigma_v \delta_r^i$ is considered next.

Lemma A.2 *Let $\mathcal{X}$ be the set of all the game states of the ESPD with the toroidal $m \times n$ grid graph as underlying graph. Then the number of game states in $\mathcal{X}$ fixed by $\sigma_v \delta_r^i$ is*

$$|F_{\sigma_v \delta_r^i}| = \begin{cases} 2^{\frac{m(n+1)}{2}} & \text{if } n \text{ is odd} \\ 2^{\frac{mn}{2}} & \text{if both } n \text{ and } i \text{ are even} \\ 2^{m(\frac{n}{2}+1)} & \text{if } n \text{ is even and } i \text{ is odd.} \end{cases}$$

Proof: The isometry $\sigma_v\delta_r^i$ shifts each column i positions to the right and then mirrors the column about the vertical axis of symmetry.

The case where i is even and $i \leq \frac{n}{2}$, illustrated in Figure A.2, is considered first. There is a one-to-one mapping between the columns in similarly coloured regions of the two game states in Figure A.2. The columns in the grey area in the top game state map to the columns in the grey area in the bottom game state, but in reverse order from left to right. Assigning strategies to the players located in the coloured areas therefore fixes the strategies of the remaining players under the isometry $\sigma_v\delta_r^i$. There are $\frac{n}{2} - i + 2\frac{i}{2} = \frac{n}{2}$ columns in the coloured areas and therefore $\frac{mn}{2}$ players in the coloured areas. Since each player can be assigned one of two strategies, it follows that $|F_{\sigma_v\delta_r^i}| = 2^{\frac{mn}{2}}$ states are fixed by $\sigma_v\delta_r^i$. The case where $i > \frac{n}{2}$ may be considered as a shift to the left by $n/2 - i$ positions; it then follows by a similar argument that $|F_{\sigma_v\delta_r^i}| = 2^{\frac{mn}{2}}$ when $i > \frac{n}{2}$.

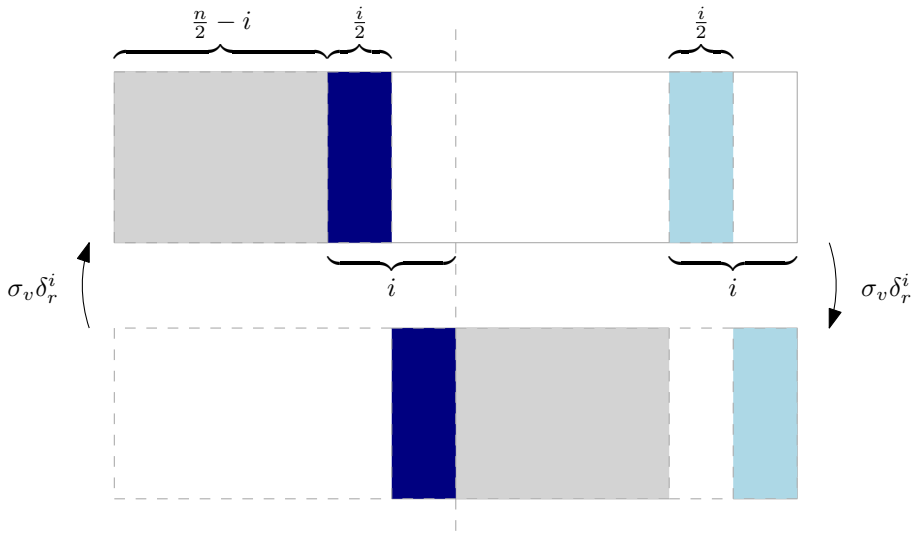

Figure A.2: *Assigning strategies to the players in the shaded areas determines the strategies of the remaining players under the isometry $\sigma_v\delta_r^i$ in the case where both n and i are even.*

The case where i is odd is similar to the case where i is even, with the exception that two columns in the game state (those coloured yellow in Figure A.3) map onto their original positions. Therefore, assigning strategies to the players in the coloured regions in Figure A.3 fixes the strategies of the remaining players under the isometry $\sigma_v\delta_r^i$. There are $\frac{n}{2} - i + 2\frac{i-1}{2} + 2 = \frac{n}{2} + 1$ columns in the coloured regions and hence $|F_{\sigma_v\delta_r^i}| = 2^{m(\frac{n}{2}+1)}$.

Finally, the case where n is odd is considered. The isometry $\sigma_v\delta_r^i$ acting on a game state is illustrated in Figures A.4 and A.5. Note that the centre column is positioned on top of the vertical axis of symmetry. Again there is a one-to-one mapping between players in the coloured areas in the top game state and the regions of same colour in the bottom game state. The number of columns that need to be assigned strategies in the case where i is even is $\frac{n-1}{2} - i + \frac{i}{2} - 1 + \frac{i}{2} + 2 = \frac{n+1}{2}$ and the case where i is odd is $\frac{n-1}{2} - i + 2 \cdot \frac{i-1}{2} + 2 = \frac{n+1}{2}$. Therefore it follows that $|F_{\sigma_v\delta_r^i}| = 2^{\frac{m(n+1)}{2}}$ for odd values of n. $\square$

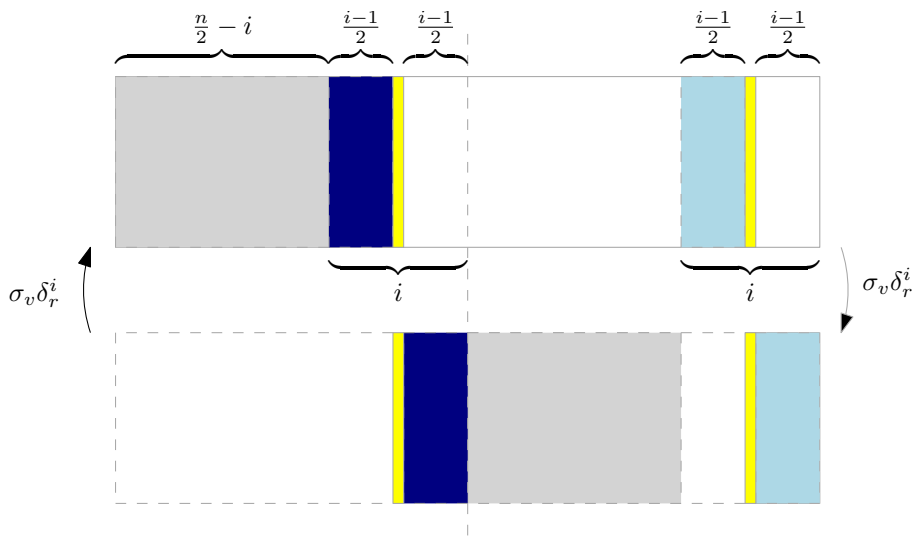

Figure A.3: *Assigning strategies to the players in the shaded areas determine the strategies of the remaining players under the isometry $\sigma_v\delta_r^i$ in the case where n is even and i is odd.*

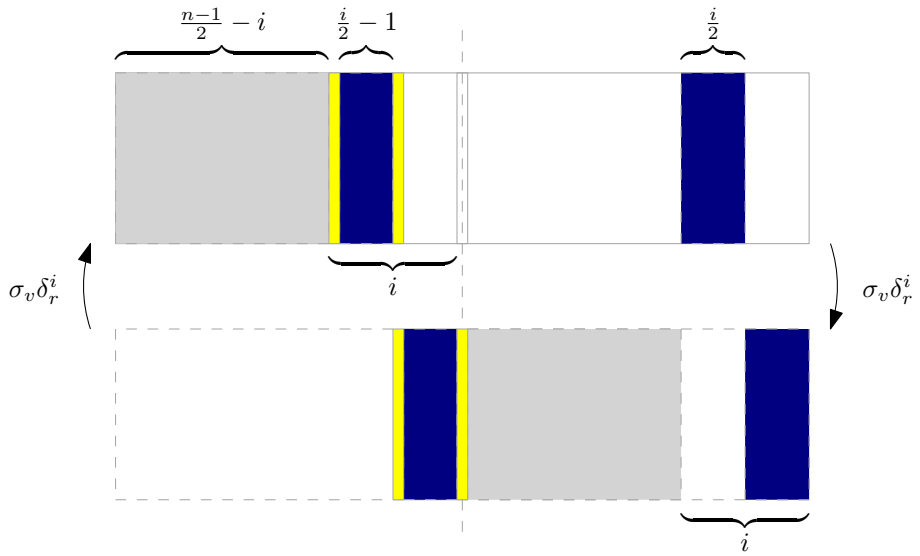

Figure A.4: *Assigning strategies to the players in the shaded areas determine the strategies of the remaining players under the isometry $\sigma_v\delta_r^i$ in the case where n is odd and i is even.*

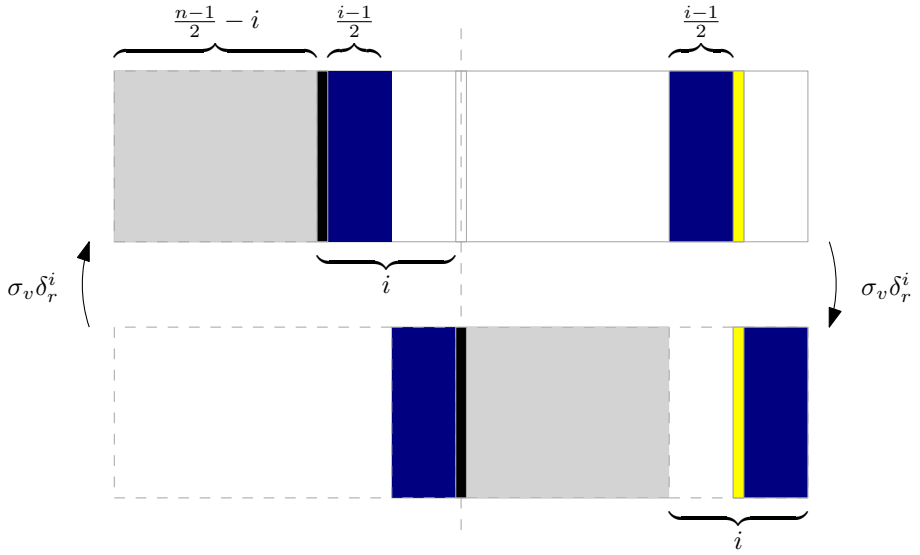

Figure A.5: *Assigning strategies to the players in the shaded areas determine the strategies of the remaining players under the isometry $\sigma_v\delta_r^i$ in the case where both n and i are odd.*

The following corollary is a direct result of the previous lemma.

Corollary A.1 *If $|F_{\sigma_v\delta_r^i}|$ is the number of game states in $\mathcal{X}$ fixed by $\sigma_v\delta_r^i$, where $\mathcal{X}$ is the set containing all the game states of the ESPD with the toroidal $m \times n$ grid graph as underlying graph, then*

$$\sum_{i=1}^{n-1} |F_{\sigma_v\delta_r^i}| = \begin{cases} (n-1)2^{\frac{m(n+1)}{2}} & \text{if } n \text{ is even} \\ (\frac{n}{2}-1)\cdot 2^{\frac{mn}{2}} + \frac{n}{2}\cdot 2^{m(\frac{n}{2}+1)} & \text{if } n \text{ is odd.} \end{cases}$$

The isometry $\sigma_h\delta_r^i$ is considered next.

Lemma A.3 *Let $\mathcal{X}$ be the set of all the game states of the ESPD with the toroidal $m \times n$ grid graph as underlying graph. Then the number of game states in $\mathcal{X}$ fixed by $\sigma_h\delta_r^i$ is*

$$|F_{\sigma_h\delta_r^i}| = \begin{cases} 2^{\frac{m}{2}\gcd(2i,n)} & \text{if } m \text{ is even} \\ 2^{\frac{m-1}{2}\gcd(2i,n)+\gcd(i,n)} & \text{if } m \text{ is odd.} \end{cases}$$

Proof: Assigning strategies to half of the players in the first column, shaded in black in Figure A.6, determines the strategies of the players in the grey shaded columns under the isometry $\sigma_h\delta_r^i$. If m is even, then assigning strategies to $\frac{m}{2}\gcd(2i,n)$ players fixes the remaining strategies.

If m is odd, then players in the middle row are mapped to the same row, but shifted to the right by i positions. Therefore, assigning strategies to $\gcd(i,n)$ players in the middle row fixes the strategies of the players in that row under the isometry $\sigma_h\delta_r^i$. Assigning strategies to $\frac{m-1}{2}\gcd(2i,n)+\gcd(i,n)$ players in the case where m is odd therefore determines the strategies of the remaining players under the isometry $\sigma_h\delta_r^i$. □

The isometry $\rho^2\delta_r^i$ is considered next.

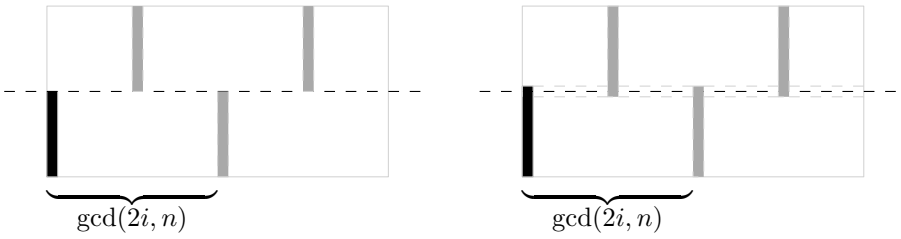

(a) m is even (b) m is odd

Figure A.6: *The grey shaded players are those players whose strategies are fixed under the isometry $\sigma_h\delta_r^i$ by assigning strategies to half of the players in the first column, shaded in black.*

Lemma A.4 *Let $\mathcal{X}$ be the set of all the game states of the ESPD with the toroidal $m \times n$ grid graph as underlying graph. Then the number of game states in $\mathcal{X}$ fixed by $\rho^2\delta_r^i$ is*

$$|F_{\rho^2\delta_r^i}| = \begin{cases} 2^{\frac{mn}{2}} & \text{if } m \text{ is even} \\ 2^{\frac{mn}{2}+\frac{1}{2}} & \text{if } m \text{ and } n \text{ are both odd} \\ 2^{\frac{mn}{2}} & \text{if } m \text{ is odd, } n \text{ and } i \text{ are both even} \\ 2^{\frac{mn}{2}+1} & \text{if } m \text{ is odd, } n \text{ is even and } i \text{ is odd.} \end{cases}$$

Proof: It can be shown that $\rho^2\delta_r^i \circ \rho^2\delta_r^i = \iota$. Therefore, assigning a strategy to a player that does not map to itself, fixes the strategy of exactly one other player. Assigning strategies to the players in the area shaded in grey in Figure A.7(a), fixes the strategies of the remaining players under the isometry $\rho^2\delta_r^i$ in the case where m is even.

In the case where m is odd, the players in the centre row have the potential to map onto their original positions under the isometry $\rho^2\delta_r^i$. Consider a player in row k and column ℓ. The isometry δ_h is equivalent to applying the function $f_h(\ell) = m-1-\ell$ to the index ℓ. A player will therefore remain in the same row after applying the isometry δ_h if $\ell = m-1-\ell$, or equivalently when $\ell = \frac{m-1}{2}$. Note that the equality can only be satisfied for odd values of m.

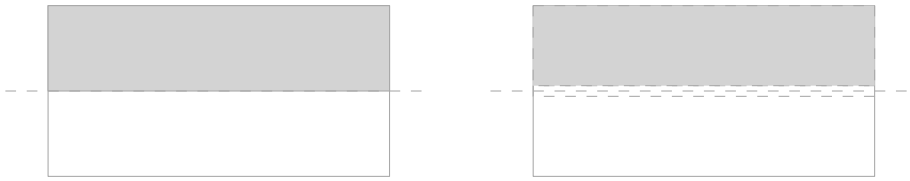

(a) (b)

Figure A.7: *Assigning strategies to the players in the shaded areas determine the remaining strategies in order for a game state to be fixed by $\rho^2\delta_r^i$ in the case (a) m is even and (b) m is odd.*

Assigning strategies to the $\frac{(m-1)n}{2}$ players in the shaded region in Figure A.7(b) determines the strategy of $mn-n$ players under the isometry $\rho^2\delta_r^i$, that is all the players excluding those in the centre row. The isometry ρ^2 is a composition of the isometries σ_v and σ_h. The position of the players in the centre row are invariant under the isometry δ_h. The effect of $\sigma_v\delta_r^i$ on the centre row is considered next. It follows by Lemma A.2 that assigning strategies to $\frac{n+1}{2}$ players if n is odd, or $\frac{n}{2}$ players if n and i are both even, or $\frac{n}{2}+1$ players if n is even and i is odd, determines the strategies of the n players in the centre row under the isometry $\rho^2\delta_r^i$. $\square$

The isometry $\delta^{i,j}$ is considered next.

Lemma A.5 *Let $\mathcal{X}$ be the set of all the game states of the ESPD with the toroidal $m \times n$ grid graph as underlying graph. Then the number of game states in $\mathcal{X}$ fixed by $\delta^{i,j}$ is*

$$|F_{\delta^{i,j}}| = 2^{\gcd[n\gcd(i,m),m\gcd(j,n)]}.$$

Proof: Applying the isometry δ_u^i a minimum of $b = \frac{m}{\gcd(i,m)}$ times will map each column to its original position. Similarly applying the isometry δ_r^j a minimum of $a = \frac{n}{\gcd(j,n)}$ times will map each row to its original position. Therefore, in order to map each player to its original position, the isometry $\delta^{i,j}$ must be applied at least $\operatorname{lcm}(a,b)$ times.

It therefore follows that assigning a strategy to a single player determines the strategies of $\operatorname{lcm}(a,b)-1$ other players. Hence fixing the strategies of $x = \frac{mn}{\operatorname{lcm}(a,b)}$ players determines the strategies of the remaining players under the isometry $\delta^{i,j}$. It follows by the identity $\operatorname{lcm}(a,b) = \frac{ab}{\gcd(a,b)}$ that

$$\begin{aligned} x &= \frac{mn\gcd(a,b)}{ab} \\ &= \gcd(a,b)\gcd(i,m)\gcd(j,n) \\ &= \gcd\left(\frac{m}{\gcd(i,m)}, \frac{n}{\gcd(j,n)}\right)\gcd(i,m)\gcd(j,n) \\ &= \gcd[m\gcd(j,n), n\gcd(i,m)]. \end{aligned}$$

Each of the $\gcd[m\gcd(j,n), n\gcd(i,m)]$ players can be assigned one of two strategies and so $|F_{\delta^{i,j}}| = 2^{\gcd[n\gcd(i,m),m\gcd(j,n)]}$. $\square$

The proof of the following Lemma is similar to the proof of Lemma A.3; the proof is therefore omitted.

Lemma A.6 *Let $\mathcal{X}$ be the set of all game states of the ESPD with the toroidal $m \times n$ grid graph as underlying graph. Then the number of games states in $\mathcal{X}$ fixed by $\sigma_v\delta_u^i$ is*

$$|F_{\sigma_v\delta_u^i}| = \begin{cases} 2^{\frac{n}{2}\gcd(2i,m)} & \text{if } n \text{ is even} \\ 2^{\frac{n-1}{2}\gcd(2i,m)+\gcd(i,m)} & \text{if } n \text{ is odd.} \end{cases}$$

The following lemma may proved in a similar fashion to Lemma A.4.

Lemma A.7 *Let $\mathcal{X}$ be the set of all the game states of the ESPD with the toroidal $m \times n$ grid graph as underlying graph. Then the number of game states in $\mathcal{X}$ fixed by $\rho^2\delta_u^i$ is*

$$|F_{\rho^2\delta_u^i}| = \begin{cases} 2^{\frac{mn}{2}} & \text{if } n \text{ is even} \\ 2^{\frac{mn}{2}+\frac{1}{2}} & \text{if } n \text{ and } m \text{ are both odd} \\ 2^{\frac{mn}{2}} & \text{if } n \text{ is odd, } m \text{ is odd and } i \text{ is even} \\ 2^{\frac{mn}{2}+1} & \text{if } n, m \text{ and } i \text{ are odd.} \end{cases}$$

The isometry $\rho^2\delta^{i,j}$ is considered next.

Lemma A.8 *If $\mathcal{X}$ is the set of all the game states of the ESPD with the toroidal $m \times n$ grid graph as the underlying graph and $|F_{\rho^2\delta^{i,j}}|$ is the number of game states in $\mathcal{X}$ fixed by $\rho^2\delta^{i,j}$, then*

$$\sum_{i=1}^{n-1}\sum_{j=1}^{m-1}|F_{\rho^2\delta^{i,j}}| = \begin{cases} (\frac{7}{4}mn - m - n + 1)2^{\frac{mn}{2}} & \text{if } m \text{ and } n \text{ are both even} \\ (\frac{3}{2}mn - \frac{3}{2}m - n + 1)2^{\frac{mn}{2}} & \text{if } m \text{ is even and } n \text{ is odd} \\ (\frac{3}{2}mn - m - \frac{3}{2}n + 1)2^{\frac{mn}{2}} & \text{if } m \text{ is odd and } n \text{ is even} \\ (m-1)(n-1)2^{\frac{mn+1}{2}} & \text{if both } m \text{ and } n \text{ are odd.} \end{cases}$$

Proof: It can be shown that $\rho^2\delta^{i,j} \circ \rho^2\delta^{i,j} = \iota$. Suppose, without loss of generality, that $\delta^{i,j}$ is the isometry that modular shifts each player's location i positions downwards and j positions to right.

Modular shifting the players in row ℓ, i positions downward, will relocate these players to row $k + i \pmod m$. Following this shift by reflection of the grid along the horizontal axis of symmetry will result in row ℓ mapping to row $-(\ell + i + 1) \pmod m$. Therefore, a row maps to its original position under $\rho^2\delta^{i,j}$ if the congruence $-(k + i + 1) \equiv k \pmod m$ is satisfied, or equivalently if

$$2k \equiv -(j + 1) \pmod m. \tag{A.1}$$

If both m and i are even, then there are no values of k satisfying (A.1). If m is even and i is odd, then exactly two values of k satisfy (A.1), namely $k = \frac{m-i-1}{2}$ or $k = \frac{2m-i-1}{2}$.

It therefore follows that in the case where both m and i are even, no player maps to its original position under the isometry $\rho^2\delta^{i,j}$. Assigning strategies to half of the players, fixes the strategies of the remaining players under the isometry $\rho^2\delta^{i,j}$. If i is odd, as shown previously, then players in exactly two rows are mapped to their original rows under the isometry $\rho^2\delta^{i,j}$. Assigning strategies to $\frac{(m-2)n}{2} = \frac{mn}{2} - n$ of the players not in these rows, fixes the strategies of the $mn - 2n$ players not contained in the aforementioned two rows.

The isometry $\rho^2\delta^{i,j}$ applied to the players in the rows mapping to their original positions under the isometry $\rho^2\delta^{i,j}$ is equivalent to applying the isometry $\delta_v\delta_r^j$ to the players in question. It follows by Lemma A.2 that strategies must be assigned to $\frac{n+1}{2}$ players if n is odd, $\frac{n}{2}$ players if n is even and j is even, or $\frac{n}{2} + 1$ players if n is even and j is odd in order to fix the strategy of the players in these rows under the isometry $\delta_v\delta_r^j$.

Hence in the case where m and n are both even,

$$|F_{\rho^2\delta^{i,j}}| = \begin{cases} 2^{\frac{mn}{2}+2} & \text{if } i \text{ and } j \text{ are both odd} \\ 2^{\frac{mn}{2}} & \text{otherwise.} \end{cases}$$

In the case where m is even, i takes on $\frac{m}{2}$ odd values and $\frac{m}{2} - 1$ even values in the double summation. Similarly if n is even, j takes on $\frac{n}{2}$ odd values and $\frac{n}{2} - 1$ even values in the double summation. Therefore,

$$\begin{aligned} \sum_{i=1}^{n-1}\sum_{j=1}^{m-1}|F_{\rho^2\delta^{i,j}}| &= \tfrac{m}{2}\tfrac{n}{2}2^{\frac{mn}{2}+2} + \left((m-1)(n-1) - \tfrac{m}{2}\tfrac{n}{2}\right)2^{\frac{mn}{2}} \\ &= \tfrac{mn}{4}2^2 2^{\frac{mn}{2}} + (\tfrac{3}{4}mn - m - n + 1)2^{\frac{mn}{2}} \\ &= (\tfrac{7}{4}mn - m - n + 1)2^{\frac{mn}{2}}. \end{aligned}$$

It follows by a similar argument as above that

$$|F_{\rho^2\delta^{i,j}}| = \begin{cases} 2^{\frac{mn}{2}} & \text{if } j \text{ is even} \\ 2^{\frac{mn}{2}+1} & \text{if } j \text{ is odd} \end{cases}$$

in the case were m is even and n is odd, and so

$$\begin{aligned} \sum_{i=1}^{m-1}\sum_{j=1}^{n-1} |F_{\rho^2\delta^{i,j}}| &= (\tfrac{m}{2}-1)(n-1)2^{\frac{mn}{2}} + \tfrac{m}{2}(n-1)2^{\frac{mn}{2}+1} \\ &= \left(\tfrac{3}{2}mn - \tfrac{3}{2}m - n + 1\right) 2^{\frac{mn}{2}}. \end{aligned}$$

In the case where m is odd and n is even,

$$|F_{\rho^2\delta^{i,j}}| = \begin{cases} 2^{\frac{mn}{2}} & \text{if } j \text{ is even} \\ 2^{\frac{mn}{2}+1} & \text{if } j \text{ is odd} \end{cases}$$

and hence

$$\begin{aligned} \sum_{i=1}^{n-1}\sum_{j=1}^{m-1} |F_{\rho^2\delta^{i,j}}| &= (m-1)\tfrac{n}{2}2^{\frac{mn}{2}+1} + (m-1)(\tfrac{n}{2}-1)2^{\frac{mn}{2}} \\ &= (\tfrac{3}{2}mn - m - \tfrac{3}{2}n + 1)2^{\frac{mn}{2}}. \end{aligned}$$

In the case where both m and n are odd, $|F_{\rho^2\delta^{i,j}}| = 2^{\frac{mn+1}{2}}$ and therefore

$$\sum_{i=1}^{n-1}\sum_{j=1}^{m-1} |F_{\rho^2\delta^{i,j}}| = (m-1)(n-1)2^{\frac{mn+1}{2}}. \quad \square$$

The proof of the following two lemmas are similar to those of the relevant lemmas above.

Lemma A.9 *Let $\mathcal{X}$ be the set of all the game states of the ESPD with the toroidal $m \times n$ grid graph as underlying graph. Then the number of game states in $\mathcal{X}$ fixed by $\sigma_v\delta^{i,j}$ is*

$$|F_{\sigma_v\delta^{i,j}}| = \begin{cases} 2^{\frac{n}{2}\gcd(2i,m)} & \text{if } n \text{ is even and } j \text{ is even} \\ 2^{\left(\frac{n}{2}-1\right)\gcd(2i,m)+2\gcd(m,i)} & \text{if } n \text{ is even and } j \text{ is odd} \\ 2^{\frac{n-1}{2}\gcd(2i,m)+\gcd(m,i)} & \text{if } n \text{ is odd.} \end{cases}$$

Lemma A.10 *Let $\mathcal{X}$ be the set of all the game states of the ESPD with the toroidal $m \times n$ grid graph as underlying graph. Then the number of game states in $\mathcal{X}$ fixed by $\sigma_h\delta^{i,j}$ is*

$$|F_{\sigma_h\delta^{i,j}}| = \begin{cases} 2^{\frac{m}{2}\gcd(2j,n)} & \text{if } m \text{ is even and } i \text{ is even} \\ 2^{\left(\frac{m}{2}-1\right)\gcd(2j,n)+2\gcd(n,j)} & \text{if } m \text{ is even and } i \text{ is odd} \\ 2^{\frac{n-1}{2}\gcd(2j,n)+\gcd(n,j)} & \text{if } m \text{ is odd.} \end{cases}$$

APPENDIX B

State graphs

Contents

This appendix contains the state graphs of the ESPD on various grids graphs (with and without wrapping) as underlying graph.

B.1 $P_2 \times P_3$

The ESPD with $P_2 \times P_3$ as underlying graph exhibits fundamentally different game dynamics across the six disjoint parameter regions in the P-T phase plane. The phase plane and the parameter regions are shown in Figure B.1. The six state graphs, one for each parameter region, are shown on pp. 116–117.

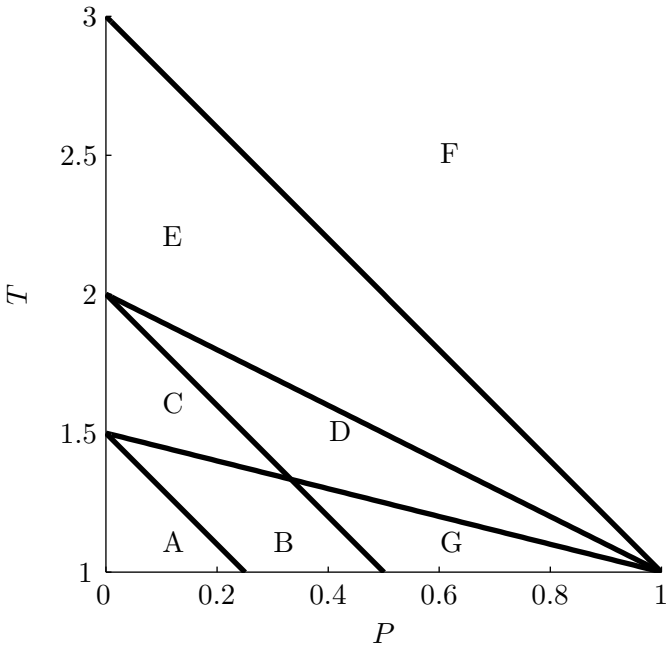

Figure B.1: *Phase plane of the ESPD with $P_2 \times P_n$ as underlying graph containing seven regions labelled A through G.*

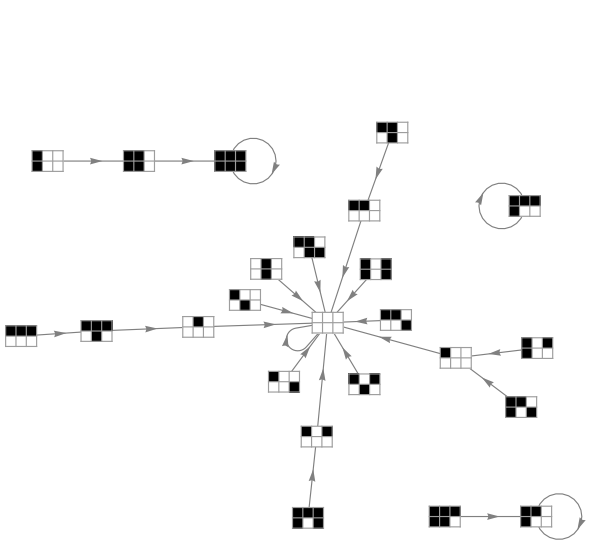

$P_2 \times P_3$: Parameter region A

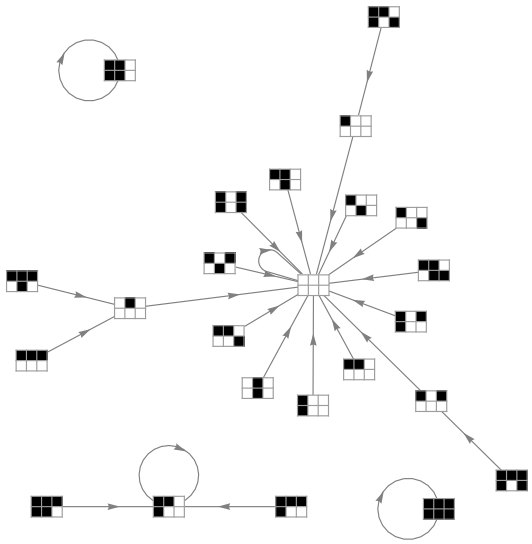

$P_2 \times P_3$: Parameter region B

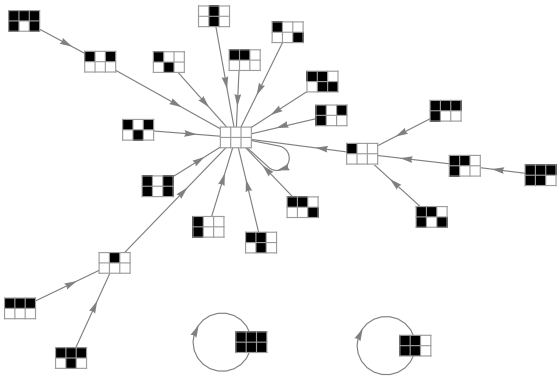

$P_2 \times P_3$: Parameter region C

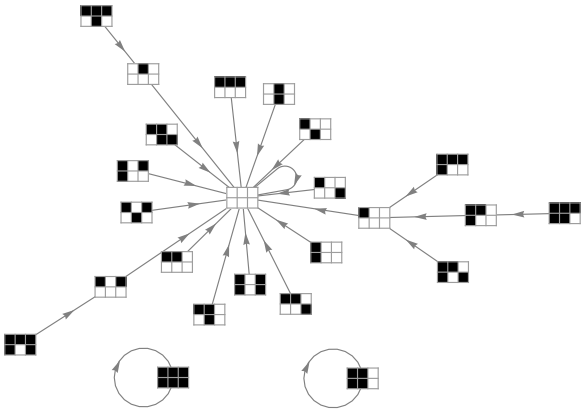

$P_2 \times P_3$: Parameter region D

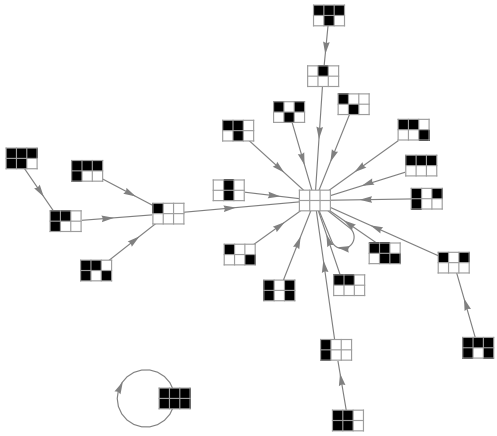

$P_2 \times P_3$: Parameter region E/F

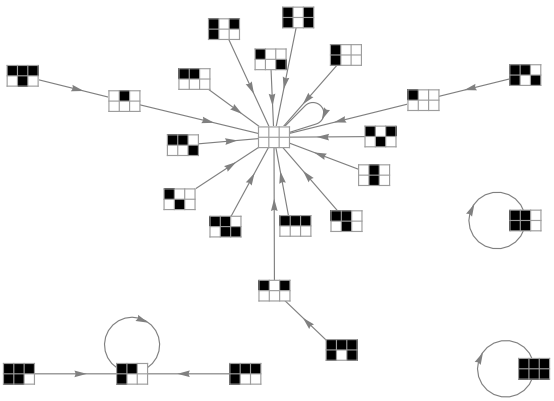

$P_2 \times P_3$: Parameter region G

B.2 $P_2 \times P_4$

The ESPD with $P_2 \times P_4$ as underlying graph exhibits fundamentally different game dynamics across the seven disjoint parameter regions in the P-T phase plane. The phase plane and the parameter regions are shown in Figure B.1. The seven state graphs, one for each parameter region, are shown below and on pp. 119–122.

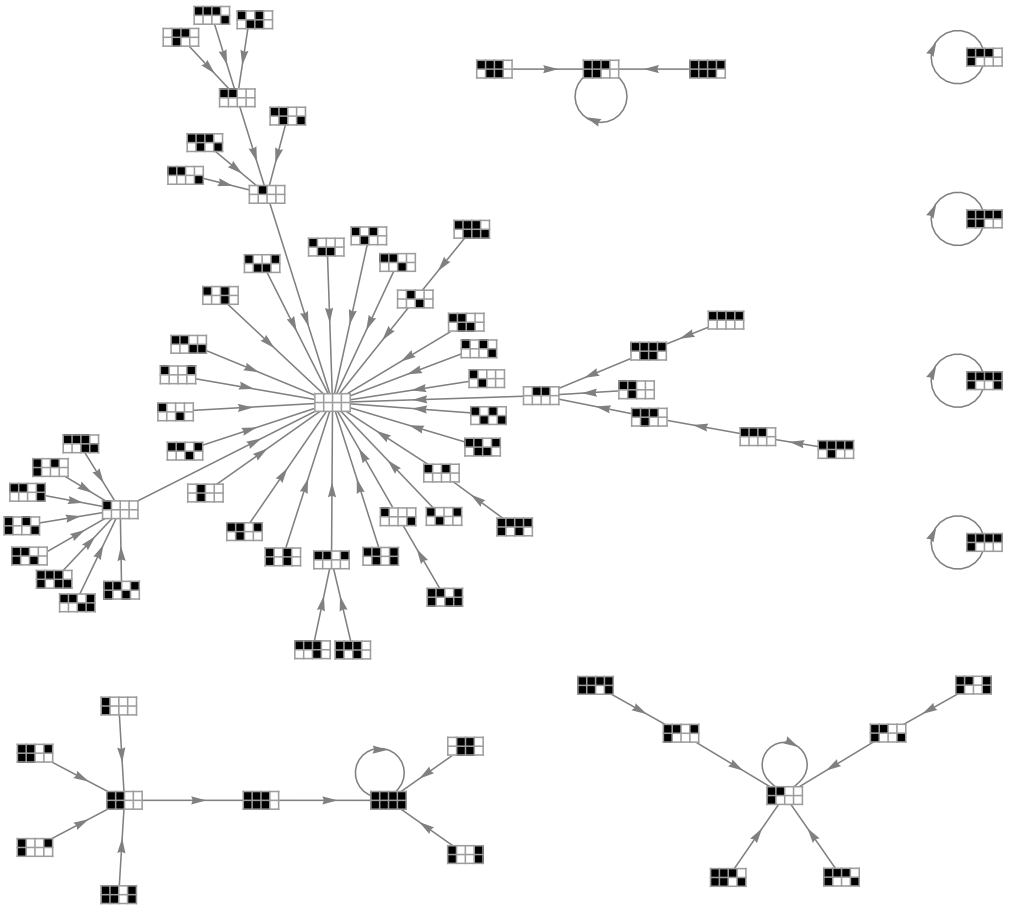

$P_2 \times P_4$: Parameter region A

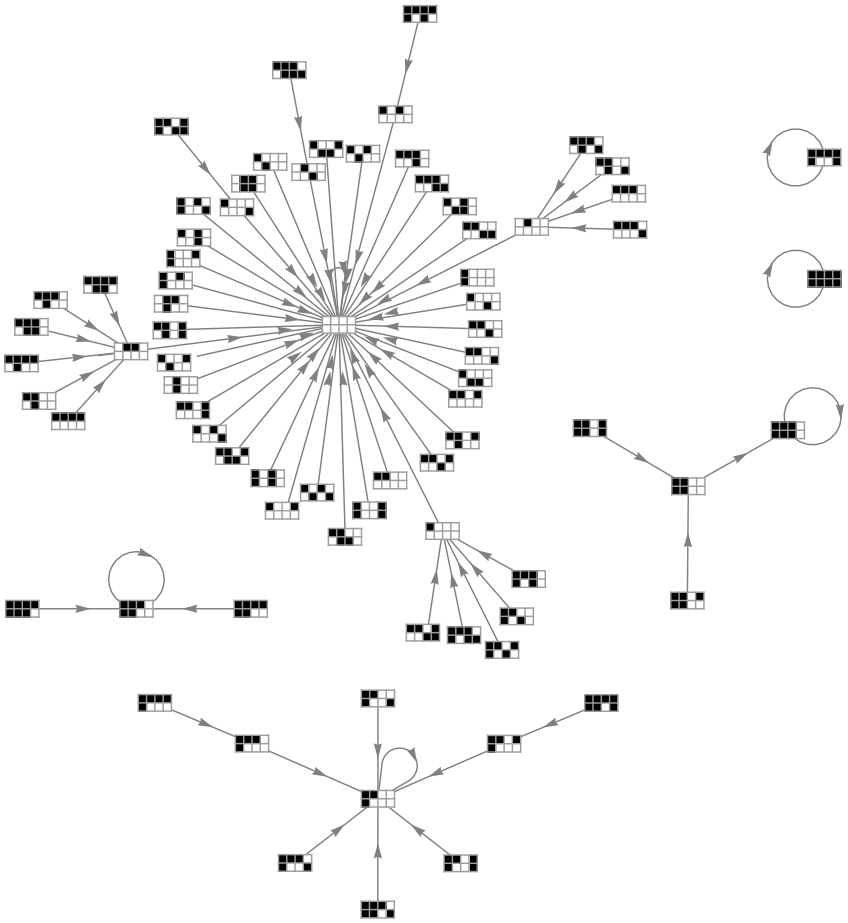

$P_2 \times P_4$: Parameter region B

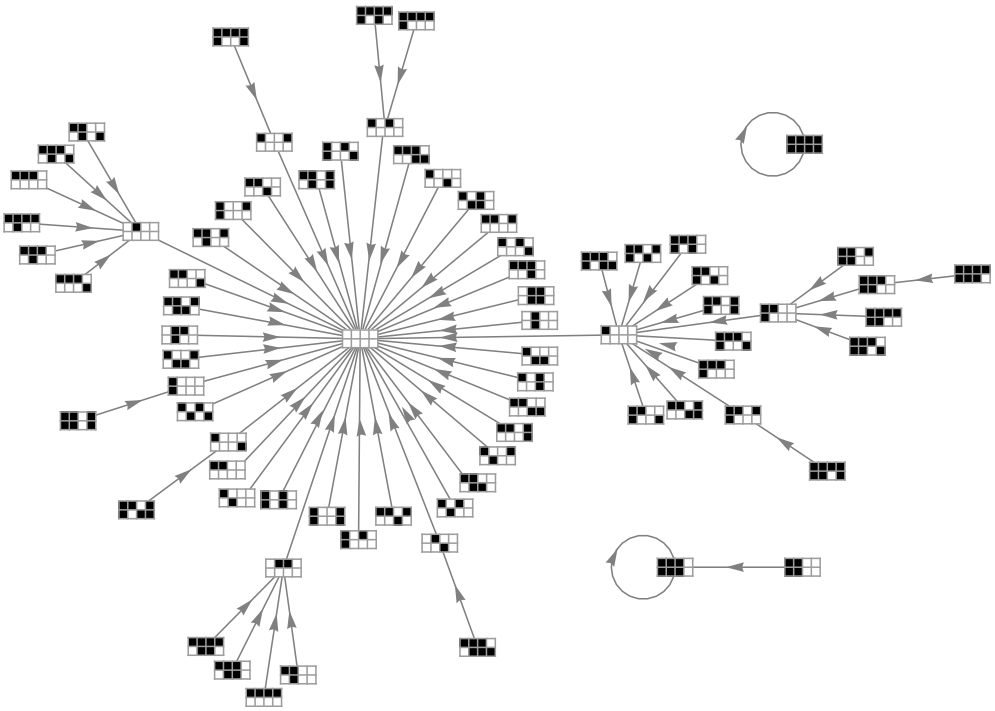

$P_2 \times P_4$: Parameter region C

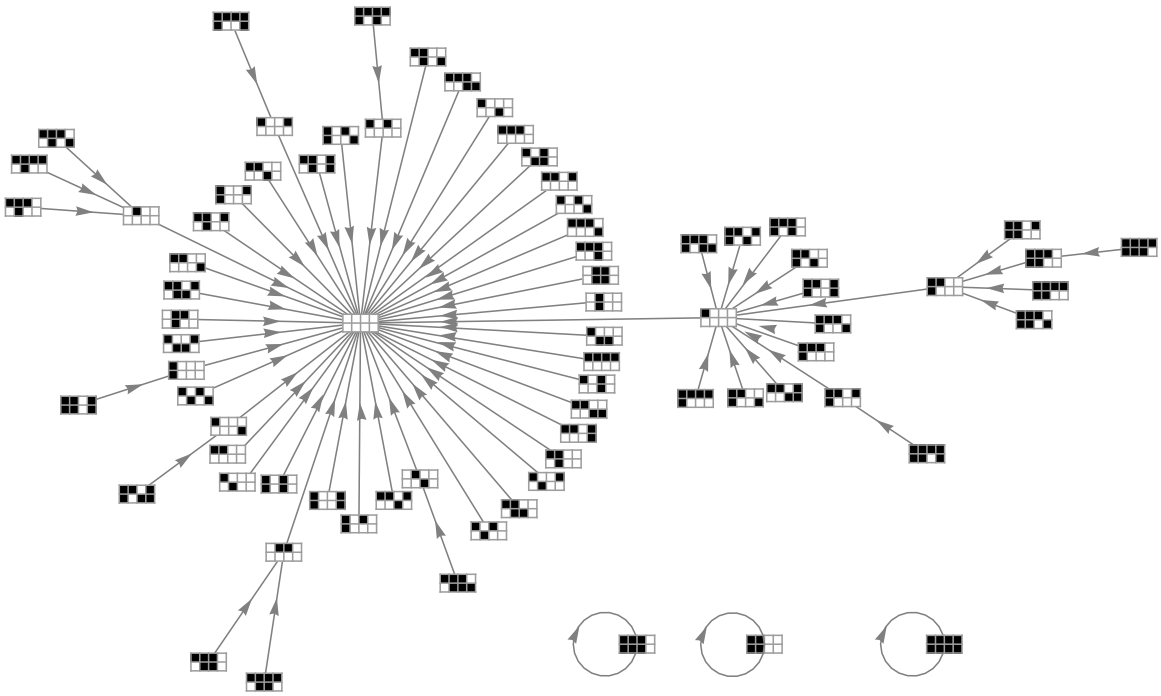

$P_2 \times P_4$: Parameter region D

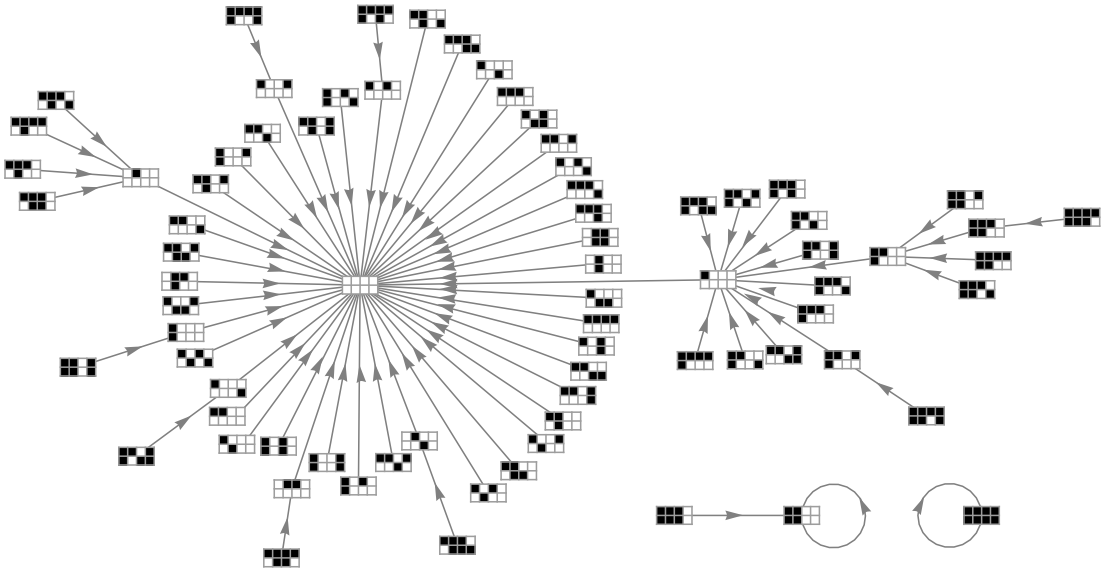

$P_2 \times P_4$: Parameter region E

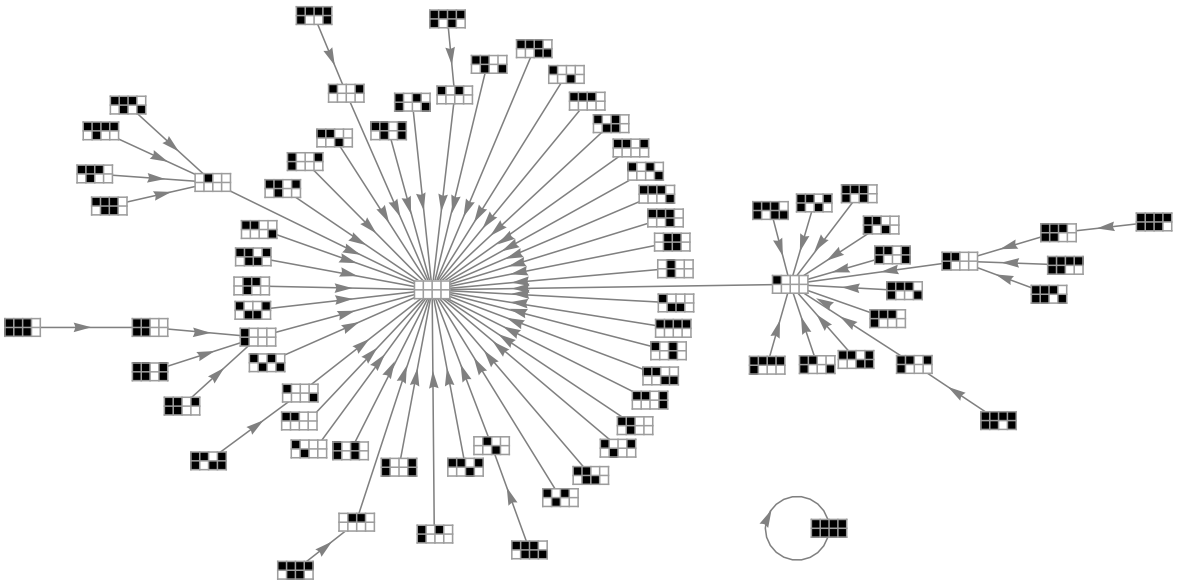

$P_2 \times P_4$: Parameter region F

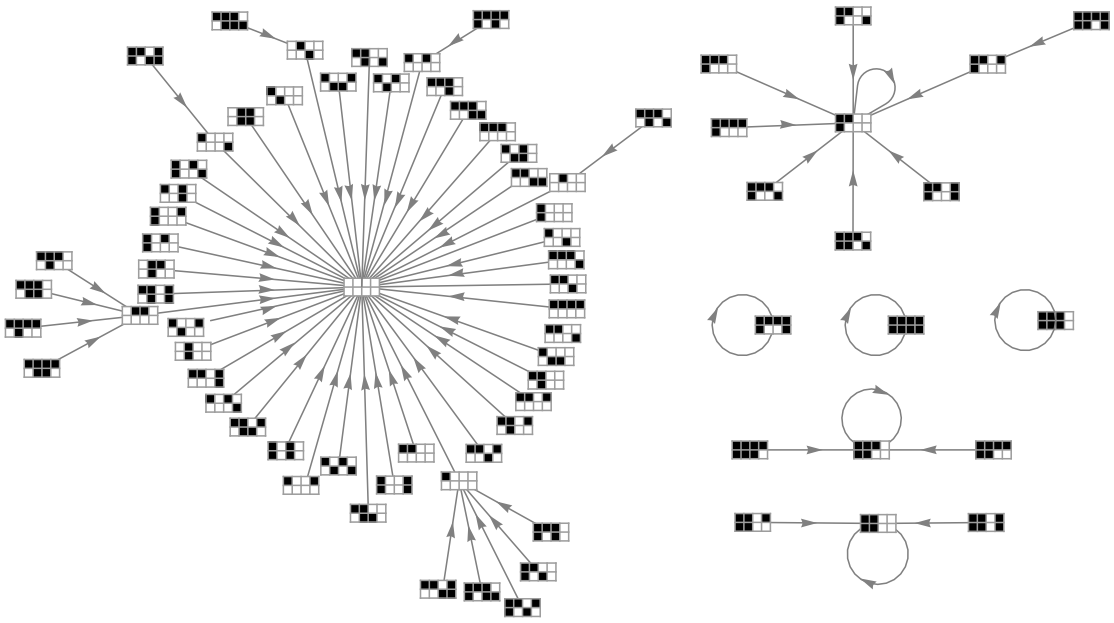

$P_2 \times P_4$: Parameter region G

B.3 $P_3 \times P_3$

The ESPD with $P_3 \times P_3$ as underlying has twenty three disjoint parameter regions in the P-T parameter space, each with a unique state graph. The phase plane indicating the aforementioned parameter regions is shown in Figure B.2. The twenty three state graphs, one for each parameter region, of the EPSD with $P_3 \times P_3$ as underlying graph are shown on pp. 124–146.

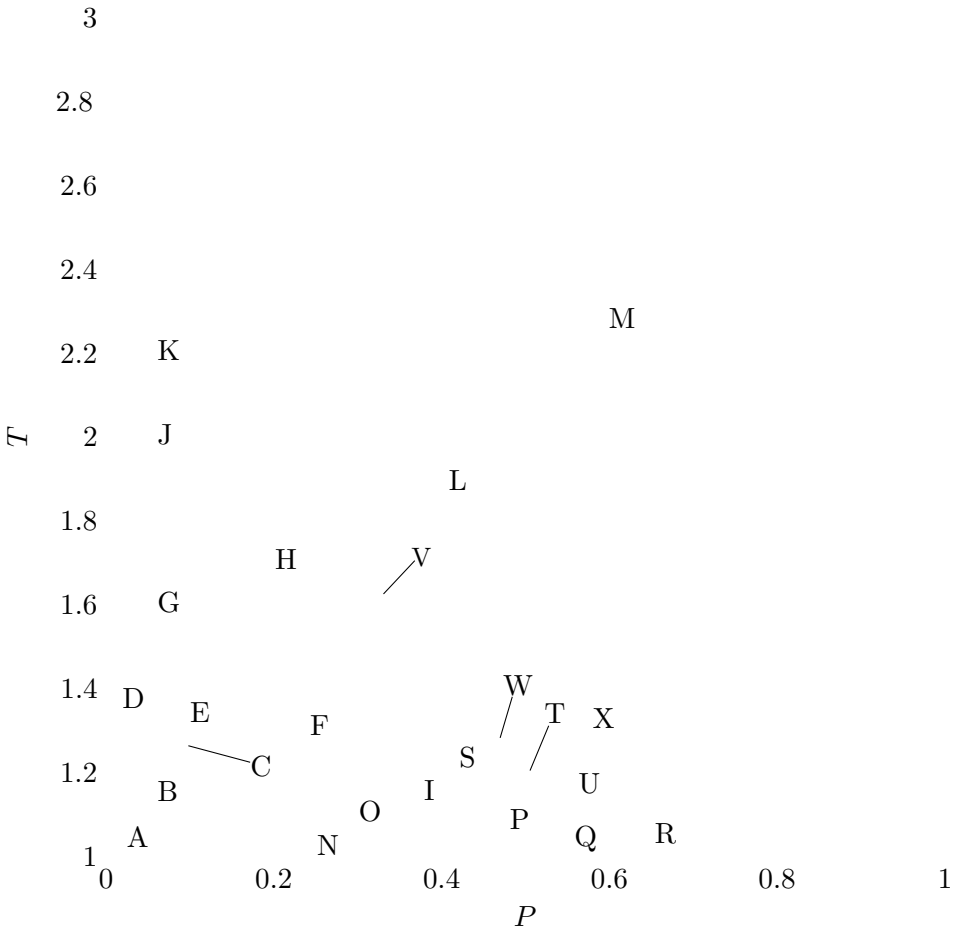

Figure B.2: *Phase plane of the ESPD with $P_3 \times P_3$ as underlying graph containing twenty three parameter regions labelled A through X.*

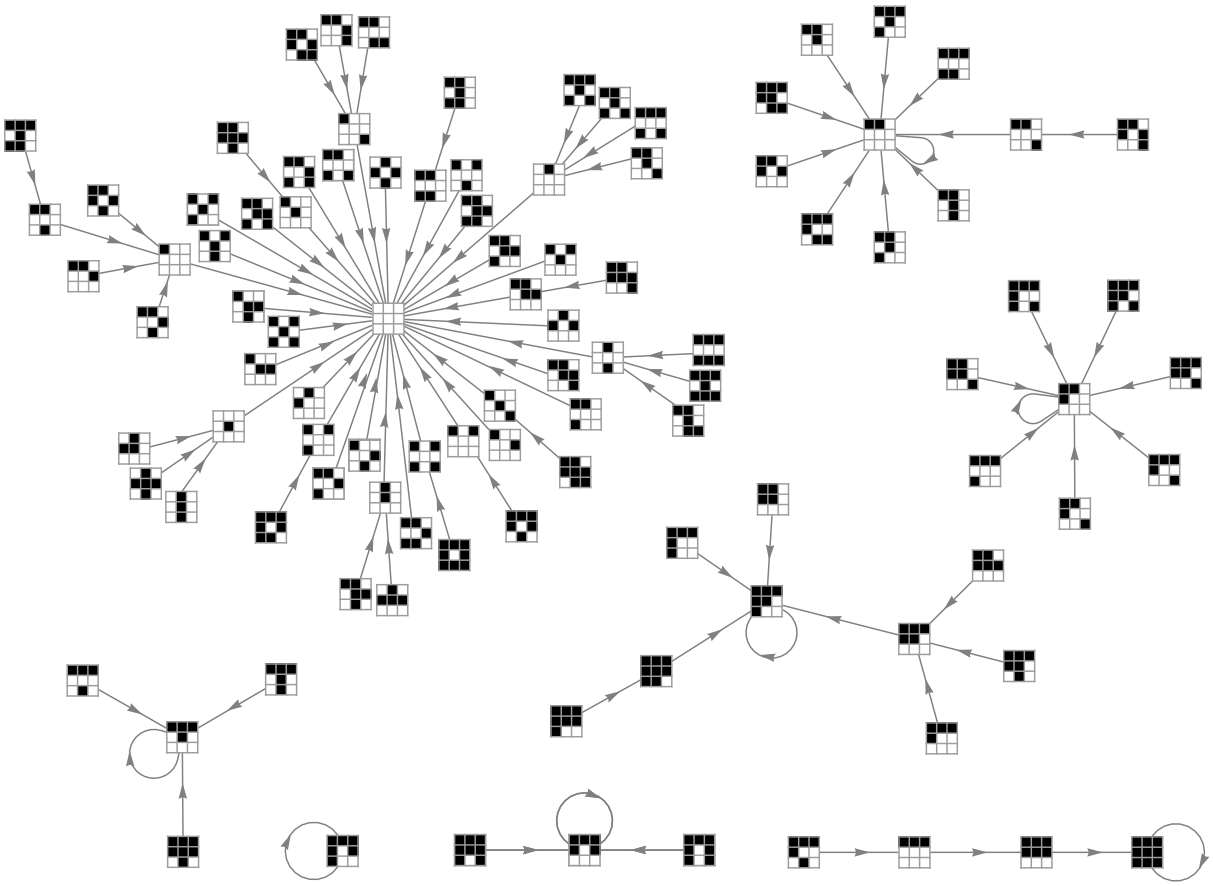

$P_3 \times P_3$: Paramter region A

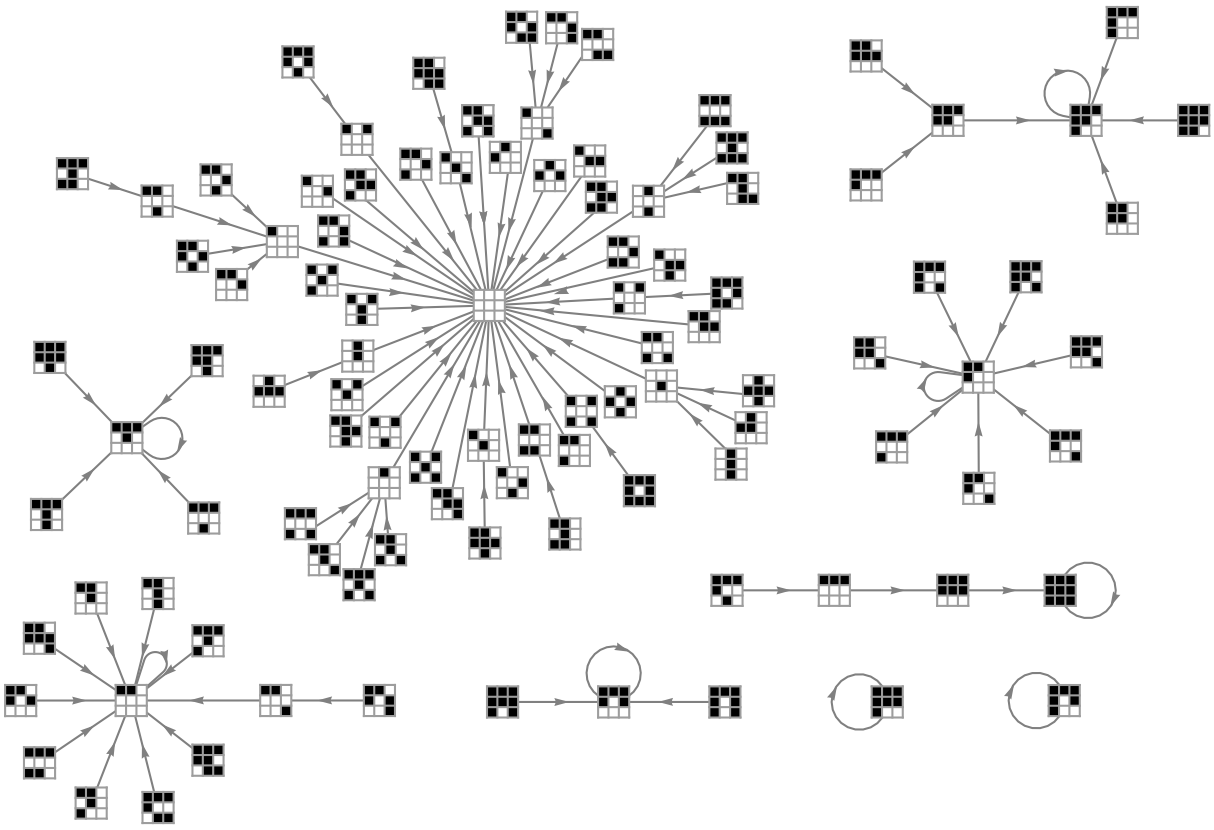

$P_3 \times P_3$: Paramter region B

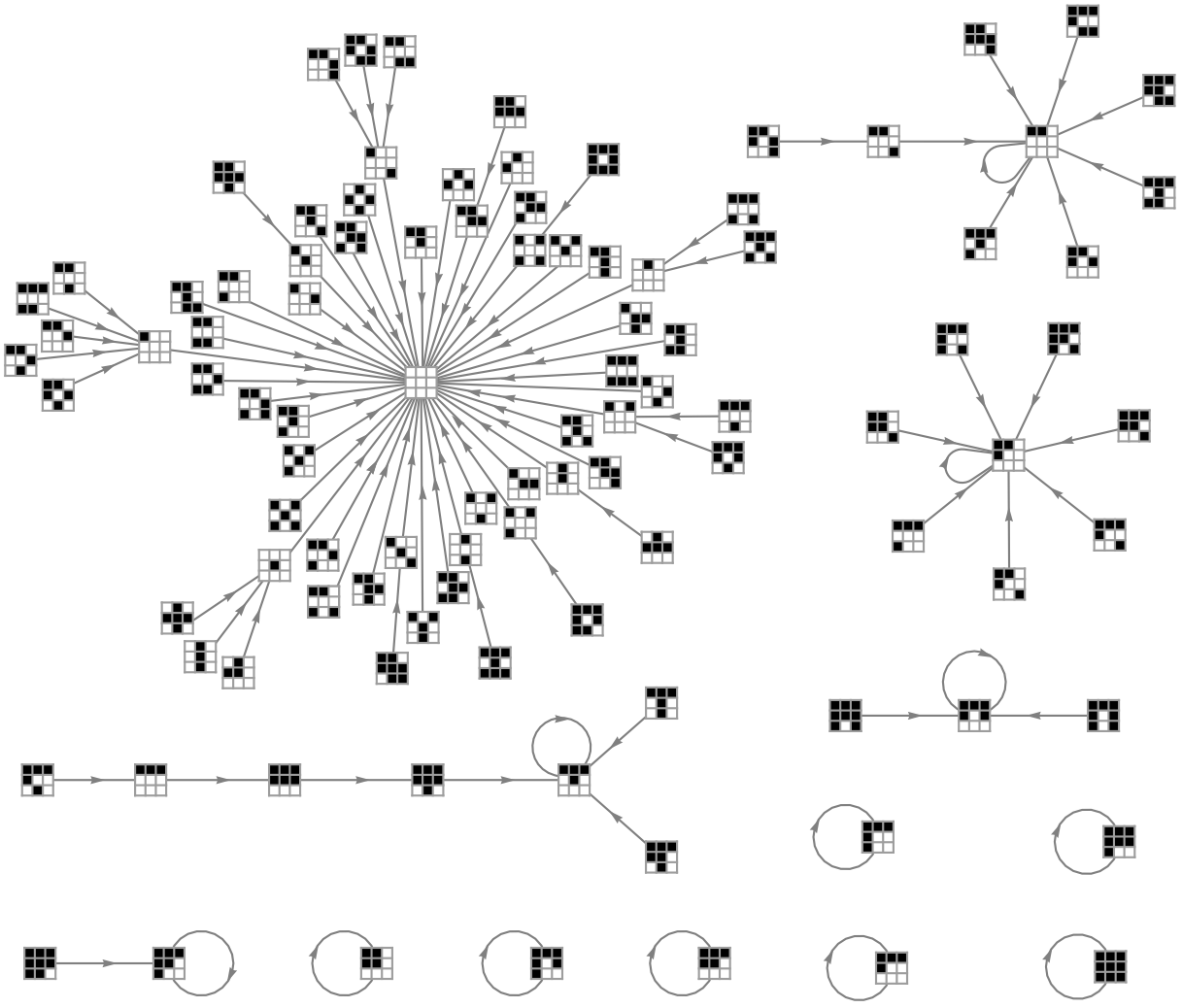

$P_3 \times P_3$: Paramter region C

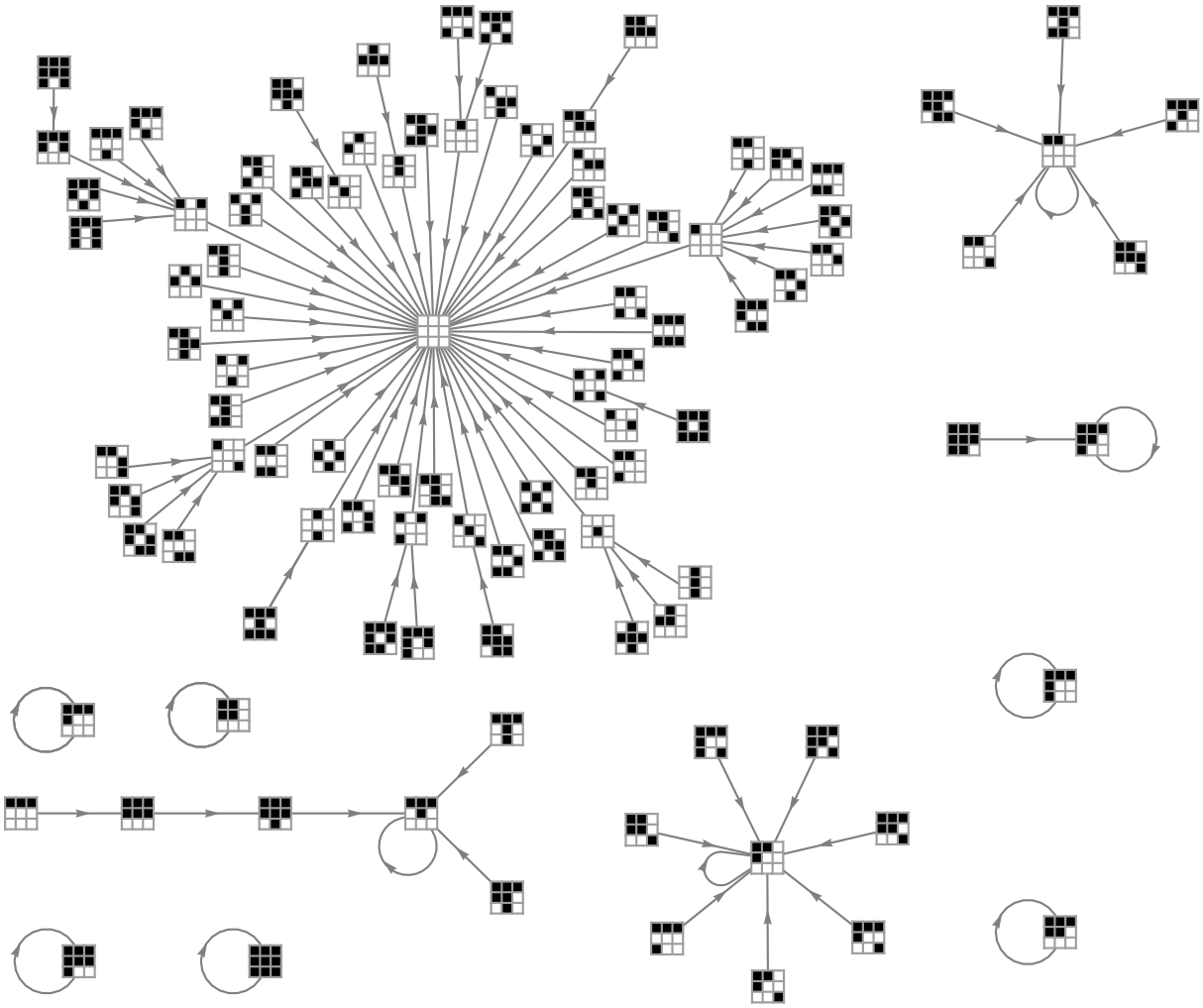

$P_3 \times P_3$: Parameter region D

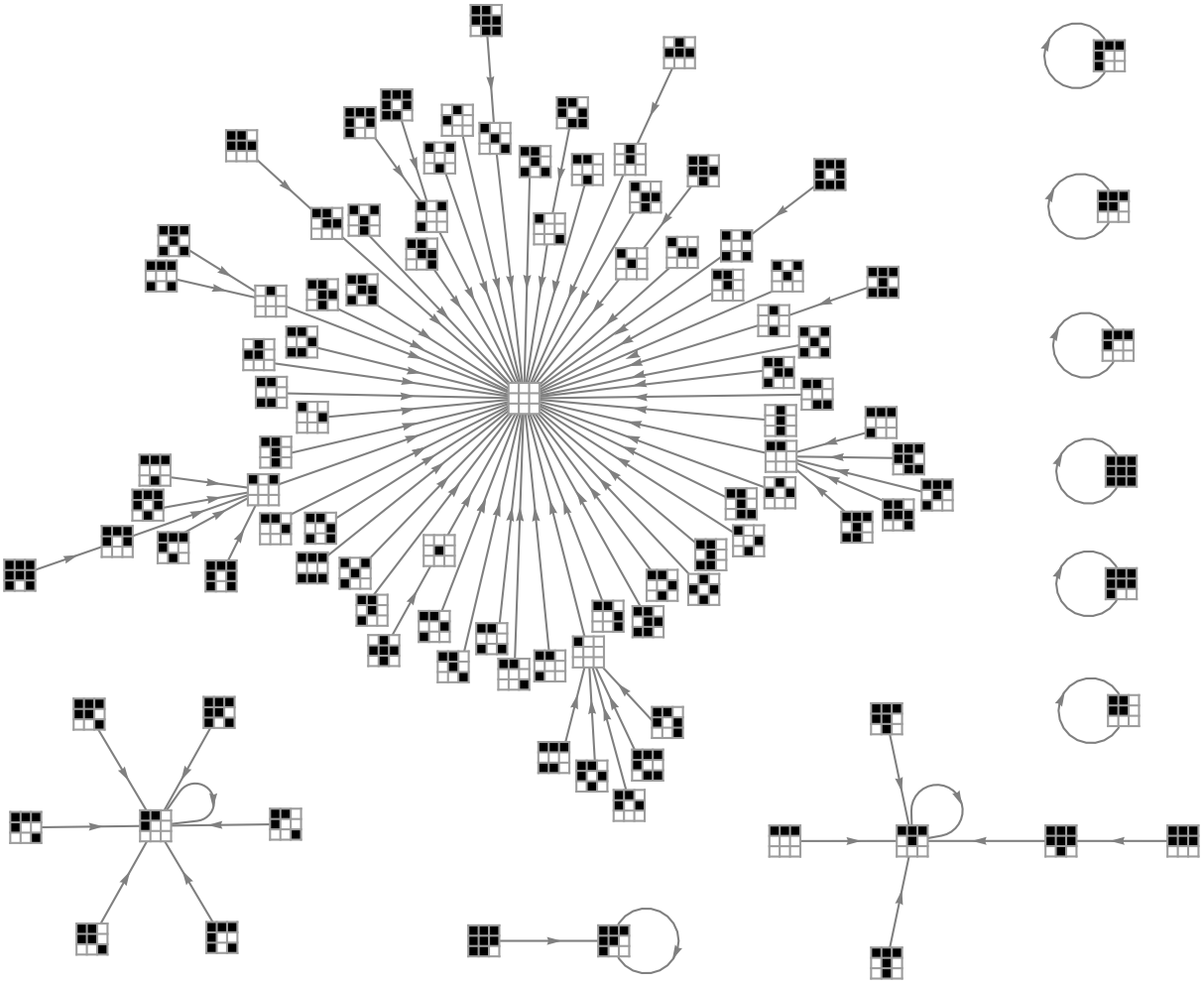

$P_3 \times P_3$: Parameter region E

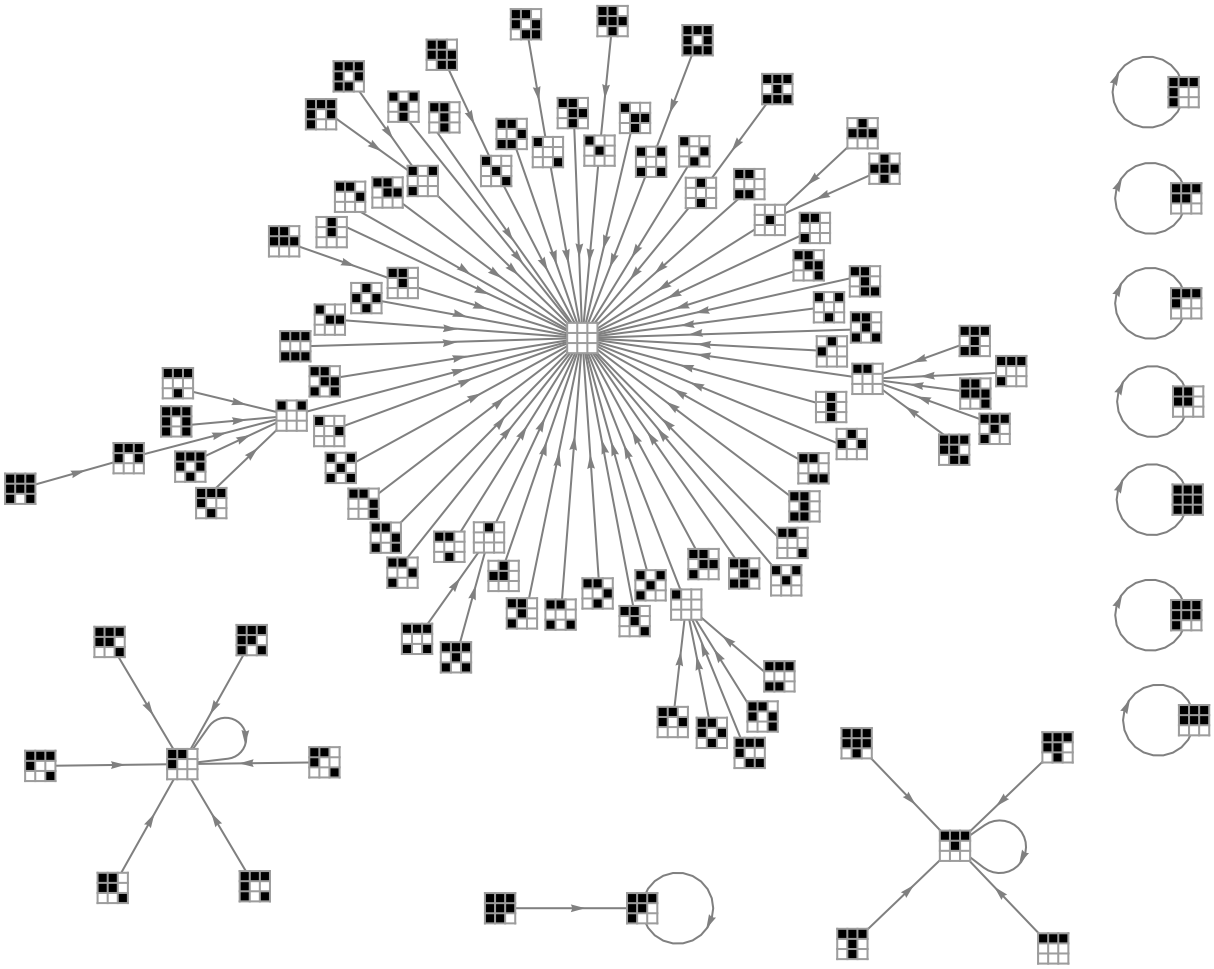

$P_3 \times P_3$: Parameter region F

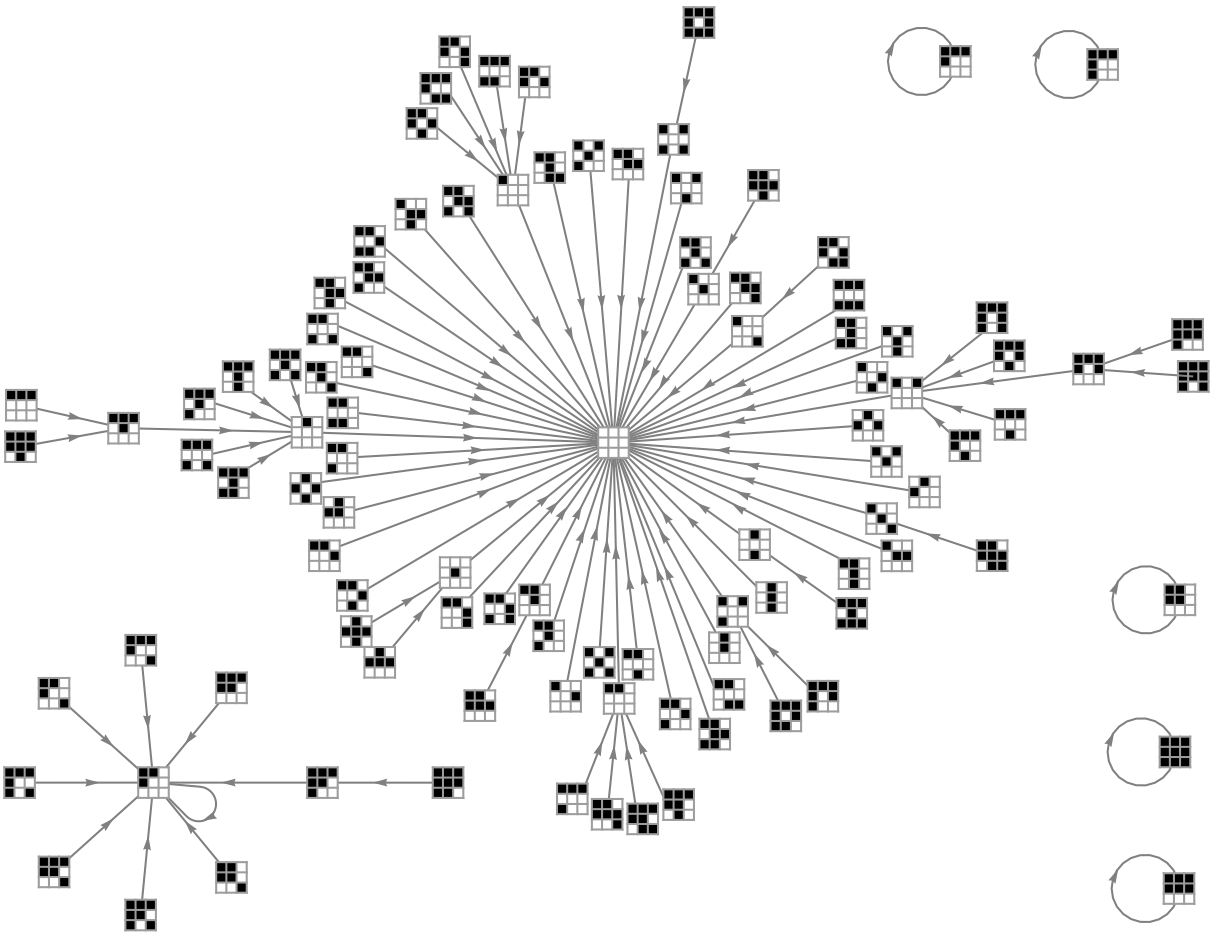

$P_3 \times P_3$: Parameter region G

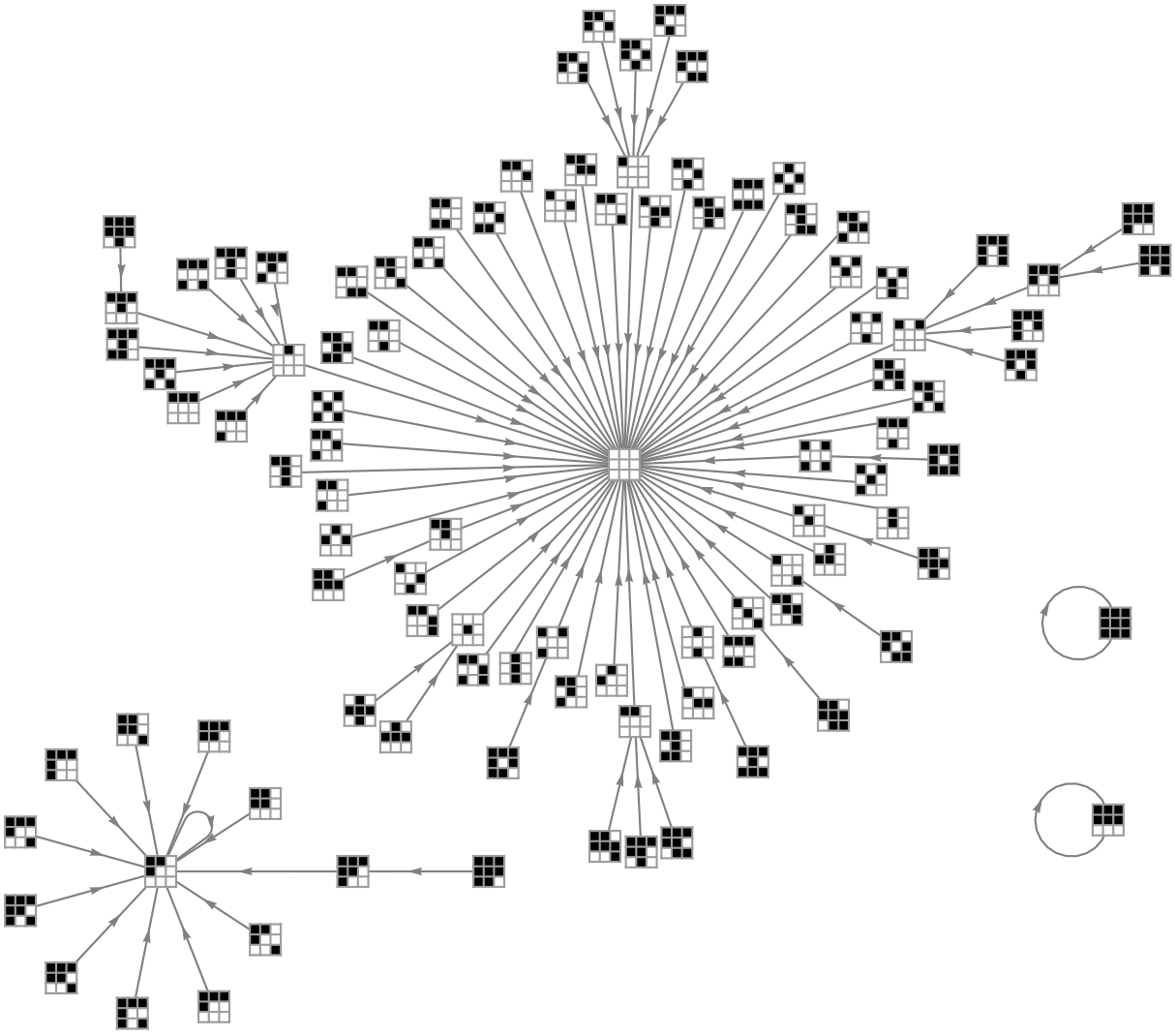

$P_3 \times P_3$: Parameter region H

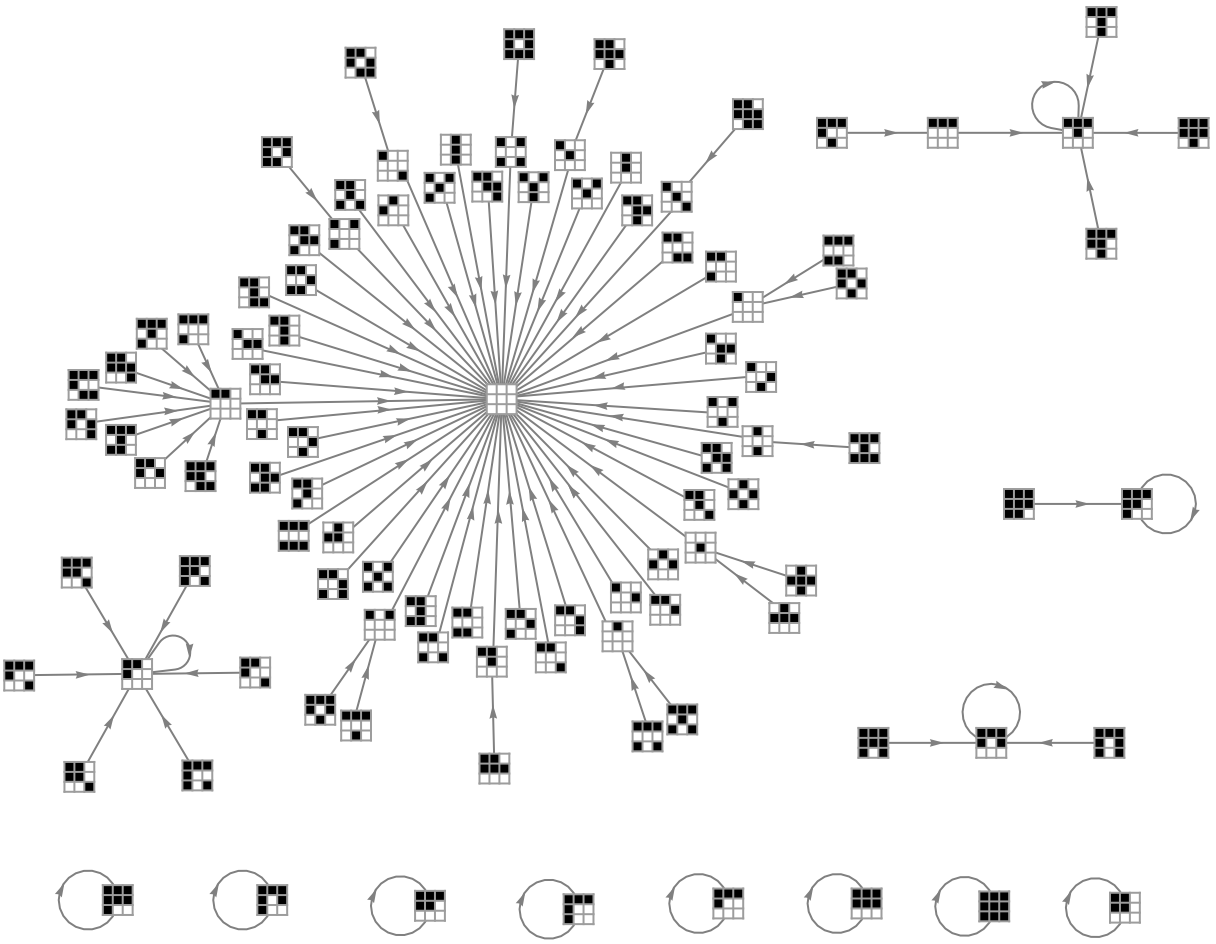

$P_3 \times P_3$: Parameter region I

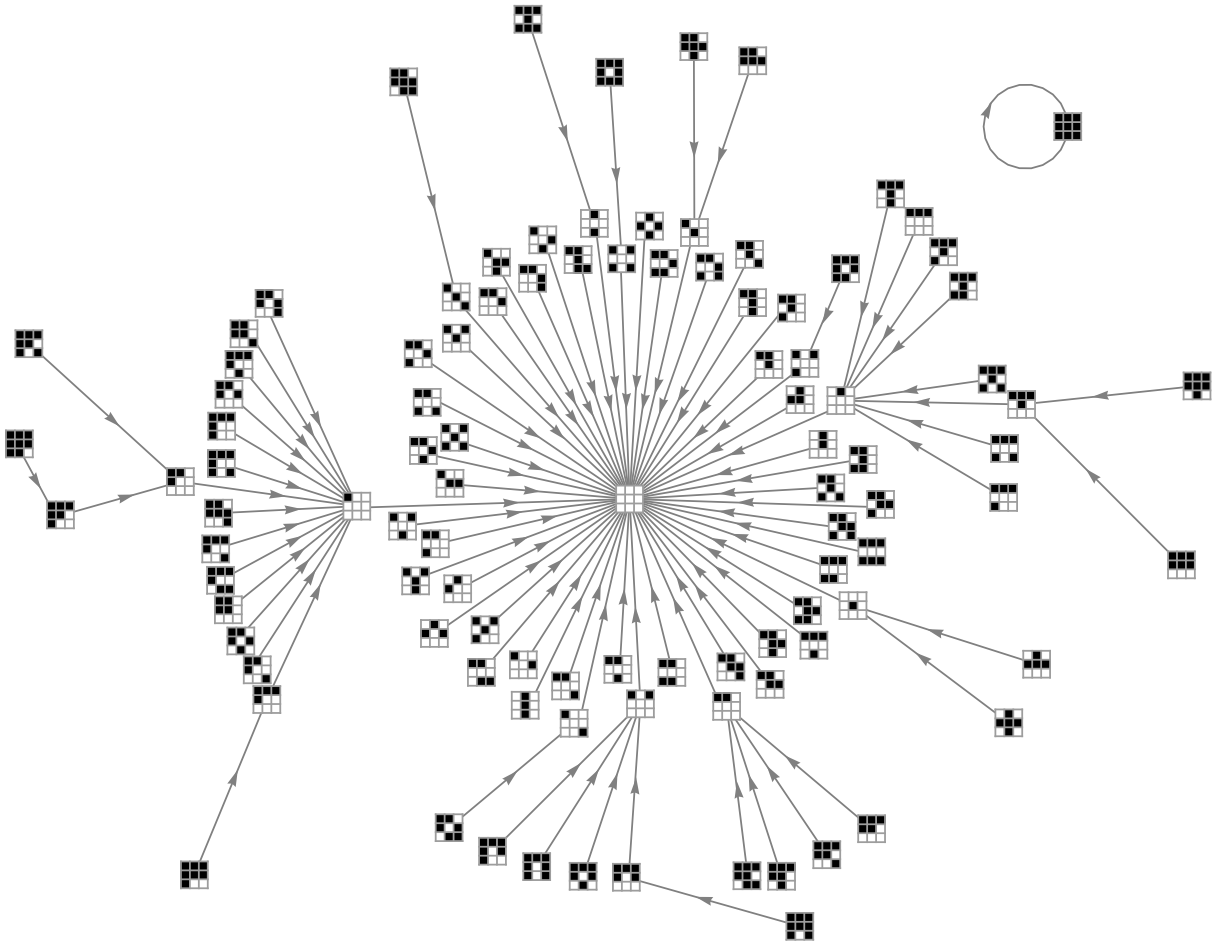

$P_3 \times P_3$: Parameter region J

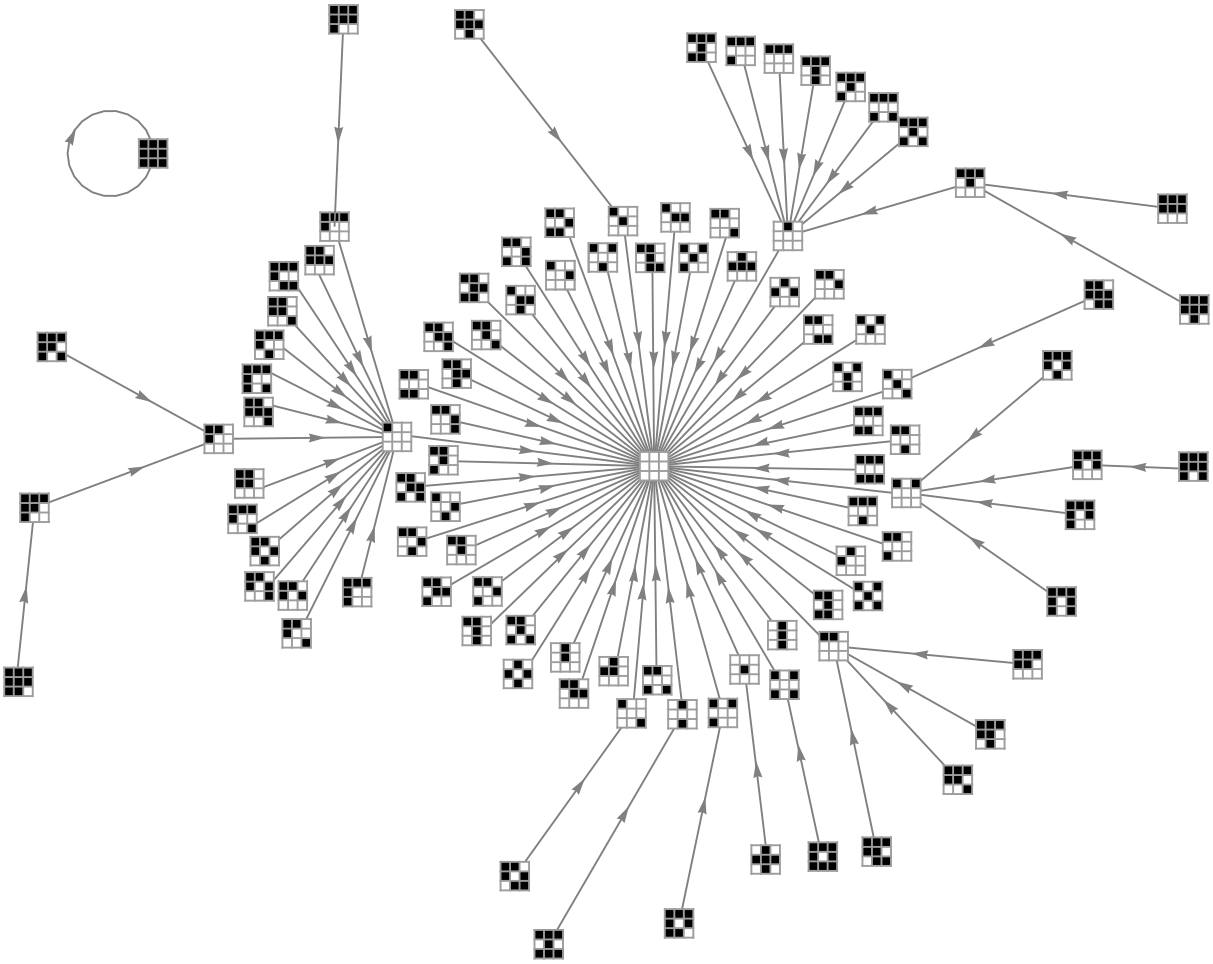

$P_3 \times P_3$: Parameter region K

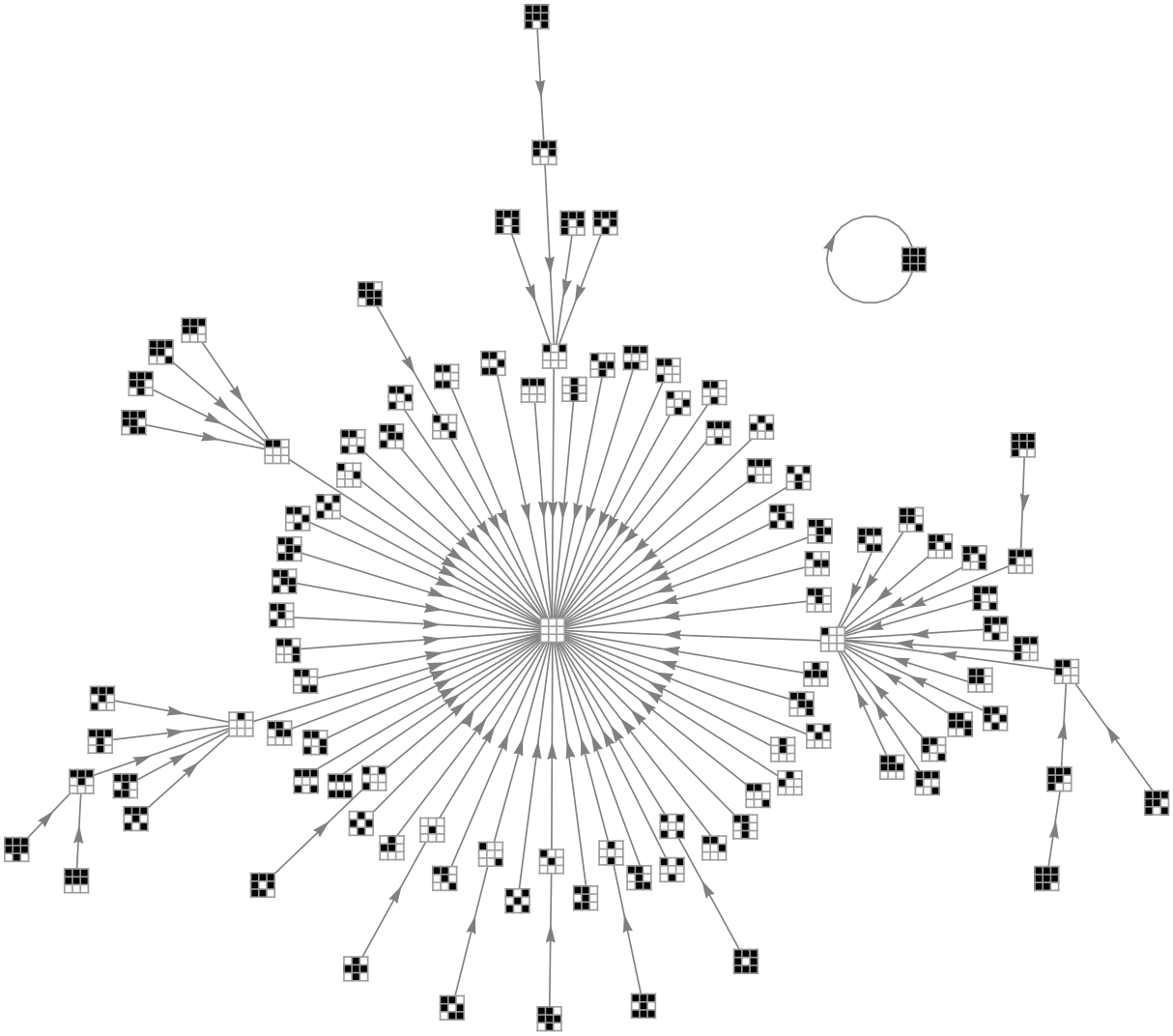

$P_3 \times P_3$: Parameter region L

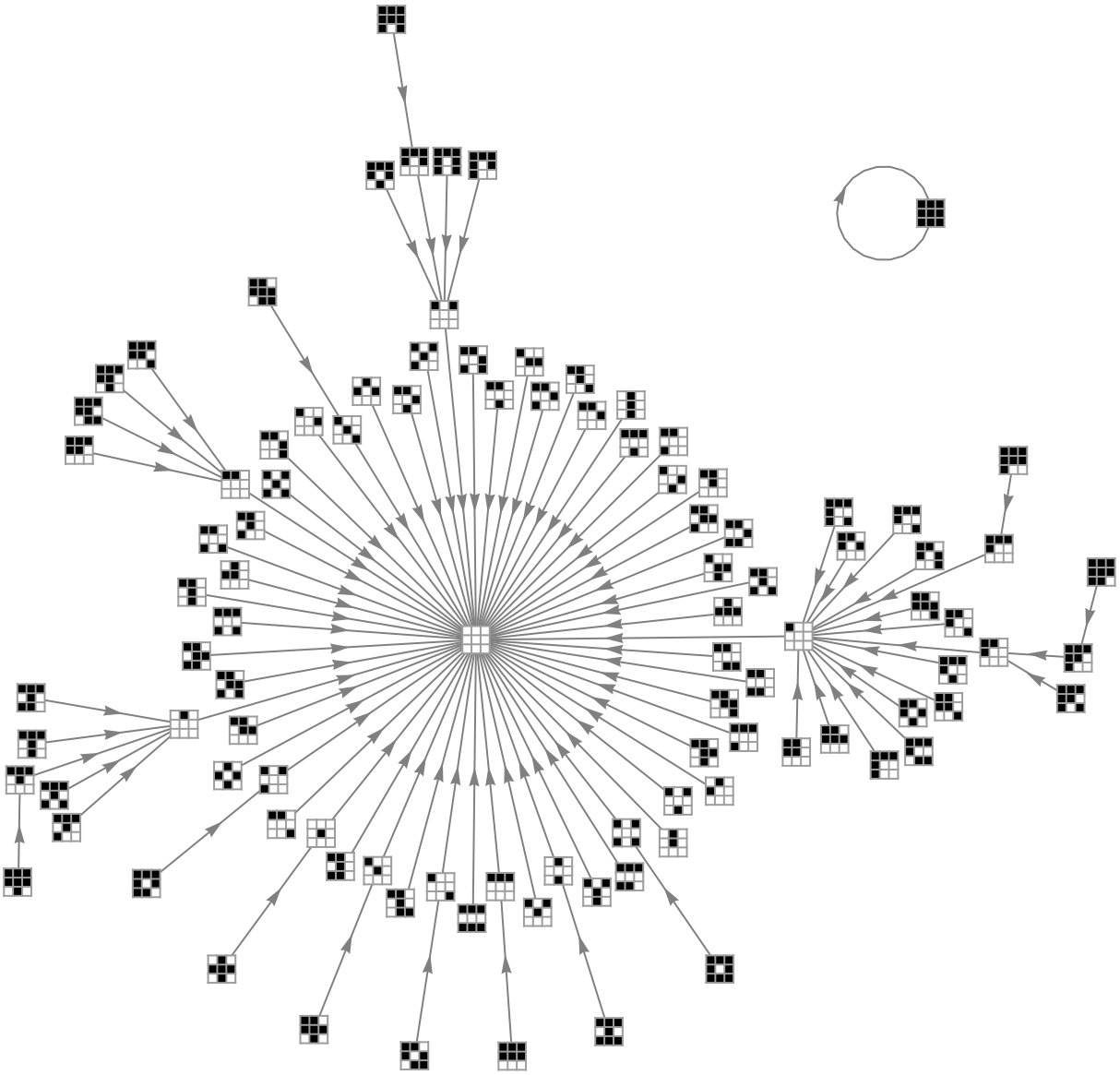

$P_3 \times P_3$: Parameter region M

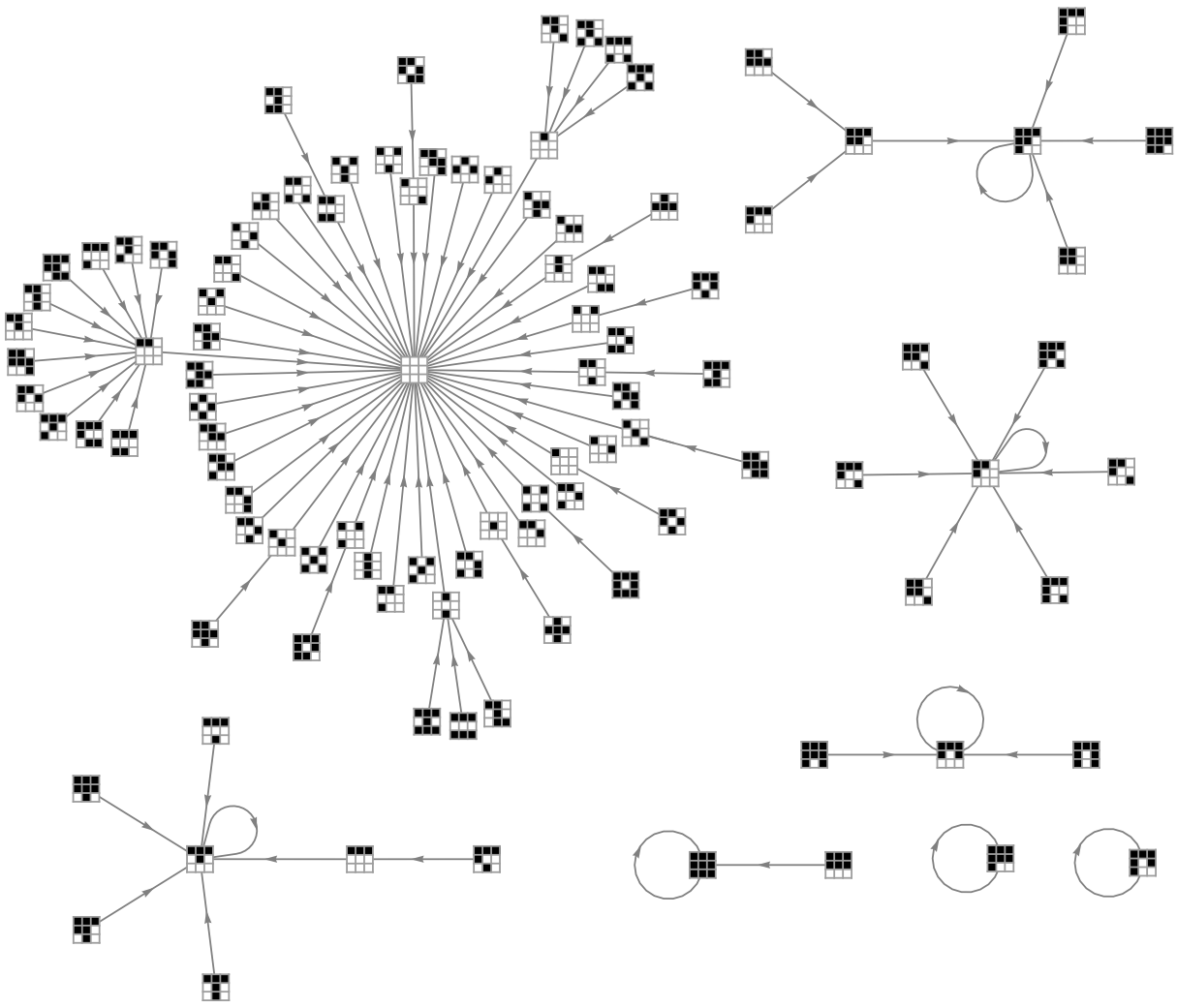

$P_3 \times P_3$: Parameter region N

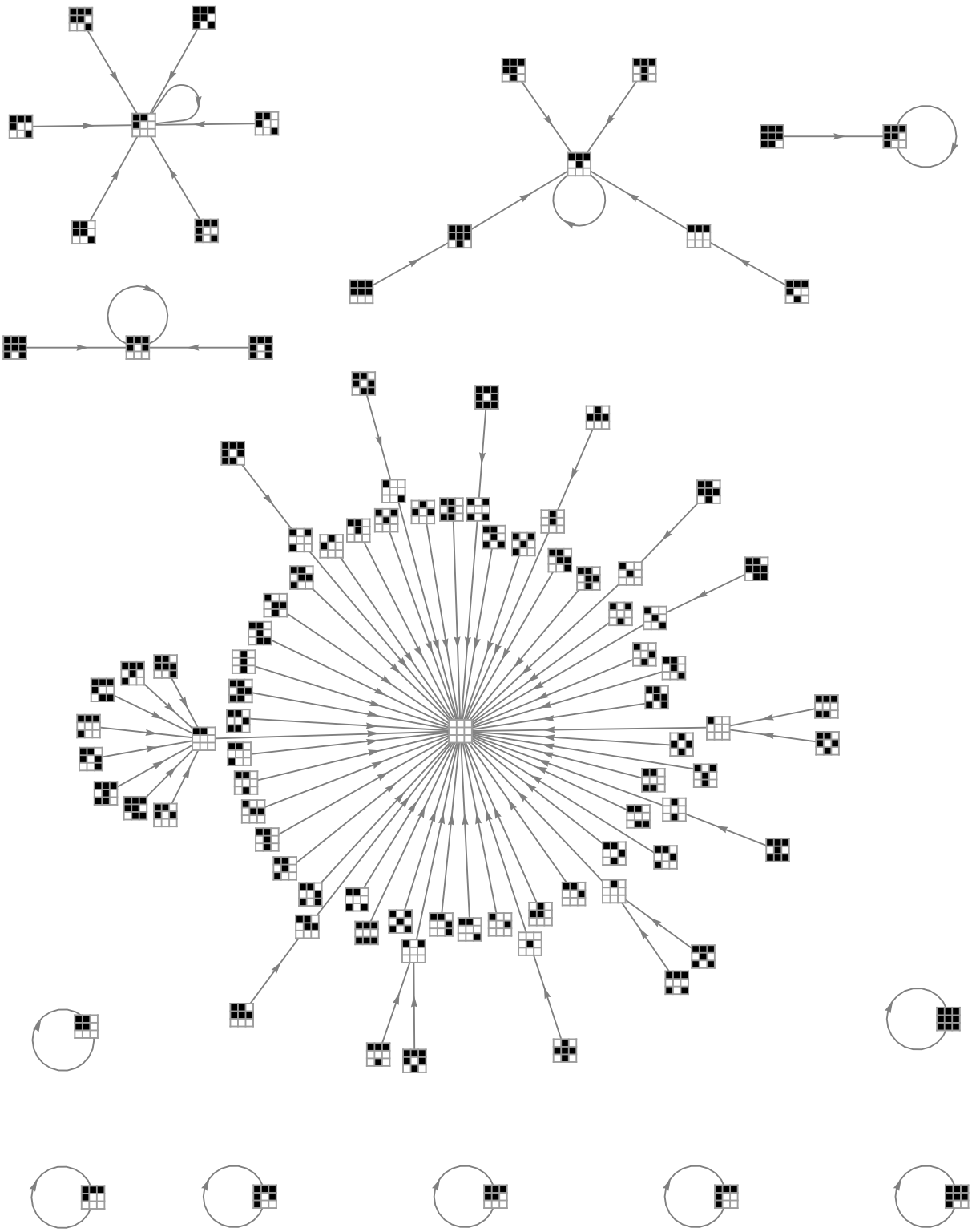

$P_3 \times P_3$: Parameter region O

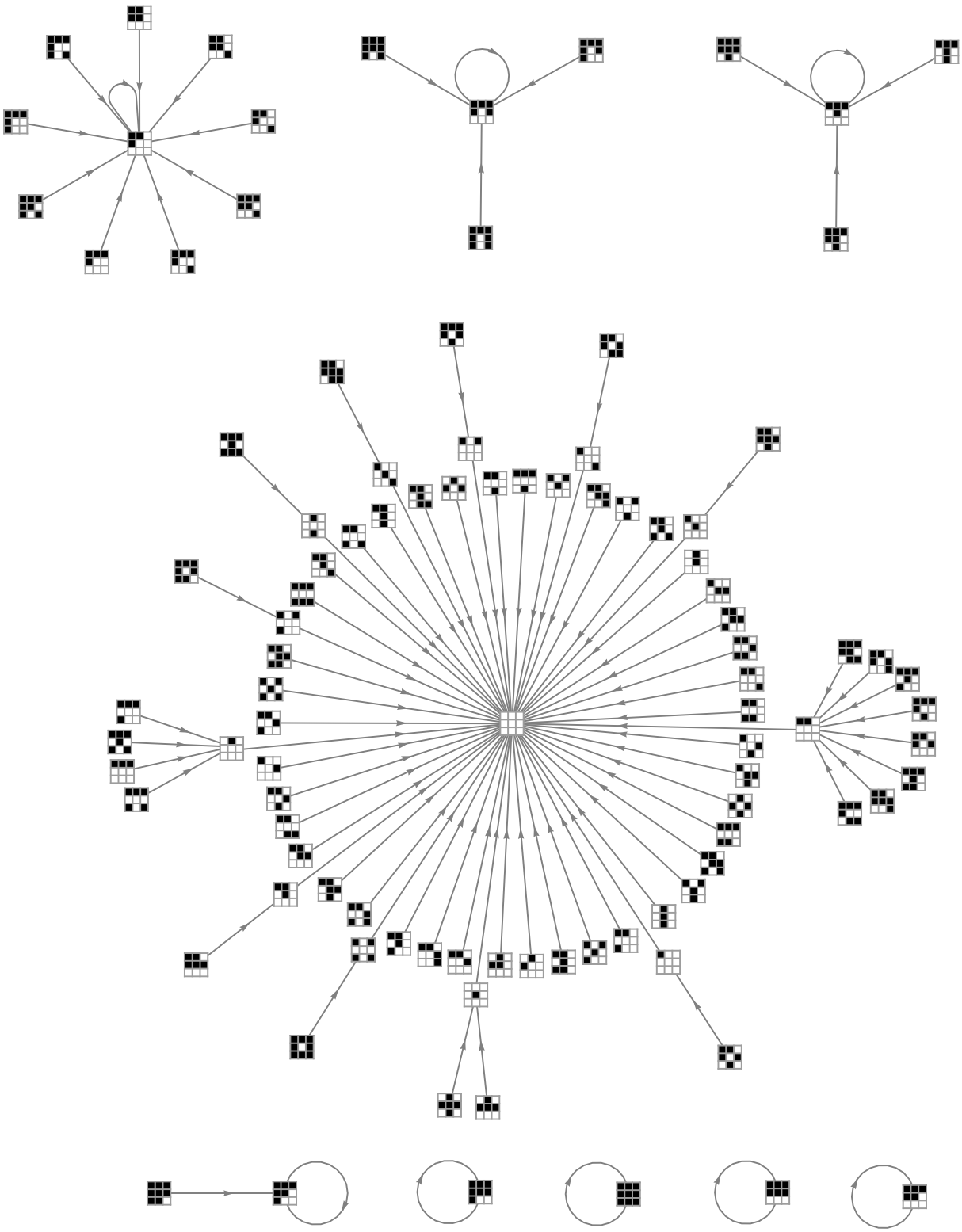

$P_3 \times P_3$: Parameter region P

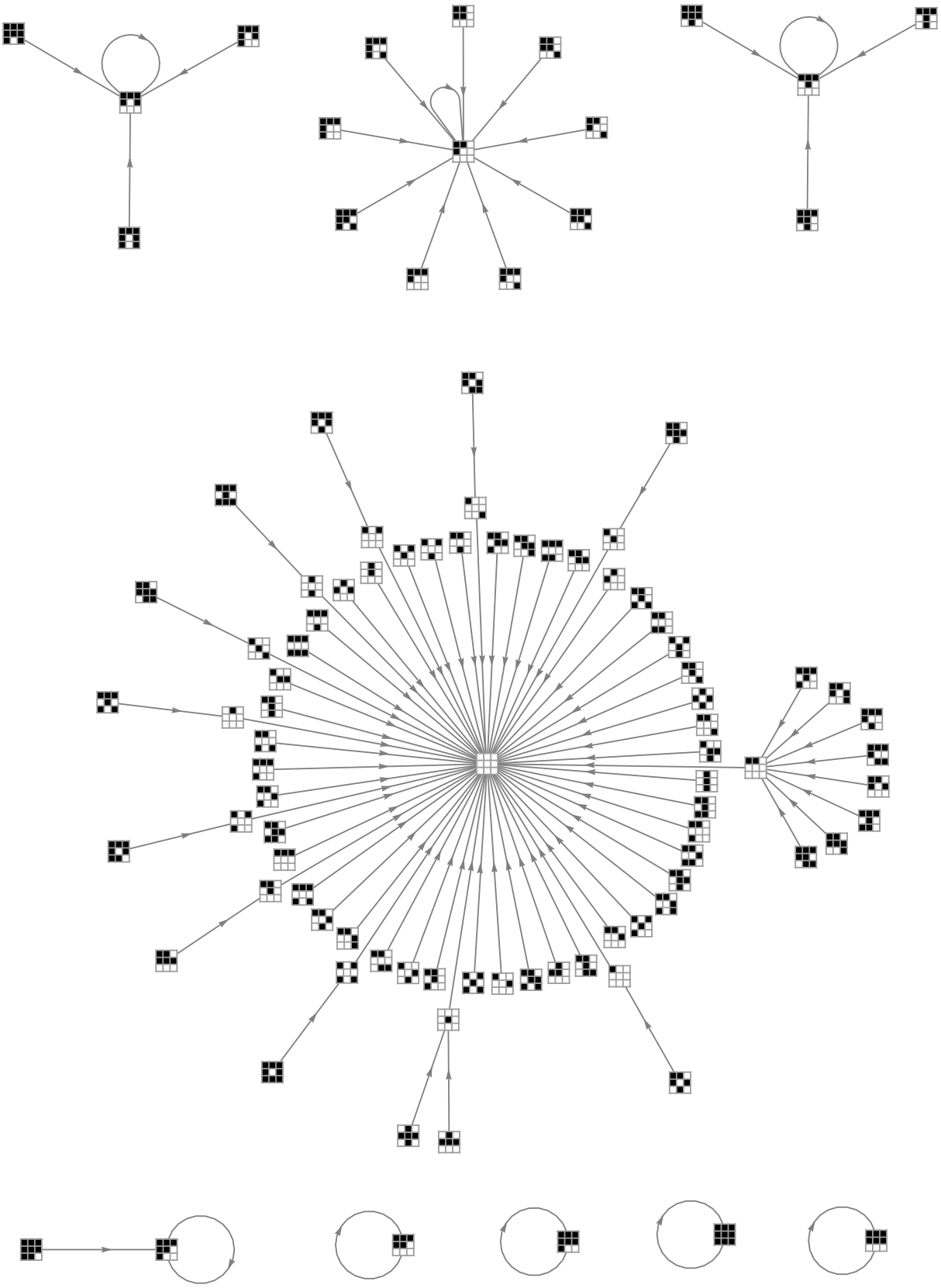

$P_3 \times P_3$: Parameter region Q

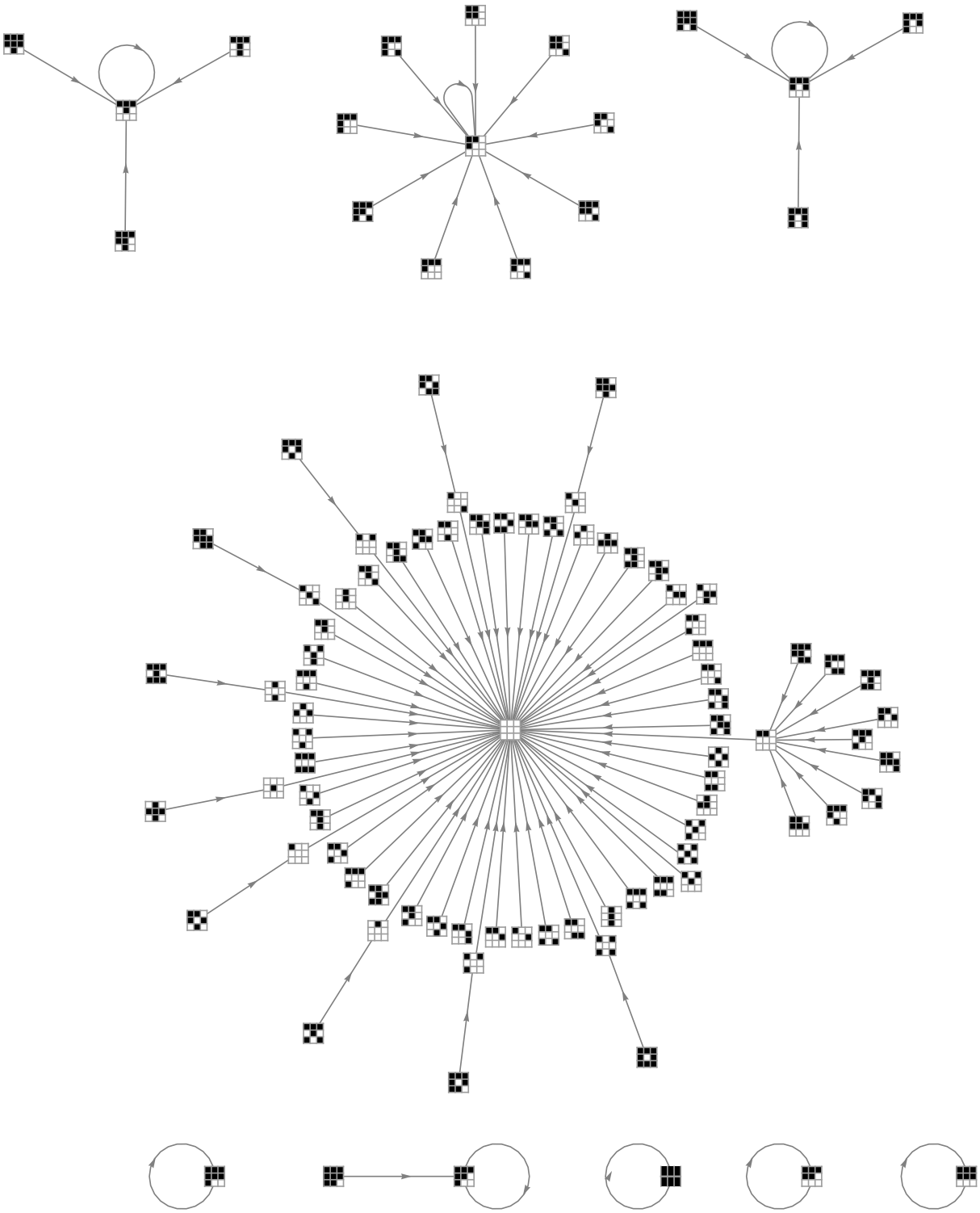

$P_3 \times P_3$: Parameter region R

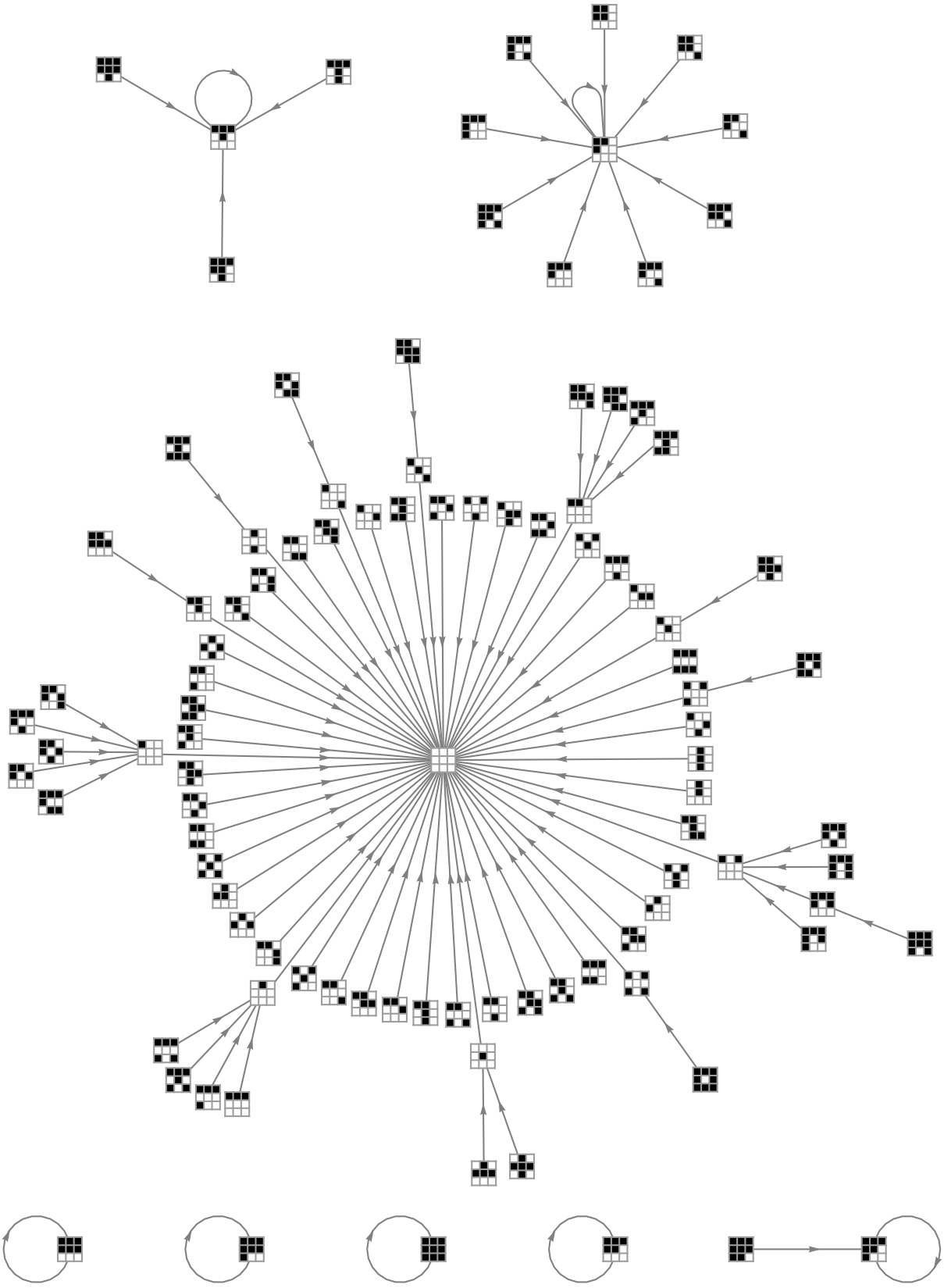

$P_3 \times P_3$: Parameter region S

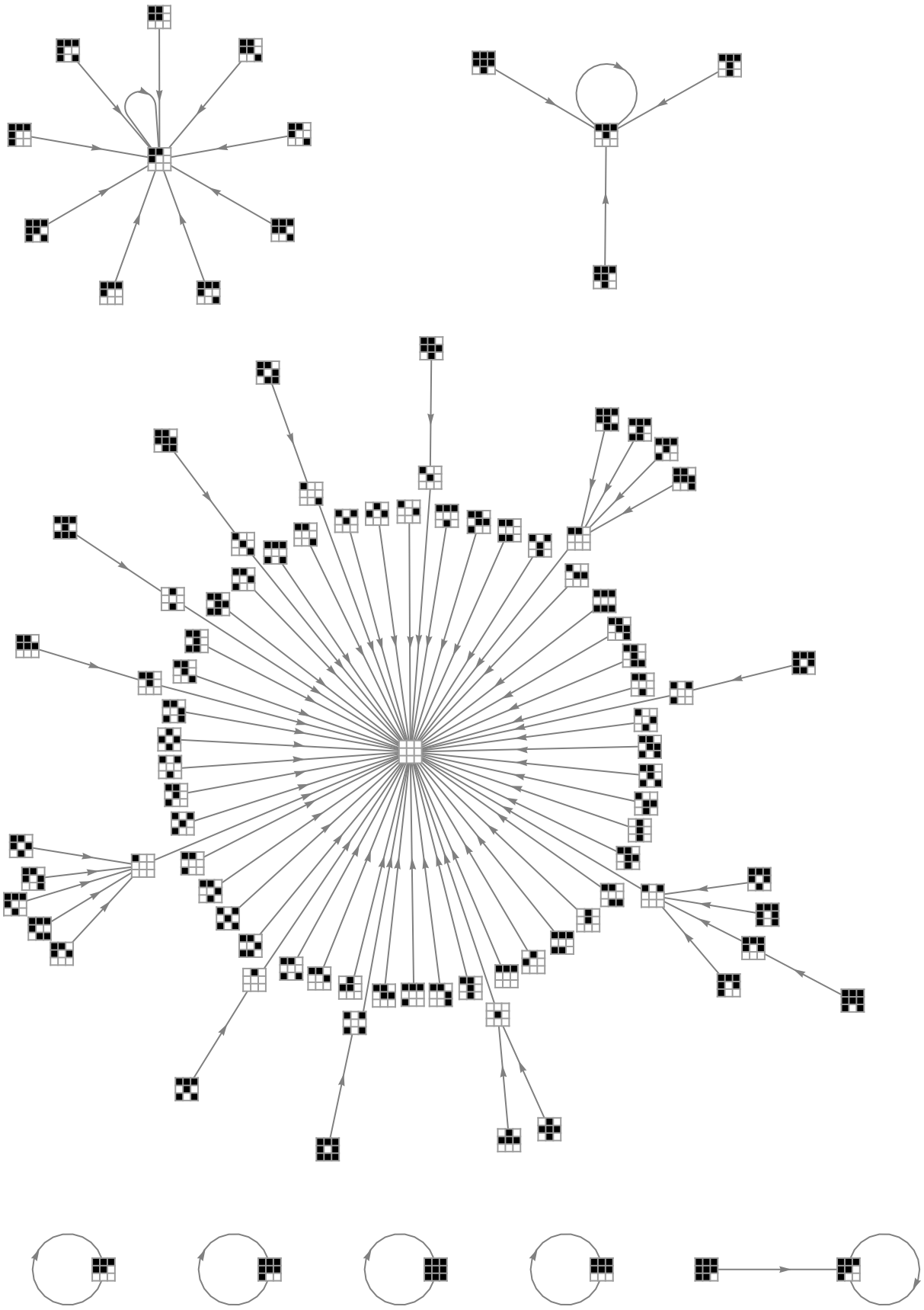

$P_3 \times P_3$: Parameter region T

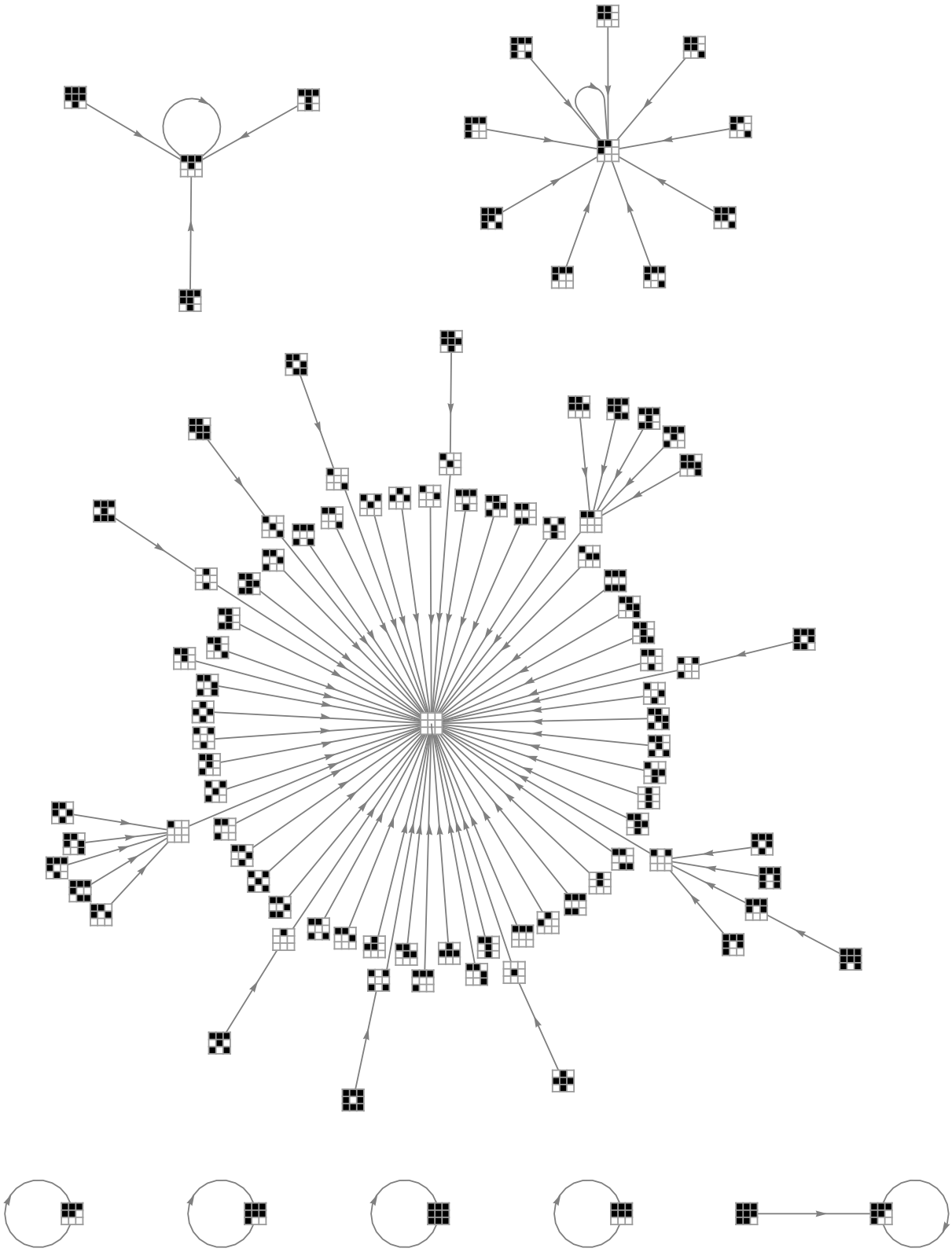

$P_3 \times P_3$: Parameter region U

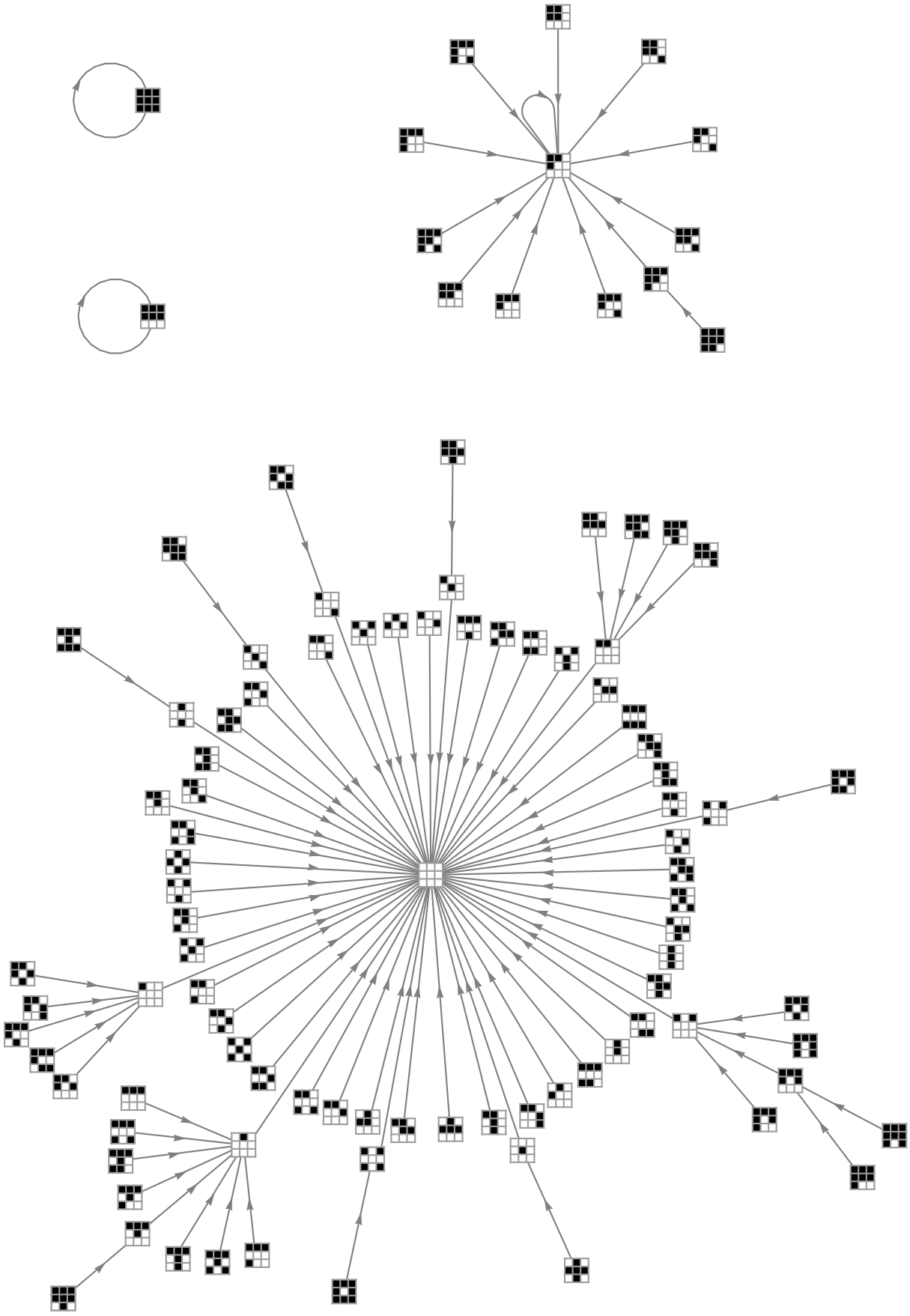

$P_3 \times P_3$: Parameter region V

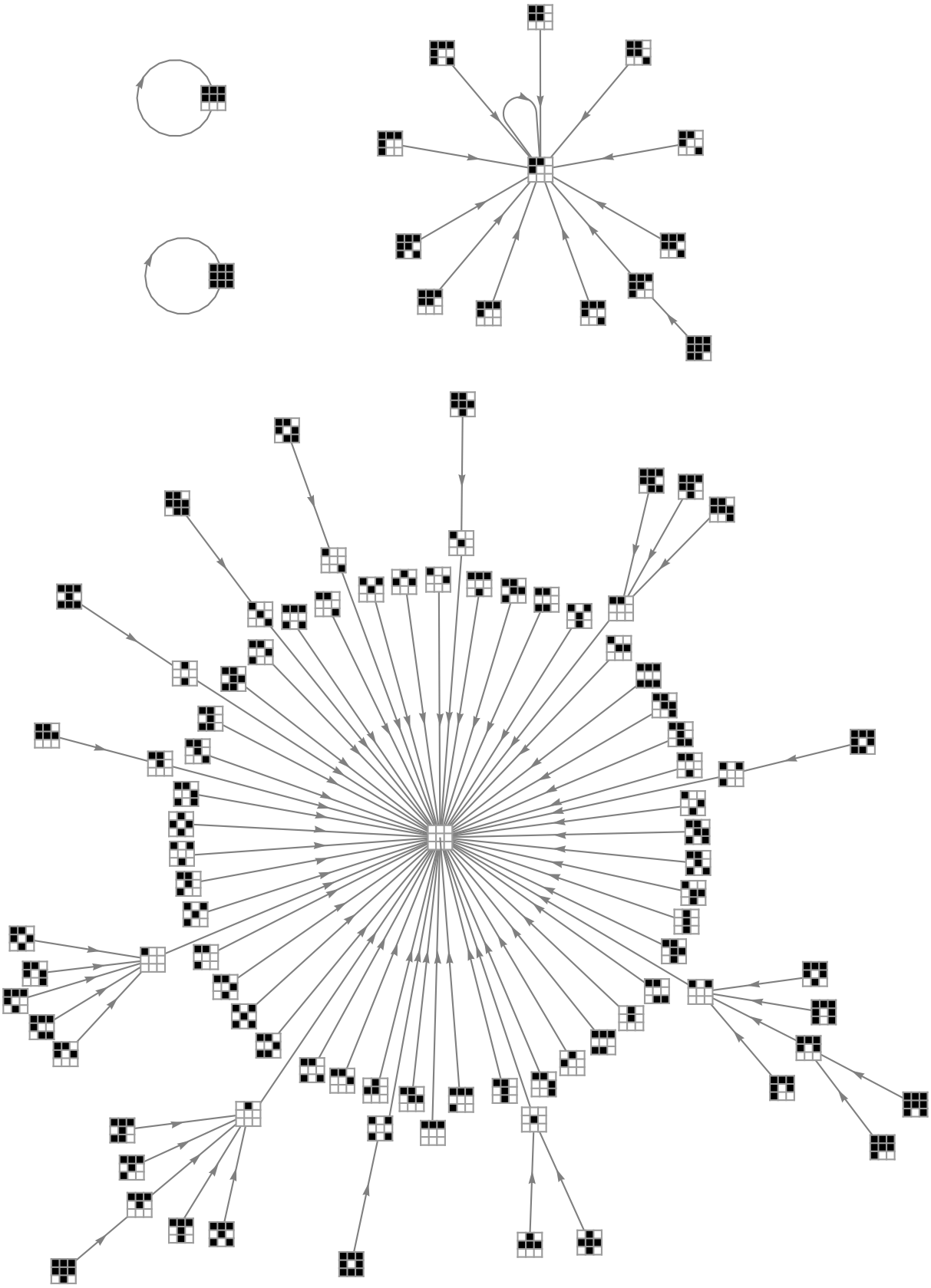

$P_3 \times P_3$: Parameter region W

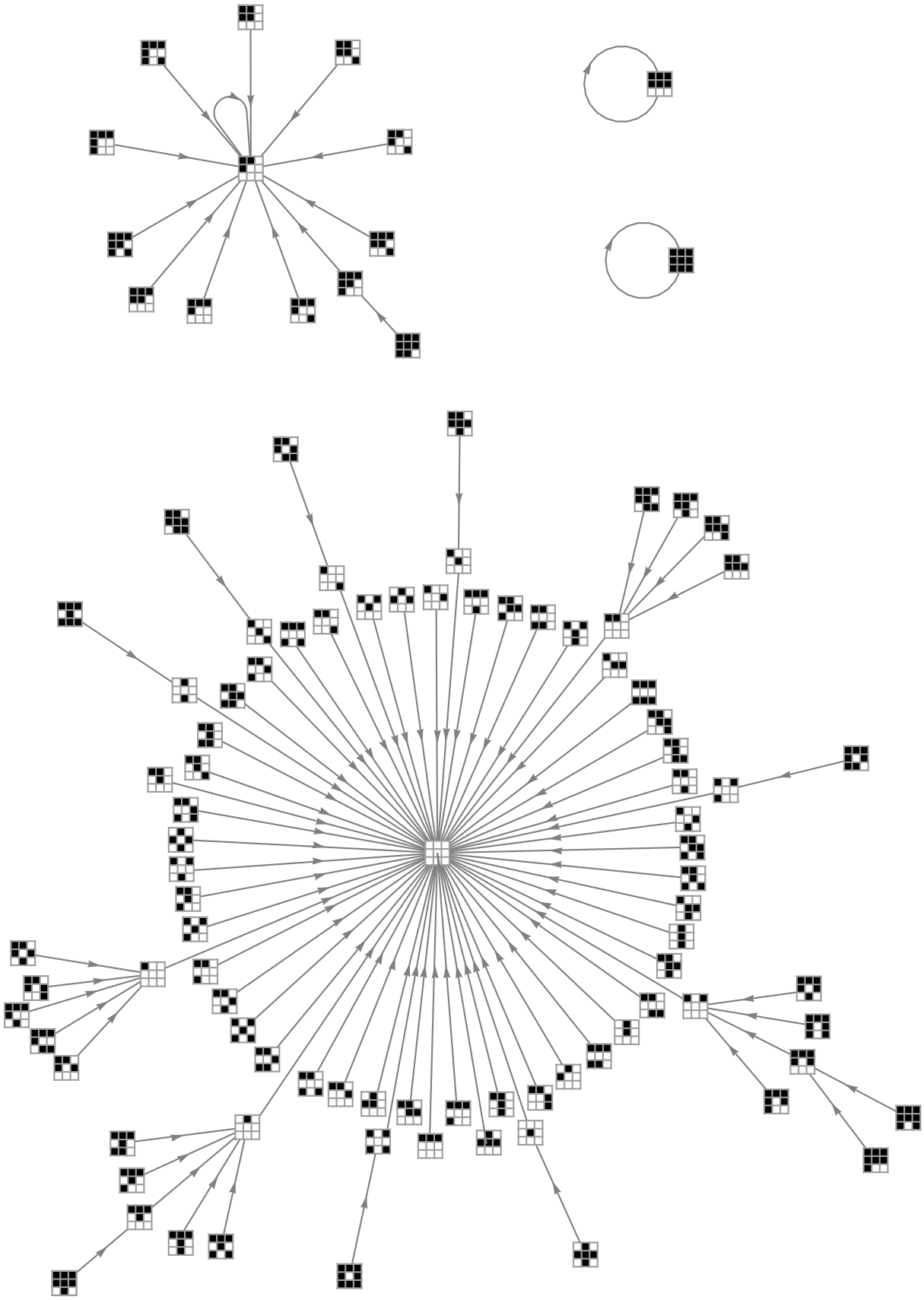

$P_3 \times P_3$: Parameter region X

B.4 $C_2 \times C_3$

The ESPD with the underlying graph $C_n \times C_m$, for values $m, n \geq 3$, admits eleven parameter regions in the *P-T* parameter space. The phase plane indicating the eleven parameter regions is shown in Figure B.3. The ESPD on smaller grid graphs exhibits equivalent game dynamics across some of the eleven parameter regions, a detailed explanation of the parameter space may be found in §6.3.1. The state graphs of the ESPD with $C_2 \times C_3$ as underlying graph are shown on p. 148.

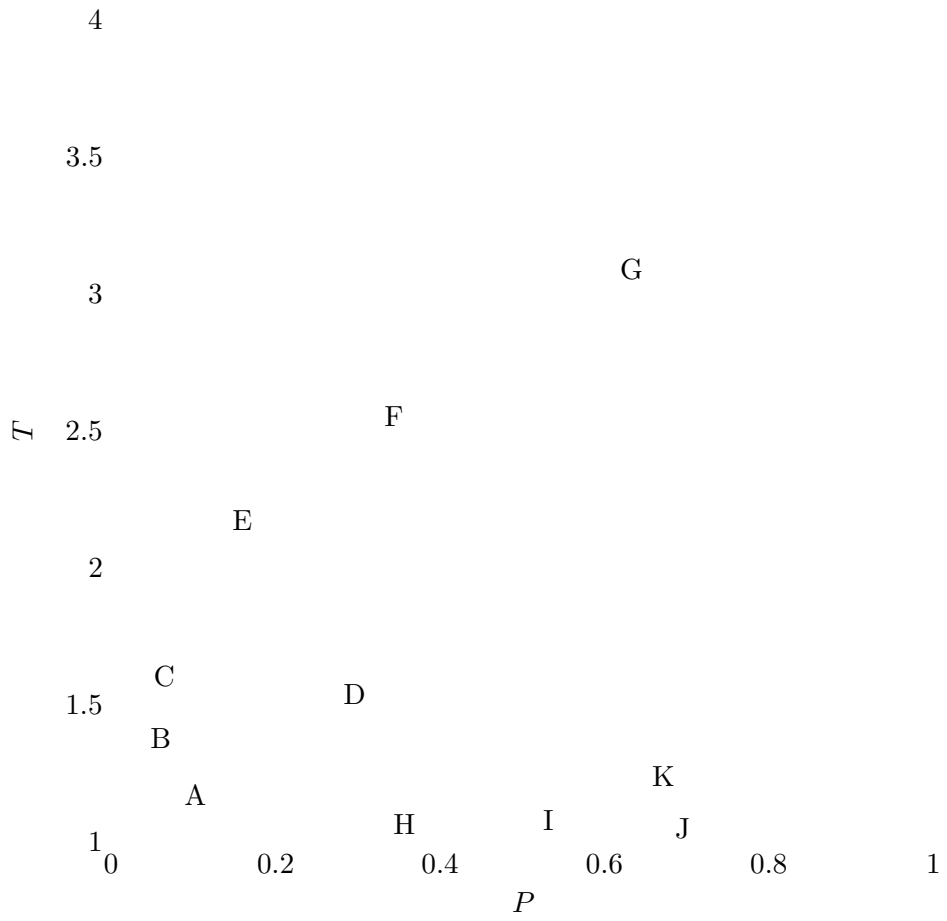

Figure B.3: *The P-T phase plane for the ESPD with $C_n \times C_m$ as the underlying graph. The eleven parameter regions are labelled A through K.*

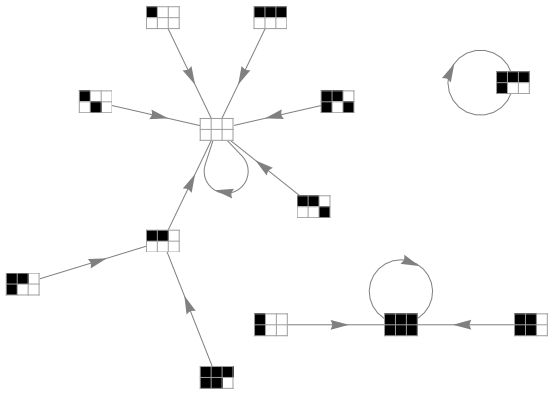

$C_2 \times C_3$: Parameter region A

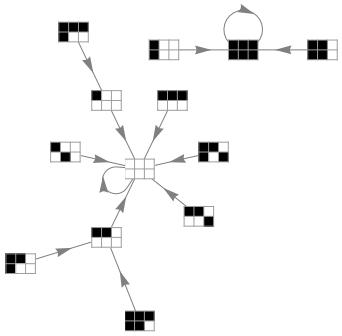

$C_2 \times C_3$: Parameter region B

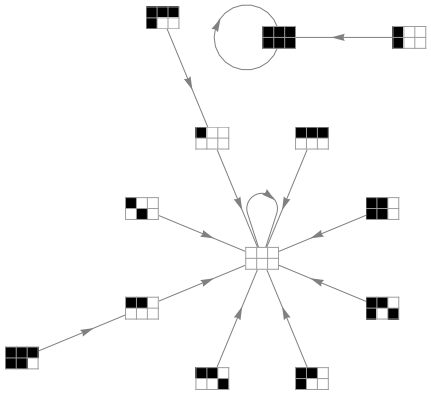

$C_2 \times C_3$: Parameter region C

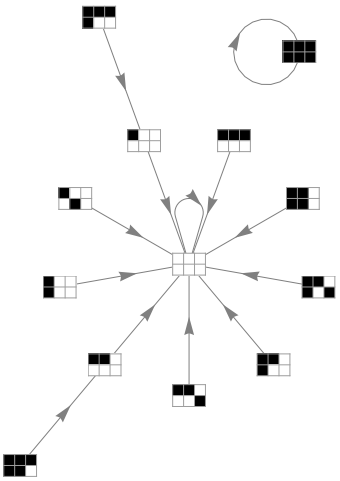

$C_2 \times C_3$: Parameter regions D, E, F, G and K

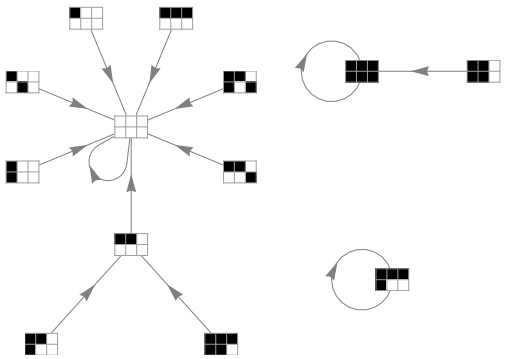

$C_2 \times C_3$: Parameter region H

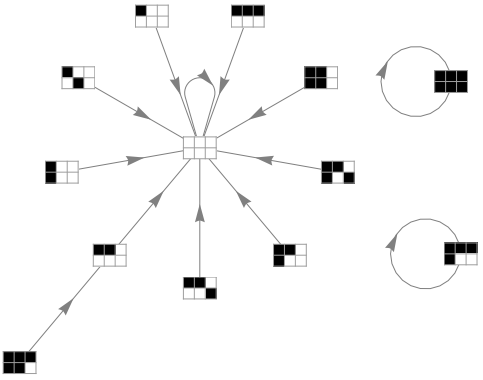

$C_2 \times C_3$: Parameter regions I and J

B.5 $C_2 \times C_4$

The ESPD with $C_2 \times C_4$ as underlying graph exhibits fundamentally different game dynamics across ten disjoint parameter regions in the P-T phase plane. The phase plane indicating the parameter regions is shown in Figure B.3. The ten state graphs, one for each parameter region, are shown below and on pp. 150–151.

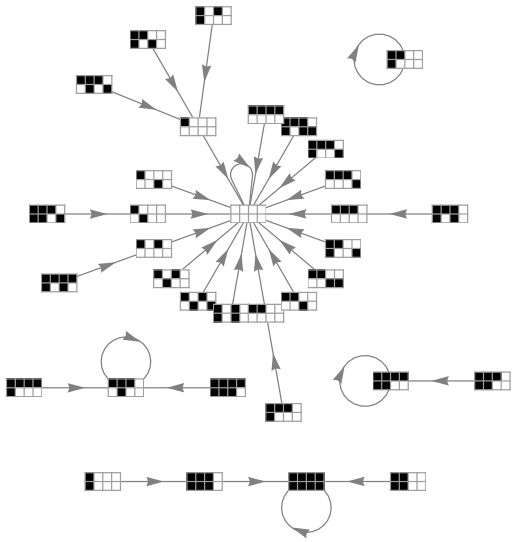

$C_2 \times C_4$: Parameter region A

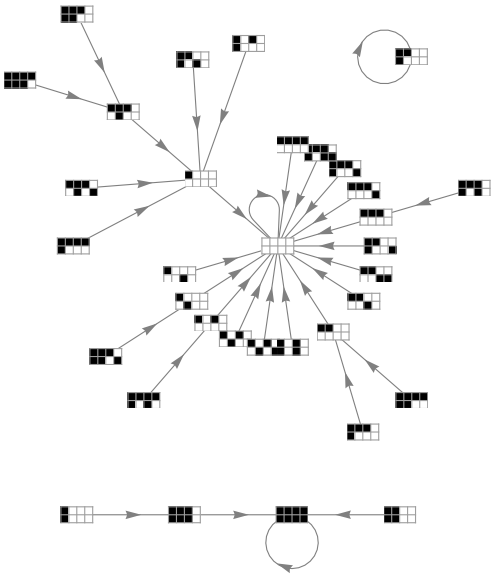

$C_2 \times C_4$: Parameter region B

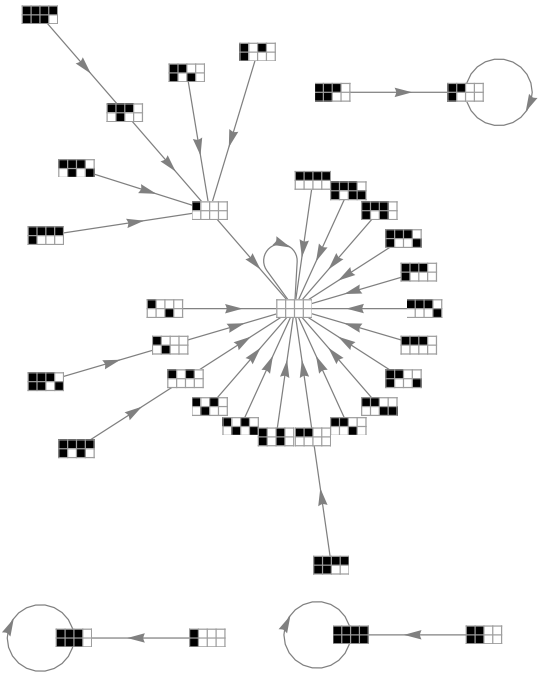

$C_2 \times C_4$: Parameter region C

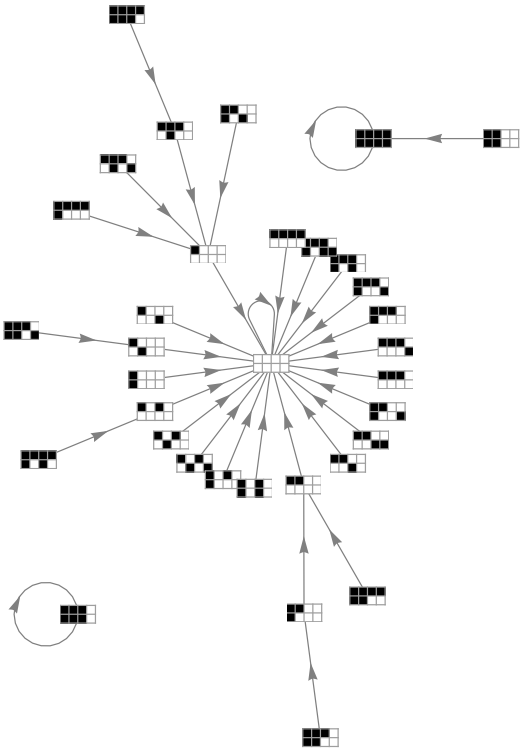

$C_2 \times C_4$: Parameter region D

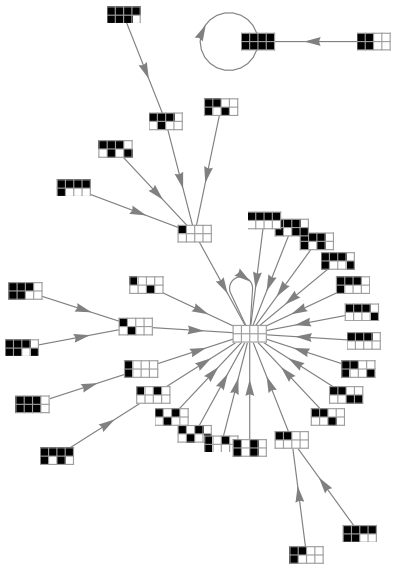

$C_2 \times C_4$: Parameter region E

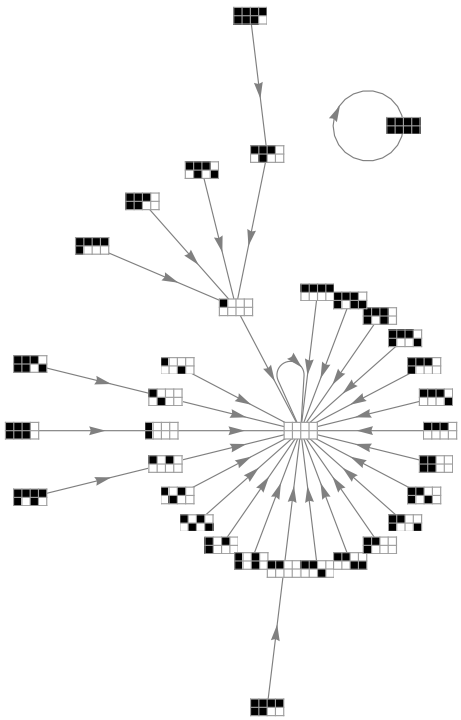

$C_2 \times C_4$: Parameter regions F and G

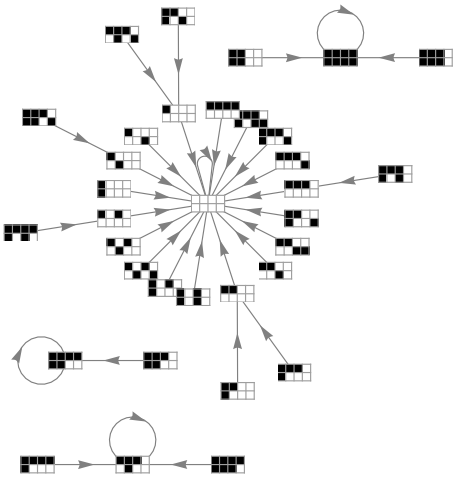

$C_2 \times C_4$: Parameter region H

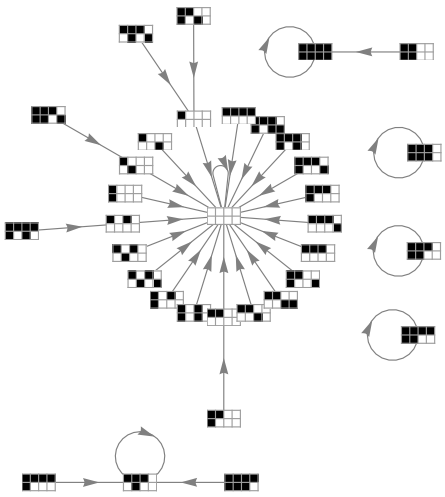

$C_2 \times C_4$: Parameter region I

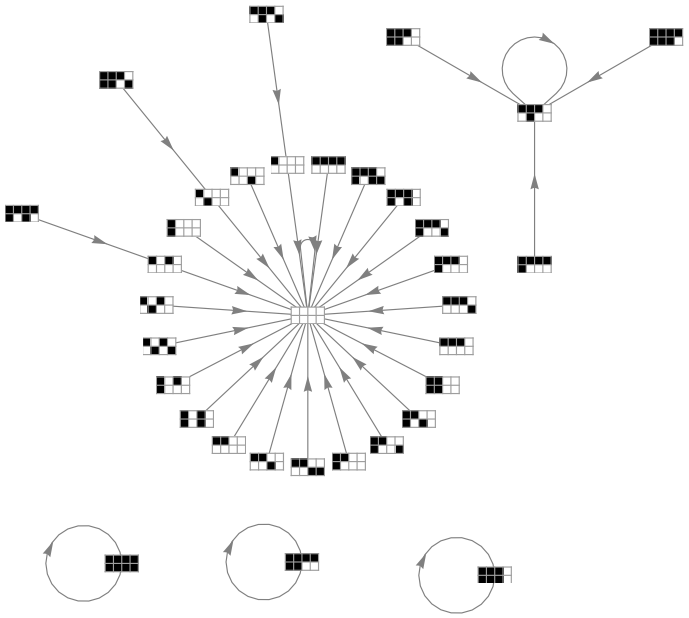

$C_2 \times C_4$: Parameter region J

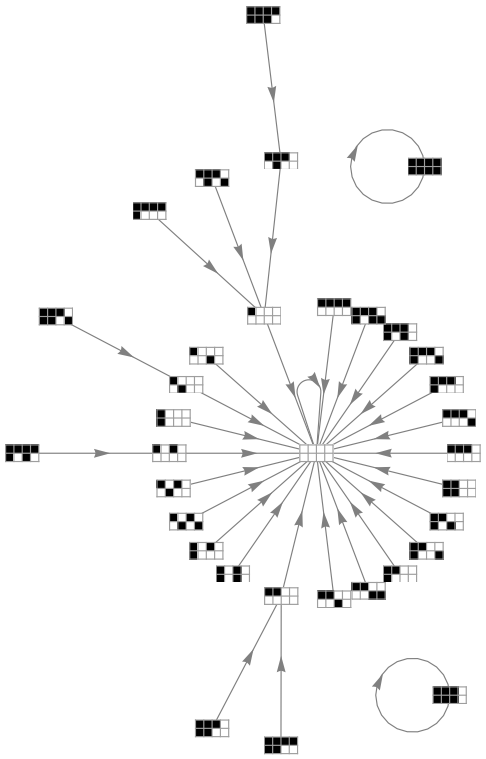

$C_2 \times C_4$: Parameter region K

B.6 $C_2 \times C_5$

The ESPD with $C_2 \times C_5$ as underlying graph exhibits fundamentally different game dynamics across eleven disjoint parameter regions in the P-T phase plane. The phase plane indicating the parameter regions is shown in Figure B.3. The eleven state graphs, one for each parameter region, are shown below and on 153–158.

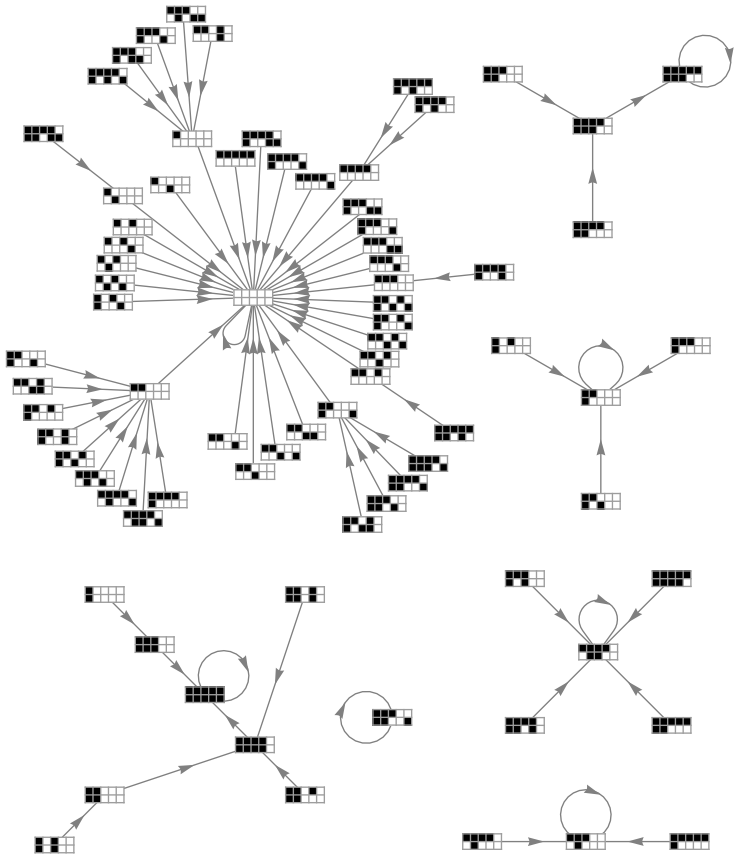

$C_2 \times C_5$: Parameter region A

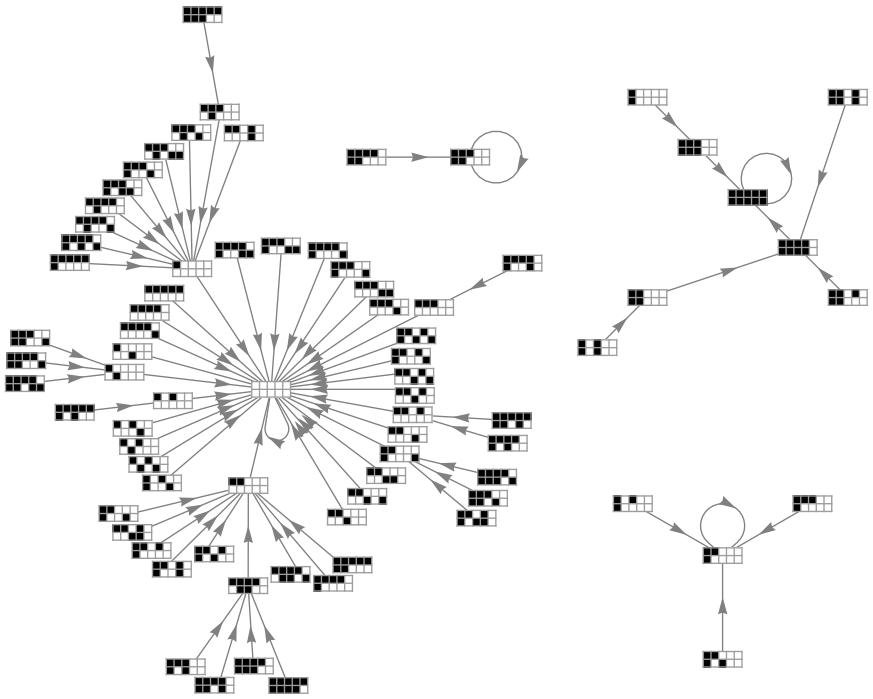

$C_2 \times C_5$:Parameter region B

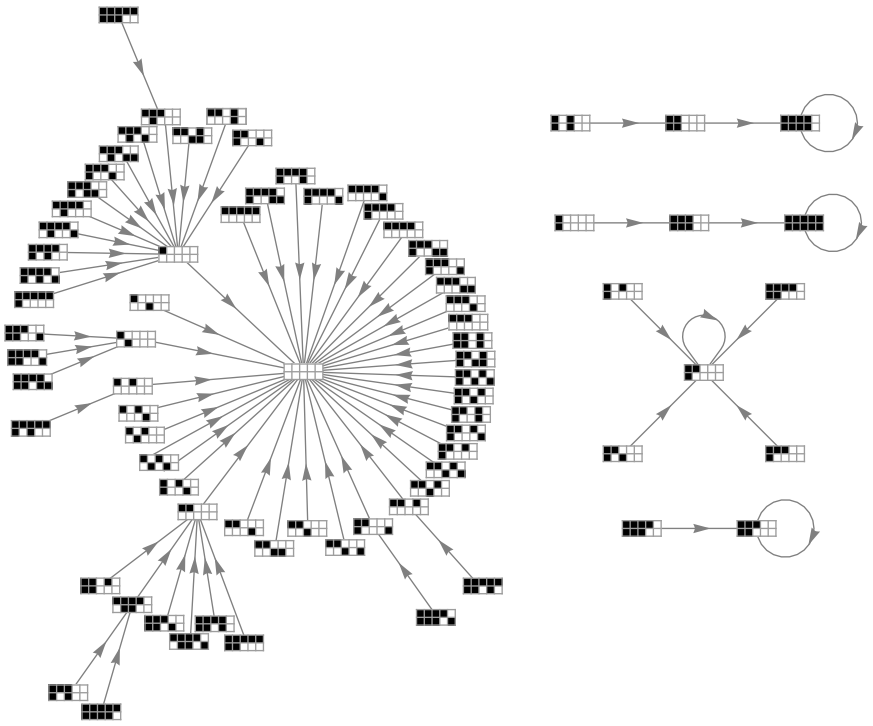

$C_2 \times C_5$: Parameter region C

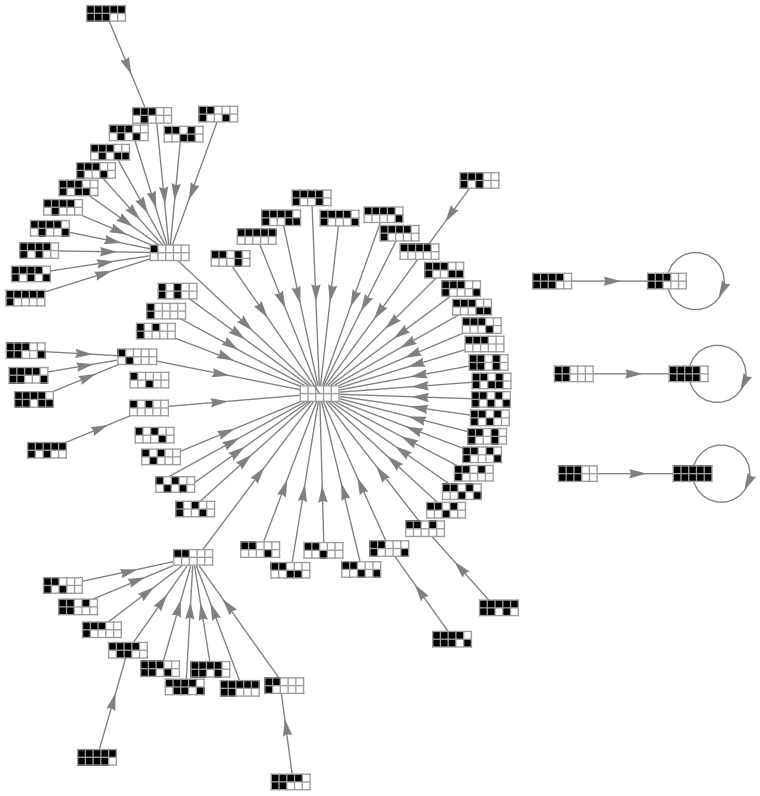

$C_2 \times C_5$: Parameter region D

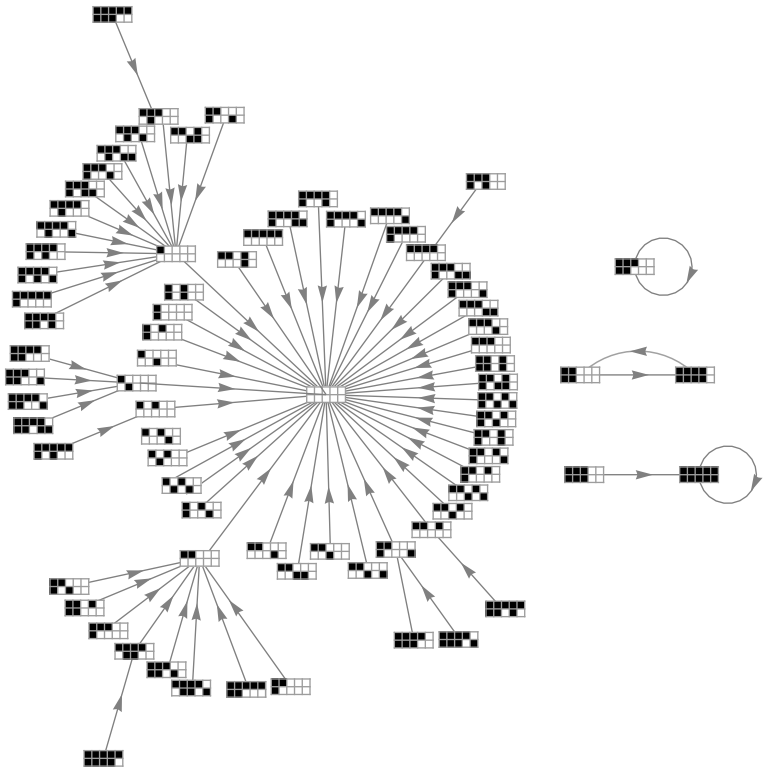

$C_2 \times C_5$: Parameter region E

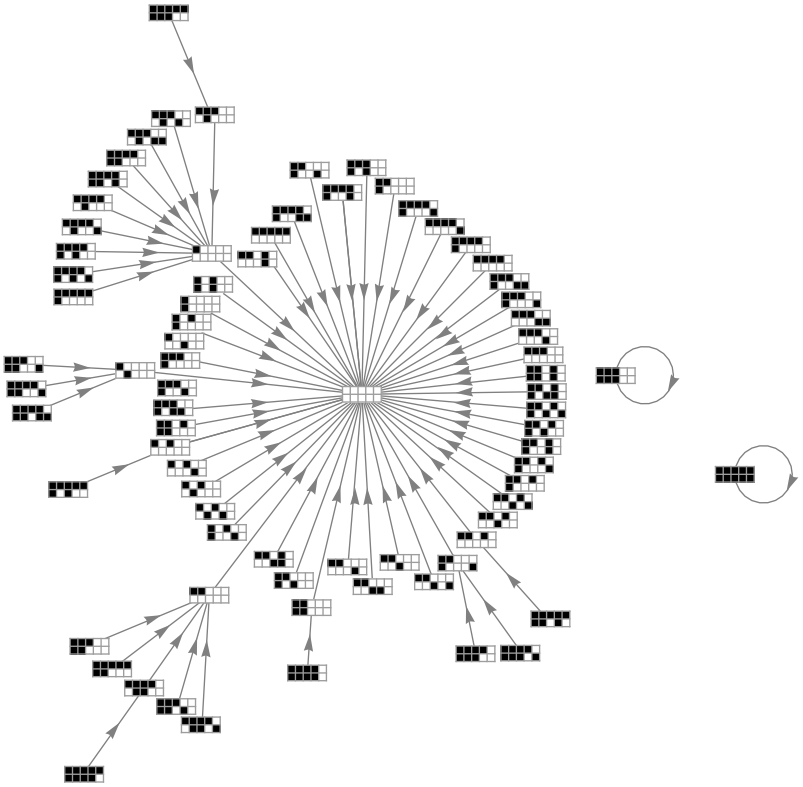

$C_2 \times C_5$: Parameter region F

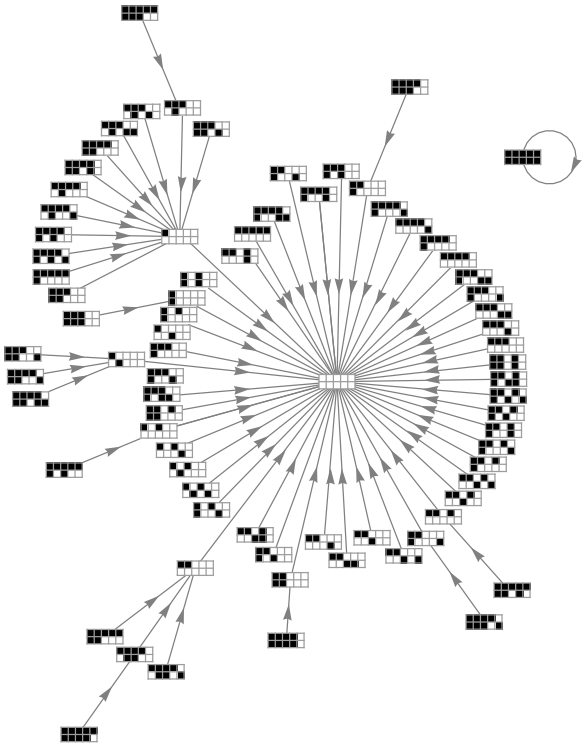

$C_2 \times C_5$: Parameter region G

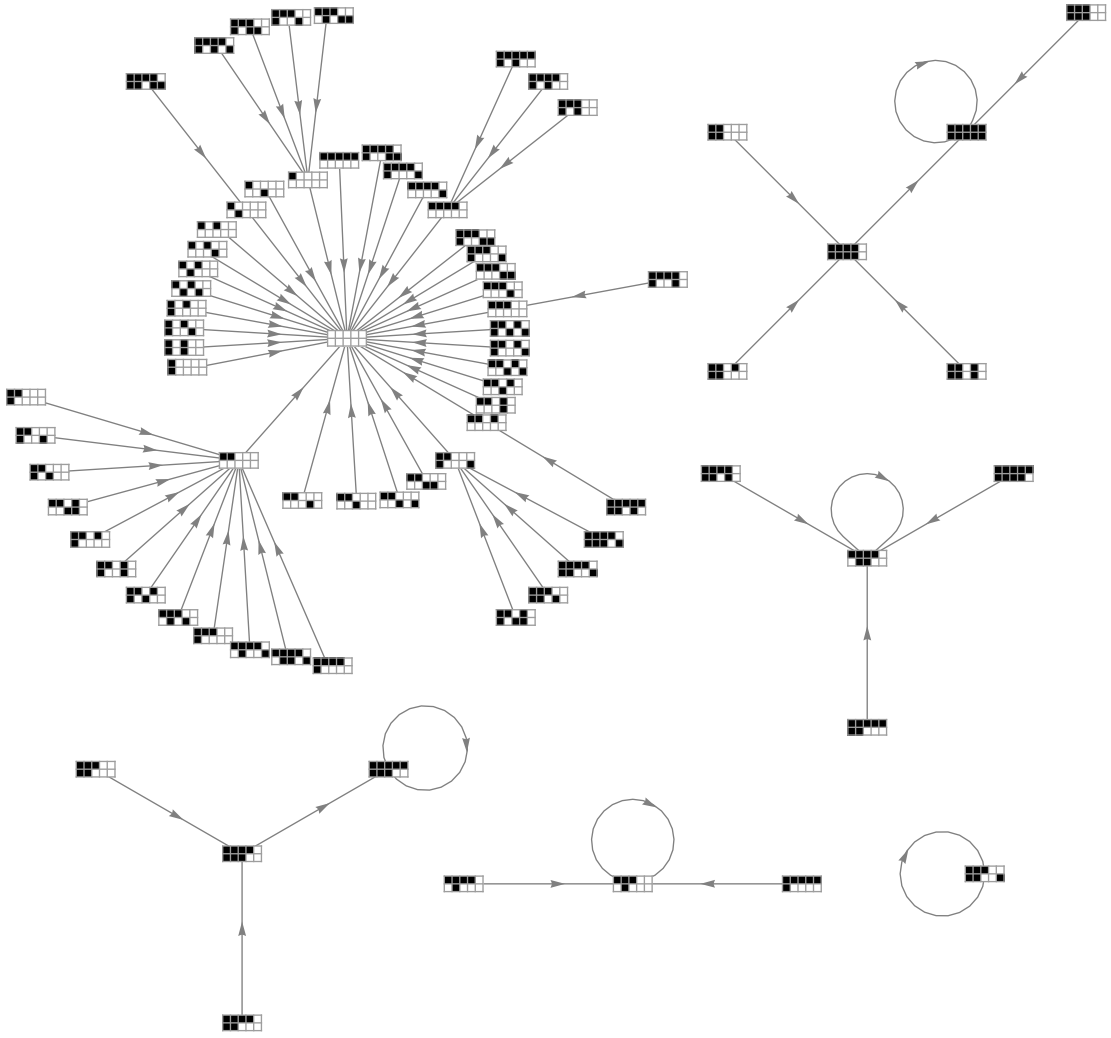

$C_2 \times C_5$: Parameter region H

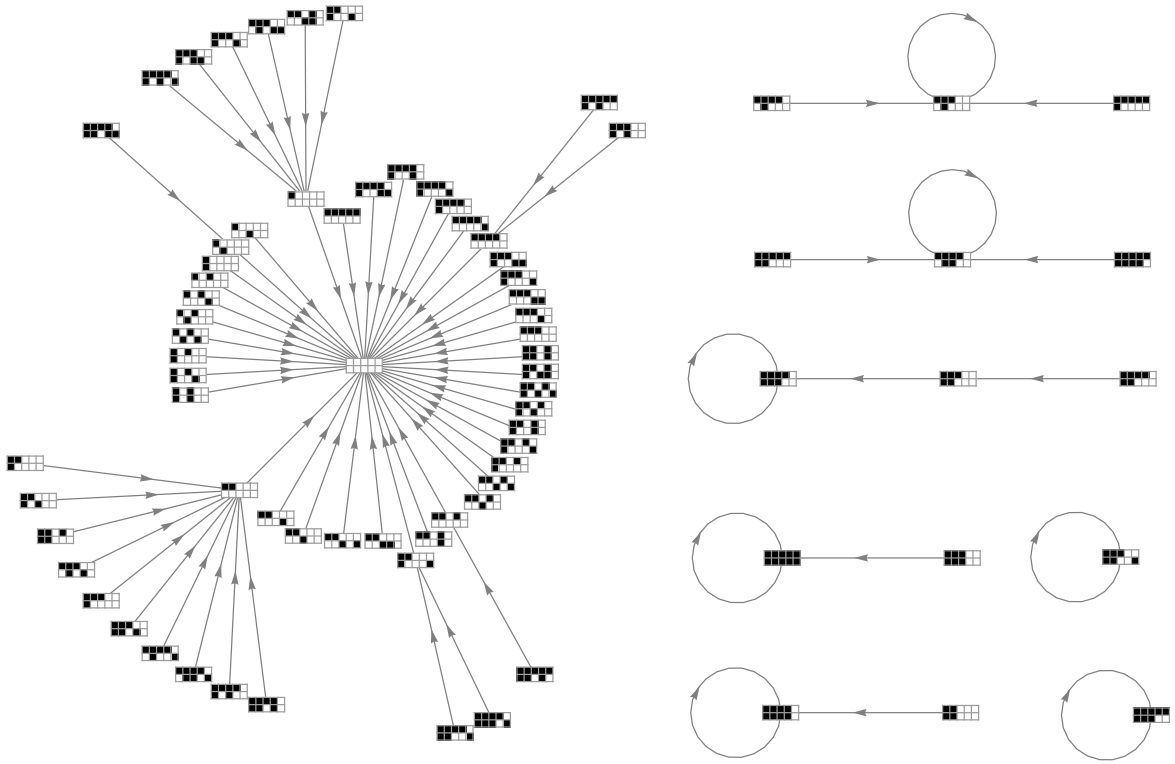

$C_2 \times C_5$: Parameter region I

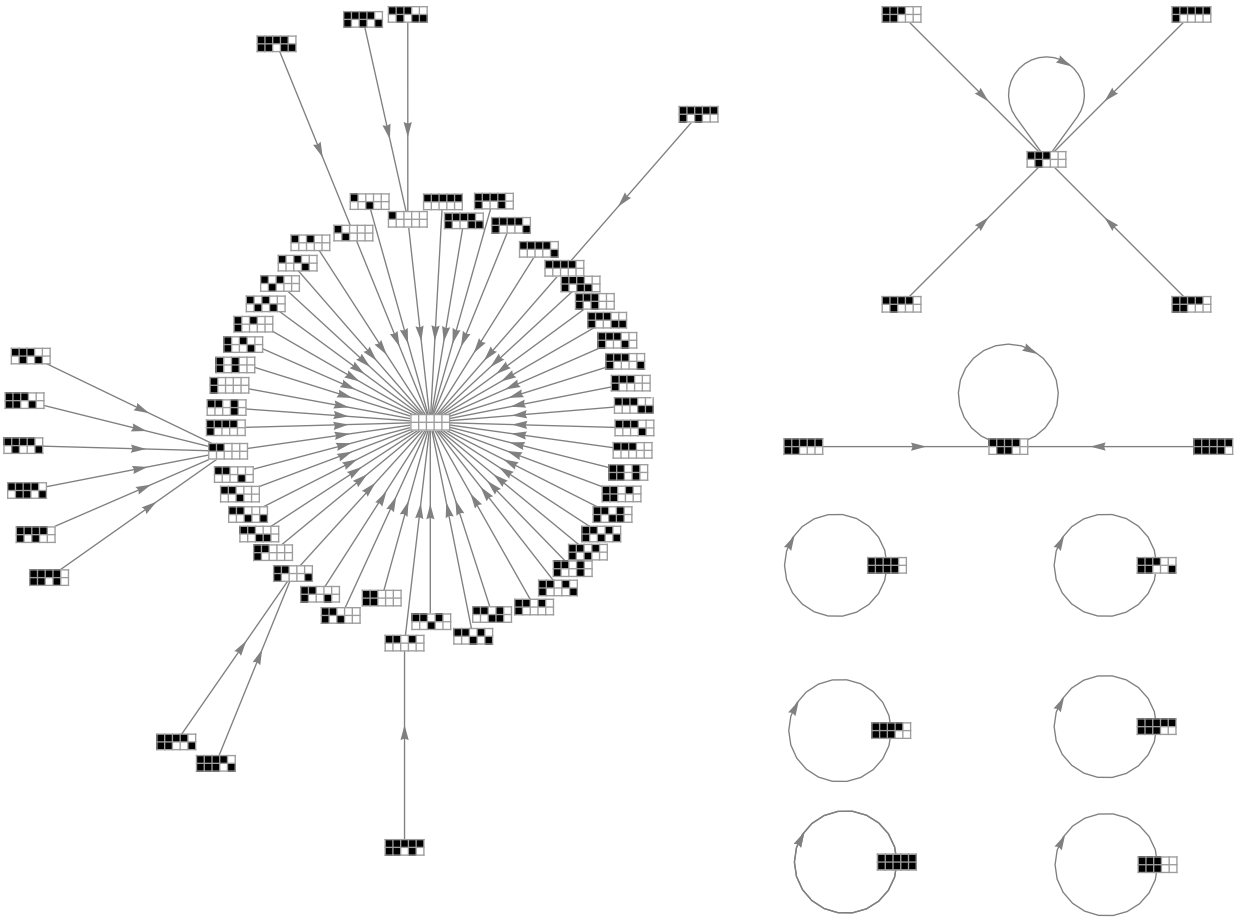

$C_2 \times C_5$: Parameter region J

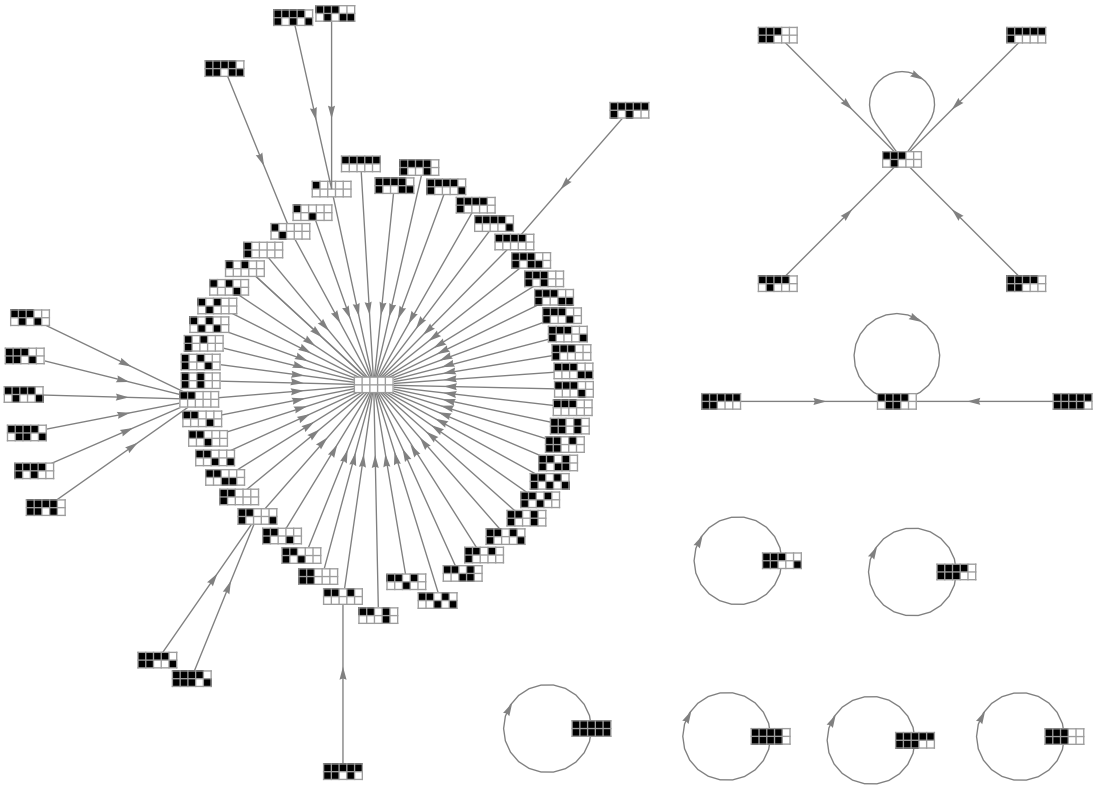

$C_2 \times C_5$: Parameter region K